To the Graduate Council:

I am submitting herewith a dissertation written by Ian James Richards entitled "Petrologic and stable isotopic studies of metamorphic fluid-rock interaction and igneous petrogenesis, Lone Mountain, Nevada." I have examined the final copy of this dissertation for form and content and recommend that it be accepted in partial fulfillment of the requirements for the degree of Doctor of Philosophy, with a major in Geology.

Dr. Theodore C. Labotka, Major Professor

We have read this dissertation
and recommend its acceptance:

Accepted for the Council:

Associate Vice Chancellor
and the Dean of the Graduate School

PETROLOGIC AND STABLE ISOTOPIC STUDIES OF METAMORPHIC FLUID-ROCK INTERACTION AND IGNEOUS PETROGENESIS, LONE MOUNTAIN, NEVADA

A Dissertation

Presented for the

Doctor of Philosophy

Degree

The University of Tennessee, Knoxville

Ian James Richards

August, 1994

ACKNOWLEDGMENTS

I wish to acknowledge all of the people who have helped me during my time as a student at the University of Tennessee.

I would like to thank my advisor, Dr. Theodore Labotka, for his patience, support and encouragement in guiding me throughout this undertaking. I am very grateful to Ted for sharing his knowledge of metamorphic petrology with me through many insightful discussions.

I would also like to thank the other members of my dissertation committee, Dr. Larry Taylor, and Dr. Steven Driese of the Department of Geological Sciences, and Dr. David Cole of the Oak Ridge National Laboratory for their efforts and assistance throughout the project. I am especially grateful to Dr. Kelsey Cook of the Department of Chemistry for agreeing to serve on my committee at a late date and at extremely short notice.

Dr. Robert Gregory is thanked for making available the facilities in the stable isotope laboratory in the Department of Geological Sciences at Southern Methodist University, and also for his continued encouragement.

I am grateful for having been provided with this opportunity by the Department of Geological Sciences at the University of Tennessee through a graduate teaching assistantship, and an extension of that assistantship. I also wish to gratefully acknowledge Dr. Claudia Mora and Dr. Steven Driese for providing me with employment in the stable isotope laboratory in the Department of Geological Sciences, which has allowed me to complete my studies while still at the University of Tennessee.

Financial support for this project was provided by National Science Foundation grant EAR-9020642 to Dr. Theodore Labotka and student research grants from the Geological Society of America, Sigma Xi, and the University of Tennessee Department of Geological Sciences.

I wish to thank the Gregory family, Bob, Susan, Steven, Jill and Bret for their generous hospitality during my stays in Dallas. Jeff and Kelly Connelly are also thanked for their hospitality in Little Rock while I was on my way to and from Dallas.

Throughout the course of this project numerous individuals have helped me obtain the analytical data necessary for its completion. These include Allen Patchen - electron microprobe, Dr. Otto Kopp and Qi Qu - X-ray fluorescence, Tony Caldanaro - cathodoluminescence, Bob McGill of the Department of Materials Engineering and Dr. Steven Driese - scanning electron microscope.

To the many friends that I have made in Knoxville and throughout the United States (space prohibits me from listing all of them), sincerest thanks for your friendship, it made my stay here very enjoyable. In particular I would like to thank Maria Leary for her companionship and support.

Finally, and most importantly, I am deeply indebted to my parents for always encouraging me and instilling in me the desire to pursue my interests, no matter where they may have taken me. While I have been away from home my family has been a constant source of support and encouragement to me. This is a debt that I can never repay.

ABSTRACT

Late Proterozoic to Cambrian carbonate, calc-silicate and pelitic rocks from Lone Mountain, Esmeralda County, Nevada, were regionally metamorphosed during Mesozoic time and then contact metamorphosed during intrusion of the Lone Mountain granitic pluton in Late Cretaceous time. The rocks were metamorphosed at a pressure of 3.5 ± 1 kbar and a temperature of 450 ± 70°C. Calc-silicate rocks were in equilibrium with H_2O-rich fluids (X_{CO_2} less than 0.05), while marbles were in equilibrium with more CO_2-rich fluids (X_{CO_2} greater than 0.2).

Essentially pure marbles consist of either calcite or dolomite with limited calcite + dolomite, and minor quartz. The stable isotopic compositions of marbles can be divided into two groups, one with positive $\delta^{13}C$ values and high $\delta^{18}O$ values, and the other with negative $\delta^{13}C$ values and low $\delta^{18}O$ values. Quartz from calcite marbles is brown- and blue-luminescent, clear, and smooth-textured, with high $\delta^{18}O$ values; whereas quartz from dolomite marbles is brown-luminescent, opaque, and rough-textured with extremely low $\delta^{18}O$ values. Low Mn/Sr ratios and high $\delta^{13}C$ and $\delta^{18}O$ values in calcite marbles indicates that their original isotopic compositions have not been significantly altered; whereas, the negative correlation between Mn/Sr and $\delta^{18}O$ in dolomite marbles indicates that they do not preserve their original oxygen isotopic compositions. The trace element compositions of dolomite marbles, loss of Sr and Na, and gain of Zn, Mn, and Fe, compared with calcite marbles, are consistent with their interaction with meteoric fluids during diagenesis. Post-metamorphic meteoric fluid-rock interaction is responsible for the negative $\delta^{13}C$ and low $\delta^{18}O$ values in marbles and the depleted $\delta^{18}O$ values of quartz and the development of authigenic quartz overgrowths and cements in dolomite marbles. Differences in behavior between dolomite versus calcite marbles requires dolomite marbles to have been more permeable than the essentially impermeable calcite marbles both before and after metamorphism.

Grossular calc-silicate rocks contain the diagnostic mineral assemblage grossular + wollastonite + diopside + albite + calcite + quartz, with or without K-feldspar, epidote, vesuvianite, and titanite. Hornblende calc-silicate rocks contain hornblende + epidote + K-feldspar + plagioclase + quartz and may also contain calcite, biotite, chlorite, titanite and magnetite. The stable isotopic composition of calcite and silicate minerals within calc-silicate rocks varies in relation to the modal abundance of the minerals, although calcite and silicate minerals approached oxygen isotopic equilibrium during metamorphism. The amount of volatiles lost by the rocks during metamorphism was calculated from mass balance relationships between the inferred protolith and the metamorphic rock. Grossular calc-silicate rocks lost significantly more CO_2 and slightly less H_2O than hornblende calc-silicate rocks during metamorphism. Differences between the amounts of fluid evolved by grossular and hornblende calc-silicate rocks are the result of differences in the original protolith mineralogy. Grossular calc-silicate rocks originally contained greater amounts of calcite, and hornblende calc-silicate rocks greater amounts of muscovite and chlorite. The volume of fluid evolved by the rocks during metamorphism resulted in a significant loss of the original protolith solid volume. The isotopic composition of carbon in calcite within the calc-silicate rocks can be explained by mostly fractional devolatilization processes; however, the oxygen isotope data requires infiltration of low ^{18}O fluids to cause the observed isotopic depletions. The amount of fluid that infiltrated grossular calc-silicate rocks was an order of magnitude greater than that which infiltrated hornblende calc-silicate rocks. Fluids in equilibrium with the most depleted calc-silicate rocks are probably of magmatic origin from the Lone Mountain pluton. During metamorphism, fluid flow occurred primarily through calc-silicate rocks; whereas marbles were essentially impermeable. Differences in the extent of fluid-rock interaction also occur within calc-silicate rocks, with grossular calc-silicate rocks interacting with significantly more fluid than hornblende calc-silicate rocks.

The Lone Mountain granitic pluton is dominated by granite with minor granodiorite and quartz monzonite. Temperatures of pluton emplacement based on garnet + biotite and hornblende + plagioclase geothermometry are between 650 and 750°C; whereas temperatures based on the oxygen isotopic compositions of quartz and feldspar are between 325 and 615 °C, indicating that some subsolidus re-equilibration of oxygen isotopes occurred after pluton emplacement. The pressure of pluton emplacement estimated from aluminum in hornblende geobarometry and from consideration of epidote + quartz and muscovite + quartz stability in conjunction with the H_2O-saturated granite solidus, is 3.5 kbar, consistent with estimates from the surrounding metamorphic rocks and is equivalent to a depth of 12 to 15 km. High whole-rock $\delta^{18}O$ values together with an intermediate initial $^{87}Sr/^{86}Sr$ ratio indicate that sedimentary or volcanic rocks must have provided a significant component of the source rocks for the granite. Lone Mountain granitic rocks could have been derived from rocks that currently surround the pluton, although isotopic data and phase equilibrium considerations negate the generation of the peraluminous Lone Mountain granitic pluton solely by the partial melting of pelitic schists. Limited chemical variation within the pluton from the most primitive parental magma composition, hornblende granodiorite, to the most evolved magma composition, garnet granite, can occur by fractional crystallization of hornblende and plagioclase; however, the well-developed foliation along the margin of the pluton and the lack of any systematic geochemical variation from the core to the rim of the pluton requires replenishment of the magma chamber to have occurred during multiple intrusive events associated with the emplacement of the pluton.

TABLE OF CONTENTS

LIST OF TABLES

LIST OF FIGURES

FIGURE PAGE

PART 1

INTRODUCTION

Fluids play a vital role during metamorphism by adding and subtracting matter and, in some instances, heat to rocks (e.g., Bickle and McKenzie, 1987; Brady, 1988), by initiating mineralogical reactions (e.g., Rice and Ferry, 1982), by affecting the chemical (e.g., Ferry, 1983) and stable isotopic (e.g., Valley, 1986) compositions of rocks, and by controlling the rheology of rocks during deformation associated with metamorphism (e.g., Etheridge and others, 1983). Metamorphic rocks maintain equilibrium with fluids by way of chemical reactions which proceed while changes in the intensive variables pressure, temperature, and fluid composition occur during metamorphism. These chemical reactions between fluids and rocks manifest themselves in the chemistry, abundance, and stable isotopic compositions of the minerals in a metamorphic rock. Therefore, the mineral assemblages and stable isotopic compositions of metamorphic rocks are monitors of the composition and amount of fluid that was present in the rocks during metamorphism.

During metamorphic fluid-rock interaction, rock type is an important controlling variable, as most pervasive fluid flow during metamorphism occurs in calc-silicate and pelitic rocks, whereas marbles interlayered with these rocks are essentially impermeable to fluids (e.g., Nabelek and others, 1984; Jamtveit and others, 1992). This is because marble protoliths, i.e., limestones and dolostones, undergo solid-state recrystallization during metamorphism, but do not experience any mineralogical changes under most conditions of metamorphism. In contrast, calc-silicate rocks and pelitic schists are much more useful indicators of metamorphic conditions and processes because the progressive metamorphism of marls and shales results in the formation of new minerals and changes in the stable isotopic compositions of the rocks as the conditions of metamorphism change.

Late Proterozoic to Cambrian carbonate, calc-silicate and pelitic sedimentary rocks exposed at Lone Mountain, Esmeralda County, Nevada, were regionally

metamorphosed at some time during the Mesozoic and then later contact metamorphosed as a result of the intrusion of the Late Cretaceous Lone Mountain granitic pluton. The purpose of this project is to conduct an integrated field, petrologic, and stable isotopic study of the metamorphic rocks surrounding the pluton, and the pluton itself, in order to better understand the role that rock type plays in fluid-rock interaction during metamorphism, and to determine the petrogenesis of the Lone Mountain granitic pluton.

This study is presented as three independent parts. Part two addresses fluid-rock interaction in carbonate rocks. The stable isotopic and trace element compositions of essentially pure calcite and dolomite marbles were examined in order to determine the fluid-rock interaction processes that affected them prior to, during, and after metamorphism. Part three continues the study of metamorphic fluid-rock interaction, but examines calc-silicate rocks. The amount and composition of fluid that interacted with grossular and hornblende calc-silicate rocks during metamorphism were determined by petrologic and stable isotopic mass balance relationships between the metamorphic rocks and their unmetamorphosed protoliths. Parts two and three also detail the pressure, temperature, and fluid composition conditions under which the carbonate and calc-silicate rocks were metamorphosed. In part four, the petrogenesis of the Lone Mountain pluton was examined by determining the conditions of pluton emplacement, the nature of the granitic source rocks, and the differentiation mechanisms that can account for the chemical and isotopic variations within the pluton.

PART TWO

CONTRASTING STABLE ISOTOPE AND TRACE ELEMENT BEHAVIOR BETWEEN CALCITE AND DOLOMITE MARBLES, LONE MOUNTAIN, NEVADA

ABSTRACT

Late Proterozoic to Cambrian carbonate, calc-silicate, and pelitic rocks from Lone Mountain, southwestern Nevada, were regionally metamorphosed during Mesozoic time and then contact metamorphosed during intrusion of the Lone Mountain granitic pluton in Late Cretaceous time. Essentially pure marbles consist of either calcite or dolomite with limited calcite + dolomite and minor quartz, muscovite, phlogopite, and rare albite, chlorite, rutile, pyrite, and graphite. The stable isotopic compositions of calcite marbles can be divided into two groups, one with positive $\delta^{13}C$ values from 3.1 to 1.4 ‰ (PDB) and high $\delta^{18}O$ values from 21.5 to 15.8 ‰ (SMOW), and the other with negative $\delta^{13}C$ values from –3.3 to –3.6 ‰ and low $\delta^{18}O$ values from 16.9 to 11.1 ‰. Dolomite marbles are similarly divided into two groups, one with positive $\delta^{13}C$ values from 1.5 to 0.2 ‰ and high $\delta^{18}O$ values from 20.4 to 14.5 ‰, and the other with negative $\delta^{13}C$ values from –0.7 to –2.9 ‰ and low $\delta^{18}O$ values from 17.7 to 14.6 ‰. The oxygen isotopic composition of brown- and blue-luminescent, clear, smooth-textured quartz from orange-luminescent calcite marbles has a relatively restricted range in $\delta^{18}O$ values from 23.9 to 18.1 ‰. In contrast, brown-luminescent, opaque, rough-textured quartz from red-luminescent dolomite marbles is extremely depleted in ^{18}O, with most $\delta^{18}O$ values between 2.0 and 7.6 ‰. Quartz from dolomite protomylonites and post-metamorphic authigenic quartz in dolomite marbles have $\delta^{18}O$ values similar to quartz from calcite marbles. Low Mn/Sr ratios, and high $\delta^{13}C$ and $\delta^{18}O$ values in calcite marbles suggest that they preserve their original stable isotopic compositions, resulting in a range in primary stable-isotopic compositions that were inherited from the sedimentary protolith of 2 ‰ in $\delta^{13}C$ and 4 ‰ in $\delta^{18}O$. Dolomite marbles have a negative correlation between Mn/Sr and $\delta^{18}O$, indicating that dolomite marbles do not preserve their original oxygen isotopic compositions. The trace-element compositions of dolomite marbles, loss of Sr and Na, and gain of Zn, Mn, and Fe, compared with calcite marbles, are consistent with interaction

with meteoric fluids during diagenesis. Dolomite marbles typically display bright luminescence intensity along the edges of fractures and veins suggesting fluid-rock interaction after metamorphism. Post-metamorphic meteoric fluid-rock interaction is responsible for the negative $\delta^{13}C$ and low $\delta^{18}O$ values in marbles, as well as the depleted $\delta^{18}O$ values of quartz in dolomite marbles, and the development of authigenic quartz overgrowths and cements in dolomite marbles. Differences in behavior between dolomite versus calcite marbles require that dolomite marbles were more permeable than the essentially impermeable calcite marbles.

INTRODUCTION

Interaction of fluids with rocks is a significant geologic process by which the chemical and isotopic compositions of both the fluids and the rocks can be altered. During metamorphic fluid-rock interaction, rock type is an important controlling variable, as most pervasive fluid flow during metamorphism occurs in calc-silicate and pelitic rocks, whereas marbles interlayered with these rocks are impermeable to fluid flow (e.g., Nabelek and others, 1984; Jamtveit and others, 1992). This is because pure limestone and dolostone undergo solid-state recrystallization during metamorphism, but do not experience any mineralogical changes under most conditions of metamorphism. Additionally, with the exception of the loss of volatile constituents as a result of devolatilization reactions, metamorphism of carbonate rocks is an isochemical process (e.g., Labotka and others, 1988 a). This comparatively inert response of marbles to metamorphism is in marked contrast to their earlier behavior during diagenesis, when the potential exists for the chemical and isotopic compositions of limestones and dolostones to be altered as a result of extensive recrystallization and transfer of chemical constituents during multiple fluid-rock interaction events (Land, 1980). Despite the loss of their original textural and chemical characteristics as a result of modification during diagenesis and metamorphism, detailed geochemical studies have been used to constrain the nature and extent of fluid-rock interaction

processes associated with the post-depositional alteration of ancient sedimentary carbonate rocks (e.g., Gao, 1990; Rumble and others, 1991).

Late Proterozoic to Cambrian carbonate, calc-silicate, and pelitic rocks from Lone Mountain, southwestern Nevada, were regionally metamorphosed during the Mesozoic and in Late Cretaceous time intruded by the Lone Mountain granitic pluton. In this study, the chemical and stable isotopic compositions of essentially pure calcite and dolomite marbles from the Wyman Formation, Reed Dolomite, and Deep Spring Formation at Lone Mountain were examined in order to determine the fluid-rock interaction processes that affected them prior to, during, and after metamorphism. Trace element and stable isotopic data were used to establish the pre-metamorphic stable isotopic composition of the marble precursor limestone and dolostone. Deviations from the original stable isotopic compositions were then attributed to either diagenesis, metamorphism, or post-metamorphic fluid-rock interaction.

The results of this study indicate that calcite marbles behaved very differently from dolomite marbles, both before and after metamorphism. Prior to metamorphism, the original trace element and stable isotopic compositions of dolomite marbles were affected during diagenesis (dolomitization), whereas, those of calcite marbles remained essentially unchanged. Following metamorphism, quartz and calcite from impermeable calcite marbles underwent closed-system re-equilibration of oxygen isotopes at temperatures below the metamorphic peak. Quartz and dolomite from permeable dolomite marbles, however, are no longer in oxygen isotopic equilibrium as a result of open-system post-metamorphic fluid-rock interaction that lowered the oxygen isotopic composition of quartz.

GEOLOGIC SETTING

Lone Mountain is located approximately 25 km west of Tonopah in Esmeralda County, Nevada. The area consists of Late Proterozoic to Cambrian sedimentary rocks that

underwent greenschist-facies regional metamorphism during Mesozoic time, followed by hornblende-hornfels-facies contact metamorphism during Late Cretaceous time, in association with the intrusion of the Lone Mountain granitic pluton (Figure 1).

The oldest rocks in the Lone Mountain area belong to the Precambrian Wyman Formation, which comprises interlayered calcite marble, calc-silicate hornfels, and minor pelitic schist. The contact between the Wyman Formation and the overlying Reed Dolomite appears conformable in western Nevada (Albers and Stewart, 1972; McKee and Moiola, 1962), and unconformable in eastern California (Nelson, 1962). The Reed Dolomite is a massive, brown to tan, medium- to coarse-grained dolomite marble that contains rare thin layers of phyllite, quartzite, and calcite marble. The Reed Dolomite is overlain by the Deep Spring Formation, the lower member of which comprises interbedded calcite and dolomite marble, minor phyllite, and lesser quartzite. At Lone Mountain, dolomite marble occurs near the base of the Deep Spring Formation making the contact with the Reed Dolomite gradational (Bonham and Garside, 1979).

Lone Mountain lies within the northern part of the Goldfield section of the Walker Lane belt, an area of structural complexity that separates the Sierra Nevada batholith to the west, from the Basin and Range province to the east (Stewart, 1988). Three main structural trends are recognized in the Lone Mountain area based on the orientations of dikes, joints, and faults (Maldonado, 1984): 1) northwest, 2) northeast, and 3) east. The major structural trend in the area is northwest, paralleling the orientation of the Walker Lane belt, the extension direction of the Lone Mountain pluton, and the dominant orientation direction of Tertiary lamprophyre dikes, which intrude both the Lone Mountain pluton and the surrounding metasedimentary rocks.

To the northeast of Lone Mountain, a northwest trending low-angle detachment fault has removed approximately 1,500 m from the stratigraphic sequence (Bonham and Garside, 1979). This fault has essentially the same upper plate and lower plate

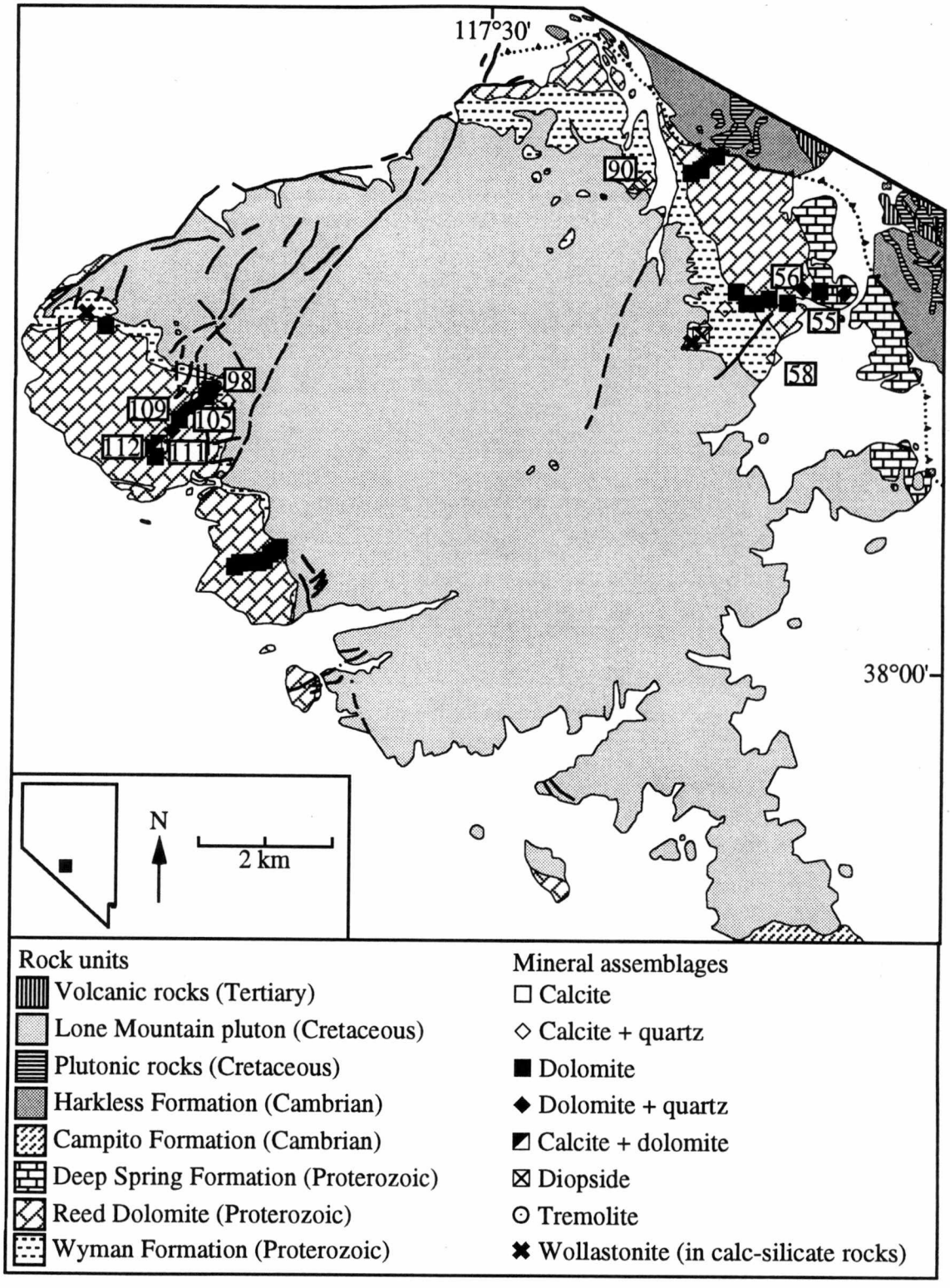

Figure 1: Geologic map of the Lone Mountain area (modified after Maldonado, 1984, and Bonham and Garside, 1979). Numbered sample locations are referred to either in figures or in the text.

stratigraphic relationships as low-angle detachment faults to the south of Lone Mountain in the Weepah Hills and at Mineral Ridge. As the Weepah detachment fault probably represents a continuation of the Mineral Ridge detachment fault (Stewart and Diamond, 1990) and the Weepah and Lone Mountain plutons are connected at shallow depth, (Albers and Stewart, 1972) the fault at Lone Mountain is presumed to be part of the Mineral Ridge-Weepah detachment fault system. Extension on these detachment faults began prior to 13 million years and probably continued up until about 6 million years before present (Stewart and Diamond, 1990).

The post-Miocene structural evolution of the Lone Mountain area includes still continuing extension on northeast trending high-angle normal faults along the northeast margin of the Lone Mountain pluton (Yount and others, 1993), which may be related to regional east-trending strike-slip faults to the north of Lone Mountain (Ekren and others, 1976; Stewart, 1985).

PETROLOGY

Three distinct lithologies are recognized within marbles based on carbonate mineralogy: 1) calcite marble, 2) dolomite marble, and 3) calcite-dolomite marble. Within the Wyman Formation only calcite marble occurs at Lone Mountain, however, dolostone and dolomite marble occur within the Wyman Formation elsewhere in Esmeralda County (McKee and Moiola, 1962), and in the White-Inyo Mountains in eastern California (Nelson, 1962). Staining of thin sections with alizarin red-S revealed either none, or less than two percent calcite in all dolomite marbles, and vice versa, such that significant amounts of coexisting calcite and dolomite were only recognized at two locations within calcite-dolomite marbles of the Reed Dolomite.

With few exceptions, marbles are essentially pure, consisting of greater than ninety-five percent carbonate, with minor quartz, muscovite, and phlogopite, and with albite, chlorite, rutile, pyrite, and graphite present in very limited abundance. With

increasing proximity to the pluton, minor amounts of tremolite and diopside + K-feldspar occur in dolomite and calcite marbles, respectively. Calcite and dolomite themselves are also close to pure, although minor amounts of impurities occur in both minerals (Table 1). Calcite in calcite marbles typically has less than 0.02 atoms per formula unit of Mg, whereas calcite in calcite-dolomite marbles is more magnesian, with up to 0.15 atoms per formula unit of Mg. Calcite in both calcite and calcite-dolomite marbles also contains greater amounts of Fe (between 200 and 500 ppm) than Mn (between100 and 400 ppm). Dolomite is close to stoichiometric, with Ca/Mg in the range 1.03 to 0.99. Like calcite, dolomite also has greater amounts of Fe (500 to 1,500 ppm) than Mn (100 to 500 ppm). The Mn and Fe contents of carbonate minerals from Lone Mountain suggest that they will be dully luminescent (Machel, and others, 1991), although both orange luminescent calcite and red luminescent dolomite typically display differing luminescent intensities. Bright luminescence commonly occurs along grain boundaries within calcite marbles and along the edges of fractures and veins in dolomite marbles, although dull or non luminescent areas also occur along fractures in dolomite marbles. The interior of calcite and dolomite grains have a uniform less intense luminescence than grain or fracture boundaries.

Marbles have a granoblastic texture in which approximately equidimensional carbonate grains have straight edges that commonly form triple junctions. Calcite marbles are coarse-grained (1 to 2 mm) and contain rare rounded quartz grains (0.2 mm) at triple junctions and along grain boundaries (Figure 2a). Dolomite marbles are finer grained than calcite marbles (0.5 to 0.2 mm) and contain smaller (0.1 mm) anhedral quartz grains (Figure 2b). In contrast to the granoblastic texture of marbles, calcite and dolomite protomylonites from within fault zones have large (1 to 0.5 mm), commonly rounded, and twinned porphyroclasts that occur within a matrix of small (100 to 25 μm), rounded, and untwinned carbonate grains that have irregular grain boundaries (Figure 2c). Calcite and dolomite protomylonites display uniformly dull cathodoluminescence intensity. Dolomite

Table 1: Representative electron microprobe analyses of calcite and dolomite from calcite marble, calcite-dolomite marble and dolomite marble

Sample	LM48	LM55-2	LM58-2	LM75-2	LM90	LM97-2	LM105-4	LM111-2	LM112
Rock type	CM	CM	CM	CM	CM	CM	CM	CDM	CDM
Mineral	C	C	C	C	C	C	C	C	C
FeO	0.14	0.09	0.14	<0.06	0.30	0.11	0.20	0.06	<0.06
MnO	<0.05	<0.05	<0.05	<0.05	0.06	<0.05	<0.05	<0.05	<0.05
MgO	<0.02	0.09	0.43	0.15	0.11	1.15	0.67	1.22	0.98
CaO	54.6	54.9	55.6	54.5	54.1	54.4	54.0	54.4	54.5
Total	54.71	55.05	56.22	54.61	54.59	55.60	54.90	55.68	55.48
Cations based on					1 oxygen				
Fe	0.002	0.001	0.002	0.000	0.004	0.002	0.003	0.001	0.000
Mn	0.000	0.000	0.000	0.000	0.001	0.000	0.000	0.000	0.000
Mg	0.000	0.002	0.011	0.004	0.003	0.028	0.017	0.030	0.024
Ca	0.998	0.996	0.987	0.996	0.992	0.970	0.980	0.969	0.975
Total	1.000	0.999	1.000	1.000	1.000	1.000	1.000	1.000	1.000

Sample	LM85	LM105-5	LM107	LM111-2	LM112	LM117	LM121
Rock type	DM	DM	DM	CDM	CDM	DM	DM
Mineral	D	D	D	D	D	D	D
FeO	0.24	0.34	0.28	0.21	0.21	0.23	0.21
MnO	<0.05	<0.05	<0.05	<0.05	<0.05	<0.05	<0.05
MgO	21.6	21.6	21.8	21.5	21.6	21.8	21.9
CaO	30.8	29.9	31.1	30.4	30.5	31.2	31.1
Total	52.67	51.92	53.17	52.12	52.37	53.21	53.25
Cations based on				2 oxygens			
Fe	0.007	0.009	0.007	0.006	0.005	0.006	0.005
Mn	0.001	0.001	0.001	0.001	0.001	0.001	0.001
Mg	0.985	0.998	0.983	0.989	0.988	0.983	0.987
Ca	1.008	0.992	1.009	1.005	1.006	1.011	1.007
Total	2.000	2.000	2.000	2.000	2.000	2.000	2.000

Note: Rock type: CM = calcite marble, DM = dolomite marble, CDM = calcite-dolomite marble. Mineral: C = calcite, D = dolomite.

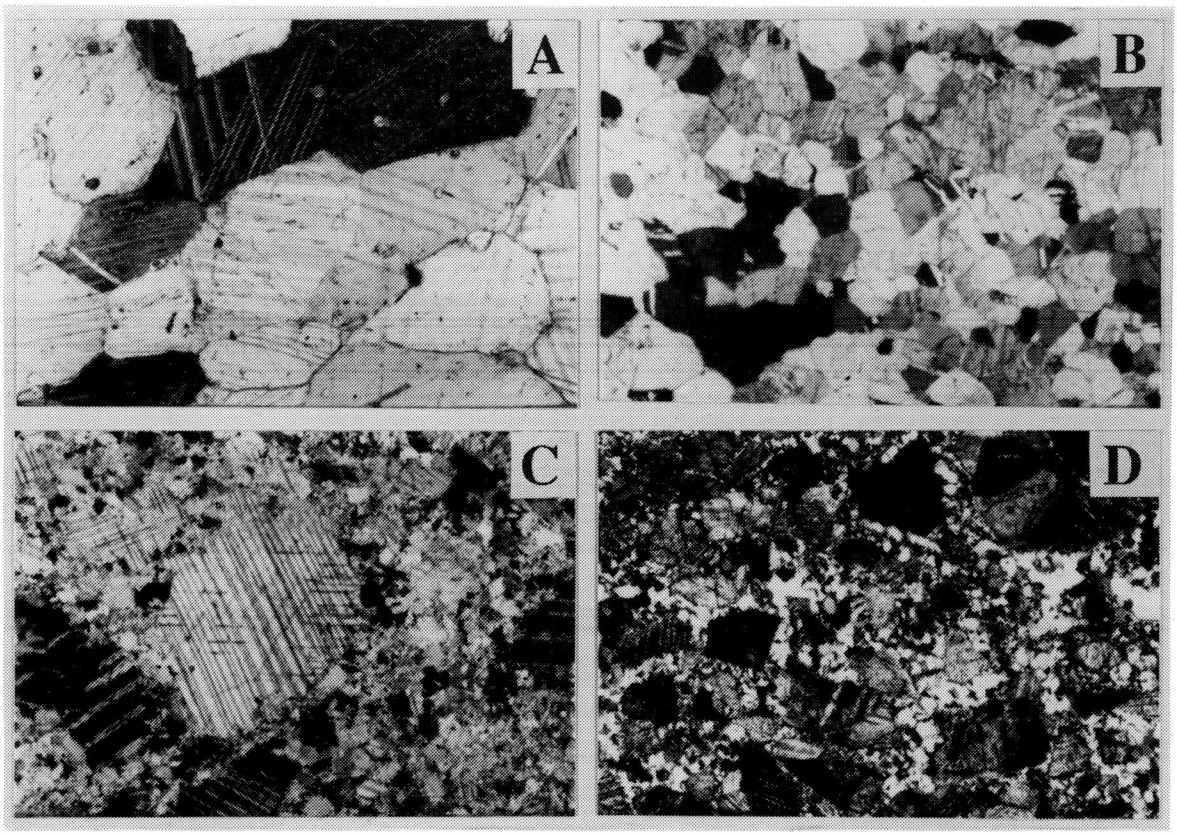

Figure 2: Photomicrographs of calcite and dolomite marbles. a) Granoblastic texture in calcite marble (LM90). b) Granoblastic texture in dolomite marble (LM109). Note that calcite marbles are coarser grained than dolomite marbles. c) Protomylonitic texture in dolomite marble (LM105-1). d) Quartz veins and quartz cements in dolomite marble (LM56). The long dimension of the field of view for each photomicrograph is 5.3 mm, and all photomicrographs were taken under cross-polarized light.

marbles also occasionally contain extensive quartz veins and microcrystalline quartz cements that fill fractures and voids, and enclose isolated dolomite grains (Figure 2d). Muscovite and phlogopite typically occur as isolated plates in both calcite and dolomite marbles, and are non-luminescent.

Observation of quartz under the binocular microscope reveals that quartz from dolomite marbles is typically opaque, whereas quartz from calcite marbles is almost always clear. Some quartz from Reed Dolomite marbles is also opaque or partially opaque such that within the Reed Dolomite, there is a gradation between opaque and clear quartz varieties. Both clear and opaque quartz from dolomite and calcite marbles have brown cathodoluminescence, with blue luminescent quartz also occasionally present in calcite marbles. Brown luminescent quartz is indicative of medium-grade metamorphic rocks, and blue luminescent quartz is indicative of high-grade metamorphic rocks (Sprunt and others, 1978; Zinkernagel, 1978), although these relationships are not always consistent, as brown luminescence occurs in many different types of quartz, and is thought to be related to lattice defects (Ramseyer and others, 1988). As a result of their widely differing environments and conditions of formation, the quartz veins and cements in dolomite marbles show a wide variety of luminescence colors, from brown, blue, and violet, to non-luminescent.

Using cathodoluminescence, it is difficult to determine differences between quartz from calcite or dolomite marbles, because they both have brown luminescence. However, further examination of quartz using the scanning electron microscope does reveal differences between quartz from calcite versus dolomite marbles. Recrystallization of quartz during metamorphism should result in the loss of any surface morphological features that are inherited from the sedimentary environment. Quartz grains from calcite and dolomite marbles have similar shapes (Figure 3a,b), but greatly differing surface features. Clear quartz grains from calcite marbles have a smooth textured surface (Figure

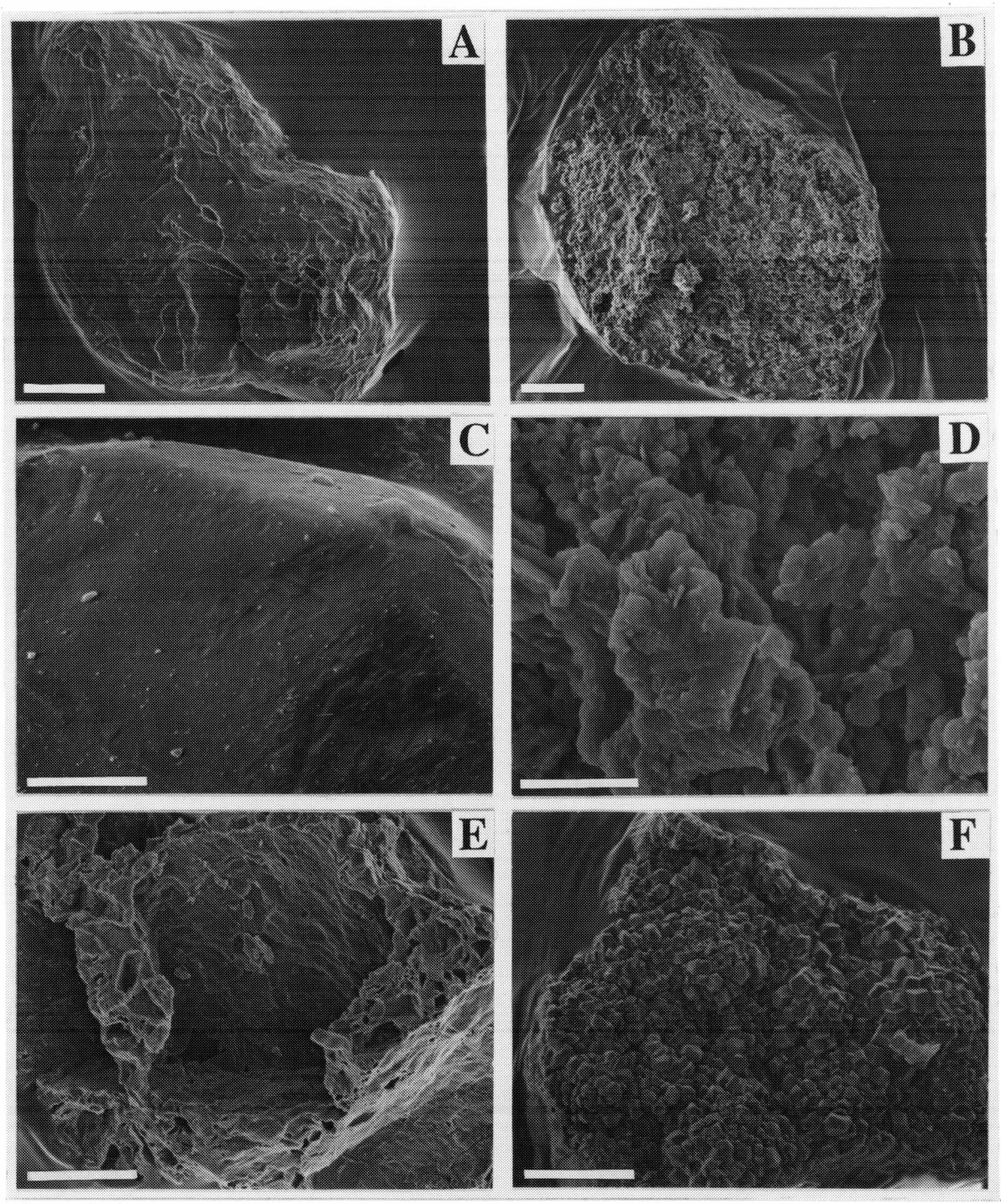

Figure 3: Scanning electron microscope photographs of quartz from calcite and dolomite marbles. a, c) Quartz from calcite marble (LM90). b, d) Quartz from dolomite marble (LM98-3). e) Post-metamorphic authigenic quartz overgrowths from dolomite marble (LM56). f) Post-metamorphic authigenic quartz cement from dolomite marble (LM56). Scale bar in a, b, e, and f is 100 μm, scale bar in c and d is 10 μm.

3c) compared with opaque quartz grains from dolomite marbles which have a rough and uneven surface (Figure 3d), that is indicative of chemical dissolution (Krinsley and Doornkamp, 1973). As well as quartz cements (Figure 3e), post-metamorphic authigenic quartz overgrowths also occur in dolomite marbles and are recognized by well-developed rhombohedral and bipyramidal terminations (Figure 3f).

CONDITIONS OF METAMORPHISM

The temperature of metamorphism estimated from calcite-dolomite cation thermometry (Anovitz and Essene, 1987) records peak metamorphic temperatures of 520 $\pm$ 50°C. More commonly, re-equilibration of calcite to lower temperatures has occurred, with temperatures more typically between 425 and 370 °C. Calcite-dolomite oxygen isotope thermometry (Sheppard and Schwarcz, 1970) also records retrograde re-equilibration, giving temperatures between 370 and 320°C.

The pre-Tertiary stratigraphic sequence in the area is approximately 10 to 12 km thick (Albers and Stewart, 1972, Bonham and Garside, 1979), indicating that the pressure at the time of intrusion of the Lone Mountain pluton was 3 to 3.5 kbar. This is corroborated by the presence of andalusite within pelitic schists of the Wyman Formation which indicates that the pressure was less than 3.8 kbar (Holdaway and Mukhopadhyay, 1993). Pressure estimates from Al in hornblende barometry using the experimental calibration of Johnson and Rutherford (1989) give pressures of between 3.0 and 4.2 kbar for the Lone Mountain granite. Accordingly, the assumed pressure of metamorphism at Lone Mountain is 3.5 $\pm$ 1 kbar.

Phlogopite is not part of the original mineral assemblage in unmetamorphosed carbonate rocks, but is inferred to occur in incipiently metamorphosed rocks as a result of the reaction:

3 dolomite + K-feldspar + H_2O = phlogopite + 3 calcite + 3 CO_2

The appearance of diopside + K-feldspar, and the disappearance of phlogopite, in calcite marbles is inferred to occur a result of the reaction:

3 calcite + phlogopite + 6 quartz = 3 diopside + K-feldspar + H_2O + 3 CO_2

and the appearance of tremolite in dolomite marbles is inferred to occur as a result of the reaction:

5 dolomite + 8 quartz + H_2O = tremolite + 3 calcite + 7 CO_2.

The observed mineral assemblages in calcite and dolomite marbles limit the composition of the fluid that was present during metamorphism (Figure 4). Fluids in equilibrium with calcite marbles (calcite + quartz + phlogopite) at 520°C have X_{CO_2} values that cannot have been less than 0.3, whereas fluids in equilibrium with dolomite marbles (dolomite + quartz + phlogopite) have X_{CO_2} values greater than 0.5 at 520°C.

WHOLE-ROCK CHEMISTRY

Whole-rock major-oxide and trace-element chemical compositions of marbles are given in Table 2. All calcite marbles are mostly CaO and CO_2, and all dolomite marbles are mostly CaO, MgO, and CO_2. Both calcite and dolomite marbles also typically have minor amounts, up to 3%, of SiO_2, although two samples (LM55-2 and LM56) contain 7.9% SiO_2 and one sample (LM58-2) contains 14.5% SiO_2. All other major oxides are usually present in amounts less than 1%.

Calcite marbles from the Wyman Formation have between 965 and 3,420 ppm Sr, whereas calcite marbles from the Reed Dolomite and Deep Spring Formation only contain between 240 and 490 ppm Sr. Dolomite marbles have less Sr than calcite marbles, consisting of up to 210 ppm Sr. Calcite marbles from the Wyman Formation and Reed Dolomite only have up to 170 ppm Mn, while calcite marbles from the Deep Spring Formation contain between 25 and 775 ppm Mn. Dolomite marbles possess greater amounts of Mn than calcite marbles, with up to 1,865 ppm Mn. Dolomite marbles also exhibit greater Fe and Zn concentrations, up to 7,175 ppm and 95 ppm, respectively, than

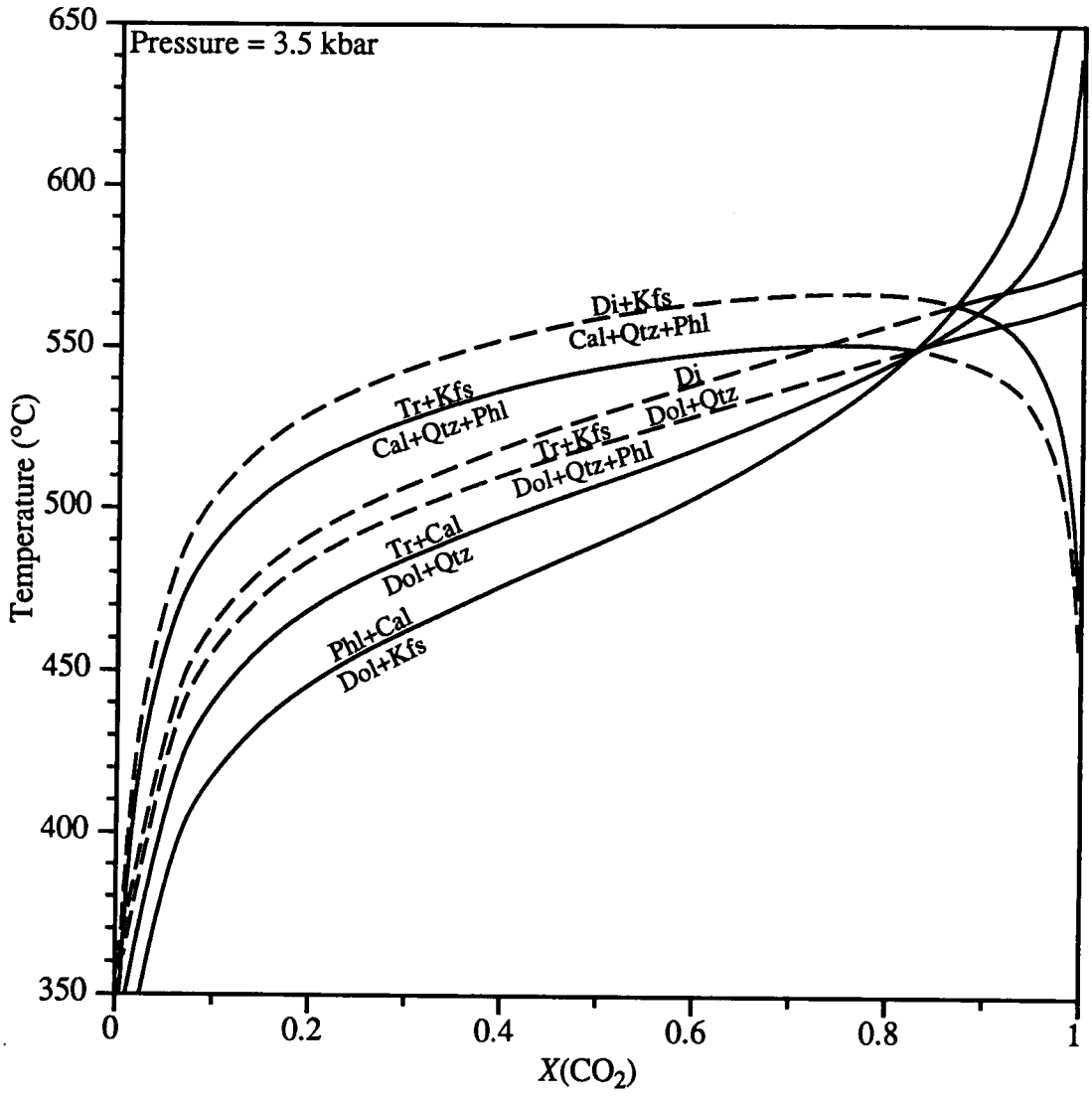

Figure 4: Isobaric T–X_{CO_2} diagram for the mineral assemblages in calcite, calcite-dolomite and dolomite marbles. The diagram was constructed at a pressure of 3.5 kbars using the computer program Vertex (Connolly, 1990), and the thermodynamic data of Holland and Powell (1991).

Table 2: Whole-rock X-ray fluorescence analyses of calcite marble, calcite-dolomite marble and dolomite marble

Sample	LM4	LM13	LM48	LM49	LM50-1	LM51	LM52	LM54	LM55-1	LM55-2	LM55-3	LM56	LM57
Rock type	DM	DM	CM	DM	DM	DM	DM	CM	CM	CM	DM	DM	DM
Formation	R	R	W	R	R	R	DS	DS	DS	DS	DS	R	R
SiO_2	0.34	0.15	1.50	0.26	0.29	0.24	3.10	3.91	0.62	7.95	1.21	7.94	0.10
TiO_2	0.01	0.01	0.03	0.01	0.03	0.01	0.02	0.06	0.01	0.13	0.01		
Al_2O_3	0.09	0.03	0.12	0.07	0.18	0.22		2.33	0.01	1.19			0.09
Fe_2O_3	0.61	1.03	0.14	0.51	0.51	0.54	0.33	0.38	0.05	2.33	1.11	0.39	0.39
MgO	21.1	21.1	0.77	21.1	21.3	21.4	20.7	1.66	1.16	0.34	20.5	20.47	21.3
CaO	30.7	30.5	55.4	31.2	31.1	31.1	30.3	50.6	55.1	45.4	29.9	28.91	31.1
Na_2O			0.02		0.01	0.02		0.05	0.02	0.10			
K_2O								0.39		0.20			
P_2O_5	0.03	0.02	0.02	0.02	0.02	0.02		0.09	0.03	0.11			0.02
CO_2	45.5	45.1	42.3	47.3	45.1	46.6	45.5	38.5	40.6	39.9	42.6	39.07	45.1
Total	98.38	97.94	100.33	100.51	98.48	100.11	99.90	97.96	97.50	97.62	95.38	96.77	98.18
S			606					480	545	288			
Mn	956	1490		867	771	1182	345	255	23	776	1268	697	432
Zn	78	85	21	80	87	86	81	34	18	16	86	83	91
Rb			22				106			14	54		3
Sr	102	96	2532	107	86	134	93	311	242	491	176	106	90

Table 2: (continued)

Sample	LM58-1	LM58-2	LM58-3	LM67-1	LM74-2	LM75-2	LM82	LM83	LM84	LM85	LM89-2	LM90	LM91
Rock type	CM	CM	CM	CM	DM	CM	DM	DM	DM	DM	CM	CM	CM
Formation	W	W	W	W	R	W	R	R	R	R	W	W	W
SiO_2	2.18	14.5	0.77	1.90	0.23	0.78	0.17	1.47	0.34	0.55	1.49	2.15	1.73
TiO_2	0.03	0.02	0.01	0.03	0.01	0.01			0.01	0.01	0.03	0.03	0.04
Al_2O_3	0.36		0.16	0.28	0.21		0.04				0.07	0.37	0.01
Fe_2O_3	0.30	0.50	0.16	0.64	0.49	0.03	0.39	0.63	0.42	0.49	0.10	0.43	0.19
MgO	1.17		1.33	0.87	21.3	0.62	21.4	21.3	21.6	22.4	0.66	1.28	0.70
CaO	53.6	45.2	55.4	53.6	31.0	55.7	31.0	30.8	30.9	30.4	55.3	53.5	54.8
Na_2O	0.02	0.02	0.02	0.03		0.01					0.02	0.02	0.02
K_2O	0.05	0.08	0.02	0.06	0.01							0.07	
P_2O_5	0.04		0.02	0.04	0.02	0.01	0.02		0.01	0.02	0.01	0.03	
CO_2	42.3	37.3	40.6	43.1	44.9	42.6	43.5	46.0	47.3	43.4	42.3	41.9	41.2
Total	100.00	97.61	98.49	100.63	98.15	99.75	96.53	100.27	100.59	97.25	99.98	99.82	98.71
S	567	184	716	573		613					619	589	591
Mn	117	170	44	111	1227		731	1142	711	1866		33	17
Zn	19	24	32	23	94	18	81	85	87	73	19	24	21
Rb	25	29		22		18				126	26	19	20
Sr	2183	1674	1397	2710	109	964	126	175	109	81	2516	2478	3420

Table 2: (continued)

Sample	LM95-2	LM97-2	LM98-3	LM103	LM104-2	LM105-1	LM105-2	LM105-3	LM105-4	LM105-5	LM106	LM107	LM108
Rock type	CM	CM	DM	DM	DM	DM	DM	DM	CM	DM	DM	DM	DM
Formation	W	W	R	R	R	R	R	R	R	R	R	R	R
SiO_2	1.53	1.73	0.24	0.24	0.57	0.67	0.37	1.08	0.88	0.37	0.24	0.28	1.43
TiO_2	0.01	0.03	0.01	0.01	0.02	0.03	0.02	0.01	0.02				0.02
Al_2O_3	0.01	0.81		0.14	0.38	0.41	0.21	0.25	0.20	0.08	0.14	0.04	0.45
Fe_2O_3	0.14	0.18	0.76	0.78	0.51	0.73	0.55	0.40	0.10	0.40	0.24	0.54	0.64
MgO	0.86	2.18	21.3	21.7	21.9	20.0	21.5	20.7	3.56	20.5	21.7	21.5	21.2
CaO	54.8	53.4	30.6	31.0	30.3	31.6	30.9	31.1	52.7	31.0	30.9	30.9	30.3
Na_2O	0.02	0.02			0.01	0.01	0.01		0.02				0.07
K_2O		0.18			0.09			0.02	0.03		0.01		
P_2O_5	0.01	0.05	0.02	0.02	0.04	0.05	0.02	0.03	0.03	0.03	0.03	0.03	0.03
CO_2	41.1	43.0	46.1	46.1	45.7	46.0	43.6	47.7	40.9	48.5	45.8	45.1	46.0
Total	98.46	101.58	99.00	99.92	99.54	99.50	97.22	101.32	98.45	100.91	99.09	98.26	100.10
S	543	527							553				
Mn	6	14	1813	860	412	615	665	514	56	548	329	560	523
Zn	19	21	73	85	73	87	91	72	25	79	75	76	89
Rb	21	22	47		28			27	18	51		88	
Sr	2196	1429	132	107	147	135	110	96	188	81	84	93	153

Table 2: (continued)

Sample	LM109	LM110	LM111-1	LM111-2	LM112	LM113-1	LM113-2	LM115-2	LM116	LM117	LM118	LM119	LM120
Rock type	DM	CM	DM	CDM	CDM	DM	CM	DM	DM	DM	DM	DM	DM
Formation	R	R	R	R	R	R	R	R	R	R	R	R	R
SiO_2	0.81	2.12	0.36	0.65	0.57	0.25	0.76	0.14	0.22	0.49	0.11	0.11	0.26
TiO_2		0.04	0.03	0.01	0.01		0.01		0.01	0.01	0.01	0.01	
Al_2O_3		0.53	0.13	0.02	0.11			0.01	0.15	0.48	0.08	0.09	0.04
Fe_2O_3	0.43	0.18	0.70	0.25	0.24	0.64	0.15	0.63	0.42	0.39	0.36	0.46	0.36
MgO	21.4	2.40	21.6	11.3	16.5	20.7	1.75	21.2	21.6	21.4	21.5	21.9	21.1
CaO	30.6	52.5	30.6	42.3	37.1	30.8	54.0	30.7	31.1	30.7	31.2	31.2	31.0
Na_2O		0.02		0.01	0.01		0.01		0.01				
K_2O		0.10		0.01	0.01					0.09			
P_2O_5	0.01	0.05	0.04	0.01	0.02	0.02	0.02	0.02	0.02	0.05	0.02	0.01	0.03
CO_2	45.3	40.3	44.7	42.7	45.2	45.1	42.4	44.8	42.9	43.9	45.6	45.8	45.5
Total	98.58	98.20	98.12	97.28	99.77	97.52	99.01	97.48	96.42	97.50	98.92	99.55	98.24
S		471		168	80		550						
Mn	408		802	172	191	1079	156	1317	617	1020	398	628	419
Zn	71	25	80	41	54	75	24	87	92	76	89	83	75
Rb	7	15		18	26		106		19	64			3
Sr	212	317	151	118	107	126	289	90	99	88	77	107	82

Table 2: (continued)

Sample	LM121	LM122
Rock type	DM	DM
Formation	R	R
SiO_2	0.32	0.17
TiO_2	0.01	0.01
Al_2O_3	0.25	0.02
Fe_2O_3	0.29	0.71
MgO	21.8	21.0
CaO	30.7	30.5
Na_2O		
K_2O	0.02	
P_2O_5	0.04	0.01
CO_2	44.9	45.9
Total	98.32	98.33
S		
Mn	310	1339
Zn	75	92
Rb	3	
Sr	98	107

Note: Rock type: CM = calcite marble, CDM = calcite-dolomite marble, DM = dolomite marble. Formation: W = Wyman Formation, R = Reed Dolomite, DS = Deep Spring Formation. All oxides given in weight percent, all elements given in parts per million, blank = below detection limit.

calcite marbles, whereas calcite marbles have greater Na concentrations, up to 715 ppm, than dolomite marbles.

STABLE ISOTOPE GEOCHEMISTRY

The carbon and oxygen isotopic compositions of calcite and dolomite, and oxygen isotopic compositions of quartz, muscovite, and phlogopite are given in Table 3. The carbon and oxygen isotopic compositions of calcite and dolomite from marbles are dependent on stratigraphic position as well as on carbonate mineralogy (Figure 5). Wyman Formation calcite marbles have positive $\delta^{13}C$ values from 3.1 to 1.4 ‰ and high $\delta^{18}O$ values from 21.5 to 15.1 ‰. Reed Dolomite and Deep Spring Formation calcite marbles, and Reed Dolomite calcite-dolomite marbles display negative $\delta^{13}C$ values from –2.5 to –3.6 ‰, and low $\delta^{18}O$ values from 16.9 to 11.1 ‰. Reed Dolomite dolomite marbles occur in two distinct populations, one with positive $\delta^{13}C$ values from 1.5 to 0.2 ‰ and $\delta^{18}O$ values from 20.1 to 15.0 ‰ and the other with negative $\delta^{13}C$ values from –0.7 to –2.9 ‰ and $\delta^{18}O$ values from 17.7 to 13.0 ‰. In calcite-dolomite marbles, coexisting calcite and dolomite preserve the expected isotopic fractionations, with dolomite enriched in both carbon and oxygen relative to calcite.

The oxygen isotopic composition of quartz from calcite marbles has a distinct range in $\delta^{18}O$ values from 23.9 to 18.1 ‰. In contrast, quartz from dolomite marbles is extremely variable in composition. Most $\delta^{18}O$ values of quartz from Reed Dolomite dolomite marbles are between 2.0 and 7.6 ‰, and quartz from dolomite protomylonites, and post-metamorphic authigenic quartz from dolomite marbles, have similar $\delta^{18}O$ values to quartz from calcite marbles. Where possible, opaque quartz and clear quartz from Reed Dolomite marbles were hand picked separately, and opaque quartz is always more depleted in ^{18}O than clear quartz (Table 3).

Muscovite $\delta^{18}O$ values vary between 10.4 and 14.9 ‰ and average 13.3 ‰, whereas phlogopite $\delta^{18}O$ values span a very similar range from 10.3 to 14.4 ‰ and

Table 3: Stable isotope analyses of calcite marble, calcite-dolomite marble and dolomite marble

Sample	$\delta^{13}C$ calcite	$\delta^{18}O$ calcite	$\delta^{13}C$ dolomite	$\delta^{18}O$ dolomite	$\delta^{18}O$ quartz	$\delta^{18}O$ phlogopite	$\delta^{18}O$ muscovite
			Wyman Formation				
LM48	2.4	20.8			23.2		
LM58-1	2.0	16.6			19.7		
LM58-2	2.0	15.8			18.4		
LM58-3	2.0	18.0					
LM67-1	2.6	18.1			21.1		
LM75-2	2.4	21.5					
LM89-2	1.7	19.8			22.9		
LM90	3.0	18.5			19.1		
LM91	3.1	18.8			21.8		
LM95-2	2.9	20.9			23.9		
LM97-2	1.4	20.4					
			Reed Dolomite				
LM4			0.9	15.0			
LM13			1.0	17.3			
LM49			1.3	15.1			
LM50-1			1.0	15.7			
LM51			1.2	17.3			
LM56			0.6	16.2	17.9		
LM57			1.1	18.4			
LM74-2			1.0	15.0			
LM82			1.2	17.5			
LM83			0.7	16.5	6.1		
LM84			1.4	17.3			
LM85			1.1	14.5			10.4
LM98-3			0.5	15.0	7.6		
LM103			1.1	16.8			
LM104-2			0.6	17.5		12.1	
LM105-1			–2.8	16.7			
LM105-2			–2.2	16.7			
LM105-3			–2.9	17.2		13.5	14.9
LM105-4	–3.6	16.6				12.9	13.8
LM105-5			–2.9	17.7	19.8	11.4	
LM106			1.0	20.4			14.9
LM107			0.5	17.1	2.0	10.7	
LM108			0.2	17.7			
LM109			0.3	17.2	3.8		
LM110	–3.4	16.9			19.7[c] 18.1[o]		
LM111-1			–2.9	15.1			
LM111-2	–3.0	12.1	–2.7	13.0	6.4		
LM112	–2.8	13.6	–2.5	14.3		11.6	
LM113-1			–2.8	15.2	11.4[c] 3.1[o]		
LM113-2	–3.3	15.8			18.1		

Table 3: (continued)

Sample	$\delta^{13}C$ calcite	$\delta^{18}O$ calcite	$\delta^{13}C$ dolomite	$\delta^{18}O$ dolomite	$\delta^{18}O$ quartz	$\delta^{18}O$ phlogopite	$\delta^{18}O$ muscovite
			Reed Dolomite				
LM115-2			1.2	17.3			
LM116			1.1	16.4			
LM117			1.4	18.5			12.7
LM118			1.3	18.8			
LM119			0.9	16.4			
LM120			1.2	18.7		14.4	
LM121			1.5	20.1		10.3	
LM122			–0.7	14.6			
			Deep Spring Formation				
LM52			–2.5	16.8	9.3		
LM54	–3.6	11.1					
LM55-1	–3.6	16.9					
LM55-2	–3.5	12.4					
LM55-3			–1.7	13.8			

Note: $\delta^{18}O$ quartz c = "clear" quartz, $\delta^{18}O$ quartz o = "opaque" quartz.

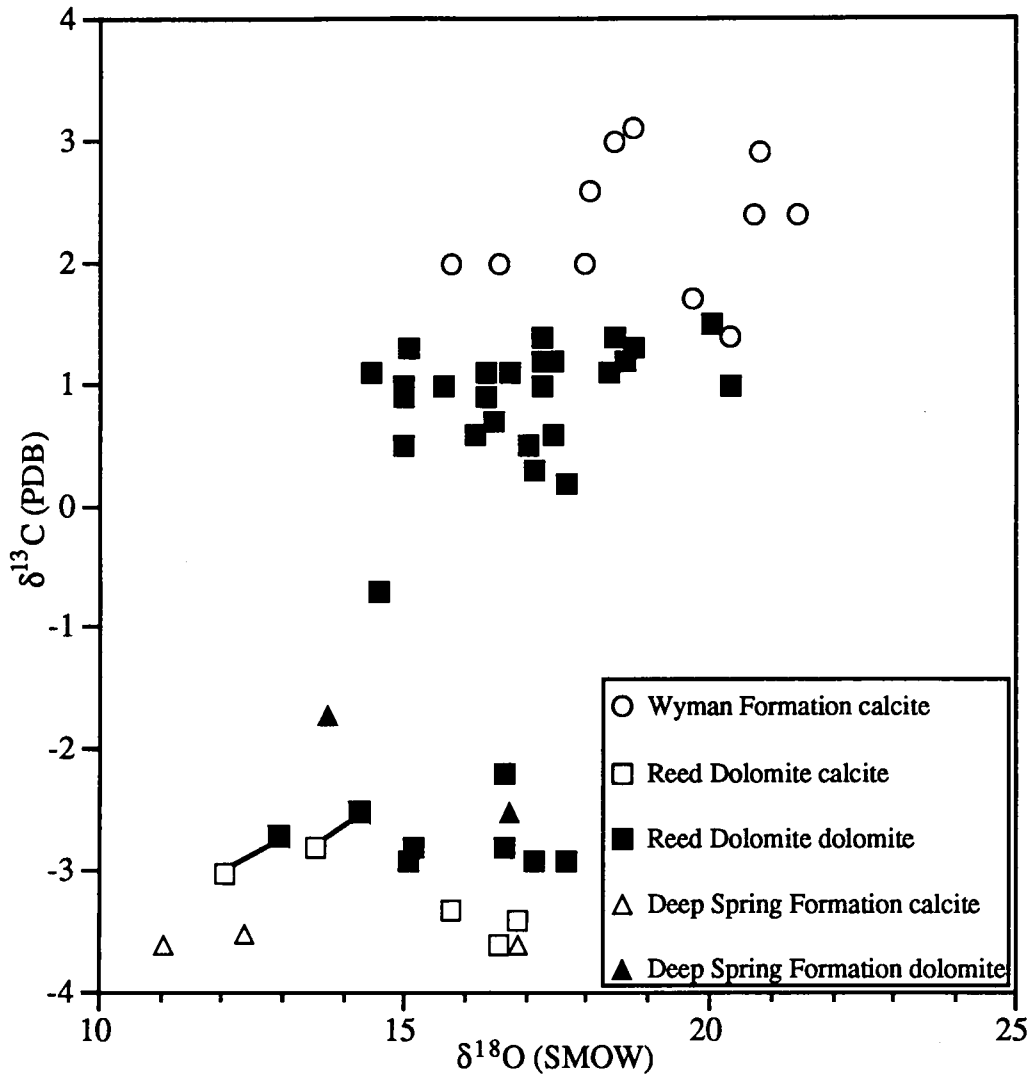

Figure 5: $\delta^{18}O$ versus $\delta^{13}C$ diagram for calcite, calcite-dolomite and dolomite marbles. Tie lines join coexisting calcite and dolomite from the same calcite-dolomite marble sample.

average 12.1 ‰. Coexisting muscovite and phlogopite from calcite and dolomite protomylonites have the expected ^{18}O fractionations, with muscovite richer in ^{18}O than phlogopite.

TRACE ELEMENTS AND CARBONATE STABLE ISOTOPES

The high Sr contents of Wyman Formation calcite marbles indicates that aragonite was present in the original mineralogy (Kinsman, 1969). Although Sr can be lost during the aragonite to calcite transition (Katz and others, 1972), any original differences in Sr content between carbonates are probably preserved during diagenesis (Brand and Veizer, 1980). The typically lower Sr contents of Reed Dolomite and Deep Spring Formation calcite marbles therefore requires either a different diagenetic history or a different precursor mineralogy for Reed Dolomite and Deep Spring Formation calcite marbles than that of Wyman Formation calcite marbles.

Dolomite marbles from Lone Mountain have Sr contents that are similar to other Precambrian and Cambrian dolostones and dolomite marbles (Weber, 1964), however, these values are lower than modern marine dolomites (Land, 1980; Veizer, 1983). Low Sr contents in carbonates can be explained by the loss of Sr during dolomitization (Katz and Matthews, 1977) or diagenesis associated with meteoric fluids (Brand and Veizer, 1980). The interpretation of the Na contents of carbonates is potentially contentious, because Na can occur as NaCl in fluid inclusions, as well as within the carbonate crystal lattice (Land and Hoops, 1973), its distribution coefficient is not well known (Land, 1980; Veizer, 1983), and it may be mobile during metamorphism (Ferry, 1983). Notwithstanding this, the Na data are consistent with the other trace element data from Lone Mountain carbonates. The decrease in Sr and Na, and increase in Mn, Fe, and Zn, in dolomite marbles compared to calcite marbles indicates that dolomitization was associated with meteoric fluids (Brand and Veizer, 1980).

The oxygen isotope compositions of calcite and dolomite marbles from Lone Mountain are similar to, but somewhat lower than the $\delta^{18}O$ compositions of unmetamorphosed Late Proterozoic to Cambrian limestones and dolostones. Late Proterozoic to Cambrian limestones have primary $\delta^{18}O$ values between 18 and 25 ‰ (Veizer and Hoefs, 1976), and Late Proterozoic to Cambrian dolostones have primary $\delta^{18}O$ values between 23 and 28 ‰ (Veizer and Hoefs, 1976). Lone Mountain $\delta^{13}C$ values are within the range of other Late Proterozoic to Cambrian carbonates which are typically between 3 and –3 ‰ (Veizer and Hoefs, 1976), although the primary carbon isotopic composition of Late Proterozoic to Cambrian carbonates may be extremely variable, ranging from 12 to –6 ‰ (e.g., Knoll and others, 1986; Lambert and others, 1987; Magaritz and others, 1991; Derry, and others, 1992; Brasier and others, 1993; Wickham and Peters, 1993).

As Lone Mountain marbles have greater than ninety-five percent carbonate, and only rocks with the low-grade mineral assemblage carbonate + quartz + muscovite + phlogopite + rutile have been considered in this study, no changes in stable isotopic composition could have occurred as a result of metamorphic devolatilization reactions. In order to determine whether the ^{18}O depletion of the marbles was caused by a low ^{18}O sedimentary protolith, by diagenetic or regional metamorphic processes, or by post-metamorphic exchange with low ^{18}O meteoric fluids, it is necessary to know the primary sedimentary stable isotopic compositions of the marble precursor limestones and dolostones, and then assess any depletions to later processes. Unfortunately, oxygen isotopic compositions of other Wyman Formation, Reed Dolomite, and Deep Spring Formation carbonates from the White-Inyo Mountains, and Mount Dunfee in southwestern Esmeralda County have also been affected by post-depositional processes (Corsetti and Kaufman, 1994; Zenger, 1976) because the $\delta^{18}O$ values from these localities span an even greater range than those from Lone Mountain, and are between approximately 7 and 22

‰. Thus, it is not possible to compare directly metamorphosed rocks with their unmetamorphosed equivalents to ascertain the effects of post-depositional processes on the stable isotopic compositions of carbonate rocks from Lone Mountain.

In conjunction with trace element data, stable isotope data can be used to assess the primary nature of the stable isotopic compositions of carbonate rocks (Veizer, 1983). Carbonate rocks with the highest $\delta^{13}C$ and $\delta^{18}O$ values have stable isotopic compositions that make the closest approach to their original stable isotopic compositions (Brand and Veizer, 1981; O'Neil, 1987), as later interaction with low ^{18}O meteoric water normally lowers the $\delta^{18}O$ values of rocks. Also, carbonate rocks with the lowest Mn/Sr ratios tend to preserve their original chemical compositions (Brand and Veizer, 1980) due to partitioning of Mn into carbonate minerals and Sr into fluids during recrystallization. Wyman Formation calcite marbles have the lowest Mn/Sr ratios, and the highest $\delta^{13}C$ and $\delta^{18}O$ values (Figure 6), which suggests that their original stable isotopic compositions have been least altered by subsequent post-depositional processes, although there is still a 6 ‰ range in the $\delta^{18}O$ values of Wyman Formation calcite marbles. This in turn, suggests that the ranges in the inferred primary stable isotopic compositions of 2 ‰ in $\delta^{13}C$, and 4 ‰ in $\delta^{18}O$ in Lone Mountain carbonate rocks were inherited from the sedimentary protolith. Calcite marbles from the Reed Dolomite and Deep Spring Formation, and calcite-dolomite marbles from the Reed Dolomite also have low Mn/Sr ratios, but typically have 4 to 5 ‰ lower $\delta^{18}O$ values than Wyman Formation calcite marbles. These low $\delta^{18}O$ values are outside the range of primary $\delta^{18}O$ values of Late Proterozoic to Cambrian carbonates, and indicates that Reed Dolomite and Deep Spring Formation calcite marbles do not preserve their original oxygen isotopic compositions. An important corollary of this is that these rocks cannot have had their $\delta^{18}O$ values lowered as a result of extensive interaction with meteoric fluids during diagenesis, otherwise they would have higher Mn/Sr ratios.

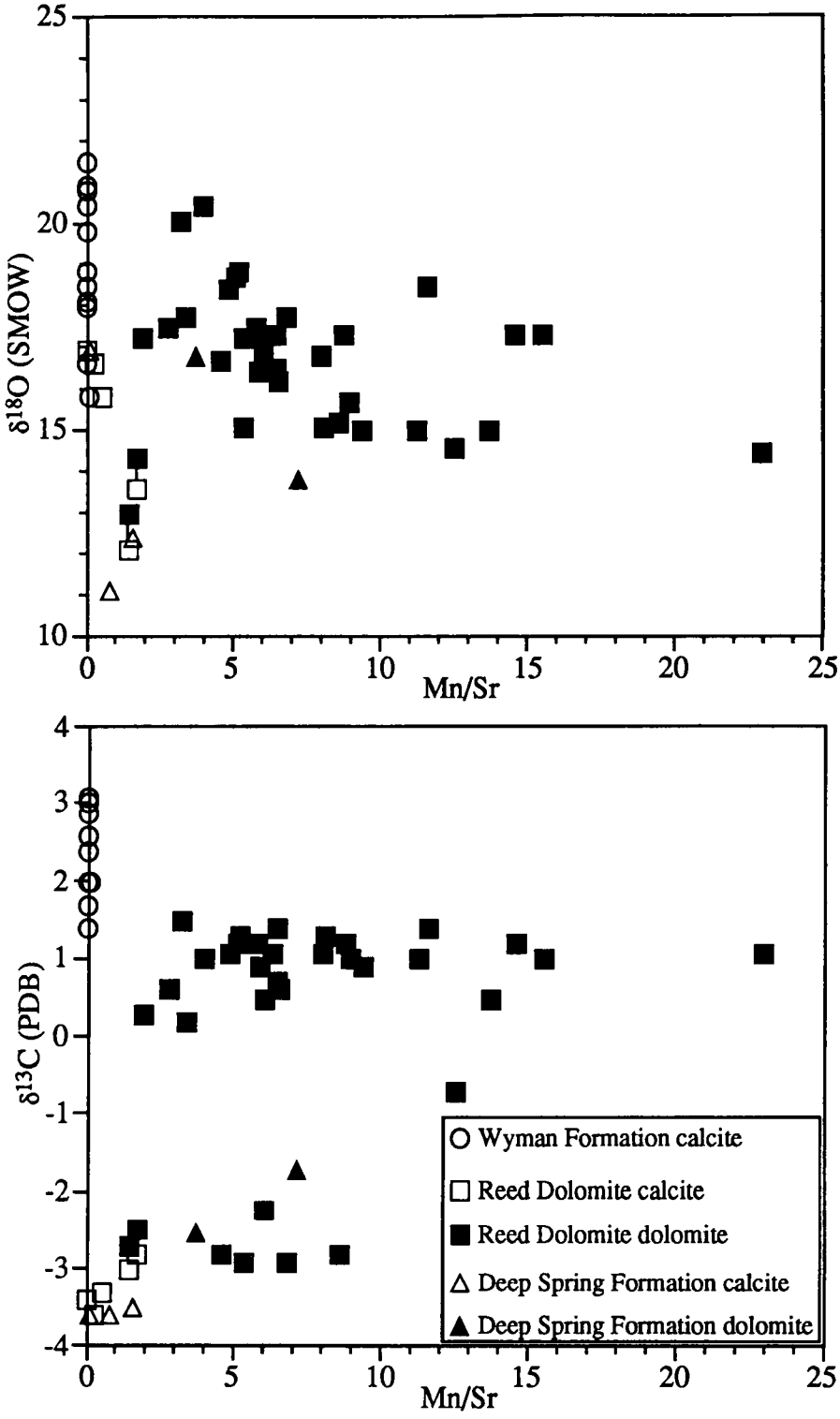

Figure 6: Mn/Sr versus $\delta^{18}O$ and $\delta^{13}C$ diagrams for calcite, calcite-dolomite and dolomite marbles. Tie lines join coexisting calcite and dolomite from the same calcite-dolomite marble sample.

Dolomite marbles show a weak negative correlation (R = 0.51) between Mn/Sr and $\delta^{18}O$, with high Mn/Sr and low $\delta^{18}O$ altered rocks and low Mn/Sr and high $\delta^{18}O$ unaltered or less altered rocks. This type of variation in Mn/Sr and $\delta^{18}O$ is indicative of carbonate rocks that have been altered by meteoric fluids during diagenesis (Veizer, 1983), and indicates that dolomite marbles do not preserve their original oxygen isotopic compositions. A negative correlation between Mn/Sr and $\delta^{13}C$ is also expected in carbonate rocks that have been altered by meteoric fluids, however, no such relationship is observed in Lone Mountain marbles. The uniformity of $\delta^{13}C$ values within both the positive and negative $\delta^{13}C$ groups and the variability in the Mn/Sr ratios, indicates that there has been a decoupling of the processes affecting the C isotopes, and the Mn and Sr compositions of Lone Mountain marbles.

Marbles that have negative $\delta^{13}C$ values also typically have depleted $\delta^{18}O$ values, strongly suggesting that the negative $\delta^{13}C$ values are not primary. At Lone Mountain, marbles with negative $\delta^{13}C$ values occur within a fault zone, where both calcite and dolomite marbles have a protomylonitic texture, in areas that were intruded by Tertiary lamprophyre dikes, or in areas where dolomite marbles are extensively fractured. Fault zones and fractures may have acted as conduits for fluid flow, which caused the observed depletions in the stable isotopic compositions of the marbles. The regional $\delta^{13}C$ stratigraphic correlation of Wyman Formation, Reed Dolomite, and Deep Spring Formation limestones and dolostones (Corsetti and Kaufman, 1994) also supports the arguments against primary negative $\delta^{13}C$ values at Lone Mountain, because the primary $\delta^{13}C$ stratigraphic curve for the region does not contain any negative $\delta^{13}C$ values within the Reed Dolomite or the lower Deep Spring Formation. That there was post-metamorphic meteoric fluid-rock interaction in Lone Mountain dolomite marbles is supported by observations of brightly luminescent rims along the margins of fractures, by the dissolution of quartz and by the development of quartz overgrowths. Thus, it is concluded

that the negative $\delta^{13}C$ values and depletions in ^{18}O of marbles are the result of post-metamorphic processes.

Modeling of the stable isotopic changes that occurred during post-metamorphic fluid rock-interaction was undertaken using open-system mass balance equations (Taylor, 1974). This approach makes several assumptions that are inappropriate to metamorphic fluid-rock interaction (Baumgartner and Rumble, 1988; Dipple and Ferry, 1992), but it is used here to ascertain the post-metamorphic fluid-rock interaction history of Lone Mountain marbles. Additionally, transport modeling of metamorphic fluid-rock interaction processes appears unwarranted in this instance in view of the apparent lack of fluid flow through marbles during metamorphism. The temperature of post-metamorphic fluid-rock interaction was taken as 370°C, based on re-equilibration temperatures determined by calcite-dolomite oxygen isotope and cation thermometry. Calculations assume that a pure dolomite marble with an initial $\delta^{18}O$ value of 20.1 ‰ interacted with a fluid that had an oxygen isotopic composition of $\delta^{18}O = -13.0$ ‰. In order to convert the initial dolomite marble into the final dolomite marble with a $\delta^{18}O$ value of 12.1 ‰, a fluid to rock ratio of 0.27 (atomic basis) is required.

QUARTZ AND CARBONATE STABLE ISOTOPES

In calcite marbles, oxygen isotopic fractionations between coexisting minerals record the expected order of ^{18}O enrichment, with quartz > calcite > muscovite > phlogopite. With one exception, quartz-calcite fractionations are between 2.3 and 3.1‰ (Figure 7). The exception, LM90, has a quartz-calcite fractionation of 0.6 ‰, which corresponds to a temperature of 525°C using the fractionation factor determined by quartz-calcite direct exchange experiments (Clayton and others, 1989). This temperature is in excellent agreement with the estimate of the temperature of metamorphism based on calcite-dolomite cation exchange thermometry. Other quartz-calcite fractionations in calcite marbles record temperatures of between 135 and 80°C, which are significantly below temperature

estimates for both metamorphism and post-metamorphic fluid-rock interaction. The rate of oxygen diffusion in quartz (Farver and Yund, 1991), calcite (Farver, 1994), and phlogopite and muscovite (Fortier and Giletti, 1991), suggests that exchange of oxygen isotopes by diffusion is inconsequential at temperatures below approximately 300°C. The low temperatures estimated using the quartz-calcite direct exchange calibration may be due to experimental artifacts (Sharp and Kirschner, 1993), use of the calibration at the lowest end of its acceptable temperature range, or the very low modal abundance of quartz in calcite marbles.

Although calcite will exchange oxygen much more readily than quartz, the lack of severely depleted $\delta^{18}O$ values of both calcite and quartz in Wyman Formation calcite marbles indicates that they did not interact with meteoric fluids after metamorphism. However, Reed Dolomite (and Deep Spring Formation) calcite marbles interlayered within the dominantly dolomite marble sequence are inferred to have had limited interaction with meteoric fluids because they contain opaque quartz that is slightly depleted in ^{18}O compared to clear quartz (Figure 7).

The $\delta^{18}O$ values of quartz from dolomite marbles are remarkably low, and are not typical of the oxygen isotopic compositions of quartz from sedimentary or metamorphic rocks (Blatt, 1987; Garlick and Epstein, 1967). This is significant, because quartz is presumed to be extremely resistant to oxygen isotopic exchange with fluids at low temperatures. As a result of the low $\delta^{18}O$ values of quartz from dolomite marbles, quartz-dolomite fractionations vary greatly between 2.1 and –15.1 (Figure 7). Negative or reversed quartz-dolomite fractionations that occur in dolomite marbles cannot possibly represent oxygen isotopic equilibrium between quartz and dolomite at any acceptable geological temperatures. The oxygen isotopic compositions of quartz from dolomite marbles are deemed to be altered and not primary because quartz from calcite marbles interlayered with dolomite marbles is not depleted in ^{18}O, and also because opaque quartz

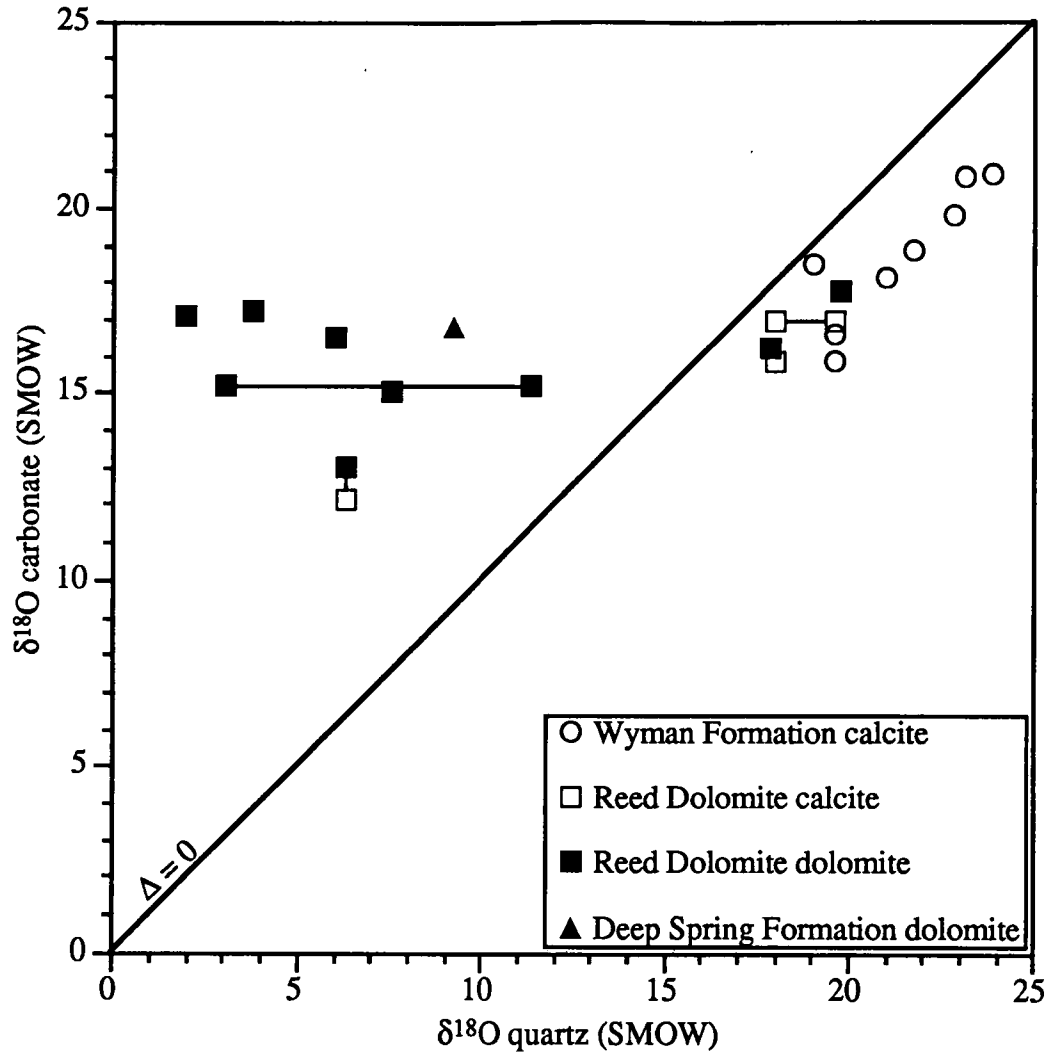

Figure 7: $\delta^{18}O$ quartz versus $\delta^{18}O$ carbonate diagram for calcite, calcite-dolomite and dolomite marbles. Horizontal tie lines join clear and opaque quartz from the same marble sample. Clear quartz always has a higher $\delta^{18}O$ value than opaque quartz. Vertical tie line joins quartz from coexisting calcite and dolomite from the same calcite-dolomite marble sample.

from dolomite marble is significantly depleted in ^{18}O compared to clear quartz from the same dolomite marble (Figure 7). The $\delta^{18}O$ depletions in quartz from dolomite marble are also inferred to have occurred after metamorphism during post-metamorphic fluid-rock interaction associated with meteoric fluids. Positive or equilibrium quartz-dolomite fractionations occur in marbles where authigenic quartz occurs as cements and overgrowths (LM56) or in protomylonites (LM105-5) that was precipitated from meteoric fluids after metamorphism. Tertiary meteoric fluid in the Lone Mountain area, and throughout western Nevada had a $\delta^{18}O$ value of approximately –13 ‰ (Taylor, 1973; O'Neil and Silberman, 1974). Thus, it is possible that hydrothermal meteoric fluids could have initially altered quartz by dissolution and then reprecipitation at temperatures of 300 to 400 °C, and then later precipitated quartz of approximately 20 ‰ as cements and overgrowths and in fractures as veins at temperatures of approximately 150°C (Figure 8).

Calcite and dolomite also behave very differently during deformation experiments. Calcite is extremely ductile, and under ideal circumstances, initially deforms by twin gliding and then by slip, although both twin gliding and slip can occur at all temperatures. In contrast to calcite, dolomite is strong, and if it deforms ductilely, it is initially by slip at temperatures less than 400°C, and then by twin gliding at temperatures greater than 500 °C. Twinning in dolomite does not occur at temperatures less than 300°C, and is usually not well developed unless the temperature is greater than 400°C (Barber and others, 1981). Although they have the potential to deform by similar mechanisms during ductile deformation, the slip and twinning systems for calcite and dolomite are quite different, with twinning and slip reinforcing each other in calcite, and competing against each other in dolomite (Wenk, 1985). For the temperatures of metamorphism appropriate for Lone Mountain calcite and dolomite marbles, greater critical shear stresses are required in order for dolomite to deform by ductile mechanisms than for calcite to do the same (Barber and others, 1981). Given that calcite and dolomite marbles experienced the same critical shear

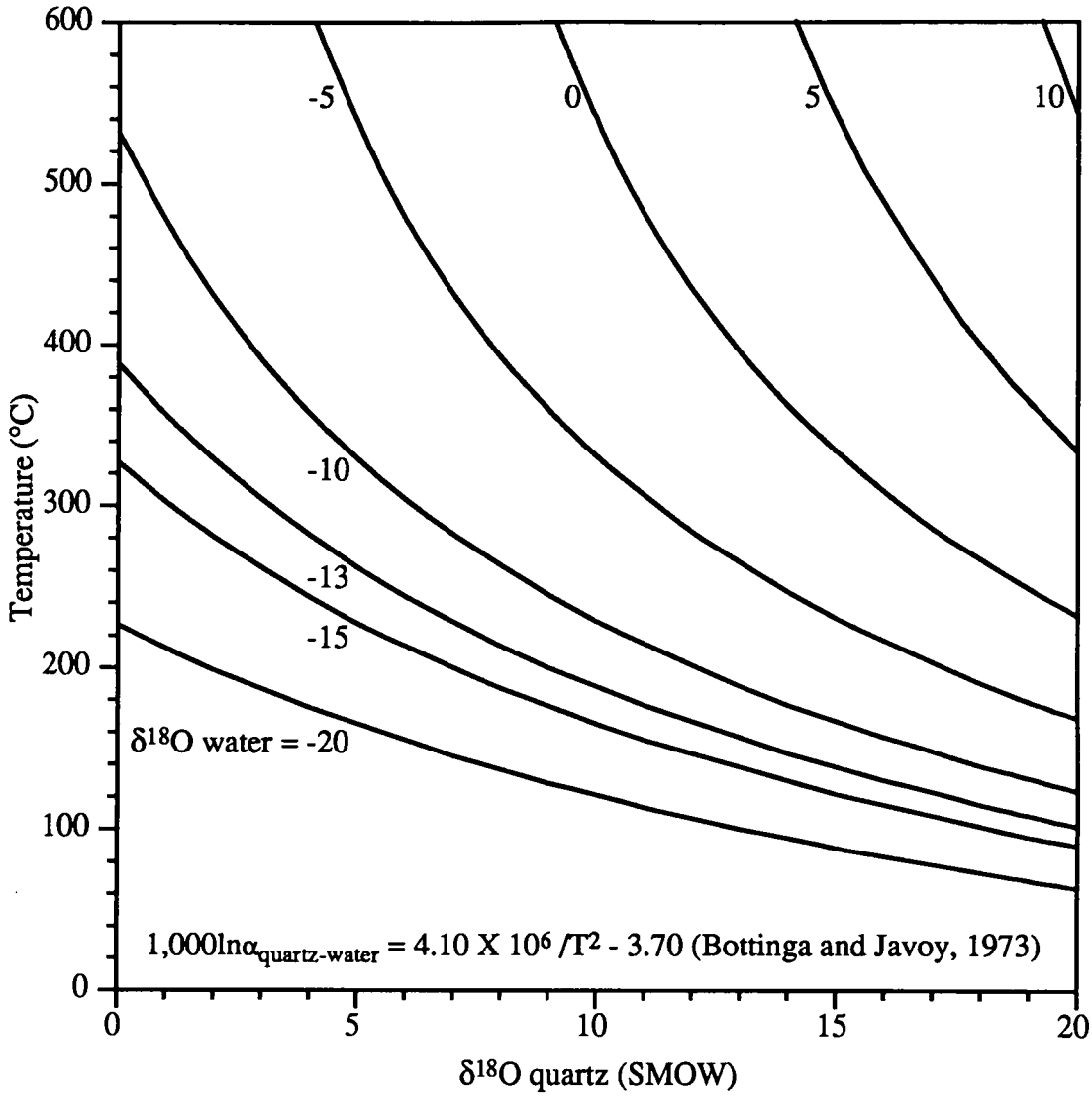

Figure 8: Temperature versus $\delta^{18}O$ quartz diagram. Diagram is contoured for $\delta^{18}O$ water based on the quartz-water fractionation factor of Bottinga and Javoy (1973). Tertiary meteoric water in western Nevada had a $\delta^{18}O$ value of –13 ‰ (Taylor, 1973; O'Neil and Silberman, 1973).

stresses during deformation and metamorphism at Lone Mountain, dolomite would only have deformed by brittle mechanisms. Field observations support this, with fractures and faults more prominent in dolomite marbles than in calcite marbles, indicating that fluid flow along fractures would have occurred more readily in dolomite marbles than in calcite marbles.

Bright luminescence along the margins of fractures in dolomite marbles indicates that there has been dissolution of dolomite associated with the flow of meteoric fluids along the fractures. Meteoric fluids would therefore contain Ca and Mg ions in solution. The dissolution of quartz is slowed by the presence of Ca and Mg ions in solution (Gratz and Bird, 1993), with Ca having the greatest affect. The greater influence of Ca in inhibiting the dissolution of quartz may explain the clear, smooth, normal ^{18}O quartz in calcite marbles versus the opaque, rough, depleted ^{18}O quartz in dolomite marbles.

CONCLUSIONS

Stable isotopic and trace element studies of marbles from Lone Mountain reveal significant differences between the behavior of limestones and calcite marbles, compared to dolostones and dolomite marbles, both before and after metamorphism. Prior to metamorphism, the trace element compositions of dolostones were affected by meteoric fluids during diagenesis (dolomitization), which resulted in a loss of Sr and Na and a gain in Zn, Mn, and Fe in dolomite marbles compared to calcite marbles. Following metamorphism, orange luminescent calcite marbles remained closed systems in which brown and blue luminescent, smooth-textured quartz and calcite re-equilibrated oxygen isotopes at temperatures below those of metamorphism. In contrast to this, red luminescent dolomite marbles were open systems, which were locally infiltrated by meteoric fluids along fractures which developed after metamorphism while the region was undergoing extension. This post-metamorphic fluid-rock interaction resulted in depleted $\delta^{13}C$ and $\delta^{18}O$ values in dolomite marbles and interlayered calcite marbles. Additionally,

meteoric fluids partially dissolved brown luminescent, rough-textured quartz in dolomite marbles thereby depleting the $\delta^{18}O$ values of quartz, such that quartz and dolomite are no longer in stable isotopic equilibrium. Authigenic quartz was then precipitated from these meteoric fluids as cements and overgrowths, and is in equilibrium with dolomite in dolomite marbles at low temperatures.

The differences in behavior between dolomite versus calcite marbles requires dolomite marbles to have maintained or developed some permeability throughout the Cretaceous and Tertiary metamorphic, plutonic, and structural events, whereas calcite marbles remained essentially impermeable. The implications of this are, that although marbles are considered to be impermeable during metamorphism, having behaved differently prior to and after metamorphism, it is possible that dolomite marbles responded differently than calcite marbles during metamorphism. Dolomite marbles are considered to be more permeable than calcite marbles, and potentially could allow some fluid flow during metamorphism. Additionally, although at Lone Mountain post-metamorphic meteoric fluids caused the ^{18}O depletions in quartz from dolomite marbles, the interaction of meteoric fluids with unmetamorphosed limestones and dolostones during post-depositional processes, such as diagenesis, has the potential to affect the stable isotopic composition of detrital quartz within carbonate rocks.

PART THREE

DIFFERENCES IN THE EXTENT OF FLUID-ROCK INTERACTION DURING METAMORPHISM BETWEEN GROSSULAR AND HORNBLENDE CALC-SILICATE ROCKS, LONE MOUNTAIN, NEVADA

ABSTRACT

Late Proterozoic to Cambrian carbonate, calc-silicate, and pelitic sedimentary rocks from Lone Mountain, southwestern Nevada, were regionally metamorphosed during Mesozoic time, and later contact metamorphosed in Late Cretaceous time as a result of the intrusion of the Lone Mountain granitic pluton. Metamorphic rocks are characterized by three distinct interlayered rock types: calcite marble, grossular calc-silicate hornfels, and hornblende calc-silicate hornfels. Calcite marbles consist almost entirely of calcite with minor amounts of quartz, phlogopite, muscovite, chlorite, albite, K-feldspar, and rutile. Grossular calc-silicate rocks contain the diagnostic mineral assemblage grossular + wollastonite + diopside + albite + calcite, with or without quartz, K-feldspar, epidote, vesuvianite, and titanite. Hornblende calc-silicate rocks contain hornblende + epidote + K-feldspar + plagioclase + calcite + quartz, and may also contain biotite, chlorite, titanite, and magnetite. Calcite in calcite marbles has $\delta^{13}C$ values between 3.1 and 1.4 ‰ (PDB), and $\delta^{18}O$ values typically between 21.5 and 18.0 ‰ (SMOW). The $\delta^{13}C$ and $\delta^{18}O$ values of calcite within calc-silicate rocks show the widest variation, with $\delta^{13}C$ = –1.3 to –10.9 ‰ and $\delta^{18}O$ = 13.9 to 11.8 ‰ in grossular calc-silicate rocks, and $\delta^{13}C$ = 2.5 to –2.8 ‰ and $\delta^{18}O$ = 16.4 to –3.3 ‰ in hornblende calc-silicate rocks. Silicate minerals in calcite marbles and grossular calc-silicate rocks have the following $\delta^{18}O$ values: quartz in calcite marbles 19.1 to 23.9 ‰, quartz in grossular calc-silicate rocks, 12.2 and 13.8 ‰, feldspar in calcite marbles and grossular calc-silicate rocks, 9.7 to 13.1 ‰, diopside and wollastonite 8.3 to 10.2 ‰, and grossular 8.3 to 10.4 ‰. Whole-rock silicate $\delta^{18}O$ values of hornblende calc-silicate rocks range from –2.4 to 16.3 ‰. These values suggest that calcite and silicate minerals approached oxygen isotopic equilibrium during metamorphism. For an estimated pressure of 3.5 kbar, the temperature of metamorphism from calcite-dolomite thermometry in marbles and mineral equilibria in calc-silicate rocks is 450 ± 70°C. Mineral assemblages within the calc-silicate rocks

were in equilibrium with H_2O-rich fluids (X_{CO_2} less than 0.05), whereas the calcite marbles were in equilibrium with more CO_2-rich fluids (X_{CO_2} greater than 0.2). The amount of volatiles lost by the rocks during metamorphism was calculated from mass balance relationships between the protolith and the metamorphic rock. Grossular calc-silicate rocks lost an average of 210 ± 32 g of CO_2 and 6 ± 2 g of H_2O per kilogram of protolith. Hornblende calc-silicate rocks lost an average of 53 ± 17 g of CO_2 and 17 ± 6 g of H_2O per kilogram of protolith. Differences between the amounts of fluid evolved by grossular and hornblende calc-silicate rocks are the result of differences in the original protolith mineralogy. Grossular calc-silicate rocks originally contained greater amounts of calcite, and hornblende calc-silicate rocks greater amounts of muscovite and chlorite. The volume of fluid evolved by calc-silicate rocks during metamorphism resulted in a significant loss of the original protolith solid volume. This loss in volume increased the permeability of the calc-silicate rocks and facilitated isotopic exchange with fluids during metamorphism. The amount of fluid that interacted with grossular calc-silicate rocks was 42 kg of H_2O per kg of rock, whereas hornblende calc-silicate rocks interacted with less fluid, 0.4 kg of H_2O per kg of rock. The isotopic composition of carbon in calcite within the calc-silicate rocks can be explained by mostly fractional devolatilization processes; however, the oxygen isotope data require infiltration of low ^{18}O fluids to cause the observed isotopic depletions. Fluids in equilibrium with the most depleted calc-silicate rocks have $\delta^{18}O$ values between 9.4 to 11.5 ‰ and are probably of magmatic origin from the Lone Mountain pluton. Both petrologic and stable isotopic evidence indicates that fluid flow occurred primarily through calc-silicate rocks during metamorphism and that marbles were essentially impermeable, and also that grossular calc-silicate rocks interacted with significantly more fluid than hornblende calc-silicate rocks.

INTRODUCTION

Rock type has been shown to be an important parameter in metamorphic fluid-rock interaction, as infiltration of externally derived fluid and pervasive fluid flow during metamorphism occurs in calc-silicate rocks, whereas calcite marbles interlayered with these rocks have been shown to be essentially impermeable to fluid flow (Nabelek, and others, 1984; Labotka and others, 1988 b; Davis and Ferry, 1993). This is in part because pure calcite marbles do not experience any mineralogical changes under most conditions of metamorphism; whereas, the minerals in calc-silicate rocks undergo continuous reactions as the conditions of metamorphism change. This typically leads to a decrease in the volume of the rocks, which increases permeability and facilitates fluid flow during metamorphism. Permeability enhancement and fluid movement during metamorphism also enables fluids and minerals in a rock to more readily attain stable isotopic equilibrium (Rumble and Spear, 1983).

In the western United States, Mesozoic low pressure regional metamorphism is associated with Mesozoic magmatism, which also caused widespread contact metamorphism (Barton, and others, 1988). At Lone Mountain in southwestern Nevada, Late Proterozoic to Cambrian carbonate, calc-silicate, and pelitic sedimentary rocks were regionally metamorphosed during Mesozoic time and were subsequently contact metamorphosed as a result of the intrusion of the Lone Mountain granitic pluton at the end of the Cretaceous Period. The amount and composition of fluid that interacted with the rocks during metamorphism were determined by petrologic and stable isotopic mass balance relationships between metamorphic rocks and their unmetamorphosed protoliths. This provided an understanding of the influence that rock type has on fluid infiltration during metamorphism.

GEOLOGIC SETTING

Lone Mountain is located approximately 25 km west of Tonopah in Esmeralda County, Nevada, within the northern part of the Goldfield section of the Walker Lane belt, a region of structural complexity that separates the Sierra Nevada batholith to the west, from the Basin and Range province to the east (Stewart, 1988). The regional geology of the area has been summarized by Albers and Stewart (1972), and Bonham and Garside (1979), and previous studies on the geology of Lone Mountain have been conducted by Sandy (1965), Phariss (1974), and Maldonado (1984). A geologic map of the area is presented in Figure 1. The area consists of Late Proterozoic to Cambrian sedimentary rocks that underwent greenschist-facies regional metamorphism during Mesozoic time. The regional metamorphic event was followed by the intrusion of the Lone Mountain granitic pluton in Late Cretaceous time, which caused contact metamorphism under hornblende-hornfels-facies conditions. The contact aureole is only a few tens of meters wide.

The oldest rocks in the Lone Mountain area belong to the Precambrian Wyman Formation which comprises calcite marble, calc-silicate hornfels, and minor pelitic schist, which are interlayered on a scale of between 2 mm and approximately 5m (Stewart, 1970; Albers and Stewart, 1972). The Wyman Formation crops out as northwest trending belts on the northeast and southwest sides of Lone Mountain and also as roof pendants in the northeastern and central parts of the Lone Mountain pluton. The base of the Wyman Formation is not exposed. The contact between the Wyman Formation and the overlying Reed Dolomite appears conformable in western Nevada (McKee and Moiola, 1962; Stewart, 1970; Albers and Stewart, 1972), and unconformable in eastern California (Nelson, 1962). The Reed Dolomite is a massive, brown to tan, medium- to coarse-grained dolomite marble which contains rare thin layers of phyllite, quartzite, and calcite marble.

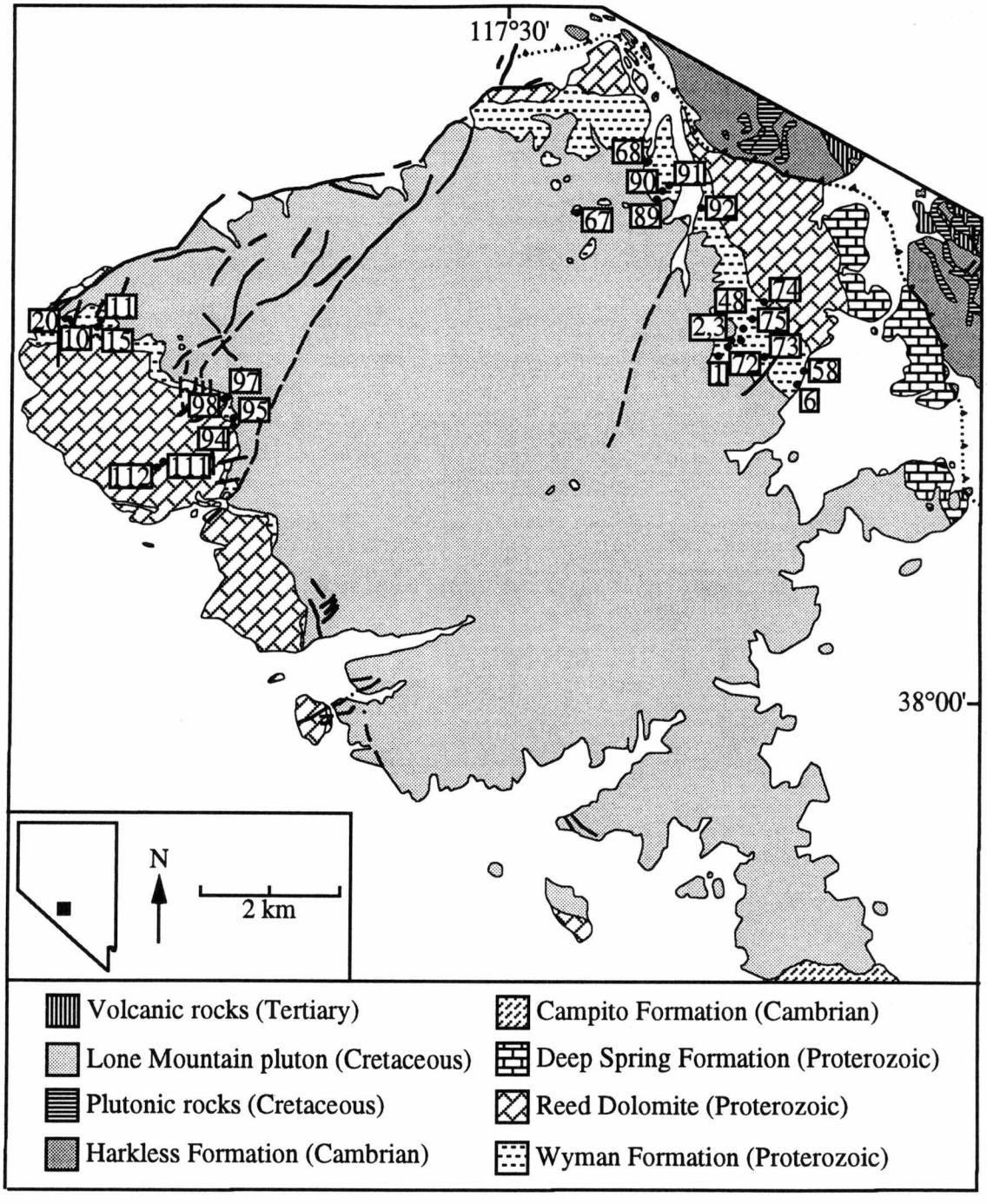

Figure 1: Geologic map of the Lone Mountain area (modified after Maldonado, 1984, and Bonham and Garside, 1979). The numbers on the map represent sample locations.

The intrusion of the Lone Mountain pluton either domed the metasedimentary rocks into a northwest-trending anticline (Maldonado, 1984), or occurred within the core of a pre-existing northwest-trending anticline (Albers and Stewart, 1972). The pluton has sharp, generally concordant contacts with the surrounding metasedimentary rocks and consists of granite, and minor granodiorite and quartz monzonite. K-Ar ages of biotite and muscovite from the Lone Mountain pluton are 69.2 ± 1.4 and 71.1 ± 1.4 million years, respectively (Silberman and others, 1975), and a Rb-Sr whole-rock isochron gives an age of 85.3 ± 4.3 million years (John and Robinson, 1989). Numerous lamprophyre and silicic porphyry dikes intrude both the Lone Mountain pluton and the surrounding metasedimentary rocks. The silicic porphry dikes have zircon fission-track ages of 22.1 ± 3.2 million years (Bonham and Garside, 1979).

PETROLOGY

Three different units are recognized within metasedimentary rocks of the Wyman Formation, on the basis of the observed mineral assemblages: 1) calcite marble, 2) grossular calc-silicate hornfels, and 3) hornblende calc-silicate hornfels. Mineral assemblages and modal abundance data for calc-silicate rocks and selected calcite marbles are given in Table 1, and average electron microprobe analyses of minerals from representative calcite marbles and calc-silicate rocks are given in Table 2. Calcite marbles contain mostly calcite, with or without minor amounts of quartz, muscovite, chlorite, phlogopite, albite, K-feldspar, and rutile at low grade, whereas at high grade, calcite marbles have the mineral assemblage calcite + quartz + diopside + K-feldspar + albite. Calcite marbles are coarse-grained (1 to 2 mm) and have a granoblastic texture in which minor rounded quartz grains (0.2 mm) occur at triple junctions and along grain boundaries. Muscovite, phlogopite, and chlorite typically occur as isolated plates within calcite.

Table 1: Mineral assemblages and modal analyses of hornblende calc-silicate hornfels, grossular calc-silicate hornfels and calcite marble

Sample	LM1	LM10	LM11	LM48	LM67-1	LM67-2	LM68-1	LM68-2	LM72	LM73
Rock type	GCS	GCS	HCS	CM	CM	GCS	GCS	HCS	CM	HCS
Calcite	12.0	3.7	0.2	95.6	94.0	16.5	4.5	76.2	93.8	35.8
Diopside	21.8	14.9				12.6	16.9		1.4	
Grossular	31.5	38.6				44.6	24.4			
Wollastonite	18.3	35.4				13.2	9.2			
Epidote			37.2			1.7	3.8	1.7		44.2
Vesuvianite		3.5					1.2			
Plagioclase	15.2	1.4	17.1			2.4	1.1	4.3	0.3	2.3
K-feldspar		0.8	21.8			2.9	34.6	2.2	2.5	3.9
Quartz	1.2	1.7	7.8	3.5	3.4	6.1	4.3	8.5	2.0	6.1
Hornblende			10.6					0.6		6.0
Biotite			3.3					6.5		
Phlogopite				0.5	0.8					
Muscovite				0.2	1.8					
Chlorite			0.7							0.1
Titanite			0.6							0.2
Rutile				0.2						
Magnetite			0.7							1.4

Sample	LM74-1	LM75-1	LM75-2	LM90	LM91	LM94	LM95-1	LM95-2	LM97-1	LM97-2
Rock type	HCS	HCS	CM	CM	CM	HCS	HCS	CM	GCS	CM
Calcite	19.3	71.8	99.2	92.8	92.5	9.4	17.5	98.1	4.2	96.6
Diopside							1.2		22.9	
Grossular									29.5	
Wollastonite									32.4	
Epidote	35.2	7.4				34.6	21.7			
Vesuvianite									3.6	
Plagioclase	1.9	1.7				7.5	3.5		6.2	
K-feldspar	3.9	4.1				9.3	13.0			
Quartz	23.4	3.2	0.8	5.6	7.4	17.0	24.6	1.5	1.2	0.2
Hornblende	13.9	2.3				17.6	10.3			
Biotite	0.4	9.0				0.2	2.0			
Phlogopite				0.8	0.1			0.1		2.4
Muscovite				0.4				0.3		0.4
Chlorite						4.4	5.7			
Titanite	0.9									
Rutile				0.4	‡			‡		0.5
Magnetite	1.1	0.5					0.5			

Note: Based on 1,000 to 1,500 points counted in thin section. Rock type: HCS = hornblende calc-silicate hornfels, GCS = grossular calc-silicate hornfels, CM = calcite marble. ‡: observed in thin section.

Table 2: Representative electron microprobe analyses of minerals from hornblende calc-silicate hornfels, grossular calc-silicate hornfels, calcite marble and calcite-dolomite marble

Sample	LM58-2	LM72	LM10	LM94	LM75-1	LM111-2	LM112	LM111-2	LM112
Mineral	Cal	Cal	Cal	Cal	Cal	Cal	Cal	Dol	Dol
Rock type	CM	CM	GCS	HCS	HCS	CDM	CDM	CDM	CDM
SiO_2									
TiO_2									
Al_2O_3									
FeO	0.14	<0.06	<0.06	0.30	0.46	<0.06	<0.06	0.21	0.21
MnO	<0.05	<0.05	<0.05	<0.05	0.05	<0.05	<0.05	<0.05	<0.05
MgO	0.43	0.07	<0.02	0.11	0.09	1.27	0.98	21.5	21.4
CaO	55.6	55.0	54.6	54.1	54.2	54.0	54.5	30.4	30.5
Na_2O									
K_2O									
Total	56.22	55.11	54.71	54.78	54.82	55.37	55.48	52.12	52.15
Cations based on				1 oxygen				2 oxygens	
Si									
Ti									
Al									
Fe^{3+}									
Fe^{2+}	0.002	0.000	0.001	0.004	0.006	0.000	0.000	0.006	0.006
Mn	0.000	0.000	0.000	0.004	0.001	0.000	0.000	0.001	0.001
Mg	0.011	0.002	0.000	0.003	0.002	0.032	0.024	0.989	0.986
Ca	0.987	0.998	0.999	0.990	0.990	0.968	0.975	1.005	1.008
Na									
K									
Total	1.000	1.000	1.000	1.001	0.999	1.000	0.999	2.001	2.001

Table 2: (continued)

Sample	LM72	LM10	LM68-1	LM95-1	LM11	LM68-2	LM75-1	LM94	LM95-1
Mineral	Di	Di	Di	Di	Hbl	Hbl	Hbl	Hbl	Hbl
Rock type	CM	GCS	GCS	HCS	HCS	HCS	HCS	HCS	HCS
SiO_2	53.8	53.5	52.1	51.2	43.2	45.4	42.5	45.6	43.9
TiO_2	<0.02	<0.02	<0.02	<0.02	0.38	0.26	0.23	0.32	0.30
Al_2O_3	0.30	0.41	0.14	0.40	11.3	9.62	10.8	9.86	10.9
FeO	<0.03	6.10	12.1	13.0	18.7	17.2	20.1	17.7	17.7
MnO	3.81	0.08	0.15	0.20	0.21	0.02	0.07	0.30	0.13
MgO	0.03	14.3	10.8	10.2	8.97	10.5	8.48	9.63	9.73
CaO	16.1	25.0	24.4	23.9	12.1	12.4	11.9	12.3	12.2
Na_2O	25.2	0.23	0.12	0.12	0.86	0.80	1.08	0.63	0.93
K_2O	0.13				1.69	1.12	1.62	0.97	1.44
Total	99.38	99.65	99.81	99.07	97.41	97.28	96.86	97.34	97.23
Cations based on		6 oxygens				23 oxygens			
Si	1.987	1.990	1.991	1.981	6.533	6.796	6.514	6.834	6.617
Ti	0.000	0.000	0.000	0.000	0.044	0.029	0.026	0.036	0.034
Al	0.013	0.018	0.006	0.018	2.022	1.695	1.959	1.742	1.930
Fe^{3+}					0.292	0.233	0.368	0.174	0.246
Fe^{2+}	0.000	0.190	0.386	0.417	2.081	1.915	2.207	2.040	1.983
Mn	0.118	0.003	0.005	0.007	0.027	0.003	0.010	0.038	0.017
Mg	0.001	0.794	0.613	0.592	2.022	2.338	1.935	2.148	2.185
Ca	0.886	0.997	0.999	0.991	1.957	1.978	1.960	1.975	1.977
Na	0.995	0.017	0.009	0.009	0.252	0.231	0.319	0.185	0.272
K	0.009				0.327	0.214	0.316	0.186	0.276
Total	4.010	4.009	4.009	4.014	15.557	15.432	15.614	15.358	15.537

Table 2: (continued)

Sample	LM97-2	LM11	LM68-2	LM58-2	LM92-1	LM11	LM94	LM10	LM68-1
Mineral	Phl	Bi	Bi	Ms	Chl	Chl	Chl	Gr	Gr
Rock type	CM	HCS	HCS	CM	CM	HCS	HCS	GCS	GCS
SiO_2	42.2	37.3	37.3	47.1	25.2	26.2	26.5	38.1	38.0
TiO_2	0.21	1.10	0.96	0.18	0.03	0.07	0.02	0.67	0.65
Al_2O_3	13.7	13.9	16.1	33.5	19.7	18.4	18.3	17.0	17.4
FeO	0.96	17.7	17.3	0.46	13.0	27.4	27.0	6.79	7.34
MnO	<0.07	0.15	<0.07	<0.07	0.18	0.19	0.21	0.06	0.11
MgO	27.0	14.2	13.1	2.45	27.5	13.9	14.6	0.08	0.06
CaO	0.08	0.07	0.11	0.07				36.2	35.2
Na_2O	0.19	0.08	0.07	0.19					
K_2O	10.1	10.0	9.64	11.2					
Total	94.38	94.50	94.64	95.10	85.62	86.09	86.54	99.98	98.81
Cations based on		11 oxygens				14 oxygens		12 oxygens	
Si	2.962	2.863	2.830	3.135	2.764	2.847	2.859	2.953	2.953
Ti	0.011	0.064	0.055	0.009	0.002	0.005	0.002	0.039	0.038
Al	1.133	1.253	1.443	2.633	2.542	2.358	2.321	1.555	1.590
Fe^{3+}								0.439	0.417
Fe^{2+}	0.056	1.136	1.100	0.026	2.118	2.490	2.436	0.001	0.060
Mn	0.001	0.010	0.003	0.000	0.017	0.018	0.020	0.004	0.007
Mg	2.825	1.623	1.483	0.244	2.522	2.253	2.342	0.009	0.006
Ca	0.006	0.006	0.009	0.005				3.007	2.931
Na	0.026	0.012	0.010	0.024					
K	0.909	0.978	0.934	0.950					
Total	7.929	7.943	7.866	7.026	9.963	9.969	9.979	8.007	8.002

Table 2: (continued)

Sample	LM68-1	LM11	LM68-2	LM94	LM95-1	LM10	LM11	LM72	LM92-1
Mineral	Epd	Epd	Epd	Epd	Epd	Ves	Ttn	Kfs	Kfs
Rock type	GCS	HCS	HCS	HCS	HCS	GCS	HCS	CM	CM
SiO_2	37.8	38.1	38.1	38.1	37.7	36.3	30.5	63.8	64.1
TiO_2	0.07	0.09	0.11	0.11	0.08	2.30	35.4		
Al_2O_3	25.8	26.4	28.7	28.7	27.9	16.1	3.47	18.9	18.8
FeO	9.17	8.48	6.35	6.35	7.25	3.63	0.41	0.02	0.07
MnO	0.03	0.08	0.01	0.01	0.02	0.04	0.00		
MgO	0.03	0.02	0.02	0.02	0.03	1.80	0.01		
CaO	21.9	23.7	23.5	23.5	23.2	35.5	28.9	0.10	0.08
Na_2O						0.13		0.45	0.56
K_2O						0.00		16.0	16.1
Total	94.71	96.80	96.78	96.78	96.17	96.62	98.79	99.35	99.73
Cations based on			8 cations			50 cations	5 oxygens	8 oxygens	
Si	3.039	2.990	2.974	2.974	2.967	17.963	1.005	2.970	2.974
Ti	0.004	0.006	0.006	0.006	0.005	0.857	0.878		
Al	2.444	2.442	2.641	2.641	2.589	9.365	0.135	1.038	1.030
Fe^{3+}	0.618	0.559	0.414	0.414	0.477				
Fe^{2+}						1.505	0.011	0.001	0.003
Mn	0.002	0.005	0.001	0.001	0.001	0.015	0.000		
Mg	0.004	0.003	0.002	0.002	0.004	1.332	0.001		
Ca	1.889	1.995	1.961	1.961	1.957	18.835	1.021	0.005	0.004
Na						0.126		0.041	0.050
K						0.003		0.953	0.951
Total	8.000	8.000	8.000	8.000	8.000	50.000	3.051	5.007	5.012

Table 2: (continued)

Sample	LM68-1	LM11	LM94	LM72	LM92-1	LM10	LM68-1	LM11	LM94
Mineral	Kfs	Kfs	Kfs	Pl	Pl	Pl	Pl	Pl	Pl
Rock type	GCS	HCS	HCS	CM	CM	GCS	GCS	HCS	HCS
SiO_2	63.5	64.6	63.9	68.1	55.3	67.0	67.9	57.1	68.1
TiO_2									
Al_2O_3	18.6	18.7	18.9	20.0	27.7	20.4	19.6	27.2	20.5
FeO	0.05	0.15	0.12	0.01	0.58	0.04	0.07	0.13	0.13
MnO									
MgO									
CaO	0.03	0.03	0.03	0.06	9.03	0.57	0.57	9.11	0.47
Na_2O	0.50	0.89	0.39	11.5	5.96	10.9	11.4	6.32	11.0
K_2O	16.3	15.8	16.2	0.06	0.29	0.10	0.10	0.18	0.14
Total	99.00	100.08	99.51	99.74	98.84	99.02	99.69	100.10	100.38
Cations based on					8 oxygens				
Si	2.973	2.982	2.972	2.982	2.518	2.956	2.979	2.561	2.960
Ti									
Al	1.026	1.015	1.035	1.029	1.487	1.062	1.016	1.438	1.051
Fe^{3+}									
Fe	0.002	0.006	0.004	0.000	0.023	0.001	0.003	0.005	0.005
Mn									
Mg									
Ca	0.002	0.002	0.002	0.003	0.441	0.027	0.027	0.437	0.022
Na	0.045	0.080	0.035	0.977	0.526	0.930	0.970	0.549	0.930
K	0.974	0.930	0.958	0.003	0.017	0.006	0.005	0.010	0.021
Total	5.023	5.015	5.007	4.994	5.010	4.981	5.001	5.000	4.989

Note: Rock type: HCS hornblende calc-silicate hornfels, GCS grossular calc-silicate hornfels, CM calcite marble, CDM calcite-dolomite marble. Mineral abbreviations after Kretz (1983).

Grossular calc-silicate rocks contain the mineral assemblage grossular + diopside + wollastonite + calcite + quartz + albite, with or without K-feldspar, vesuvianite, epidote, and titanite, in which grossular occurs as large euhedral porphyroblasts (up to 1 cm), with a few small (0.1 mm) inclusions of diopside and calcite, and is set within a weakly foliated matrix dominated by bladed wollastonite, euhedral diopside, and minor feldspar, quartz, and epidote. Vesuvianite, where present, occurs as 0.5 mm subhedral porphyroblasts with numerous diopside and quartz inclusions. Hornblende calc-silicate rocks contain the mineral assemblage hornblende + plagioclase + K-feldspar + epidote + quartz, and may also contain calcite, biotite, chlorite, titanite, and magnetite. Hornblende calc-silicate rocks are generally fine grained (0.2 to 0.05 mm) and have a very well developed foliation defined by alternating layers of calcite and silicate layers. Within the silicate layers, mafic layers that consist of intergrown euhedral hornblende, subhedral epidote, and biotite, are typically separated from felsic layers that are composed of intergrown quartz and feldspar.

Calcite in calcite marbles and calc-silicate rocks is essentially pure $CaCO_3$ with less than 0.01 atoms of Mg, Mn, and Fe per formula unit. Dolomite within the Reed Dolomite has Ca/Mg in the restricted range 0.99 to 1.03 indicating that it is essentially stoichiometric and, like calcite, has less than 0.01 atoms of Mg, Mn, and Fe per formula unit. Calcite within Reed Dolomite dolomite marbles is more magnesian, with up to 0.15 atoms of Mg per formula unit.

Diopside occurs in grossular calc-silicate rocks, in calcite marbles at high metamorphic grade, and very rarely in hornblende calc-silicate rocks. In calcite marbles, diopside is close to $CaMgSi_2O_6$, with Fe/(Fe+Mg) in the range 0.06 to 0.13. In calc-silicate rocks diopside is more iron-rich with Fe/(Fe+Mg) between 0.17 and 0.43 in grossular calc-silicate rocks and between 0.38 and 0.46 in hornblende calc-silicate rocks.

Amphiboles in hornblende calc-silicate rocks are calcic, varying between edenitic

hornblende and magnesio-hornblende (Leake, 1978), such that Fe/(Fe+Mg) varies between 0.44 and 0.61, Na/(Na+K) is in the range 0.42 to 0.54, and there are 6.2 to 7.0 atoms of Si per formula unit, and 1.5 to 2.4 atoms of Al per formula unit.

Phlogopite in calcite marbles has a very restricted range in composition with Fe/(Fe+Mg) = 0.01 to 0.02, Na/(Na+K) = 0.01 to 0.03, 2.7 to 3.0 atoms of Si per formula unit, and 0.01 to 0.04 atoms of Ti per formula unit. Biotite in hornblende calc-silicate rocks has Fe/(Fe+Mg) = 0.39 to 0.47, Na/(Na+K) = 0.01 to 0.02, and 2.8 to 2.9 atoms of Si per formula unit, and 0.03 to 0.06 atoms of Ti per formula unit. Muscovite in calcite marbles has Fe/(Fe+Mg) = 0.09 to 0.11, Na/(Na+K) = 0.02, and 0.01 to 0.02 atoms of Ti per formula unit. Chlorite in hornblende calc-silicate rocks has Fe/(Fe+Mg) = 0.40 to 0.56, and 2.7 to 2.9 atoms of Si per formula unit, and chlorite in calcite marbles has Fe/(Fe+Mg) = 0.02, and 2.6 atoms of both Si and Al per formula unit.

Garnet in grossular calc-silicate rocks is a grossular-andradite solid solution $Ca_3(Fe,Al)_2Si_3O_{12}$, with 2.9 to 3.0 atoms of Ca per formula unit, and $Al/(Al+Fe^{3+})$ = 0.73 to 0.91 and less than 0.01 atoms of Mg, Mn, and Fe^{2+} per formula unit. Epidote in calc-silicate rocks has Al/(Al+Fe) = 0.71 to 0.91. Vesuvianite in grossular calc-silicate rocks has 18.7 to 18.9 atoms of Ca per formula unit, 17.8 to 18.0 atoms of Si per formula unit, and Fe/(Fe+Mg) = 0.51 to 0.57. Titanite in calc-silicate rocks typically has between 0.98 and 1.00 cations each of Si and Ca, with Ti varying between 0.85 and 0.87, and Al between 0.13 and 0.15.

K-feldspar in both marbles and calc-silicate rocks is essentially constant in composition with K/(K+Na) = 0.92 to 0.97. Plagioclase varies in composition that is dependent on rock type, but is uniform in composition within samples. In grossular calc-silicate rocks, and calcite marbles, plagioclase is albite, with Ca/(Ca+Na) = 0.00 to 0.04, while plagioclase in hornblende calc-silicate rocks is generally more calcic, varying between andesine and labradorite with Ca/(Ca+Na) = 0.37 to 0.69, although in one

hornblende calc-silicate rock, LM94, the plagioclase is albite with Ca/(Ca+Na) = 0.01 to 0.03.

Wollastonite, quartz, and rutile are assumed to be pure $CaSiO_3$, SiO_2, and TiO_2, respectively.

WHOLE-ROCK CHEMISTRY

Whole-rock major-element chemical analyses are given in Table 3 for the samples listed in Table 1. All calcite marbles are mostly CaO and CO_2, with less than 3% SiO_2, and typically less than 1% of the other elements. Calcite marbles and calc-silicate rocks differ in that calc-silicate rocks are much more variable in composition with significantly more SiO_2 and Al_2O_3, and greater amounts of FeO, MgO, Na_2O, and K_2O than calcite marbles have. Because of the variability of the thickness of the layering in Lone Mountain metasedimentary rocks, different whole-rock compositions occur within the same rock type, thus, for the purposes of comparison of whole-rock compositions between calc-silicate rocks, only rocks that have less than approximately 3 weight percent CO_2 are considered, e.g., grossular calc-silicate hornfels samples LM10 and LM68-1, and hornblende calc-silicate hornfels samples LM11, LM94 and LM95-1. Hornblende calc-silicate rocks have significantly more Al_2O_3 and K_2O than grossular calc-silicate rocks, and slightly more SiO_2, FeO, MgO, and Na_2O, whereas grossular calc-silicate rocks contain substantially more CaO than hornblende calc-silicate rocks.

STABLE ISOTOPE GEOCHEMISTRY

The stable isotopic compositions of Lone Mountain metamorphic and granitic rocks are given in Table 4. There is a correlation between the $\delta^{13}C$ and $\delta^{18}O$ values of calcite in Lone Mountain metamorphic rocks, with marbles having high $\delta^{13}C$ and $\delta^{18}O$ values and calc-silicate rocks having low $\delta^{13}C$ and $\delta^{18}O$ values (Figure 2). Calcite from low grade calcite marbles has $\delta^{13}C$ values between 3.1 and 1.7 ‰ (PDB), and $\delta^{18}O$ values between 21.5 and 15.8 ‰ (SMOW). High-grade calcite marble, LM72, has a $\delta^{13}C$ value similar

Table 3: Whole-rock X-ray fluorescence analyses of hornblende calc-silicate hornfels, grossular calc-silicate hornfels and calcite marble

Sample	LM1	LM10	LM11	LM48	LM67-1	LM67-2	LM68-1	LM68-2	LM72	LM73
Rock type	GCS	GCS	HCS	CM	CM	GCS	GCS	HCS	CM	HCS
SiO_2	45.4	49.9	52.0	1.50	1.90	43.7	47.0	17.0	1.62	42.1
TiO_2	0.08	0.18	0.36	0.03	0.03	0.26	0.28	0.21	0.02	0.52
Al_2O_3	2.03	4.02	20.3	0.12	0.28	4.99	6.09	7.99	0.24	14.6
FeO	1.08	1.59	6.67	0.13	0.58	2.25	2.14	1.74	0.12	5.30
MnO	0.06	0.05	0.06		0.01	0.05	0.04	0.03		0.11
MgO	0.60	1.21	1.52	0.77	0.87	1.35	0.95	0.59	0.35	1.88
CaO	43.7	41.1	11.9	55.4	53.6	38.1	37.9	36.7	55.3	26.2
Na_2O	0.06	0.32	1.37	0.02	0.02	0.73	0.08	0.65	0.02	0.66
K_2O	0.02	0.22	3.98		0.03	1.43	1.52	0.13	0.08	1.94
CO_2	6.66	1.61		42.3	43.1	6.87	3.65	35.7	40.0	6.12
Total	99.65	100.20	98.19	100.31	100.49	99.73	99.69	100.76	97.77	99.54

Sample	LM74-1	LM75-1	LM75-2	LM90	LM91	LM94	LM95-1	LM95-2	LM97-1	LM97-2
Rock type	HCS	HCS	CM	CM	CM	HCS	HCS	CM	GCS	CM
SiO_2	53.5	12.0	0.78	2.15	1.74	53.4	53.5	1.53	36.8	1.73
TiO_2	0.61	0.20	0.01	0.03	0.04	0.70	0.67	0.01	0.20	0.03
Al_2O_3	13.0	9.04		0.37	0.01	15.3	16.8	0.01	5.34	0.81
FeO	4.05	2.06	0.03	0.39	0.17	6.40	5.69	0.13	1.60	0.16
MnO	0.13	0.04				0.11	0.08		0.03	
MgO	1.46	0.96	0.62	1.28	0.70	2.53	2.16	0.86	1.94	2.18
CaO	19.8	39.1	55.7	53.5	54.8	13.6	12.9	54.8	41.8	53.4
Na_2O	0.66	0.43	0.01	0.02	0.02	1.25	1.18	0.02	0.06	0.02
K_2O	1.86	1.07		0.07		3.50	4.90		0.01	0.18
CO_2	4.73	35.8	42.6	41.9	41.2	2.44	1.85	41.1	12.0	43.0
Total	99.83	100.64	99.73	99.74	98.70	99.21	99.72	98.44	99.69	101.51

Note: Rock type: HCS = hornblende calc-silicate hornfels, GCS = grossular calc-silicate hornfels, CM = calcite marble.

Table 4: Stable isotope analyses of hornblende calc-silicate hornfels, grossular calc-silicate hornfels, calcite marble, granite and pelitic schist

Sample	$\delta^{13}C$ calcite	$\delta^{18}O$ calcite	$\delta^{18}O$ whole-rock	$\delta^{18}O$ quartz	$\delta^{18}O$ feldspar	$\delta^{18}O$ grossular	$\delta^{18}O$ diopside	$\delta^{18}O$ wollastonite
			Hornblende calc-silicate hornfels					
LM2	–0.8	15.5	15.4					
LM3			14.4					
LM6	0.9	14.1	13.2					
LM11			1.2					
LM15			9.7					
LM20	0.3	10.8	2.5					
LM68-2	2.5	15.2	12.8					
LM73	–2.8	12.3	11.5					
LM74-1	–0.6	14.9	14.1					
LM75-1	1.9	16.4	16.3					
LM92-2	–0.9	12.6	11.2					
LM92-3	2.4	14.5	12.1					
LM94	0.0	–3.3	–2.4					
LM95-1	0.6	5.1	4.9					
LM98-1	–0.5	14.1	11.7					
			Grossular calc-silicate hornfels					
LM1	–1.3	12.1			10.1	8.3	9.7	8.9
LM10	–10.9	13.9			11.8	9.6		8.3
LM67-2	–1.4	12.8		13.8	13.1	10.4	9.6	
LM68-1	–1.5	11.8			9.7	9.4	10.2	9.1
LM97-1	–2.0	12.8		12.2	10.5	9.8		10.7
			Calcite marble					
LM48	2.4	20.8		23.2				
LM58-1	2.0	16.6		19.7				
LM58-2	2.0	15.8						
LM58-3	2.1	18.0						
LM67-1	2.6	18.1		21.1				
LM72	1.8	14.9			12.3			
LM75-2	2.4	21.5						

Table 4: (continued)

Sample	$\delta^{13}C$ calcite	$\delta^{18}O$ calcite	$\delta^{18}O$ whole-rock	$\delta^{18}O$ quartz	$\delta^{18}O$ feldspar	$\delta^{18}O$ grossular	$\delta^{18}O$ diopside	$\delta^{18}O$ wollastonite
				Calcite marble				
LM89-2	1.7	19.8		22.9				
LM90	3.0	18.5		19.1				
LM91	3.1	18.8		21.8				
LM92-1	2.4	13.0						
LM95-2	3.0	20.9		23.9				
LM97-2	1.4	20.4						
				Granite				
LM115-1			9.7		8.6			
LM123			9.0	10.9	9.1			
LM125			9.2	11.3	8.7			
LM131-2			12.2	10.8	9.6			
LM134-2			11.7	11.6	9.9			
LM138			10.1	11.0	9.2			
LM140			9.5	11.5	9.1			
LM142			9.5	11.4	8.9			
LM144			10.3	11.1	8.5			
LM146			9.2	10.7	9.4			
				Pelitic schist				
LM5			15.9					
LM12			9.3					
LM14			7.8					
LM59-1			14.6					
LM93			13.9					

Note: Whole-rock $\delta^{18}O$ values for hornblende calc-silicate hornfels are for the silicate mineral fraction.

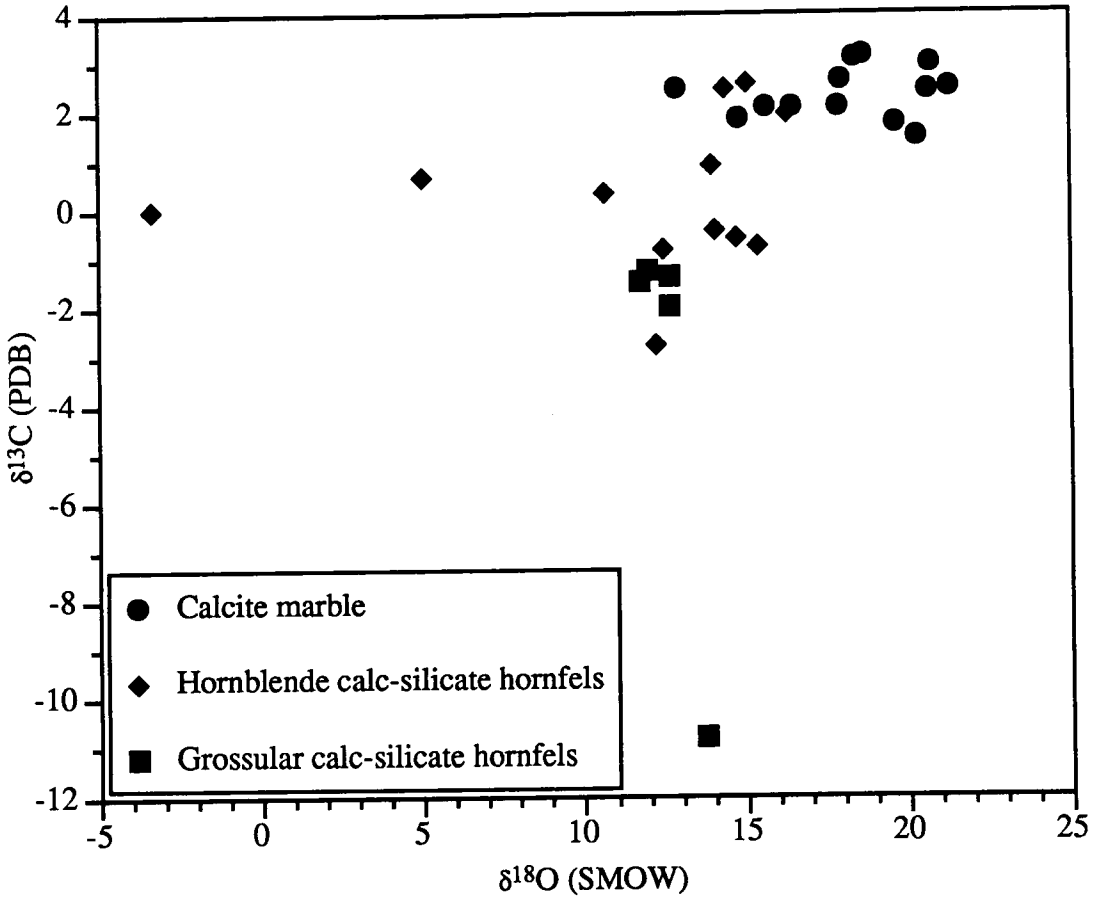

Figure 2: $\delta^{18}O$ versus $\delta^{13}C$ for calcite in hornblende calc-silicate hornfels, grossular calc-silicate hornfels and calcite marble.

to that of low-grade calcite marbles, 1.8 ‰, but has a lower $\delta^{18}O$ value, 14.9 ‰. Calcite in grossular calc-silicate rocks has $\delta^{13}C$ values between –1.3 and –2.0 ‰, with the exception of LM10, which has a very low $\delta^{13}C$ value of –10.9, and has $\delta^{18}O$ values between 11.8 and 13.9 ‰. Hornblende calc-silicate rocks show the widest variation in calcite isotopic compositions with $\delta^{13}C$ values ranging from 2.4 to –2.8 and with $\delta^{18}O$ values typically between 12.3 and 13.4‰; however, two samples, LM94 and LM95-1, have very low $\delta^{18}O$ values of 5.1 and –3.3‰, respectively. The $\delta^{13}C$ and $\delta^{18}O$ values of samples collected from the same location generally show a wide range in stable isotopic composition that is dependent on rock type, with calc-silicate rocks depleted in both carbon and oxygen compared to calcite marbles. Calcite marble and grossular calc-silicate hornfels from sample location LM97 have a 7.6 ‰ difference in oxygen isotopic composition and a 3.4 ‰ difference in carbon isotopic composition. Calcite marble and hornblende calc-silicate hornfels collected from sample location LM95 have a 15.8 ‰ difference in $\delta^{18}O$, and a 2.4 ‰ difference in $\delta^{13}C$. Differences in stable isotopic composition also exist between calc-silicate rocks at sample location LM68, with grossular calc-silicate hornfels depleted in both ^{13}C and ^{18}O relative to hornblende calc-silicate hornfels.

Whole-rock $\delta^{18}O$ values for the silicate mineral fraction of hornblende calc-silicate rocks show a broad range in $\delta^{18}O$ values from –2.4 to 16.3 ‰, resulting in calcite-whole-rock silicate fractionations that are typically between 0.1 and 2.5 ‰. The whole-rock silicate mineral fraction of grossular calc-silicate rocks have $\delta^{18}O$ values that have a narrow range, from 8.0 to 9.2 ‰, so that calcite-whole-rock silicate fractionations in grossular calc-silicate rocks are greater than in hornblende calc-silicate rocks, varying between 3.1 and 5.4 ‰. The oxygen isotopic composition of quartz has a narrow range in $\delta^{18}O$ values that is also dependent on rock type. Quartz from calcite marbles has $\delta^{18}O$ values from 19.1 to 23.9 ‰, whereas quartz from grossular calc-silicate rocks has lower

$\delta^{18}O$ values, between 12.2 and 13.8 ‰. Feldspar $\delta^{18}O$ values from high-grade calcite marble and grossular calc-silicate rocks are between 9.7 and 13.1 ‰. Diopside and wollastonite in grossular calc-silicate rocks have $\delta^{18}O$ values that are similar to each other, between 8.3 and 10.2 ‰, although diopside is always about 0.9 ‰ enriched in ^{18}O compared to wollastonite, and grossular in grossular calc-silicate rocks has $\delta^{18}O$ values from 8.3 to 10.4 ‰.

Granitic rocks have whole-rock $\delta^{18}O$ values of between 9.0 and 12.2 ‰. These $\delta^{18}O$ values are higher than those of normal igneous granitic rocks (Taylor, 1978), and are representative of granites that were either derived from or exchanged oxygen with sedimentary or volcanic rocks or their metamorphosed equivalents. The whole-rock $\delta^{18}O$ values are intermediate between those of quartz and feldspar, with quartz $\delta^{18}O$ values between 10.7 and 11.6 ‰, and feldspar $\delta^{18}O$ values between 8.5 and 9.9 ‰.

Pelitic schists have whole-rock $\delta^{18}O$ values between 15.9 and 7.8 ‰. The high $\delta^{18}O$ values, between 15.9 and 13.9 ‰, occur in rocks from the eastern side of the pluton, and the low $\delta^{18}O$ values, 9.3 and 7.8 ‰, occur in rocks from the northwestern side of the pluton. The high $\delta^{18}O$ values are typical of shales and their metamorphosed equivalents (Garlick and Epstein, 1967; Savin and Epstein, 1970).

CONDITIONS OF METAMORPHISM

The pre-Tertiary stratigraphic sequence in the area is approximately 10 to 12 km thick (Albers and Stewart, 1972; Bonham and Garside, 1979), indicating that the pressure at the time of the intrusion of the Lone Mountain pluton was 3 to 3.5 kbar. This is corroborated by the presence of andalusite within pelitic schists that indicates that the pressure was less than 3.8 kbar (Holdaway and Mukhopadhyay, 1993). Pressure estimates from aluminum in hornblende geobarometry from the Lone Mountain granite give pressures of between 3.0 and 4.2 kbar using the experimental calibration of Johnson

and Rutherford (1989). Accordingly, the pressure of metamorphism at Lone Mountain is 3.5 ± 1 kbar.

The temperature of metamorphism estimated from calcite-dolomite thermometry, based on the magnesium content of calcite coexisting with dolomite (Anovitz and Essene, 1987) in calcite-dolomite marbles of the Reed Dolomite, overlying the Wyman Formation, records peak metamorphic temperatures of between 500 and 520°C. In calcite marbles, the divariant mineral assemblages calcite + quartz, and calcite + quartz + phlogopite, requires that fluids in equilibrium with calcite marbles during metamorphism must have had X_{CO_2} values greater than 0.2 at temperatures of around 500°C (Figure 3).

Most hornblende calc-silicate rocks contain the mineral assemblage hornblende + plagioclase + K-feldspar + epidote + quartz + biotite + calcite (Table 1). Within the system SiO_2-Al_2O_3-MgO-CaO-K_2O-H_2O-CO_2, this mineral assemblage, including an H_2O-CO_2 fluid, defines an isobaric invariant point that is located at a temperature of 490°C with X_{CO_2} = 0.098 at 3.5 kbar (Figure 3). All grossular calc-silicate rocks contain coexisting grossular, plagioclase, calcite, quartz, and wollastonite. Within the system SiO_2-Al_2O_3-CaO-CO_2, this mineral assemblage, again in the presence of an H_2O-CO_2 fluid, defines an invariant point at a temperature of 637°C with X_{CO_2} = 0.121 at 3.5 kbar (Figure 3). All grossular calc-silicate rocks also contain diopside, and many contain vesuvianite (Table 1). In the system SiO_2-Al_2O_3-MgO-CaO-H_2O-CO_2, mineral equilibria among grossular, diopside, plagioclase, wollastonite, calcite, quartz and vesuvianite, occur at more H_2O-rich conditions than those of the invariant point (Hochella and others, 1982; Valley and others, 1985; Labotka and others, 1988 b) (Figure 3).

In calcite marbles, minerals are close to pure end-members in composition (Table 2), so there is little effect on temperature or fluid composition if activities of minerals are used to calculate mineral equilibria. However, minerals in calc-silicate rocks are not

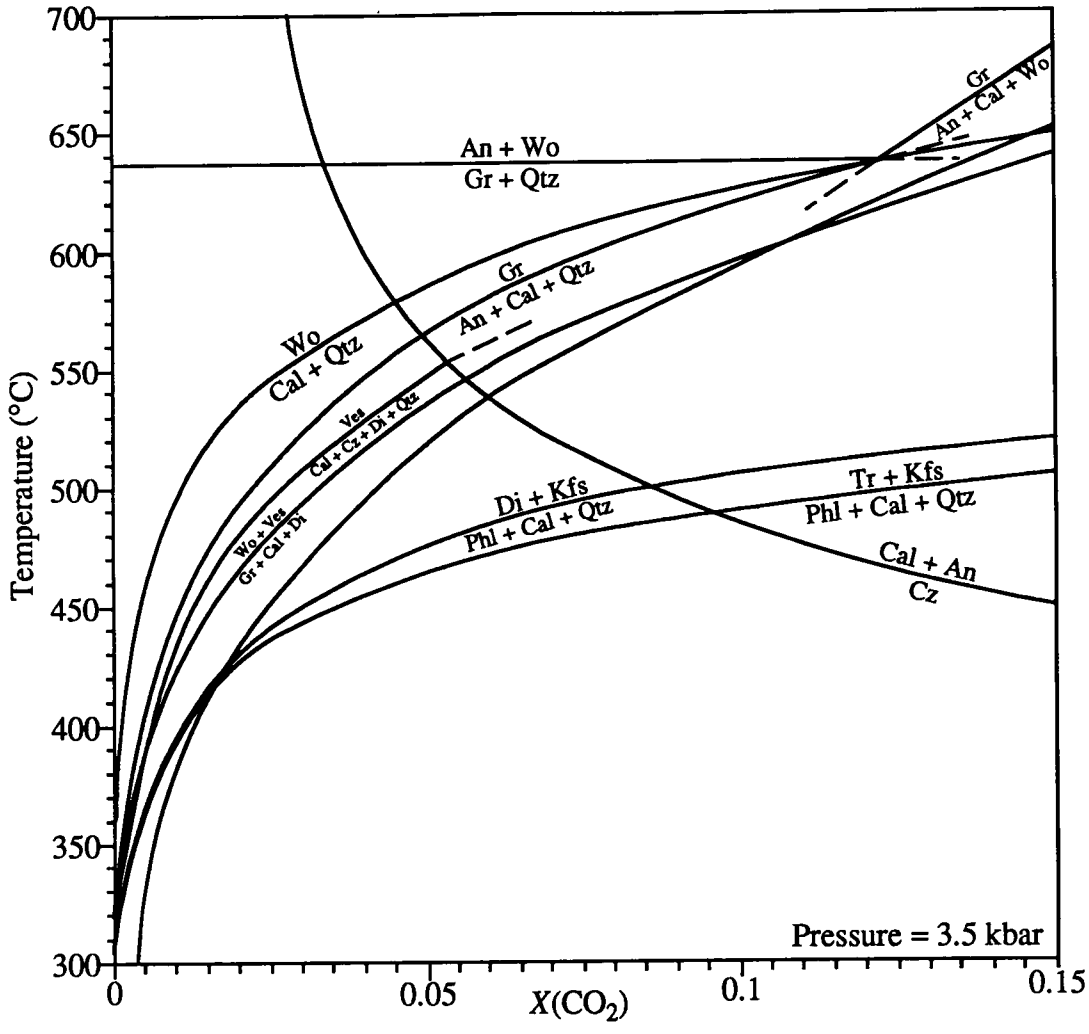

Figure 3: Isobaric T–X_{CO_2} diagram for the mineral assemblages in hornblende calc-silicate hornfels, grossular calc-silicate hornfels and calcite marble. The diagram was constructed using the computer program Vertex (Connolly, 1990) and the thermodynamic data of Holland and Powell (1991). The thermodynamic data of Holland and Powell (1991) was used in preference to that of Berman (1988), because it more closely reflects the experimental data of Zhu and others (1994) in the system SiO_2-Al_2O_3-CaO-CO_2, which is appropriate for Lone Mountain grossular calc-silicate rocks.

close to simple end member compositions (Table 2), so that recalculation of mineral equilibria using ideal ionic activities, drastically alters the locations of the mineral equilibria from those of the simple end-member systems. In particular, in grossular calc-silicate rocks the plagioclase is albite whereas the end-member reaction requires the plagioclase to be anorthite. This shifts plagioclase-bearing equilibria to much lower temperatures and much more H_2O-rich fluid compositions. Using calculated activities the invariant point in grossular calc-silicate rocks occurs at a temperature of 390°C and $X_{CO_2} = 0.001$. This is approximately 250°C lower in temperature and two orders of magnitude lower in X_{CO_2} than the simple end member system in grossular calc-silicate rocks. Similarly, consideration of calculated activities on the invariant point in hornblende calc-silicate rocks also lowers temperature and X_{CO_2}, and places the invariant point at a temperature of 430°C and $X_{CO_2} = 0.047$.

On the basis of on calcite-dolomite thermometry in marbles, and mineral equilibria in calc-silicate rocks, the temperature of metamorphism at Lone Mountain is taken to be 450 ± 70°C. On the scale of an outcrop, interlayered marbles and calc-silicate rocks at Lone Mountain must have experienced the same pressure and temperature conditions during metamorphism. Therefore, while the absolute values of X_{CO_2} for each mineral assemblage depend on the precise location of mineral equilibria, irrespective of the temperature, there is a progression in which fluid composition in marbles, hornblende calc-silicate rocks, and grossular calc-silicate rocks, was increasingly more H_2O-rich. Accordingly, fluid compositions in grossular calc-silicate hornfels, hornblende calc-silicate hornfels, and calcite marbles, are taken to be $X_{CO_2} = 0.002$, 0.05, and greater than 0.2, respectively.

FLUID-ROCK INTERACTION DURING METAMORPHISM

The amount of fluid evolved by Lone Mountain calc-silicate rocks during metamorphism was calculated using mass balance relationships between a protolith and a metamorphic

rock, assuming that metamorphism was isochemical except for loss of H_2O and CO_2 (Labotka and others, 1984; 1988 b). The mass balance relationship is $\mathbf{y} = \mathbf{Ax}$, where **y** is a vector representing the whole-rock chemical composition, **A** is a matrix representing the compositions of the minerals in the rock, and **x** is a vector representing the abundances of the minerals in the rock. The initial mass balance calculation determines the abundances of protolith minerals in the metamorphic rock. The abundances of protolith minerals are then used to recalculate the whole-rock chemical composition. Using this whole-rock chemical composition, except for H_2O and CO_2, the abundances of metamorphic minerals in the metamorphic rock are calculated. The result gives the total amount of H_2O and CO_2 that was evolved by the rock over its entire metamorphic history. Average mineral compositions from marbles and calc-silicate rocks (Table 2), and calc-silicate whole-rock compositions (Table 3) were used in the mass balance calculations. The H_2O and CO_2 contents of minerals were determined from mineral stoichiometry.

The protolith mineral assemblage for Lone Mountain calc-silicate rocks was assumed to be the mineral assemblage in low grade calcite marbles, i.e., calcite + quartz + muscovite + chlorite + albite + rutile, with or without K-feldspar. This mineral assemblage also occurs elsewhere within unmetamorphosed (?) Wyman Formation rocks (Stewart, 1970), and is common to other low grade carbonate rocks (e.g., Rice, 1977). Although, calcite is the only carbonate observed in rocks of the Wyman Formation at Lone Mountain, dolomite is a very common constituent of low-grade carbonate rocks, and occurs elsewhere within the Wyman Formation in western Nevada (McKee and Moiola, 1962; Sonderman, 1971) and eastern California (Nelson, 1962; Zenger, 1976). Phlogopite also occurs within Lone Mountain marbles, although it is thought not to be part of the original mineral assemblage but rather to have formed from reactions between

calcite, quartz, muscovite, and chlorite. Protolith mineral abundances, expressed as grams of mineral per kilogram of rock, are given in Table 5.

The mineral assemblage in the metamorphic rock was taken as the major observed mineral assemblage in each sample (Table 1). This excludes from consideration the minor amounts of epidote in grossular calc-silicate rocks and chlorite in hornblende calc-silicate rocks, such that the amount of H_2O evolved from calc-silicate rocks determined by mass balance are considered to be minimum estimates. In grossular calc-silicate rocks the metamorphic rock mineral assemblage is grossular + wollastonite + diopside + calcite + K-feldspar + albite, with or without vesuvianite, and in hornblende calc-silicate rocks, different combinations of K-feldspar, hornblende, plagioclase, epidote, quartz, biotite, calcite, and titanite. Metamorphic rock mineral abundances, expressed as grams of mineral per kilogram of rock, are given in Table 5.

The amount of CO_2 and H_2O lost by calc-silicate rocks during metamorphism is also given in Table 5. Grossular calc-silicate rocks lost an average of 210 ± 32 g (4.8 ± 0.7 mol) of CO_2 and 6 ± 2 g (0.3 ± 0.1 mol) of H_2O per kilogram of protolith, compared with hornblende calc-silicate rocks, which lost an average of 53 ± 17 g (1.2 ± 0.4 mol) of CO_2 and 17 ± 6 g (0.9 ± 0.3 mol) of H_2O per kilogram of protolith. The volume of fluid evolved by calc-silicate rocks during metamorphism resulted in a significant loss of the original protolith solid volume. The loss of CO_2 and H_2O from the rocks during metamorphism resulted in an average loss of $28\ \% \pm 3\ \%$ and $12\ \% \pm 6\ \%$ of the original solid rock volume of grossular and hornblende calc-silicate rocks, respectively. In grossular calc-silicate rocks the average volume of the evolved fluid was equivalent to $60\ \% \pm 8\ \%$ of the original solid volume of the protolith, and in hornblende calc-silicate rocks the average volume of the evolved fluid was equivalent to $18\ \% \pm 8\ \%$ of the original solid volume. This was calculated using volumes of H_2O and CO_2 of 21.5 and 45.3 cm^3/mol, respectively, appropriate for a temperature of 450°C and pressure of 3.5

Table 5: Mass balance between protolith and metamorphic rock

Grossular calc-silicate hornfels

Sample	Protolith							Metamorphic rock										
	Cal	Qtz	Rt	Ab	Ms	Chl	Kfs	Wo	Grs	Di	Ab	Cal	Kfs	Ves	H_2O	CO_2	V_{solid}	V_{fluid}
LM1	616	325	1	17	24	18		555	50	47	16	76	16		3	239	30	67
LM10	561	320	1	37	43	38		498	55	72	36	29	28	43	5	235	31	67
LM67-2	555	257	2	48	28	57	52	355	101	100	47	134	70		8	187	26	54
LM68-1	538	299	2	8	114	40		416	131	55	5	27	78	57	8	225	31	65
LM97-1	613	225	1	41	65	55		270	104	92	39	243	44	40	8	166	23	49
X	576	285	1	30	55	42	10	435	88	73	29	102	47	47	6	210	28	60
σ	36	43	1	17	37	16		113	35	23	17	90	26	9	2	32	3	8

Hornblende calc-silicate hornfels

Sample	Protolith							Metamorphic rock											
	Cal	Qtz	Rt	Ab	Ms	Chl	Kfs	Hbl	Pl	Kfs	Ep	Cal	Bt	Qtz	Ttn	H_2O	CO_2	V_{solid}	V_{fluid}
LM11	188	162	3	129	368	151		176	149	232	283			38	8	24	83	19	31
LM68-2	683	16	2	126	133	40			209	47		655	65	4	4	8	20	1	8
LM73	397	151	4	92	228	128		192	154	142	97	287		53	9	19	52	12	20
LM74-1	311	277	5	88	218	101		154	153	138	82	213		190	12	16	45	10	18
LM75-1	718		2	19	211	50				44	219	637	46			9	43	9	15
LM94	219	240	6	92	231	177	35	234	73	177	222	68		123	13	21	67	18	25
LM95-1	207	202	6	83	260	150	93	215	129	257	145	70		89	13	21	61	15	8
X	389	175	4	90	236	114	64	194	144	148	175	322	55	83	10	17	53	12	18
σ	225	91	2	36	70	53	41	32	44	83	79	265	14	67	4	6	20	6	8

Note: Grams of mineral per kilogram of protolith and metamorphic rock. X = mean, σ = standard deviation. H_2O, CO_2 = grams of H_2O and CO_2 lost during metamorphism. V_{solid} = percentage of protolith solid volume lost during metamorphism. V_{fluid} = percentage of protolith solid volume lost as fluid during metamorphism. Mineral abbreviations after Kretz (1983).

kbar (Burnham and others, 1969; Shmonov and Shmulovich, 1974). The average composition of the fluid evolved by the rocks during metamorphism was $X_{CO_2} = 0.93$ in grossular calc-silicate rocks, and $X_{CO_2} = 0.56$ in hornblende calc-silicate rocks.

Differences in the amount and composition of fluid evolved by grossular and hornblende calc-silicate rocks is a result of differences in the modal abundances of minerals in the protolith. Grossular calc-silicate rocks contained an average of 576 grams of calcite per kilogram of protolith, whereas hornblende calc-silicate rocks only contained an average of 389 grams of calcite per kilogram of protolith. This resulted in grossular calc-silicate rocks losing 157 grams more of CO_2 per kilogram of protolith than hornblende calc-silicate rocks lost. Similarly, hornblende calc-silicate rocks contained an average of 236 and 114 grams of muscovite and chlorite per kilogram of protolith, respectively, whereas grossular calc-silicate rocks only contained 55 and 42 grams of muscovite and chlorite per kilogram of protolith, respectively. This caused hornblende calc-silicate rocks to have lost an average of 11 more grams of H_2O per kilogram of protolith than grossular calc-silicate rocks.

FLUID INFILTRATION DURING METAMORPHISM

The composition of the fluid evolved by calc-silicate rocks during metamorphism differed significantly from the composition of the fluid with which the rocks were in equilibrium during metamorphism. Grossular calc-silicate rocks are in equilibrium with essentially pure H_2O, but they evolved very close to pure CO_2. Hornblende calc-silicate rocks were also in equilibrium with H_2O-rich fluids, but evolved more CO_2-rich fluids. The difference between the evolved fluid composition and the equilibrium fluid composition indicates that the calc-silicate rocks were infiltrated by substantial amounts of H_2O-rich fluids during metamorphism.

The effects of fluid infiltration in calc-silicate rocks during metamorphism are also recorded in the stable isotopic compositions of the calc-silicate rocks. Unlike many

other contact metamorphic terranes, at Lone Mountain, because of the prior regional metamorphic event, and the variation in rock type, there is not a progression from unmetamorphosed rocks to their metamorphosed equivalents. Accordingly, the oxygen isotopic composition of the calc-silicate rock protoliths can only be inferred, using the $\delta^{18}O$ values of Lone Mountain pelitic schists and calcite marbles. Appropriate mixtures of calcite and silicate minerals give hypothetical precursor whole-rock $\delta^{18}O$ values for Lone Mountain calc-silicate rocks of between 16.5 and 18.6 ‰. These values are considerably less than their present values, and indicate that calc-silicate rocks had their isotopic compositions lowered during metamorphism.

The amount of carbon lost from the calc-silicate rocks during metamorphism, together with the carbon stable isotopic data indicate that decarbonation of calc-silicate rocks was mostly fractional, i.e., that the CO_2 was removed from the rock as soon as it was evolved (Figure 4), although not all decarbonation was fractional such that CO_2 was also released periodically during batch decarbonation. This style of decarbonation has the implication that nearly pure H_2O must have infiltrated the calc-silicate rocks in order to remove the CO_2 effectively, as soon as it was evolved from the rocks.

Although decarbonation reactions can account for the depleted $\delta^{13}C$ values in calc-silicate rocks, similar calculations for oxygen isotopes in calc-silicate rocks indicate that the $\delta^{18}O$ values of calc-silicate rocks cannot have been depleted by decarbonation reactions alone (Figure 5). This is because decarbonation will only cause a small change in the $\delta^{18}O$ values of calc-silicate rocks, as there is only a minor amount of oxygen as CO_2 in calc-silicate rocks (Valley, 1986). The depletion of ^{18}O in calc-silicate rocks must therefore have been caused by exchange with externally derived fluids. The depletions in ^{18}O and ^{13}C of calc-silicate rocks are strongly correlated with both the modal abundance of calcite, expressed as weight percent CO_2 (Figure 6), and also with the loss of solid volume of the calc-silicate rocks (Figure 7). The loss in solid volume, as

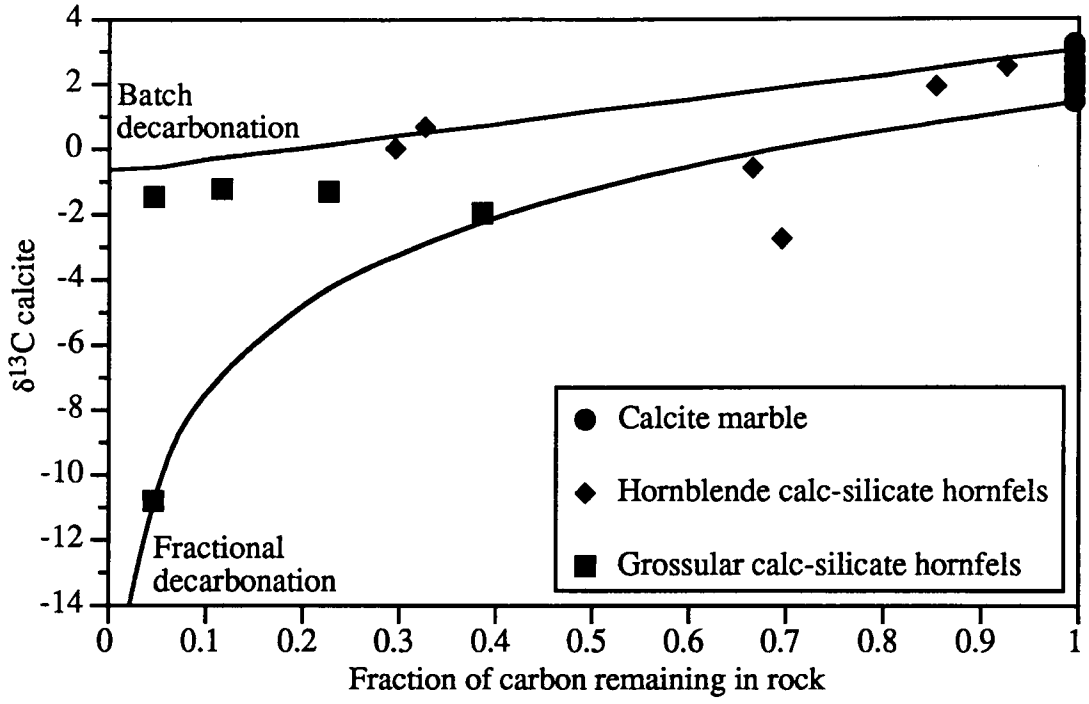

Figure 4: $\delta^{13}C$ calcite versus the fraction of carbon remaining in the rock for hornblende calc-silicate hornfels, grossular calc-silicate hornfels and calcite marble. The theoretical batch decarbonation curve was calculated using the equation $\delta^{13}C_{final} = \delta^{13}C_{initial} - (1-F)$ 1,000 $\ln\alpha$. The theoretical fractional decarbonation curve was calculated using the equation $\delta^{13}C_{final} = \delta^{13}C_{initial} + 1{,}000\ (F^{(\alpha-1)} - 1)$. $\delta^{13}C_{initial} = 3.0$ ‰ for batch decarbonation and 1.4 ‰ for fractional decarbonation. Both the batch and fractional decarbonation curves were calculated using the calcite-CO_2 fractionation factor of Chacko and others (1991) at 450 °C.

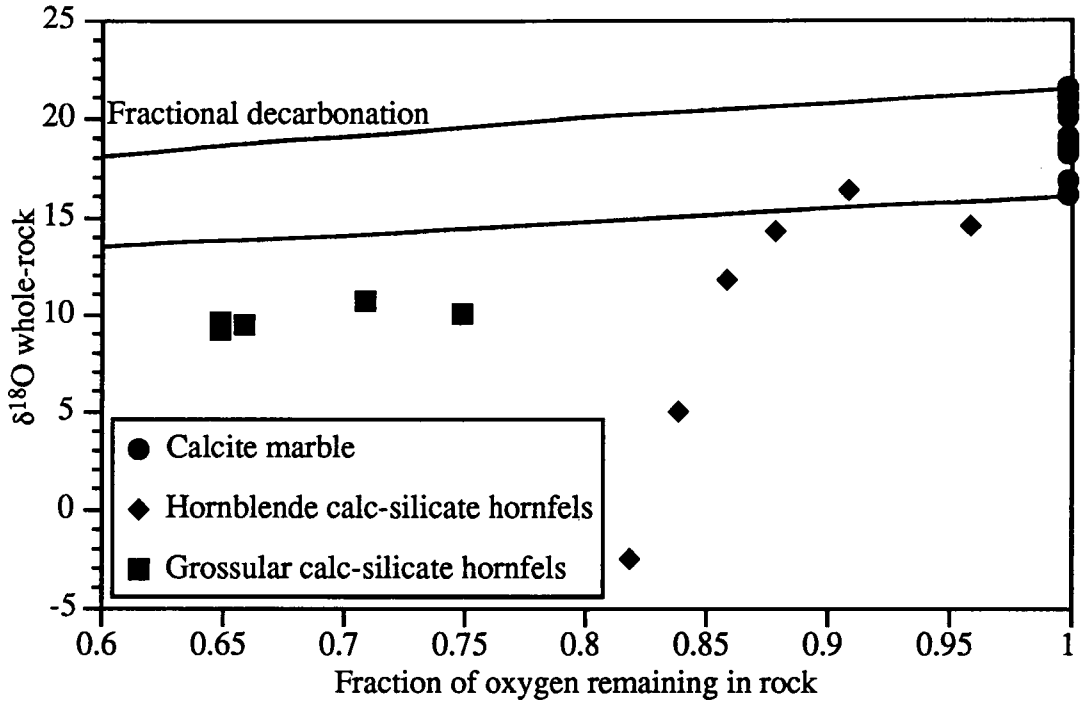

Figure 5: $\delta^{18}O$ whole-rock versus the fraction of oxygen remaining in the rock for hornblende calc-silicate hornfels, grossular calc-silicate hornfels and calcite marble. The theoretical fractional decarbonation curve was calculated using the equation $\delta^{18}O_{final} = \delta^{18}O_{initial} + 1{,}000\ (F^{(\alpha-1)} - 1$. $\delta^{18}O_{initial} = 21.5$ and 16.1 ‰. The fractional decarbonation curve was calculated using the calcite-CO_2 fractionation factor of Chacko and others (1991) at 450 °C.

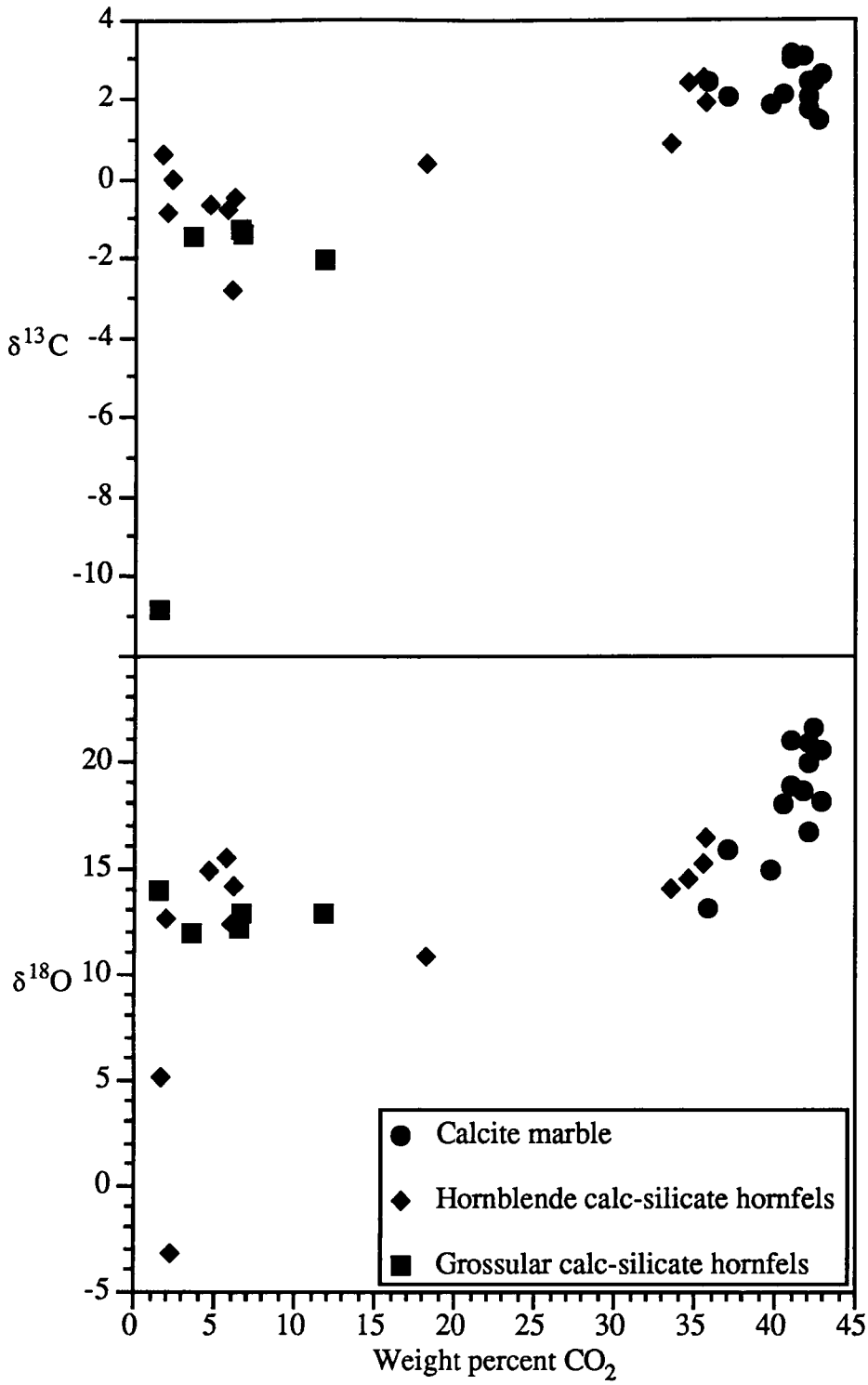

Figure 6: $\delta^{13}C$ and $\delta^{18}O$ of calcite versus weight percent CO_2 of calcite for hornblende calc-silicate hornfels, grossular calc-silicate hornfels and calcite marble.

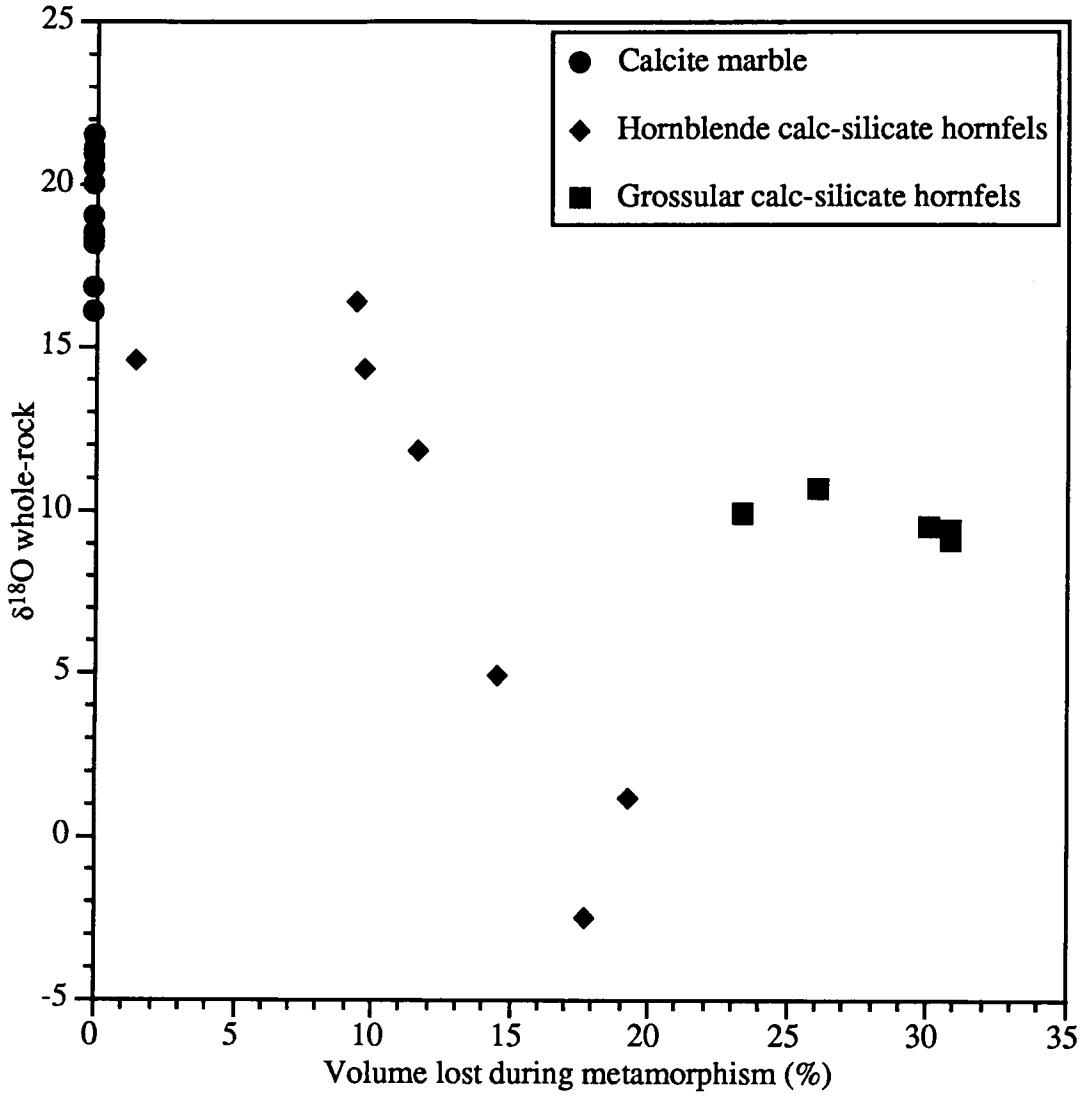

Figure 7: $\delta^{18}O$ whole-rock versus volume lost during metamorphism for hornblende calc-silicate hornfels, grossular calc-silicate hornfels and calcite marble.

a result of increased permeability due to devolatilization reactions among minerals in calc-silicate rocks, facilitated fluid flow during metamorphism allowing stable isotopic exchange to occur between rocks and fluid (Rumble and others, 1982; Nabelek and others, 1984; 1992). In contrast to calc-silicate rocks, no changes in the stable isotopic compositions of Lone Mountain calcite marbles could have occurred as a result of metamorphic decarbonation reactions, as marbles typically have greater than ninety-five percent calcite, and therefore have lost essentially none of their original CO_2.

Systematic relationships between the modal abundance of calcite, the loss of solid volume in calc-silicate rocks, and the $\delta^{18}O$ values of the metamorphic rocks indicate that rock type exerts a first order influence on the flow of fluid through the rocks. This is confirmed by the lack of any recognizable correlation between calcite $\delta^{18}O$ values of specific rock types and distance from the pluton (Figure 8), which suggests that fluid flow was channeled along the calc-silicate rock layers.

The amount of fluid that infiltrated the calc-silicate rocks while they were undergoing devolatilization reactions during metamorphism was determined by mass balancing the fluid that was evolved from the rocks with an appropriate amount of H_2O that was infiltrating the rock, until the equilibrium fluid composition was achieved (Ferry, 1980). The extent of devolatilization that grossular calc-silicate rocks underwent required the infiltration of an extraordinary amount of water, an average of 43 ± 7 kg of H_2O per kg of rock. For hornblende calc-silicate rocks, the water that infiltrated the metamorphic rock was substantially less than that which infiltrated grossular calc-silicate rocks, 395 ± 124 g of H_2O infiltrated every kg of rock. This is equivalent to a fluid/rock ratio, by mass, of 43 in grossular calc-silicate rocks and 0.40, two orders of magnitude smaller, in hornblende calc-silicate rocks. Mass balance calculations using stable isotopes (Taylor, 1974) give fluid/rock ratios, in mass units, of between 0.42 and 0.91,

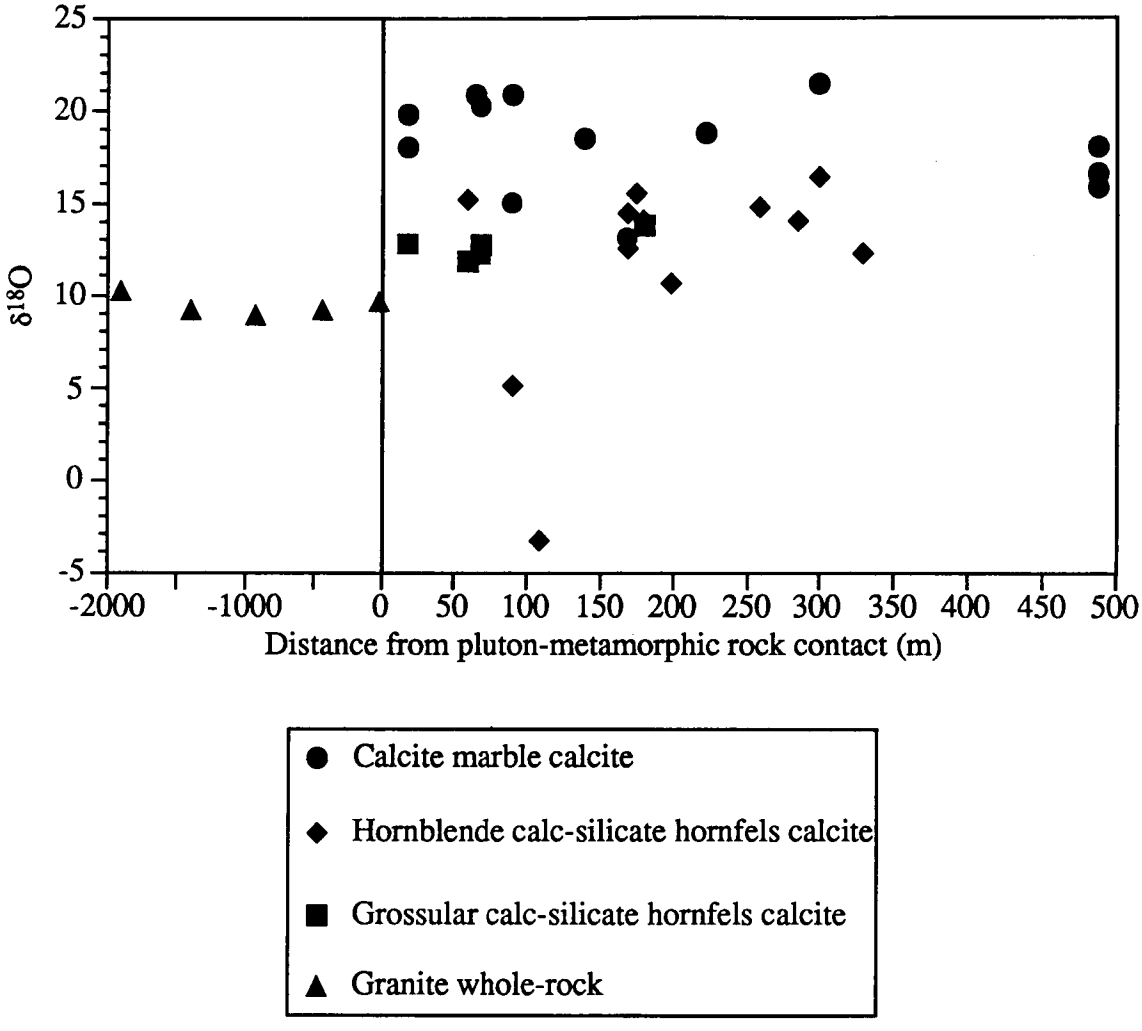

Figure 8: $\delta^{18}O$ calcite from hornblende calc-silicate hornfels, grossular calc-silicate hornfels and calcite marble, and $\delta^{18}O$ whole-rock from granite versus distance from the pluton-metamorphic rock contact.

with an average of 0.68, in grossular calc-silicate rocks, and 0.15 to 0.75, with an average of 0.49, in hornblende calc-silicate rocks.

Thus, for hornblende calc-silicate rocks both petrologic and stable isotopic fluid/rock ratios are in good agreement as they have similar values, but for grossular calc-silicate rocks there are significant differences between petrologic and stable isotopic fluid/rock ratios. Discrepancies between petrologic and stable isotopic fluid/rock ratios in grossular calc-silicate hornfelses are the result of the petrologic and stable isotopic systems within grossular calc-silicate rocks recording different responses to metamorphism. It is for this reason, that the utility of fluid/rock ratios has been questioned, as they cease to record the amount of fluid that flowed through the rock, i.e. the fluid flux, once the infiltrating fluid and the rock have attained equilibrium (Baumgartner and Ferry, 1991).

SOURCE OF INFILTRATING FLUID

Fluid flow during metamorphism is a complex process, and there is considerable debate as to whether fluids flow in the direction of increasing temperature (Ferry, 1991; Ferry and Dipple, 1991; Dipple and Ferry, 1992) or decreasing temperature during metamorphism (Nabelek and others, 1984; 1992; Labotka and others, 1988 b; Hanson, 1992; Bowman and others, 1994). In order to determine the direction of fluid movement during metamorphism, the source of the infiltrating fluid must be known. Meteoric fluid is probably not a major source of externally derived fluid, because the depth of emplacement of the Lone Mountain pluton is at the limit at which meteoric hydrothermal systems develop (Criss and Taylor, 1986). Two other possible major sources of externally derived fluid are, magmatic fluid from the Lone Mountain pluton, and metamorphic fluid from the surrounding metamorphic rocks.

The Lone Mountain pluton has a radius of between 4 and 5 km. If magmatic fluids flowed outward from the pluton into the surrounding country rocks, the effects

would only be observed within 435 to 350 m of the pluton (Dipple and Ferry, 1992). Grossular calc-silicate rocks occur as roof pendants and along the margins of the Lone Mountain pluton and are thus confined to within 180 m of the pluton. Similarly, hornblende calc-silicate rocks were only observed as far as 330 m from the pluton. These distances meet the criteria that the fluids that infiltrated the metamorphic rocks may have flowed in the direction of decreasing temperature away from the pluton. Phase equilibrium constraints indicate that fluids that infiltrated the calc-silicate rocks must have been essentially pure H_2O, a criterion that magmatic fluids also adhere to. Fluids that infiltrated the calc-silicate rocks are assumed to have been in equilibrium with the most depleted grossular calc-silicate rocks at the temperatures of metamorphism. This requires that the fluids had $\delta^{18}O$ values of between 11.5 and 9.4 ‰. This is within the range of the $\delta^{18}O$ values that magmatic fluids from the Lone Mountain granite would have had, which was between 8.5 and 9.9 ‰, derived from the range in $\delta^{18}O$ values of feldspar from the Lone Mountain pluton. The lowering of the original $\delta^{18}O$ values in calc-silicate rocks to values that are close to those of the Lone Mountain granite also strongly suggests that the calc-silicate rocks were infiltrated by fluids that were in equilibrium with the granite.

Fluids in equilibrium with calcite and quartz in calc-silicate protoliths at a temperature of 150°C have $\delta^{18}O$ values of between 2.3 and 5.4 ‰, based on the oxygen isotopic fractionations between quartz and water (Bottinga and Javoy, 1973), and calcite and water (O'Neil and others, 1969), respectively. If the ambient temperature of the country rocks prior to pluton emplacement was higher than 150°C, due to the prior regional metamorphic event, then the $\delta^{18}O$ values of fluids within the metamorphic rocks would have ranges similar to those in equilibrium with calc-silicate rocks during metamorphism, 12.5 to 12.8 ‰ at 300°C. The isotopic composition of the fluids initially in the rocks would also increase as a result of interaction with high ^{18}O rocks during

metamorphism. Thus the range in $\delta^{18}O$ values of fluid present in the sedimentary rocks prior to metamorphism suggests that may also have been a possible source of fluid that infiltrated the metamorphic rocks. Thus, it is not possible to unequivocally determine the source of the fluids that infiltrated the calc-silicate rocks, although these are presumed to have been magmatic fluids emanating from the Lone Mountain granitic pluton, because the pluton is the only possible source that could have provided sufficient quantities of fluid to account for the large fluid-rock ratios measured in the grossular calc-silicate rocks.

A MODEL FOR GROSSULAR AND HORNBLENDE CALC-SILICATE HORNFELS METAMORPHISM

A statistical analysis of the whole-rock chemical compositions of hornblende and grossular calc-silicate rocks was performed in order to determine whether the two calc-silicate rock types have different whole-rock chemical compositions. The Wilcoxon rank sum test was used to test the hypothesis that the whole-rock chemical compositions of grossular and hornblende calc-silicate rocks are different at the 5 % significance level (Table 6). In order for the Wilcoxon rank sum test to be valid, the weight percent oxides of the calc-silicate rocks must be independent of each other, both within each calc-silicate rock type and between grossular and hornblende calc-silicate rocks. The Wilcoxon rank sum test is a nonparametric statistical test, so it does not consider the weight percent oxide values themselves, but their ranks, and so is resistant to outliers in the data and is also robust when applied to small sample populations. Also shown for comparison are the results of an unpaired t-test that is the parametric equivalent of the Wilcoxon rank sum test. This test assumes that the data have a normal distribution. There is little difference between the results of the two statistical tests indicating that the results of the statistical analysis are rigorous and that TiO_2, Al_2O_3, FeO, CaO, Na_2O, and K_2O can each be used to distinguish grossular calc-silicate rocks from hornblende calc-

Table 6: Statistical analysis of calc-silicate hornfels whole-rock chemical compositions

	Wilcoxon rank sum test			Unpaired t-test		
	Mean rank			Mean		
Variable	Grossular calc-silicate hornfels	Hornblende calc-silicate hornfels	p-value	Grossular calc-silicate hornfels	Hornblende calc-silicate hornfels	p-value
SiO_2	5.80	7.00	0.5698	44.55	40.49	0.6424
TiO_2	3.90	8.36	0.0344	0.20	0.47	0.0236
Al_2O_3	3.00	9.00	0.0045	4.49	13.86	0.0010
FeO	3.80	8.43	0.0284	1.73	4.56	0.0122
MnO	4.70	7.79	0.1403	0.05	0.08	0.0863
MgO	5.20	7.43	0.2912	1.21	1.59	0.3165
CaO	9.60	4.29	0.0118	40.52	22.91	0.0073
Na_2O	3.80	8.43	0.0278	0.25	0.89	0.0096
K_2O	4.00	8.29	0.0424	0.64	2.48	0.0488
CO_2	6.80	6.29	0.8075	12.39	6.15	0.4207

Note: If a variable has a p-value of less than 0.05, it indicates that grossular and hornblende calc-silicate rocks are different at the 5% significance level.

silicate rocks. It is therefore concluded that the whole-rock chemical compositions of grossular and hornblende calc-silicate rocks are significantly different.

Although grossular and hornblende calc-silicate rocks have different whole-rock chemical compositions, their protoliths had the same mineralogy. Model protoliths for grossular and hornblende calc-silicate rocks differ in that grossular calc-silicate hornfels protoliths are dominated by calcite and quartz, whereas hornblende calc-silicate hornfels protoliths contain significant amounts of muscovite and chlorite as well as quartz and calcite. To understand the differences in metamorphic histories between grossular and hornblende calc-silicate rocks, model reaction histories were determined for representative calc-silicate rocks, grossular calc-silicate hornfels LM10, and hornblende calc-silicate hornfels LM73 (Table 7). These particular samples were chosen because they have modal abundances and evolved fluid amounts and compositions that are similar to the average for each calc-silicate rock type. Simple end member mineral compositions in the system SiO_2-Al_2O_3-MgO-CaO-K_2O-H_2O-CO_2 were used to compare the two different calc-silicate rock types. As textural relationships among the minerals in calc-silicate rocks are complex, the actual reactions that occurred among the minerals in the rock to produce the observed final mineral assemblage can only be inferred.

Initially similar reactions occurred among the protolith minerals in both grossular and hornblende calc-silicate rocks. In the initial protolith mineral assemblage, calcite, quartz, muscovite, and chlorite reacted with one another to produce phlogopite and anorthite. In hornblende calc-silicate rocks, chlorite was used up before muscovite, so calcite, quartz, and muscovite continued to react to produce K-feldspar and plagioclase, while in grossular calc-silicate rocks, muscovite was used up before chlorite, so that calcite, quartz, and chlorite reacted to form diopside and anorthite. Calcite, quartz, and phlogopite then reacted to form diopside and K-feldspar, which produced the mineral

Table 7: Metamorphism of model grossular and hornblende calc-silicate rocks

Grossular calc-silicate hornfels LM10

	Protolith					Metamorphic rock		
Calcite	561	544	542	509	507	60	48	41
Quartz	320	311	309	270	269	0	0	0
Plagioclase	37	42	43	43	43	43	12	0
Muscovite	43	0	0	0	0	0	0	0
Chlorite	38	2	0	0	0	0	0	0
Rutile	2	2	2	2	0	0	0	0
Phlogopite		45	45	0	0	0	0	0
Diopside			4	74	74	74	74	70
K-feldspar				30	30	30	30	31
Titanite					4	4	4	4
Wollastonite						520	506	503
Grossular							54	54
Vesuvianite								23
Total	1000	946	944	928	927	730	727	726
H_2O loss		5	5	7	9	9	9	8
CO_2 loss		8	9	23	24	221	226	229

Hornblende calc-silicate hornfels LM73

	Protolith				Metamorphic rock	
Calcite	397	335	316	311	281	271
Quartz	151	119	96	93	21	21
Plagioclase	92	112	161	161	161	83
Muscovite	228	75	0	0	0	0
Chlorite	128	0	0	0	0	0
Rutile	4	4	4	0	0	0
Phlogopite		161	161	161	56	56
K-feldspar			52	52	122	122
Titanite				10	10	10
Tremolite					122	122
Epidote						97
Total	1000	805	791	788	773	781
H_2O loss		17	20	20	22	20
CO_2 loss		27	35	38	51	55

Note: Grams of mineral per kilogram of rock in going from protolith to metamorphic rock by reactions described in text. H_2O and CO_2 loss are cumulative losses after each reaction.

assemblage observed in high-grade calcite marbles. Conversion of rutile to titanite by the reaction rutile + calcite + quartz = titanite + CO_2, occurred in both grossular and hornblende calc-silicate rocks. At this stage grossular calc-silicate rocks were completely dehydrated by the loss of 9 g of H_2O, but had only lost 24 g of CO_2, from the original kilogram of protolith. The fluid that had thus far been evolved from grossular calc-silicate rocks had an average composition of $X_{CO_2} = 0.52$. In marked contrast to this, hornblende calc-silicate rocks had already lost most of their H_2O, 20 g, and a large portion, 38 g, of their CO_2. This fluid had $X_{CO_2} = 0.44$. In grossular calc-silicate rocks, after phlogopite was exhausted, calcite and quartz reacted to form wollastonite which released an additional 197 g of pure CO_2. Grossular and vesuvianite then formed by reactions such as anorthite + wollastonite + calcite = grossular + CO_2, and anorthite + wollastonite + calcite + diopside + H_2O = vesuvianite + CO_2, and produced the mineral assemblage observed in grossular calc-silicate rocks. At the same time, the minerals in hornblende calc-silicate rocks reacted to produce tremolite and epidote by reactions associated with the invariant point, calcite + quartz + phlogopite = tremolite + K-feldspar + H_2O + CO_2, and calcite + anorthite + H_2O = epidote + CO_2. Grossular calc-silicate rocks evolved a total of 8 g of H_2O and 229 g of CO_2, of composition X_{CO_2} = 0.92, while hornblende calc-silicate rocks lost 20 g of H_2O and 55 g of CO_2 with a composition that had $X_{CO_2} = 0.53$.

The subtle differences in whole-rock chemistry and protolith mineral abundances between grossular and hornblende calc-silicate rocks resulted in their having vastly different metamorphic reaction histories. This resulted in grossular calc-silicate rocks being infiltrated by approximately two orders of magnitude more fluid than hornblende calc-silicate rocks. Correlations between the modal abundance of calcite, the solid volume lost during metamorphism, and the stable isotopic compositions of metamorphic rocks together with the lack of any kind of systematic variation in the stable isotopic

composition of the metamorphic rocks with distance from the Lone Mountain pluton indicates that in detail fluid flow was primarily through grossular calc-silicate layers, with some fluid flow through hornblende calc-silicate layers, with interlayered marble layers remaining essentially impermeable.

PART FOUR

PETROGENESIS OF THE LONE MOUNTAIN GRANITIC PLUTON

ABSTRACT

The Late Cretaceous Lone Mountain granitic pluton intrudes Late Proterozoic to Cambrian metasedimentary rocks in southwestern Nevada, and consists of granite with minor granodiorite and quartz monzonite. Temperatures of pluton emplacement estimated from the partitioning of iron and magnesium between garnet and biotite and from edenite exchange between hornblende and plagioclase, are between 650 and 750 °C; whereas temperatures based on the oxygen isotopic compositions of quartz and feldspar are lower, at between 325 and 615 °C, indicating that some subsolidus re-equilibration of isotopes occurred after pluton emplacement. Estimates of the pressure of pluton emplacement from aluminum in hornblende geobarometry, from consideration of the stability of epidote plus quartz and from the stability of muscovite + quartz in conjunction with the water-saturated granite solidus all suggest pressures of crystallization of around 3.5 kbar. This pressure is consistent with that estimated from the country rocks surrounding the pluton and is equivalent to a depth of pluton emplacement of between 12 and 15 km. High whole-rock $\delta^{18}O$ values, between 9.0 and 12.2 ‰, together with an initial $^{87}Sr/^{86}Sr$ ratio of 0.7071, indicate that sedimentary or volcanic rocks must have provided a significant component of the source rocks for the granite. Lone Mountain granitic rocks could have been derived from rocks that currently surround the pluton, although isotopic data and phase equilibrium considerations negate the generation of peraluminous Lone Mountain granitic magma solely by the partial melting of Lone Mountain pelitic schists. Chemical variation in the pluton from the most primitive parental magma composition, hornblende granodiorite, to the most evolved magma composition, garnet granite, can occur by fractional crystallization of hornblende and plagioclase; however, the well-developed foliation along the margin of the pluton and the lack of any systematic geochemical variation from the core to the rim of the

pluton requires replenishment of the magma chamber to have occurred during multiple intrusive events associated with the emplacement of the Lone Mountain pluton.

INTRODUCTION

Although granitoid magmas are generated from a variety of source rocks in many different geologic settings, they all have broadly similar mineralogies and chemical compositions. Notwithstanding their general similarities, granitoids have distinctive petrological and geochemical characteristics that allow both primary magmatic processes and the nature of the magma source rocks to be identified. Both radiogenic and stable isotopic studies are particularly useful in determining granite petrogenesis, inferring the nature of the magma source rocks, and deciding whether rocks preserve their primary igneous characteristics or have been altered by secondary processes.

In the western United States, regional studies using Pb, Sr, Nd, and O isotopic systems have been able to characterize distinct crustal regimes, which are manifested in the Mesozoic and Cenozoic granitic rocks of the region (Zartman, 1974; Farmer and DePaolo, 1983; Solomon and Taylor, 1989; Kistler, 1990). In very general terms, the results of these studies indicate that distinctly different source rocks are responsible for the generation of granitic rocks in the western United States, with peraluminous granitoids derived from Precambrian sialic rocks and metaluminous granitoids derived from Phanerozoic rocks that have upper mantle affinities.

The aim of this study is to determine the petrogenesis of the Late Cretaceous Lone Mountain granitic pluton in southwestern Nevada. A chemical and stable isotopic study of the Lone Mountain pluton was undertaken in order determine the conditions of emplacement, the possible source rocks of the granitic magma, and the primary igneous differentiation processes.

GEOLOGIC SETTING

Mesozoic and Cenozoic plutonism in the western United States produced the Sierra Nevada and Peninsular Ranges batholiths, and numerous isolated plutons throughout the Cordillera. Details of the Mesozoic plutonism in the Cordillera have been summarized by Miller and Barton (1990): Middle to Late Jurassic plutonism was widespread, but not particularly voluminous, and varied in composition from gabbro to granite, with potassic rocks dominant. Cretaceous plutonism was both widespread, and voluminous, becoming more intense and compositionally more felsic and peraluminous with time, such that granodiorite and granite are abundant, and mafic rocks are insignificant.

The Lone Mountain granitic pluton (Figure 1) is one of several large intrusions that occurs to the east of the Sierra Nevada batholith in the Cordillera. The Lone Mountain pluton is Late Cretaceous in age, with a Rb-Sr whole-rock age of 85.3 $\pm$ 4.3 million years (John and Robinson, 1989) and with K-Ar dating of muscovite and biotite giving ages of 69.2 $\pm$ 1.4, and 71.1 $\pm$ 1.4 million years, respectively (Silberman and others, 1975). The 85 million year Rb-Sr age probably represents the age of emplacement of the Lone Mountain pluton, whereas the younger, 70 million year K-Ar age represents a cooling age associated with the beginning of uplift and extension of the terrane.

The Lone Mountain pluton is dominated by granitic rocks, but other igneous rocks also occur associated with the pluton. The oldest igneous rocks exposed in the area are gabbros, which intrude the metasedimentary rocks surrounding the pluton, and occur as isolated roof pendants in the granite (Bonham and Garside, 1979). The 113.0 $\pm$ 3.0 million year K-Ar age of hornblende from the gabbro probably represents a minimum age, because heating of the gabbro during emplacement of the granite would have caused the loss of radiogenic Ar from hornblende (Bonham and Garside, 1979). Magnetic and gravity highs associated with the Lone Mountain pluton indicate that gabbro underlies the main granite pluton (Synder, written communication 1983, in John and Robinson,

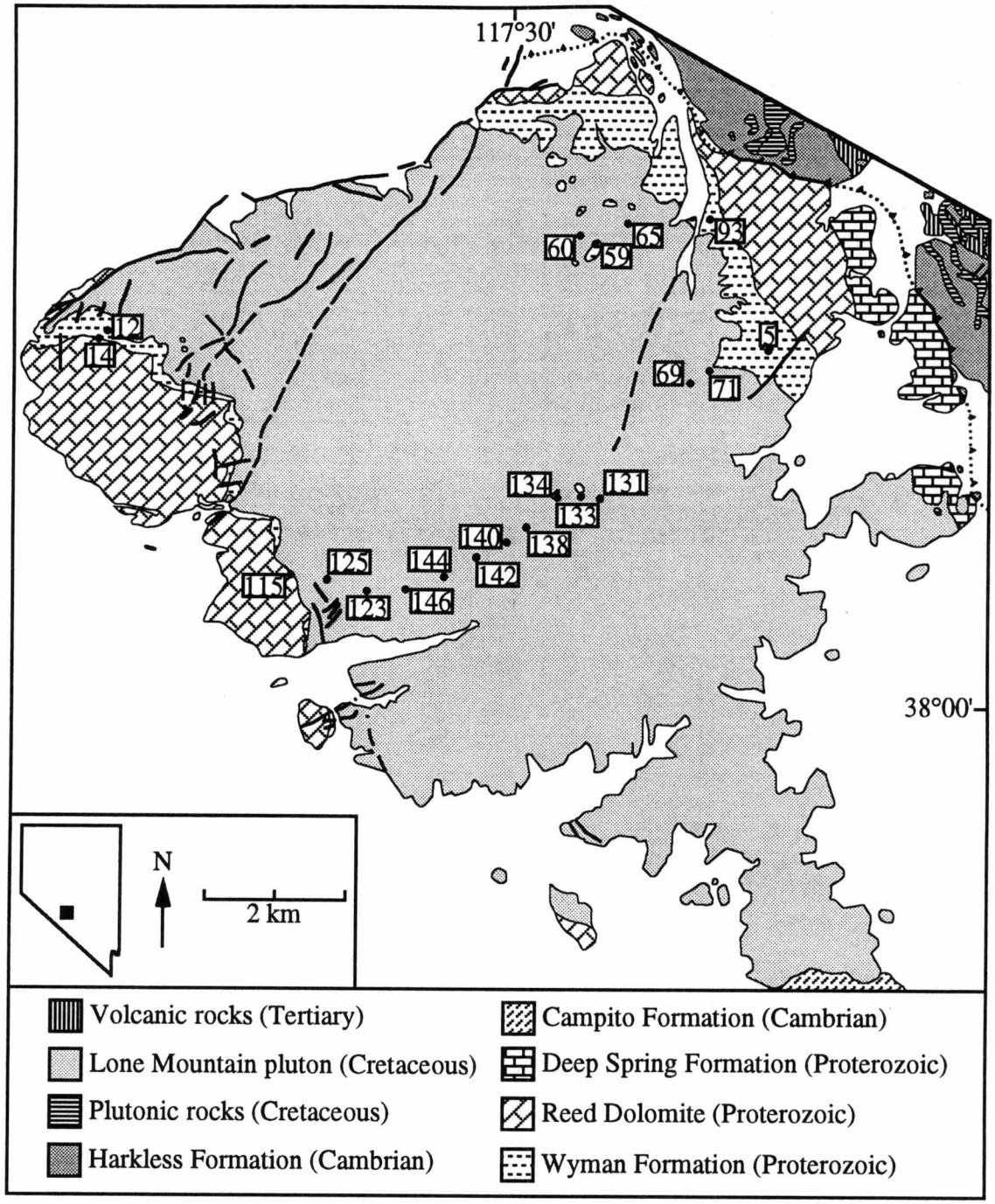

Figure 1: Geologic map of the Lone Mountain area (modified after Maldonado, 1984, and Bonham and Garside, 1979). The numbers on the map represent sample locations.

1989). Numerous lamprophyre and silicic porphyry dikes also intrude both the Lone Mountain pluton and the surrounding metasedimentary rocks. The silicic porphry dikes have zircon fission-track ages of 22.1 $\pm$ 3.2 million years (Bonham and Garside, 1979).

The Lone Mountain pluton intruded Late Proterozoic to Cambrian marbles, calc-silicate hornfelses, and pelitic schists, with pluton emplacement either doming the metasedimentary rocks into a northwest-trending anticline (Maldonado, 1984), or occurring within the core of a pre-existing northwest-trending anticline (Albers and Stewart, 1972). In general, the pluton has sharp, generally concordant contacts with the surrounding metasedimentary rocks, and the pluton itself displays a well-developed foliation along its margin that is parallel to the layering in the wall rocks. The rocks surrounding the pluton underwent greenschist facies regional metamorphism before intrusion of the pluton and were subsequently contact metamorphosed in association with the emplacement of the pluton.

WHOLE-ROCK CHEMISTRY

Whole-rock major and trace element analyses, together with CIPW norms for granitic rocks are given in Table 1. Granitic rocks of the Lone Mountain pluton have chemical compositions indicating that they are calc-alkaline and metaluminous to peraluminous (Figure 2). These rocks also have a high, and relatively restricted range in silica, with between 76.4 and 68.8 weight percent SiO_2. On Harker variation diagrams (Figure 3), most of the major oxides and trace elements decrease with increasing SiO_2. Although these overall trends were observed in the chemistry of the granites, there is no systematic variation in granite chemistry from the core to the rim of the pluton.

The whole-rock major and trace element compositions of gabbro associated with the Lone Mountain pluton, and pelitic schists surrounding the pluton are given in Table 2. Both gabbro and pelitic schist have lower SiO_2, higher TiO_2, Al_2O_3, Fe_2O_3, MnO,

Table 1: Whole-rock X-ray fluorescence analyses and CIPW norms of granite

Sample	LM60	LM65	LM69	LM71	LM115-1	LM 123	LM 125
SiO_2	76.4	75.1	76.4	76.2	68.8	71.4	70.2
TiO_2	0.01	0.01	0.04	0.03	0.34	0.28	0.30
Al_2O_3	13.8	14.4	13.3	14.5	17.1	15.3	16.7
Fe_2O_3	0.71	0.49	0.39	0.37	2.03	1.59	1.86
MnO	0.06	0.04	0.05	0.03	0.04	0.03	0.04
MgO	0.22	0.14	0.01	0.09	0.52	0.43	0.43
CaO	1.22	1.18	0.82	1.45	2.01	1.41	2.01
Na_2O	3.63	4.04	5.48	4.77	5.09	4.26	4.98
K_2O	4.96	5.11	3.65	4.20	3.80	4.53	4.34
P_2O_5	0.02		0.01		0.08	0.06	0.08
Total	101.04	100.56	100.15	101.62	99.81	99.34	100.93
Cu	15	14	20	14	8	9	10
V					19	18	16
Cr					18		
Co					4	4	4
Ni	6	6	9	6	6	6	5
Zn	31	33	77	34	34	29	22
Pb	32	34	55	30	27	26	23
Rb	190	191	165	154	247	175	181
Sr	512	485	520	479	886	637	782
Y	15	13	19	20	28	16	22
Zr	381	372	308	317	506	306	383
Nb	8	9	12	8	9	6	7
Mo	6	8	11	7	2	1	
Ba	1346	1344	1478	1255	1552	1504	1615
quartz	32.82	28.90	29.13	29.10	18.30	24.69	18.52
corundum	0.27	0.10			1.17	0.97	0.36
orthoclase	29.31	30.20	21.57	24.82	22.46	26.77	25.65
albite	30.71	34.18	46.37	40.36	43.07	36.05	42.14
anorthite	5.92	5.85	0.97	5.80	9.45	6.60	9.45
diopside			1.45	1.19			
hypersthene	1.95	1.31		0.30	4.54	3.58	4.07
ilmenite	0.02	0.02	0.08	0.06	0.65	0.53	0.57
apatite	0.05		0.02		0.19	0.14	0.19

Table 1: (continued)

Sample	LM 131-2	LM 134-2	LM 138	LM 140	LM 142	LM144	LM 146
SiO_2	74.6	71.3	71.5	71.0	71.5	73.2	68.9
TiO_2	0.23	0.26	0.30	0.26	0.24	0.31	0.32
Al_2O_3	14.7	16.6	16.1	15.9	16.0	15.0	17.6
Fe_2O_3	1.23	1.39	1.50	1.43	1.38	1.75	1.58
MnO	0.03	0.04	0.03	0.03	0.03	0.04	0.03
MgO	0.26	0.31	0.33	0.40	0.30	0.42	0.44
CaO	1.44	2.24	1.84	2.01	1.77	2.03	2.25
Na_2O	4.53	5.16	4.53	4.58	4.74	4.70	4.77
K_2O	4.19	4.48	4.67	4.29	4.40	3.69	4.71
P_2O_5	0.03	0.08	0.06	0.06	0.05	0.09	0.07
Total	101.24	101.87	100.90	99.94	100.46	101.31	100.68
Cu	11	10	9	12	11	12	13
V	17	16	17	16	17	17	18
Cr							32
Co	4	4	4	4	4	5	5
Ni	4	5	5	6	5	7	8
Zn	24	23	25	25	25	33	25
Pb	23	22	23	25	22	24	24
Rb	156	195	181	147	184	157	190
Sr	668	733	764	787	731	740	859
Y	16	21	21	20	18	19	24
Zr	301	366	378	374	349	401	450
Nb	6	8	6	7	7	8	8
Mo	1	1			1		
Ba	1505	1375	1923	1728	1614	1635	1944
quartz	27.91	18.46	21.96	22.16	22.00	25.89	16.75
corundum	0.21		0.43	0.21	0.38		0.73
orthoclase	24.76	26.48	27.60	25.35	26.00	21.81	27.83
albite	38.33	43.66	38.33	38.75	40.11	39.77	40.36
anorthite	6.95	8.93	8.74	9.58	8.45	9.04	10.71
diopside		1.42				0.38	
hypersthene	2.58	2.24	3.14	3.25	2.94	3.63	3.52
ilmenite	0.44	0.49	0.57	0.49	0.46	0.59	0.61
apatite	0.07	0.19	0.14	0.14	0.12	0.21	0.16

Note: All Fe as Fe_2O_3. All oxides in weight percent, all elements in parts per million, blank = below detection limit.

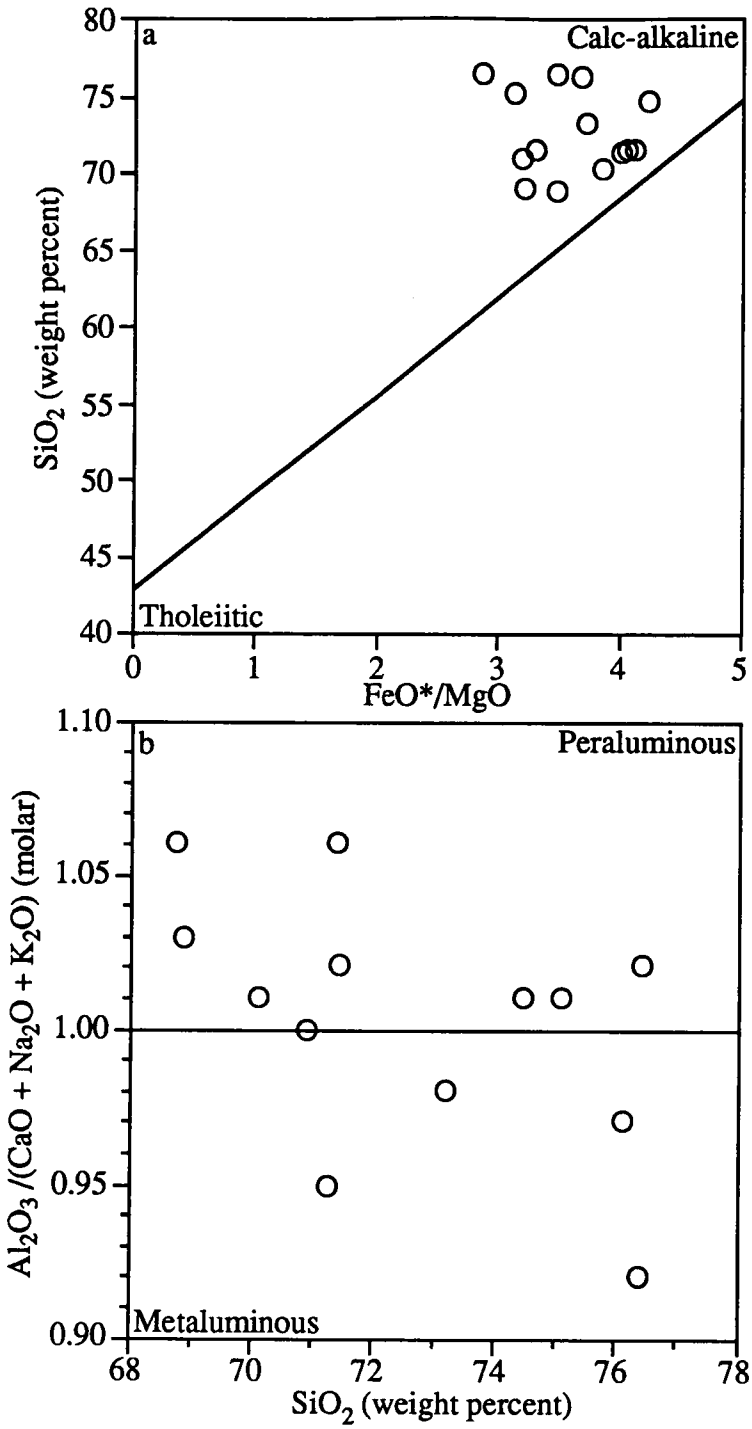

Figure 2: Chemical composition of granitic rocks. a) Weight percent silica versus total FeO divided by MgO. The division between calc-alkaline and tholeiitic is taken from Miyashiro (1974). b) Molar $Al_2O_3/(CaO + Na_2O + K_2O)$ ratio versus weight percent silica. The division between metaluminous and peraluminous is taken from Shand (1951).

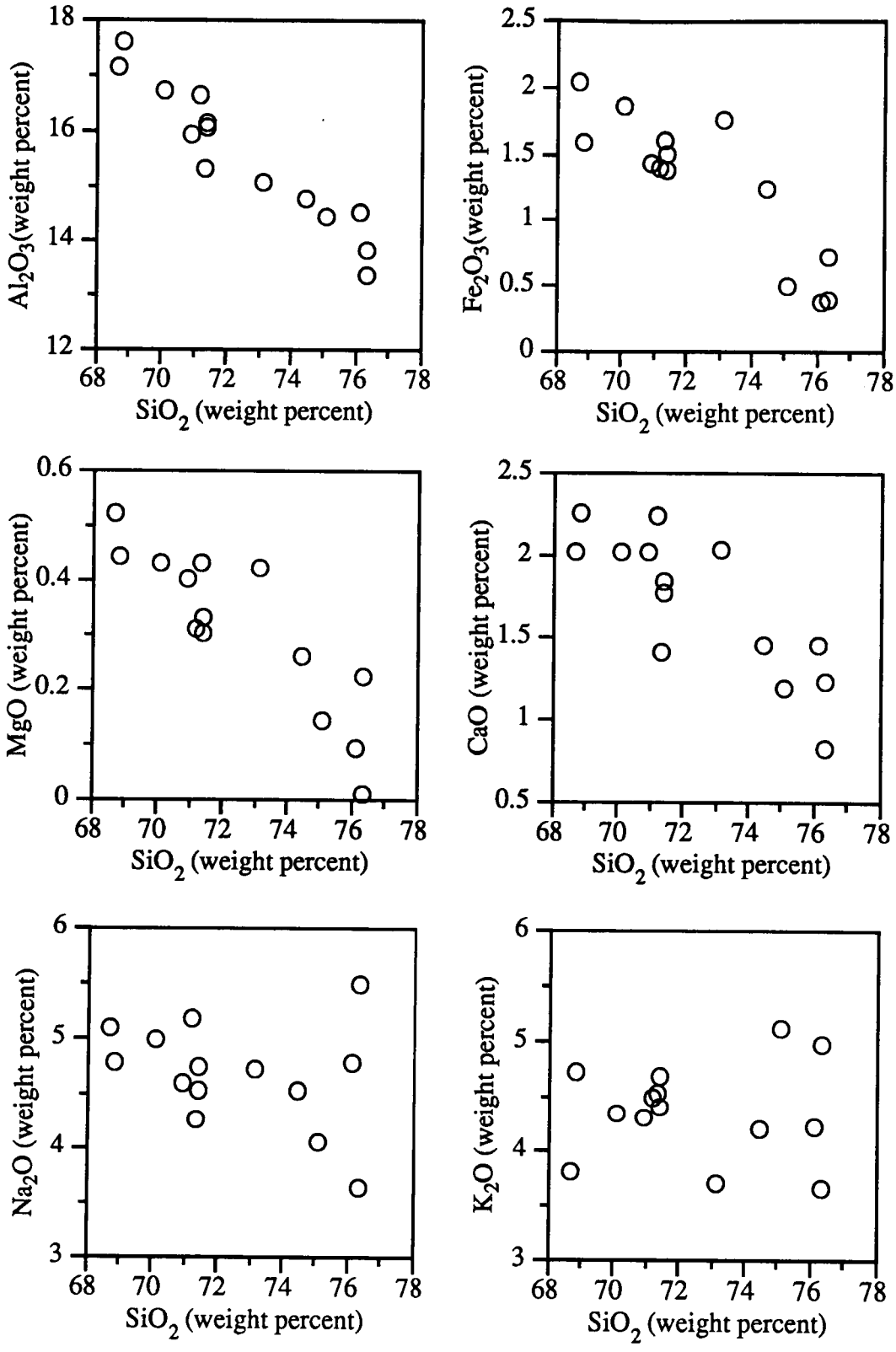

Figure 3: Harker variation diagrams for selected major and trace elements.

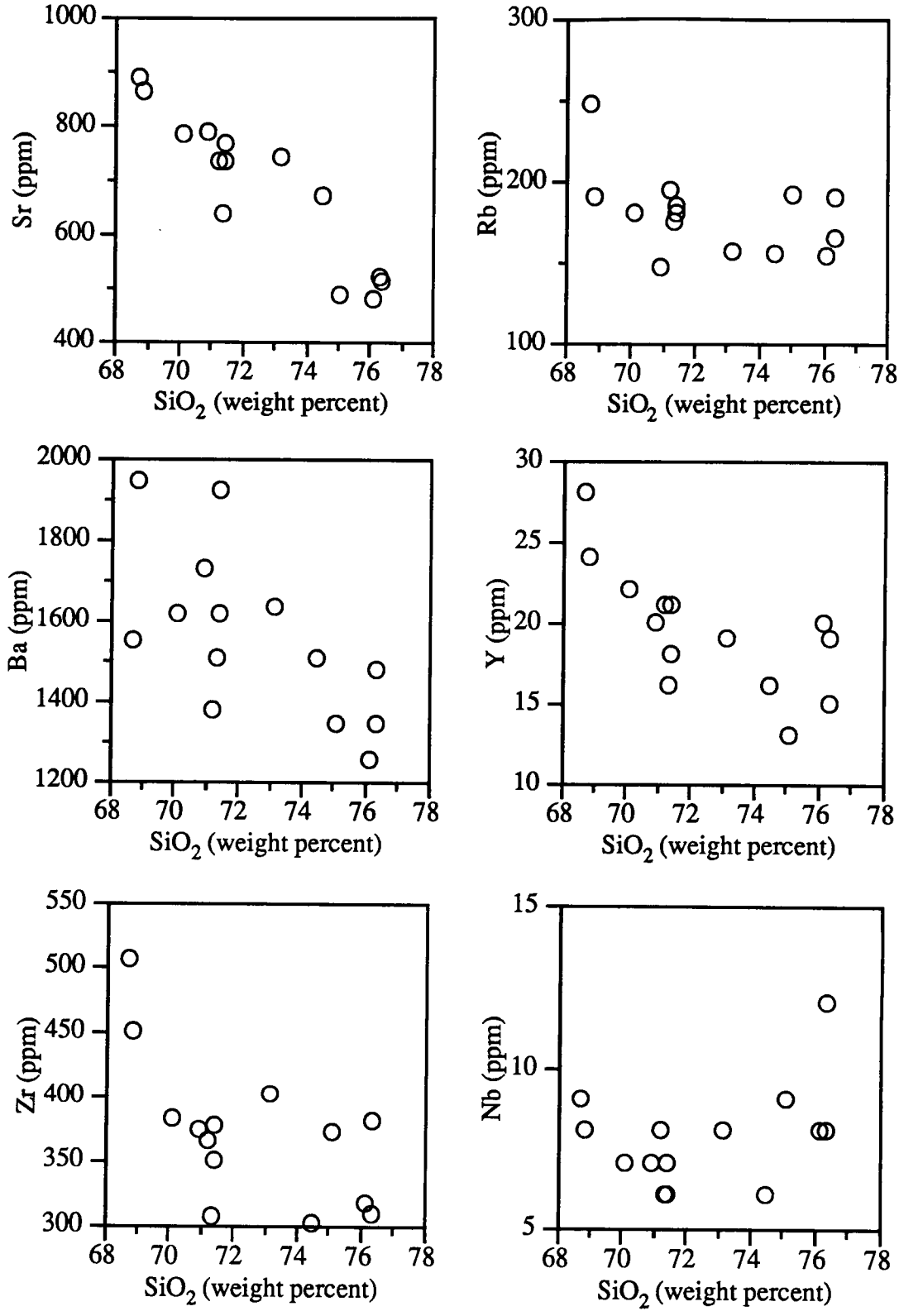

Figure 3: (continued)

Table 2: Whole-rock X-ray fluorescence analyses of pelitic schist and gabbro

Sample	LM5	LM 12	LM 14	LM 59-1	LM 93	LM133-4	T179D
Rock type	P	P	P	P	P	G	G
SiO_2	50.8	47.2	49.6	51.5	53.6	47.4	48.2
TiO_2	0.84	0.93	0.81	0.88	0.81	1.55	1.2
Al_2O_3	22.4	24.4	22.2	24.7	19.6	19.5	19.7
Fe_2O_3	6.50	8.37	7.46	5.98	8.11	8.10	8.6
MnO	0.08	0.07	0.07	0.07	0.07	0.09	0.13
MgO	2.23	2.74	2.41	1.94	2.53	7.51	7.2
CaO	1.16	0.60	1.65	0.47	1.06	2.94	2.3
Na_2O	1.08	1.11	1.74	1.03	1.47	10.2	10.9
K_2O	3.87	4.76	3.94	4.85	4.00	0.98	1.7
P_2O_5	0.10	0.11	0.10	0.11	0.13	0.13	n.d.
LOI	9.64	7.85	8.92	8.63	8.26	n.d.	n.d.
Total	98.66	98.11	98.82	100.19	99.65	100.97	99.93
Cu	45	91	68	52	64	28	n.d.
V	145	73	68	168	26	140	n.d.
Cr	129	94	105	143	86	99	n.d.
Co	18	25	21	16	24	23	n.d.
Ni	37	63	59	14		181	n.d.
Zn	269	316	277	329	288	58	n.d.
Pb		2				11	n.d.
As	4	1	3	4	4	n.d.	n.d.
Rb	143	189	135	170	149	71	n.d.
Sr	215	111	361	194	330	1213	n.d.
Y	n.d.	n.d.	n.d.	n.d.	n.d.		n.d.
Zr	133	104	158	150	179	188	n.d.
Nb	n.d.	n.d.	n.d.	n.d.	n.d.	5	n.d.
Ba	716	528	392	810	580	1267	n.d.

Note: All Fe as Fe_2O_3. All oxides in weight percent, all elements in parts per million, blank = below detection limit, n.d. = not determined, LOI = loss on ignition. Rock type: P = pelitic schist, G = gabbro. Sample T179D is from Bonham and Garside (1979).

MgO, and P_2O_5 than granite. Gabbro has higher CaO and lower K_2O than granite; whereas pelitic schist has lower CaO and similar K_2O to granite.

PETROGRAPHY AND CONDITIONS OF EMPLACEMENT

The Lone Mountain pluton is mostly composed of granite with subordinate granodiorite and quartz monzonite (Figure 4). Lone Mountain granitic rocks are primarily composed of quartz, plagioclase, and K-feldspar, with minor amounts of biotite, muscovite, garnet, hornblende, epidote, chlorite, titanite, magnetite, and apatite. Granitic rocks are typically panidiomorphic granular or hypautomorphic granular, although porphyritic rocks are common on the outer margin of the pluton.

Plagioclase feldspar usually occurs as 2 to 5 mm euhedral to subhedral phenocrysts and occasionally as 0.5 mm subhedral inclusions in alkali feldspar and is locally altered to muscovite, epidote, and quartz. Plagioclase is unzoned and is oligoclase (An_{11-16}) in composition except where it occurs as inclusions in alkali feldspar where it is albite (An_{0-2}) (Table 3). Alkali feldspar in Lone Mountain granitic rocks is usually similar in size to plagioclase, except in porphyritic rocks where it occurs as large phenocrysts, up to 2 cm in size. Alkali feldspar is perthitic and is uniform in composition, Or_{95}, throughout the pluton (Table 4). Occasional intergrowths of alkali and plagioclase feldspar display a myrmekitic texture.

Garnet in Lone Mountain granitic rocks typically occurs as 0.5 mm euhedral to subhedral phenocrysts that do not contain any inclusions and are extremely spessartine-rich, with up to 28 weight percent MnO (Table 5). Garnets are zoned, some have manganese and magnesium concentrations higher in the core than in the rim and calcium and iron concentrations higher in the rim than in the core (Figure 5). The texture as well as the high spessartine content suggests that garnet in the Lone Mountain pluton is a primary igneous phase (Green, 1977; Abbott, 1981; Allan and Clarke, 1981; Miller and Stoddard, 1981).

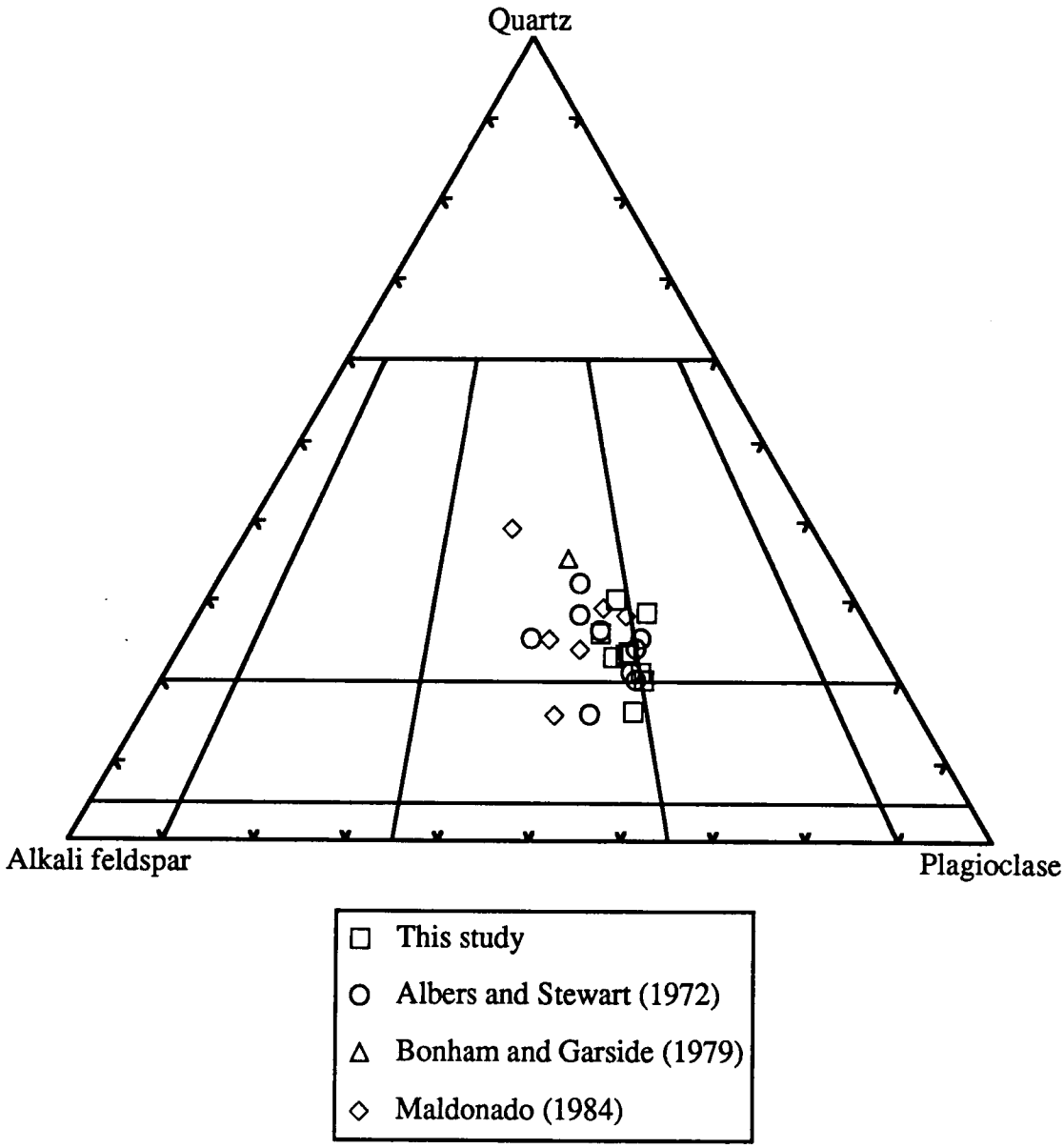

Figure 4: Modal abundances of quartz, plagioclase and alkali feldspar in Lone Mountain granitic rocks.

Table 3: Representative electron microprobe analyses of plagioclase from granite

Sample	LM134-2	LM134-2	LM134-2	LM134-2	LM65	LM65	LM65	LM65	LM65
SiO_2	65.2	65.0	63.9	65.1	63.5	64.1	67.7	64.3	63.8
Al_2O_3	21.9	22.4	22.8	22.5	23.0	22.8	20.5	22.7	23.0
FeO	2.29	<0.06	<0.06	<0.06	3.64	3.22	0.51	3.16	3.67
CaO	0.06	2.75	3.38	2.59	0.03	0.05	0.02	0.08	<0.02
Na_2O	10.3	9.99	9.67	9.94	9.43	9.68	11.2	9.64	9.45
K_2O	0.18	0.14	0.14	0.19	0.13	0.19	0.12	0.20	0.13
Total	99.82	100.22	99.93	100.30	99.68	99.99	100.16	100.11	100.10
Cations based on					8 oxygens				
Si	2.872	2.852	2.821	2.852	2.809	2.825	2.956	2.832	2.813
Al	1.135	1.159	1.186	1.163	1.200	1.185	1.056	1.178	1.196
Fe	0.108	0.129	0.160	0.122	0.172	0.152	0.024	0.149	0.173
Ca	0.002	0.000	0.001	0.001	0.001	0.002	0.001	0.003	0.000
Na	0.875	0.850	0.827	0.845	0.809	0.827	0.951	0.823	0.807
K	0.010	0.008	0.008	0.946	0.008	0.011	0.007	0.011	0.007
Total	5.002	4.998	5.003	4.994	4.999	5.002	4.995	4.996	4.996

Table 4: Representative electron microprobe analyses of alkali feldspar from granite

Sample	LM134-2	LM134-2	LM134-2	LM65	LM65	LM65	LM65	LM65	LM65
SiO_2	64.2	63.4	63.9	63.9	64.4	63.8	64.1	64.3	64.1
Al_2O_3	18.9	18.9	19.0	18.9	18.9	18.8	18.7	18.9	18.9
FeO	<0.03	<0.03	<0.03	0.03	<0.03	<0.03	0.03	0.03	0.04
CaO	0.13	0.09	0.02	0.03	0.07	0.04	0.06	<0.02	0.03
Na_2O	0.77	0.48	0.54	0.49	0.60	0.53	0.56	0.61	0.63
K_2O	15.7	16.2	15.9	16.3	16.2	16.3	16.3	16.2	16.2
Total	99.63	99.06	99.32	99.61	100.23	99.42	99.71	99.98	99.85
Cations based on					8 oxygens				
Si	2.977	2.966	2.971	2.971	2.975	2.973	2.976	2.974	2.971
Al	1.030	1.039	1.039	1.033	1.028	1.029	1.025	1.030	1.033
Fe	0.000	0.001	0.001	0.002	0.001	0.001	0.002	0.002	0.002
Ca	0.005	0.003	0.001	0.001	0.003	0.002	0.002	0.000	0.001
Na	0.069	0.044	0.049	0.044	0.054	0.048	0.051	0.055	0.057
K	0.926	0.966	0.946	0.967	0.956	0.966	0.965	0.957	0.955
Total	5.007	5.019	5.007	5.018	5.017	5.019	5.021	5.018	5.019

Table 5: Representative electron microprobe analyses of garnet from granite

Sample	LM65	LM65	LM65	LM65	LM65	LM65	LM65	LM65
SiO_2	36.0	36.1	36.1	35.1	35.3	35.1	35.3	35.2
TiO_2	0.14	0.16	0.11	0.48	0.57	0.52	0.55	0.56
Al_2O_3	20.0	19.9	20.4	19.0	19.1	19.2	18.9	18.9
FeO	13.6	13.5	11.9	11.7	11.2	11.0	10.6	10.8
MnO	22.7	22.5	24.2	26.5	27.0	27.6	28.2	28.1
MgO	0.47	0.48	0.40	0.46	0.51	0.55	0.58	0.54
CaO	5.55	5.78	5.49	3.52	3.43	3.21	3.35	3.31
Total	98.51	98.40	98.56	96.84	97.06	97.25	97.43	97.33
Cations based on				12 oxygens				
Si	2.982	2.990	2.982	2.983	2.984	2.970	2.982	2.981
Ti	0.009	0.010	0.006	0.030	0.036	0.033	0.035	0.035
Al	1.954	1.944	1.983	1.901	1.903	1.914	1.884	1.882
Fe	0.943	0.932	0.820	0.834	0.792	0.781	0.748	0.762
Mn	1.594	1.581	1.691	1.907	1.936	1.981	2.016	2.013
Mg	0.058	0.059	0.049	0.058	0.064	0.069	0.073	0.068
Ca	0.493	0.513	0.486	0.320	0.311	0.291	0.303	0.301
Total	8.033	8.029	8.018	8.035	8.026	8.039	8.041	8.043

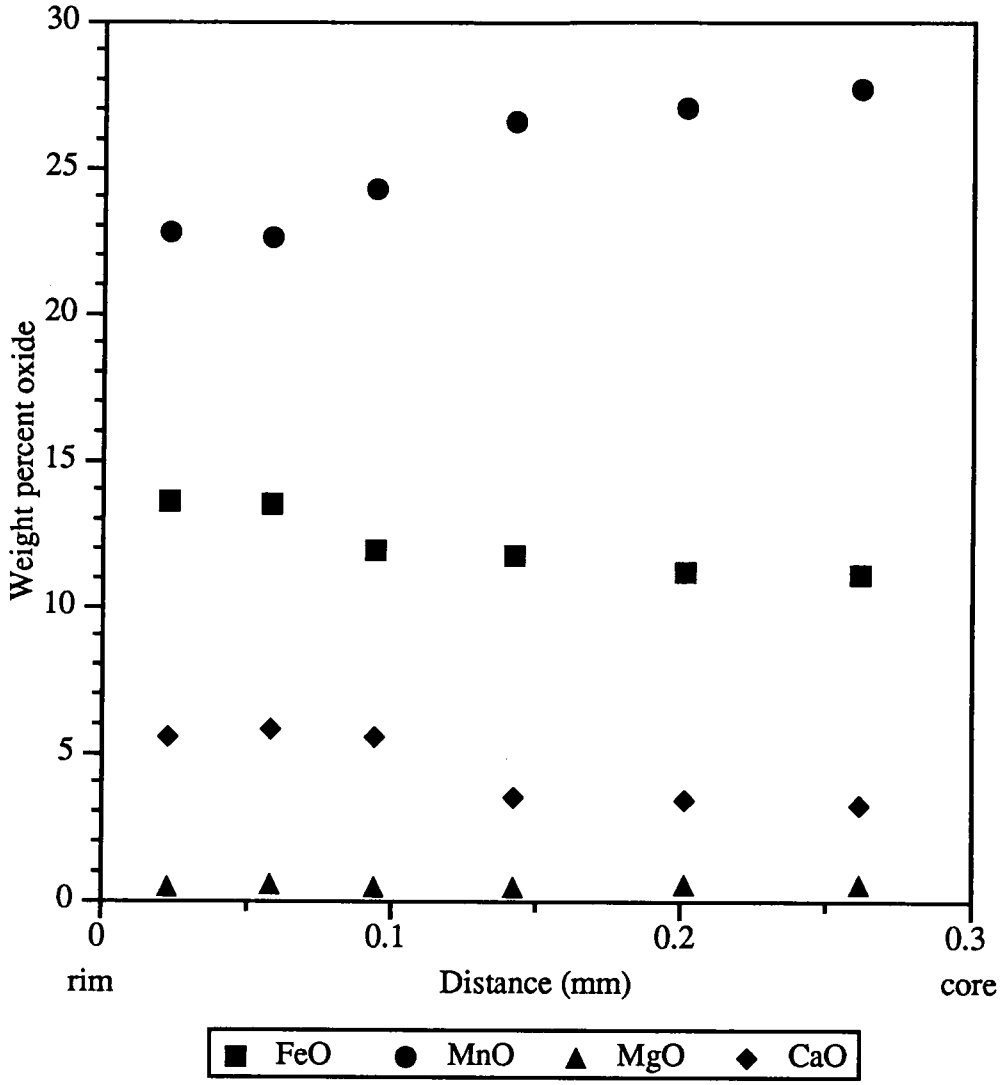

Figure 5: Compositional zoning profile for garnet phenocryst from Lone Mountain garnet granite.

Biotite is the most widespread mafic mineral in the Lone Mountain pluton and occurs as isolated 1 to 2 mm aggregates that are pleochroic (pale yellow to tan brown) and commonly altered to chlorite. Biotite has Fe/(Fe + Mg) ratios in the range 0.71 to 0.78, Na/(Na + K) less than 0.02, and between 0.28 and 0.34 atoms pfu of Al as tetrahedral aluminum. Biotite in the Lone Mountain pluton is less aluminous and has higher Fe/(Fe + Mg) and Na/(Na + K) ratios than biotite in the pelitic schists surrounding the pluton (Table 6), whereas chlorite is similar in composition in both rocks (Table 7).

The temperature of pluton emplacement was estimated using the garnet + biotite thermometer. Although based on the partitioning of iron and magnesium between garnet and biotite, the garnet biotite thermometer is sensitive to other components in both minerals. Ferry and Spear (1978) suggest that their experimental derivation of the garnet biotite thermometer should not be used without a correction for other components if the ratio (Ca + Mn)/(Ca + Mn + Fe + Mg) in garnet is greater than 0.15. In garnets from Lone Mountain granitic rocks this ratio is approximately 0.7. Accordingly, garnet compositions were corrected using the Ca-Mg-Fe-Mn garnet mixing model of Berman (1990) and the temperature then calculated using the calibration of Ferry and Spear (1978). Temperatures of pluton emplacement are estimated at between 690 and 650°C.

Muscovite is the most common mineralogical indicator of peraluminous granitoids; however, its origin is also the most problematic because both textural and chemical criteria used to distinguish primary magmatic muscovite from secondary altered muscovite are not always conclusive. Several distinct parageneses of muscovite occur within the granitic rocks of the Lone Mountain pluton. Euhedral to subhedral 2 to 3 mm muscovite that occurs as individual grains between quartz and feldspar, and 1 to 2 mm muscovite plates intergrown with biotite are of possible primary magmatic origin. Muscovite rims on biotite and very fine-grained muscovite associated with epidote within plagioclase are clearly secondary alteration products, and subhedral 2 to 3 mm

Table 6: Representative electron microprobe analyses of biotite from granite and pelitic schist

Sample	LM65	LM65	LM65	LM12	LM12	LM12	LM12	LM12
Rock type	G	G	G	P	P	P	P	P
SiO_2	35.0	34.6	33.6	30.86	30.3	33.1	28.2	34.8
TiO_2	2.03	2.09	1.97	0.19	0.18	0.68	0.24	0.44
Al_2O_3	19.1	19.7	19.3	18.5	22.5	24.4	23.7	26.1
FeO	23.7	23.6	26.4	26.5	22.4	19.6	24.9	15.9
MnO	0.88	0.79	0.73	0.03	0.17	0.04	0.18	0.18
MgO	5.37	5.46	4.17	9.80	11.2	7.48	9.80	6.81
CaO	<0.02	<0.02	<0.02	0.10	0.04	0.16	0.08	0.17
Na_2O	0.13	0.11	0.08	0.06	0.08	0.27	0.15	0.36
K_2O	9.45	8.98	9.15	8.70	8.59	10.2	8.97	10.6
Total	95.65	95.33	95.40	94.70	95.43	95.78	96.16	95.36
Cations based on				11 oxygens				
Si	2.718	2.691	2.659	2.475	2.353	2.512	2.211	2.596
Ti	0.119	0.122	0.117	0.012	0.010	0.039	0.014	0.025
Al	1.751	1.803	1.799	1.745	2.058	2.186	2.190	2.297
Fe	1.542	1.531	1.742	1.777	1.451	1.243	1.637	0.996
Mn	0.058	0.052	0.049	0.002	0.011	0.003	0.012	0.011
Mg	0.622	0.632	0.491	1.172	1.292	0.847	1.147	0.759
Ca	0.000	0.000	0.000	0.009	0.003	0.013	0.007	0.013
Na	0.020	0.017	0.012	0.009	0.012	0.040	0.022	0.052
K	0.937	0.890	0.923	0.890	0.850	0.984	0.899	1.014
Total	7.766	7.738	7.792	8.091	8.040	7.867	8.139	7.763

Note: Rock type: G = granite, P = pelitic schist.

Table 7: Representative electron microprobe analyses of chlorite from granite and pelitic schist

Sample	LM65	LM65	LM65	LM12	LM12	LM12	LM12	LM12	LM12
Rock type	G	G	G	P	P	P	P	P	P
SiO_2	24.5	24.2	24.3	24.9	24.9	25.5	24.9	25.4	23.8
TiO_2	0.10	0.11	0.06	0.10	0.03	0.10	0.06	0.23	0.09
Al_2O_3	19.7	19.9	20.5	19.6	19.3	20.0	19.4	20.3	21.1
FeO	28.9	28.8	28.9	29.4	30.1	29.8	29.6	28.9	29.3
MnO	1.88	1.85	1.94	0.26	0.15	0.20	0.16	0.25	0.24
MgO	11.0	11.2	10.3	11.8	11.5	10.9	12.0	12.0	11.2
Total	86.14	86.08	86.11	85.98	85.99	86.49	86.20	87.16	85.75
Cations based on	14 oxygens								
Si	2.715	2.681	2.699	2.749	2.759	2.794	2.743	2.750	2.635
Ti	0.008	0.010	0.005	0.008	0.003	0.008	0.005	0.019	0.007
Al	2.579	2.607	2.678	2.542	2.515	2.575	2.524	2.592	2.755
Fe	2.685	2.673	2.683	2.712	2.788	2.729	2.731	2.616	2.708
Mn	0.177	0.174	0.183	0.024	0.014	0.018	0.015	0.023	0.023
Mg	1.823	1.860	1.709	1.937	1.902	1.784	1.972	1.938	1.853
Total	9.987	10.005	9.957	9.972	9.981	9.908	9.990	9.938	9.981

Note: Rock type: G = granite, P = pelitic schist.

muscovite within feldspar may also be of secondary origin. Muscovite in granitic rocks is typically enriched in Si, Mg, and Fe compared to ideal muscovite as a result of celadonite exchange, $SiAl_{-1}(Mg,Fe)Al_{-1}$. (Miller and others, 1981), and muscovite of primary magmatic origin usually contains more Ti, Al, and Na, and less Si and Mg than coexisting secondary muscovite (Miller and others, 1981). The chemical composition of inferred texturally primary muscovite from the Lone Mountain granitic pluton does have greater amounts of Ti, Al, and Na, and less Si and Mg than secondary muscovite (Table 8), although this is based on only one analysis of inferred primary muscovite. Thus, both textural and chemical criteria suggest that there may be magmatic muscovite in the Lone Mountain pluton, but this conclusion is not definitive.

Epidote of possible magmatic origin occurs in hornblende-biotite granodiorite. Textural criteria, as proposed by Zen and Hammarstrom (1984), that suggest that some of the epidote in Lone Mountain granitic rocks is a primary igneous phase include epidote that occurs as isolated euhedral grains within biotite and euhedral to subhedral epidote that is either completely enclosed within resorbed hornblende or occurs on the margins of embayments within resorbed hornblende. Secondary, very fine-grained epidote also occurs as an alteration product of plagioclase intergrown with very fine-grained muscovite, and often in association with magnetite and plagioclase. Although as with muscovite, textural evidence of primary epidote is inconclusive, chemical differences also exist between primary magmatic epidote and secondary altered epidote. Compositional data for magmatic epidote indicate that it is very restricted in composition with the pistacite component, $Ps = Fe^{3+}/(Fe^{3+} + Al)$, of primary igneous epidote between Ps_{25} and Ps_{33} (Naney, 1983; Zen and Hammarstrom, 1984; Tulloch, 1986). Inferred primary igneous epidote from the Lone Mountain pluton has compositions of Ps_{27} and Ps_{30} (Table 9), suggesting that it is a primary igneous phase. Secondary epidote resulting from the alteration of plagioclase has compositions between

Table 8: Representative electron microprobe analyses of muscovite from granite and pelitic schist

Sample	LM65	LM65	LM65	LM65	LM12	LM12	LM12	LM12	LM12
Rock type	G	G	G	G	P	P	P	P	P
Texture	S	S	S	P					
SiO_2	46.6	46.1	46.1	46.0	45.6	45.2	45.4	45.7	45.4
TiO_2	0.04	0.04	0.08	0.37	0.73	0.71	0.69	0.68	0.69
Al_2O_3	32.2	33.2	33.4	33.6	36.1	36.0	36.1	36.1	36.1
FeO	3.50	3.14	2.89	1.75	1.32	1.30	1.32	1.11	1.13
MnO	0.09	0.10	0.10	<0.05	<0.05	<0.05	<0.05	<0.05	<0.05
MgO	1.19	0.91	1.05	1.50	0.60	0.69	0.54	0.62	0.61
CaO	<0.02	0.02	<0.02	<0.02	<0.02	<0.02	0.02	0.02	<0.02
Na_2O	0.15	0.16	0.16	0.27	0.79	0.82	0.81	0.81	1.21
K_2O	11.2	11.3	11.4	11.1	10.2	10.2	10.3	10.4	10.3
Total	94.92	94.89	95.15	94.51	95.31	94.98	95.16	95.33	95.51
Cations based on	11 oxygens								
Si	3.158	3.122	3.113	3.104	3.036	3.023	3.028	3.037	3.023
Ti	0.002	0.002	0.004	0.019	0.036	0.036	0.035	0.034	0.035
Al	2.576	2.651	2.660	2.673	2.827	2.834	2.838	2.827	2.831
Fe	0.199	0.178	0.163	0.099	0.074	0.072	0.074	0.062	0.063
Mn	0.005	0.006	0.005	0.000	0.000	0.000	0.000	0.001	0.001
Mg	0.120	0.092	0.106	0.151	0.059	0.068	0.053	0.062	0.060
Ca	0.000	0.002	0.001	0.001	0.000	0.000	0.001	0.001	0.000
Na	0.020	0.020	0.021	0.035	0.102	0.106	0.105	0.104	0.156
K	0.965	0.976	0.980	0.954	0.864	0.873	0.874	0.879	0.873
Total	7.045	7.049	7.054	7.036	6.998	7.014	7.007	7.008	7.042

Note: Rock type: G = granite, P = pelitic schist. Texture: S = secondary, P = primary.

Table 9: Representative electron microprobe analyses of epidote from granite

Sample	LM134-2	LM134-2	LM134-2	LM134-2	LM134-2
Texture	S	S	S	P	P
SiO_2	37.5	37.4	37.5	37.2	36.9
TiO_2	0.14	0.08	0.03	0.05	0.05
Al_2O_3	27.5	26.2	26.7	22.4	23.3
FeO	7.78	9.26	8.49	13.7	12.2
MnO	0.30	0.64	0.39	0.24	0.31
MgO	0.03	<0.02	0.20	0.03	0.36
CaO	23.3	22.8	22.6	22.6	21.6
Total	96.60	98.14	97.76	98.09	96.55
Cations based on			8 cations		
Si	2.949	2.960	2.975	2.984	2.993
Ti	0.008	0.004	0.002	0.003	0.003
Al	2.550	2.445	2.496	2.122	2.231
Fe	0.511	0.614	0.563	0.922	0.829
Mn	0.020	0.043	0.026	0.017	0.022
Mg	0.003	0.001	0.023	0.004	0.044
Ca	1.958	1.933	1.915	1.948	1.878
Total	8.000	8.000	8.000	8.000	8.000
Fe/(Fe+Al)	0.17	0.20	0.18	0.30	0.27

Note: All Fe reported as FeO. Texture: S = secondary, P = primary.

Ps_0 and Ps_{24}, (Tulloch, 1979; 1986), secondary epidote formed by the alteration of plagioclase in Lone Mountain granitic rocks has compositions between Ps_{17} and Ps_{20} (Table 9), consistent with its secondary origin.

If epidote and muscovite in the Lone Mountain granitic pluton are of primary magmatic origin, then they have the potential to be used as pressure indicators, because of the intersection of the granite solidus with the stability limits of muscovite and epidote (Figure 6). On the basis of phase equilibria, granitic plutons in which muscovite and epidote are magmatic phases, could have been emplaced at pressures anywhere between 4.4 and 2.4 kbar. The specific conditions of emplacement are highly dependent on oxygen fugacity, the activity of H_2O in the granitic melt, and the composition of the granitic melt. Low oxygen fugacities shift the stability limit of epidote to higher pressures, and low water activities shift the granite solidus to higher temperatures.

Hornblende occurs within hornblende granodiorite of the Lone Mountain granitic pluton. Hornblende typically appears as euhedral to subhedral bladed grains, up to 5 mm in size, that often have embayed and resorbed margins and epidote inclusions. Hornblende varies in composition (Table 10), displaying a complex chemical zonation with rim compositions enriched in Al, Fe, and Na, and depleted in Si and Mg relative to core compositions. The total aluminum content of hornblende in calc-alkaline granitic rocks has been shown to be a function of pressure. Initial empirical calibrations (Hammarstrom and Zen, 1986; Hollister and others, 1987) were based on pressures determined from rocks of the contact aureoles of the plutons. More recently, the barometer has been calibrated directly by experiment (Johnson and Rutherford, 1989; Schmidt, 1992), using natural granite and tonalite samples in reversed experiments at pressures of 2 to 13.5 kbar, and temperatures between 655 and 780°C. Use of the total aluminum content in hornblende as a barometer requires the equilibrium assemblage quartz + plagioclase + K-feldspar + hornblende + biotite + titanite + magnetite or

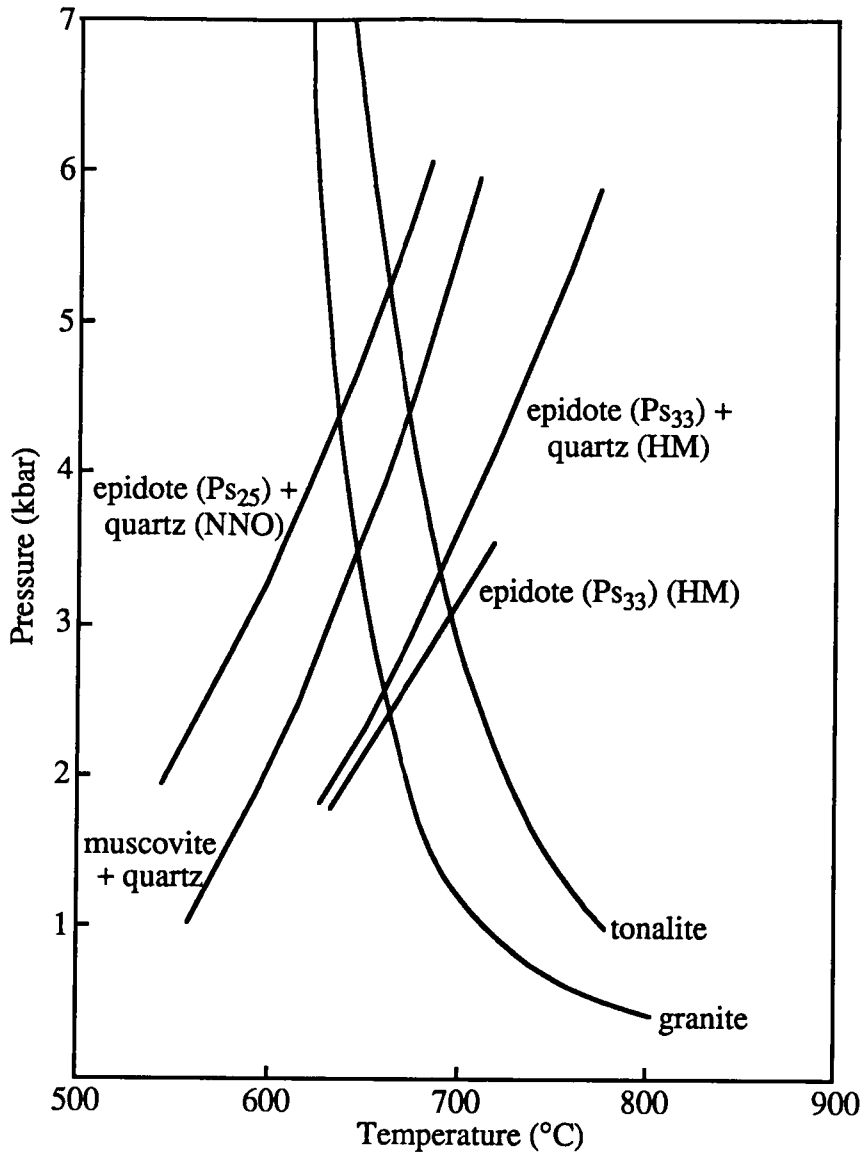

Figure 6: Pressure-temperature phase diagram for mineral equilibria in granitic rocks. Epidote (Ps_{33}) curve at the hematite-magnetite (HM) buffer is from Holdaway (1972). Epidote (Ps_{33}) + quartz curve at the hematite-magnetite buffer and epidote (Ps_{25}) + quartz curve at the nickel-nickel oxide buffer (NNO) are from Liou (1973). Muscovite + quartz curve is from Chatterjee and Johannes (1974). Tonalite and granite water saturated solidi curves are from Wyllie (1977).

Table 10: Representative electron microprobe analyses of amphibole from granite

Sample	LM134-2	LM134-2	LM134-2	LM134-2	LM134-2	LM134-2	LM134-2	LM134-2	LM134-2	LM134-2	LM134-2	LM134-2	LM134-2
SiO_2	42.9	41.5	43.0	42.9	43.2	42.9	42.8	43.3	43.0	42.8	42.0	41.6	40.9
TiO_2	0.89	0.39	0.86	0.98	0.80	0.89	0.90	0.73	0.82	0.87	0.87	0.48	0.38
Al_2O_3	8.34	9.78	8.44	8.47	8.32	8.42	8.54	8.29	8.24	8.38	8.63	9.24	9.76
FeO	21.2	21.9	21.4	21.4	20.9	20.9	22.1	20.7	21.1	22.3	23.6	23.2	24.1
MnO	1.08	1.08	1.19	1.07	1.07	1.04	1.11	1.11	1.09	1.15	1.12	1.11	1.00
MgO	8.30	7.72	8.32	8.17	8.70	8.43	7.82	8.94	8.25	7.67	6.93	7.06	6.15
CaO	11.1	11.3	11.1	10.9	10.9	11.1	11.0	11.1	11.2	11.0	11.1	11.4	11.2
Na_2O	1.72	1.43	1.77	1.81	1.81	1.80	1.65	1.80	1.74	1.76	1.57	1.34	1.35
K_2O	1.12	1.59	1.11	1.15	1.12	1.14	1.10	1.09	0.98	1.12	1.21	1.32	1.54
Total	96.62	96.63	97.22	96.78	96.83	96.60	97.01	97.04	96.39	97.05	97.01	96.62	96.35
Cations based on							23 oxygens						
Si	6.704	6.536	6.688	6.694	6.722	6.698	6.689	6.721	6.727	6.700	6.628	6.577	6.529
Ti	0.105	0.047	0.101	0.115	0.093	0.105	0.105	0.085	0.096	0.103	0.103	0.057	0.045
Al	1.536	1.815	1.547	1.559	1.525	1.550	1.573	1.515	1.521	1.545	1.605	1.723	1.837
Fe	2.766	2.878	2.782	2.794	2.720	2.725	2.880	2.680	2.768	2.912	3.108	3.064	3.220
Mn	0.142	0.143	0.157	0.141	0.140	0.137	0.147	0.146	0.145	0.152	0.149	0.149	0.135
Mg	1.934	1.812	1.928	1.900	2.019	1.962	1.821	2.067	1.926	1.789	1.630	1.665	1.465
Ca	1.863	1.901	1.857	1.819	1.820	1.860	1.846	1.843	1.872	1.846	1.883	1.932	1.912
Na	0.522	0.437	0.534	0.548	0.545	0.544	0.498	0.541	0.527	0.535	0.479	0.411	0.416
K	0.224	0.320	0.221	0.229	0.222	0.228	0.220	0.215	0.195	0.223	0.243	0.267	0.313
Total	15.796	15.889	15.815	15.799	15.806	15.809	15.779	15.813	15.777	15.805	15.828	15.845	15.872

ilmenite to be present in granitic rocks, a criterion that is satisfied by Lone Mountain hornblende granodiorite. The increase in total aluminum content in hornblende with increasing pressure is mainly due to tschermakite exchange, $Al^{IV}Si_{-1}Al^{VI}(Mg,Fe)_{-1}$, in hornblende (Hollister and others, 1987; Johnson and Rutherford, 1989; Schmidt, 1992), while edenite exchange, $Na\square_{-1}Al^{IV}Si_{-1}$, in hornblende is temperature rather than pressure dependent (Blundy and Holland, 1990; 1992 a; b; Schmidt, 1992). Despite there being both pressure and temperature controls on the chemical composition of hornblende, its use as a barometer is not precluded (Hammarstrom and Zen, 1992; Rutherford and Johnson, 1992; Poli and Schmidt, 1992). The positive correlation of total aluminum with Fe/(Fe + Mg) and the negative correlation of total aluminum with Na (Figure 7), is consistent with both tschermak and edenite substitution in Lone Mountain hornblendes. The total aluminum content of Lone Mountain hornblende gives pressures of between 3.0 and 4.2 kbar, with an average of 3.3 kbar, using the calibration of Johnson and Rutherford (1989), and temperatures of between 680 and 745°C using the calibration of Blundy and Holland (1990).

Pressure determinations from country rocks that were intruded by the Lone Mountain pluton are in good agreement with those estimated from the pluton itself. The pre-Tertiary stratigraphic thickness in the Lone Mountain area was 10 to 12 km (Albers and Stewart, 1972; Bonham and Garside, 1979), suggesting that the pressure at the time of intrusion of the Lone Mountain pluton was 3 to 3.5 kbar. The presence of andalusite in pelitic schists adjacent to the pluton indicates that the pressure must have been less than 3.8 kbar (Holdaway and Mukhopadhyay, 1993).

OXYGEN ISOTOPE GEOCHEMISTRY

Oxygen isotopic data for the Lone Mountain granitic pluton and associated rocks are given in Table 11. Granitic rocks have whole rock $\delta^{18}O$ values of between 9.0 and 12.2 ‰. These $\delta^{18}O$ values are higher than those of normal igneous granitic rocks (Taylor,

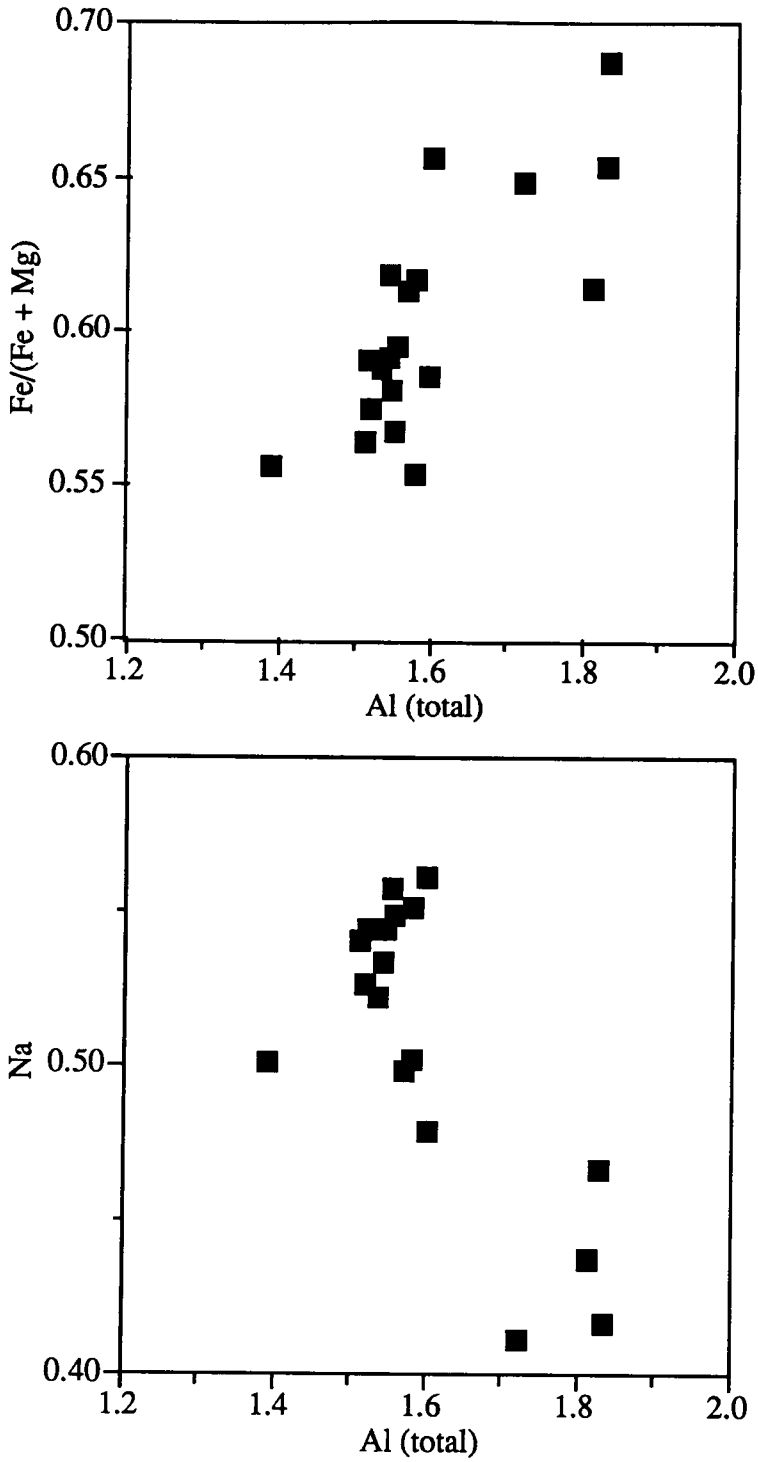

Figure 7: Compositional variation in hornblende from Lone Mountain hornblende granodiorite.

Table 11: Stable isotope analyses of granite, pelitic schist and gabbro

Sample	$\delta^{18}O$ whole rock	$\delta^{18}O$ quartz	$\delta^{18}O$ feldspar
	Granite		
LM115-1	9.7		8.6
LM123	9.0	10.9	9.1
LM125	9.2	11.3	8.7
LM131-2	12.2	10.8	9.6
LM134-2	11.7	11.6	9.9
LM138	10.1	11.0	9.2
LM140	9.5	11.5	9.1
LM142	9.5	11.4	8.9
LM144	10.3	11.1	8.5
LM146	9.2	10.7	9.4
	Pelitic schist		
LM5	15.9		
LM12	9.3		
LM14	7.8		
LM59-1	14.6		
LM93	13.9		
	Gabbro		
LM133-4	5.9		

1978), and are representative of granites that were either derived from or exchanged oxygen with sedimentary or volcanic rocks or their metamorphosed equivalents. The oxygen isotopic composition of quartz ranges from 10.7 to 11.6 ‰, and feldspar from 8.5 to 9.9 ‰, so that quartz–feldspar fractionations, $\Delta^{18}O$, are between 1.2 and 1.6 ‰, and the expected ^{18}O fractionations occur with quartz always heavier in ^{18}O than feldspar. This suggests that the whole-rock $\delta^{18}O$ values of the granite are close to those of the magma from which the granite crystallized. Assuming that the oxygen isotopic fractionation of feldspar is equivalent to that of albite and K-feldspar, using the fractionation factors of Clayton and others (1989), quartz-feldspar fractionations correspond to temperatures of between 325 and 615°C. Typical quartz-feldspar fractionations for igneous rocks are between 1.0 and 2.0 ‰ (Taylor, 1978), so that Lone Mountain granitic rocks have undergone some subsolidus re-equilibration after emplacement. The lack of severely depleted feldspar $\delta^{18}O$ values and the absence of reversals in $\delta^{18}O$ between feldspar and quartz indicate that the Lone Mountain granitic pluton was not subjected to extensive meteoric hydrothermal activity after emplacement. This interpretation is also consistent with estimates of the depth of pluton emplacement, 10 to 12 km, which is typical of the limit at which hydrothermal circulation of meteoric fluids occurs in granitic systems (Criss and Taylor, 1986).

Gabbro has a $\delta^{18}O$ value of 5.9 ‰, indicating that it is definitely of mantle origin. Pelitic schists have whole-rock $\delta^{18}O$ values that are dependent on geographic location. High $\delta^{18}O$ values, between 15.9 and 13.9 ‰, occur on the eastern side of the pluton, and low $\delta^{18}O$ values, 9.3 and 7.8 ‰, occur on the northwestern side of the pluton. The high $\delta^{18}O$ values are typical of shales and their metamorphosed equivalents (Garlick and Epstein, 1967; Savin and Epstein, 1970), whereas the low $\delta^{18}O$ values are more problematic. There is no difference in the mineralogy of pelitic schists between the east and west side of the pluton and also no significant difference in modal abundance of

minerals to account for the different oxygen isotopic compositions. It is therefore proposed that these rocks acquired their low $\delta^{18}O$ compositions as a result of interaction with low ^{18}O fluids, probably associated with either the intrusion of Tertiary dikes or the development of northeast trending normal faults, which are both prevalent on the northwestern side of the pluton.

NATURE OF GRANITIC SOURCE ROCKS

For most granites it is not possible to determine unambiguously the source rocks from which they were derived. This is because potential crustal source rocks are likely to be inhomogeneous, and therefore, so will granitic magmas that are derived from them (Miller and others, 1988). Nevertheless, it is still meaningful to attempt to determine granitoid source rock compositions in order to provide insight into granitoid petrogenesis.

The geographic location of the Lone Mountain pluton (Figure 8) is consistent with the available isotopic data, whole-rock $\delta^{18}O$ values in the range 9.0 to 12.2 ‰, and an initial $^{87}Sr/^{86}Sr$ ratio of 0.7071 (John and Robinson, 1989), that place it in subzone V of the central zone of Solomon and Taylor (1989). This suggests that the source rocks of the Lone Mountain pluton had a probable volcanic component (Solomon and Taylor, 1989). The only volcanic rocks exposed in the Lone Mountain area are the Tertiary volcanic rocks that crop out to the northeast of the pluton. The young age of these rocks precludes them from being considered as possible source rocks of the Cretaceous Lone Mountain granite. This does not eliminate older volcanic or volcanogenic sedimentary rocks at depth from being the source of the Lone Mountain pluton, however, the Lone Mountain pluton does intrude the oldest known rocks in the region, so these should also be considered as possible source rocks for the granite, because the high viscosity of granitic magmas suggests that they cannot migrate very far from their source regions.

Figure 8: Isotopic provinces map of the western United States. Lead isotopic provinces are given as Roman numerals, I, II and III, are separated from each other by small dashed lines, and are from Zartman (1974). Oxygen isotopic provinces are given as letters, EZ = eastern zone, CZ = central zone and WZ = western zone, are separated from each other by solid lines, and are from Solomon and Taylor (1989). The central zone is divided into two subzones, V to the west, and S to the east, by the $^{87}Sr/^{86}Sr_{initial} = 0.708$ and $\varepsilon Nd = -7$ line. Neodymium isotopic provinces are given as numbers, 1, 2, and 3, are separated from each other by large dashed lines, and are from Bennett and DePaolo (1987).

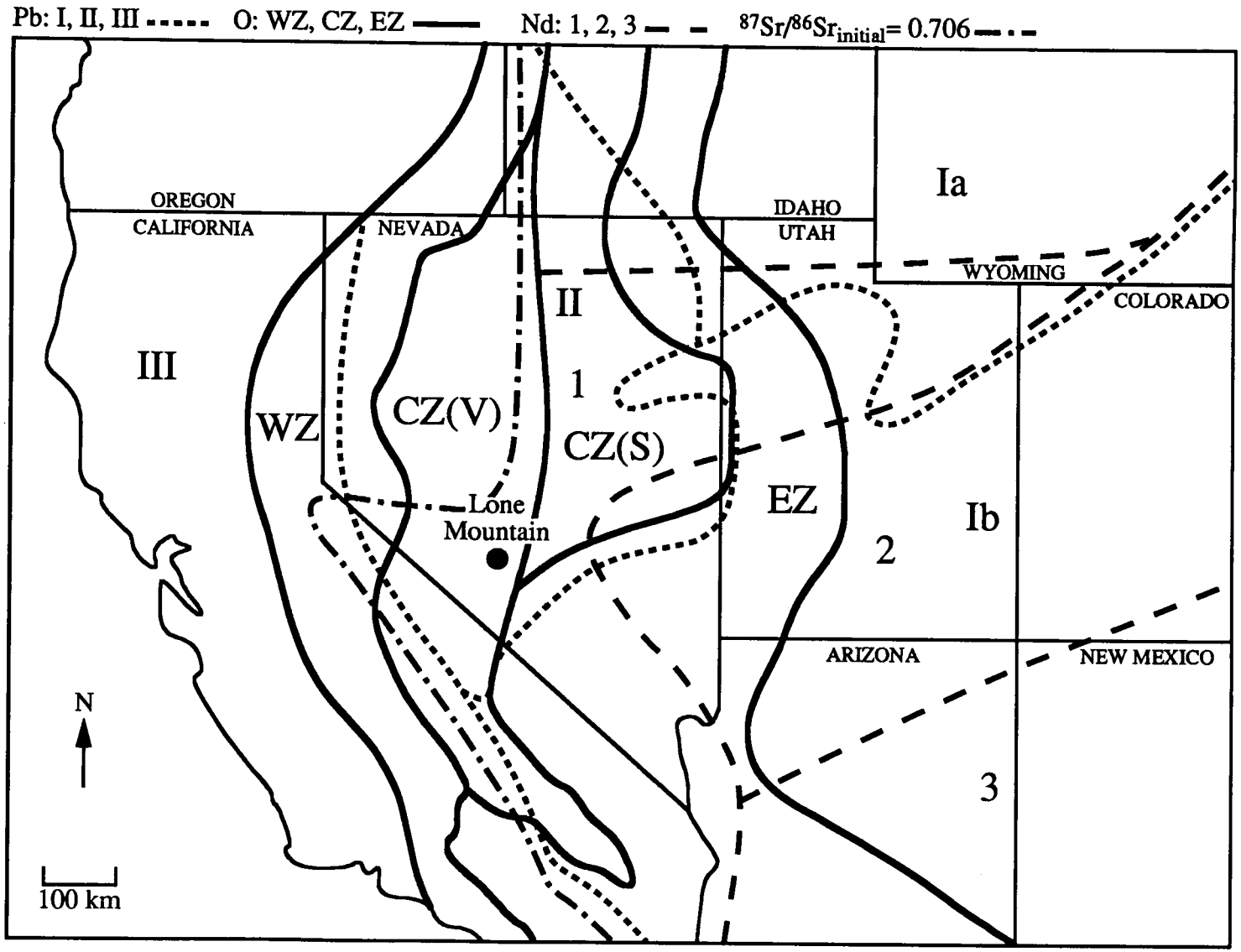
Pb: I, II, III
O: WZ, CZ, EZ
Nd: 1, 2, 3
$^{87}Sr/^{86}Sr_{initial}$= 0.706
OREGON
CALIFORNIA
NEVADA
IDAHO
UTAH
WYOMING
COLORADO
ARIZONA
NEW MEXICO
Ia
II
III
1
WZ
CZ(V)
CZ(S)
EZ
Ib
2
3
Lone Mountain
N
100 km

The high $\delta^{18}O$ values of the Lone Mountain granitic pluton could have been attained by partial melting of sedimentary or metamorphosed rocks, however, in this instance partial melting of pelitic schists would produce a magma that would have both a $\delta^{18}O$ value, and an initial $^{87}Sr/^{86}Sr$ ratio that are too high. The complete absence of sedimentary xenoliths within Lone Mountain granitic rocks rules out assimilation of sedimentary rocks during pluton emplacement as a mechanism to impart a high ^{18}O signature to the granite. The melting of the limited volume of pelitic schists exposed in the vicinity of the Lone Mountain pluton is unlikely to be able to provide enough material to produce the volume of granitic magma sufficient to crystallize the Lone Mountain pluton. Additionally, Lone Mountain pelitic schists have the mineral assemblage chlorite + biotite + muscovite + quartz, with or without andalusite, and tourmaline. Garnet has also been reported from pelitic schists in the area (Bonham and Garside, 1979), and feldspar is generally absent. Such mica-rich and plagioclase-poor pelitic schists are also unlikely to produce sufficient quantities of magma to crystallize the Lone Mountain pluton because they have low melt productivity (Patino Douce and Johnston, 1991).

Geophysical evidence suggests that gabbro underlies much of the Lone Mountain pluton. Oxygen isotopic data from Lone Mountain gabbro, a whole rock $\delta^{18}O$ value of 5.9 ‰, however, eliminates it as a possible source rock of the Lone Mountain granitic pluton because its $\delta^{18}O$ value is too low. Differentiation of a gabbroic parent would only increase its oxygen isotopic composition by 1 or 2 ‰ at most (Taylor, 1978). Such rocks would also presumably have initial $^{87}Sr/^{86}Sr$ ratios that are also too low.

GRANITE PETROGENESIS

Granitic rocks of the Lone Mountain pluton all have broadly similar mineral assemblages, major and trace element chemistries and oxygen isotopic compositions. The limited variation in the chemical and isotopic characteristics throughout the pluton

suggests that all of the granitic rocks have had very similar histories. The most likely cause of the variation within the pluton is fractional crystallization from a common parental magma. That fractional crystallization occurred in the Lone Mountain pluton is strongly indicated by depletions in both major and trace elements as the granitic rocks becomes more felsic. Fractional crystallization of hornblende is thought to be a major factor in producing the calc-alkaline trend in igneous rocks (Cawthorn and O'Hara, 1976). The systematic decrease in CaO, Al_2O_3, TiO_2 and Fe_2O_3, with increasing SiO_2, support the removal of hornblende from the magma, as these elements are preferentially partitioned into hornblende relative to the magma (Cawthorn, 1976). Similarly, the decrease in CaO, Al_2O_3, Na_2O, and Sr, with increasing SiO_2 indicates that plagioclase was also a fractionating phase in Lone Mountain granites. Qualitatively, removal of amphibole and plagioclase from a metaluminous diopside-normative magma by fractional crystallization can produce a peraluminous corundum-normative magma (Cawthorn and Brown, 1976), and thereby account for the chemical variations observed within the Lone Mountain pluton. Therefore, hornblende granodiorite, with a relatively low silica content is considered to be an appropriate parental magma for the Lone Mountain granitic rocks. Garnet granite is considered to be a late stage differentiate, and the most highly evolved of the Lone Mountain granitic rocks because it is the most peraluminous, and also because of the extremely high manganese contents of the garnets (Green, 1977; Miller and Stoddard, 1981)

Quantitative least squares mass balance mixing calculations were carried using XLFRAC (Stormer and Nicholls, 1978). Whole-rock chemical compositions used in the mass balance calculations were taken from Table 1, and mineral chemical compositions of hornblende and plagioclase were taken from Tables 10 and 3, respectively. For the parental magma composition, metaluminous hornblende granodiorite, LM134-2, removal of hornblende and plagioclase by fractional crystallization can produce a

daughter magma composition, peraluminous garnet granite LM65. This requires 31 percent crystallization of the parent magma, with 20 percent hornblende and 80 percent plagioclase. The sum of the squares of the residuals in the least squares mass balance calculation was 1.2. This relatively low value indicates that the fractional crystallization model provides an acceptable solution to the least squares problem.

It should be stressed, however, that while a simple fractional crystallization model can explain the overall chemical variation within the pluton, in detail the actual relationships between the granitic rocks are more complex. Field evidence, in the form of a well developed foliation along the margin of the granite, which is parallel to the layering in country rocks, suggests that protoclastic deformation occurred during intrusion of the magma. This indicates that successive pulses of magma were intruded into the cooled outer portions of the pluton as it was crystallizing from the outer margin inwards. Several episodes of magmatic intrusion are also supported by the lack of geochemical variation in the Lone Mountain pluton, which have no discernible systematic trend in chemistry with distance from the rim to the core of the pluton. Therefore, rather than a simple fractional crystallization model, a model of replenishment of a magma chamber that is undergoing fractional crystallization better explains the field and chemical data. That simple fractional crystallization alone was not responsible for the generation of the Lone Mountain pluton is also supported by the oxygen isotopic compositions of the granitic rocks. Fractional crystallization is incapable of producing the 3 ‰ variation in the oxygen isotopic composition of the Lone Mountain granitic rocks. As the oxygen isotopic composition of the source rocks will essentially be the same as the oxygen isotopic composition of the granite, variations in the extent of partial melting of the granitic source rocks may explain the variation in the oxygen isotopic composition of the granite. Therefore, the overall mechanism of

differentiation of granitic rock throughout the Lone Mountain pluton was dominated by fractional crystallization, with some contribution by variable degrees of partial melting.

REFERENCES CITED

Abbott, R. N., 1981, AFM liquidus projections for granitic magmas, with special reference to hornblende, biotite, and garnet: Canadian Mineralogist, v. 19, p. 103-110.

Al-Aasm, I. S., Taylor, B. E., and South, B., 1990, Stable isotope analysis of multiple carbonate samples using selective acid extraction: Chemical Geology, v. 80, p. 119-125.

Albers, J. P., and Stewart, J. H., 1972, Geology and mineral deposits of Esmeralda County, Nevada: Nevada Bureau of Mines and Geology Bulletin 78, p. 80.

Allan, B. D., and Clarke, D. B., 1981, Occurrence and origin of garnets in the South Mountain Batholith, Nova Scotia: Canadian Mineralogist, v. 19, p. 19-24.

Anovitz, L. M., and Essene, E. J., 1987, Phase equilibria in the system $CaCO_3$-$MgCO_3$-$FeCO_3$: Journal of Petrology, v. 28, p. 389-414.

Barber, D. J., Heard, H. C., and Wenk, H.-R., 1981, Deformation of dolomite single crystals from 20–800°C: Physics and Chemistry of Minerals, v. 7, p. 271-286.

Barton, M. D., Battles, D. A., Bebout, G. E., Capo, R. C., Christensen, J. N., Davis, S. R., Hansen, R. B., Michelsen, C. J., and Trim, H. E., 1988, Mesozoic contact metamorphism in the western United States, *in* Ernst, W. G., ed., Metamorphism and crustal structure of the western United States: Rubey Volume 7: Englewood-Cliffs, New Jersey, Prentice-Hall, p.110-178.

Baumgartner, L. P., and Ferry, J. M., 1991, A model for coupled fluid-flow and mixed-volatile mineral reactions with applications to regional metamorphism: Contributions to Mineralogy and Petrology, v. 106, p. 273-285.

Baumgartner, L. P., and Rumble, D., III., 1988, Transport of stable isotopes: I: Development of a kinetic continuum theory for stable isotope transport: Contributions to Mineralogy and Petrology, v. 98, p. 417-430.

Bennett, V. C., and DePaolo, D. J., 1987, Proterozoic crustal history of the western United States as determined by neodymium isotopic mapping: Geological Society of America Bulletin, v. 99, p. 674-685.

Berman, R. G., 1988, Internally consistent thermodynamic data for minerals in the system Na_2O-K_2O-CaO-MgO-FeO-Fe_2O_3-Al_2O_3-SiO_2-TiO_2-H_2O-CO_2: Journal of Petrology, v. 29, p. 445-522.

Berman, R. G., 1990, Mixing properties of Ca-Mg-Fe-Mn garnets: American Mineralogist, v. 75, p. 328-344.

Bickle, M. J., and McKenzie, D., 1987, The transport of heat and matter by fluids during metamorphism: Contributions to Mineralogy and Petrology, v. 95, p. 384-392.

Blatt, H., 1987, Oxygen isotopes and the origin of quartz: Journal of Sedimentary Petrology, v. 57, p. 373-377.

Blundy, J. D., and Holland, T. J. B., 1990, Calcic amphibole equilibria and a new amphibole-plagioclase geothermometer: Contributions to Mineralogy and Petrology, v. 104, p. 208-224.

Blundy, J. D., and Holland, T. J. B., 1992 a, "Calcic amphibole equilibria and a new amphibole-plagioclase geothermometer": Reply to the comments of Hammarstrom and Zen, and Rutherford and Johnson: Contributions to Mineralogy and Petrology, v. 111, p. 269-272.

Blundy, J. D., and Holland, T. J. B., 1992 b, "Calcic amphibole equilibria and a new amphibole-plagioclase geothermometer"-reply to the comment of Poli and Schmidt: Contributions to Mineralogy and Petrology, v. 111, p. 278-282.

Bonham, H. F., Jr., and Garside, L. J., 1979, Geology of the Tonopah, Lone Mountain, Klondike and Northern Mud Lake quadrangles, Nevada: Nevada Bureau of Mines and Geology Bulletin 92, p. 142.

Borthwick, J., and Harmon, R. S., 1982, A note regarding ClF_3 as an alternative to BrF_5 for oxygen isotope analysis: Geochimica et Cosmochimica Acta, v. 46, p. 1665-1668.

Bottinga, Y., and Javoy, M., 1973, Comments on oxygen isotope geothermometry: Earth and Planetary Science Letters, v. 20, p. 250-265.

Bowman, J. R., Willett, S. D., and Cook, S. J., 1994, Oxygen isotopic transport and exchange during fluid flow: one-dimensional models and applications: American Journal of Science, v. 294, p. 1-55.

Brady, J. B., 1988, The role of volatiles in the thermal history of metamorphic terranes: Journal of Petrology, v. 29, p. 1187-1213.

Brand, U., and Veizer, J., 1980, Chemical diagenesis of a multicomponent carbonate system - 1: trace elements: Journal of Sedimentary Petrology, v. 50, p. 1219-1236.

Brand, U., and Veizer, J., 1981, Chemical diagenesis of a multicomponent carbonate system - 2: stable isotopes: Journal of Sedimentary Petrology, v. 51, p. 987-997.

Brasier, M. D., Khomentovsky, V. V., Corfield, R. M., 1993, Stable isotopic calibration of the earliest skeletal fossil assemblages in eastern Siberia (Precambrian-Cambrian boundary): Terra Nova, v. 5, p. 225-232.

Burnham, C. W., Holloway, J. R., and Davis, N. F., 1969, Thermodynamic properties of water to 1000°C and 10, 000 bars: Geological Society of America Special Paper 132, p. 96.

Cawthorn, R. G., 1976, Some chemical controls on igneous amphibole compositions: Geochimica et Cosmochimica Acta, v. 40, p. 1319-1328.

Cawthorn, R. G., and Brown, P. A., 1976, A model for the formation and crystallization of corundum-normative calc-alkaline magmas through amphibole fractionation: Journal of Geology, v. 84, p. 467-476.

Cawthorn, R. G., and O'Hara, M. J., 1976, Amphibole fractionation in calc-alkaline magma genesis: American Journal of Science, v. 276, p. 309-329.

Chacko, T., Mayeda, T. K., Clayton, R. N., and Goldsmith, J. R., 1991, Oxygen and carbon isotope fractionations between CO_2 and calcite: Geochimica et Cosmochimica Acta, v. 55, p. 2867-2882.

Chatterjee, N. D., and Johannes, W., 1974, Thermal stability and standard thermodynamic properties of synthetic $2M_1$-muscovite $KAl_2[AlSi_3O_{10}(OH)_2]$: Contributions to Mineralogy and Petrology, v. 48, p. 89-114.

Clayton, R. N., Goldsmith, J. R., and Mayeda, T. K., 1989, Oxygen isotope fractionation in quartz, albite, anorthite and calcite: Geochimica et Cosmochimica Acta, v. 53, p. 725-733.

Connolly, J. A. D., 1990, Multivariable phase diagrams: an algorithm based on generalized thermodynamics: American Journal of Science, v. 290, p. 666-718.

Corsetti, F. A., and Kaufman, A. J., 1994, Chemostratigraphy of Neoproterozoic-Cambrian units, White-Inyo region, eastern California and western Nevada: Implications for global correlation and faunal distribution: Palaios, v. 9, p. 211-219.

Criss, R. E., and Taylor, H. P., Jr., 1986, Meteoric-hydrothermal systems, *in* Valley, J. W., O'Neil, J. R., and Taylor, H. P., Jr., eds., Stable isotopes in high temperature geological processes: Reviews in Mineralogy, v. 16, p.373-424.

Davis, S. R., and Ferry, J. M., 1993, Fluid infiltration during contact metamorphism of interbedded marble and calc-silicate hornfels, Twin Lakes area, central Sierra Nevada, California: Journal of Metamorphic Geology, v. 11, p. 71-88.

Derry, L. A., Kaufman, A. J., and Jacobsen, S. B., 1992, Sedimentary cycling and environmental change in the Late Proterozoic: Evidence from stable and radiogenic isotopes: Geochimica et Cosmochimica Acta, v. 56, p. 1317-1329.

Dipple, G. M., and Ferry, J. M., 1992, Fluid flow and stable isotopic alteration in rocks at elevated temperatures with applications to metamorphism: Geochimica et Cosmochimica Acta, v. 56, p. 3539-3550.

Ekren, E. B., Bucknam, R. C., Carr, W. J., Dixon, G. L., and Quinlivan, W. D., 1976, East-trending structural lineaments in central Nevada: United States Geological Survey Professional Paper 986, 16 p.

Etheridge, M. A., Wall, V. J., and Vernon, R. H., 1983, The role of the fluid phase during regional metamorphism and deformation: Journal of Metamorphic Geology, v. 1, p. 205-226.

Farmer, G. L., and DePaolo, D. J., 1983, Origin of Mesozoic and Tertiary granite in the western United States and implications for pre-Mesozoic crustal structure 1. Nd and Sr isotopic studies in the geocline of the northern Great Basin: Journal of Geophysical Research, v. 88, p. 3379-3401.

Farver, J. R., 1994, Oxygen self-diffusion in calcite: dependence on temperature and water fugacity: Earth and Planetary Science Letters, v. 121, p. 575-587.

Farver, J. R., and Yund, R. A., 1991, Oxygen diffusion in quartz: dependence on temperature and water fugacity: Chemical Geology, v. 90, p. 55-70.

Ferry, J. M., 1980, A case study of the amount and distribution of heat and fluid during metamorphism: Contributions to Mineralogy and Petrology, v. 71, p. 373-385.

Ferry, J. M., 1983, Mineral reactions and element migration during metamorphism of calcareous sediments from the Vassalboro Formation, south-central Maine: American Mineralogist, v. 68, p. 334-354.

Ferry, J. M., 1991, Dehydration and decarbonation reactions as a record of fluid infiltration, *in* Kerrick, D. M., ed., Contact Metamorphism: Reviews in Mineralogy, v. 26, p. 351-393.

Ferry, J. M., and Dipple, G. M., 1991, Fluid flow, mineral reactions, and metasomatism: Geology, v. 19, p. 211-214.

Ferry, J. M., and Spear, F. S., 1978, Experimental calibration of partitioning of Fe and Mg between biotite and garnet: Contributions to Mineralogy and Petrology, v. 66, p. 113-117.

Fortier, S. M., and Giletti, B. J., 1991, Volume self-diffusion of oxygen in biotite, muscovite, and phlogopite micas: Geochimica et Cosmochimica Acta, v. 55, p. 1319-1330.

Gao, G., 1990, Geochemical and isotopic constraints on the diagenetic history of a massive stratal, late Cambrian (Royer) dolomite, Lower Arbuckle Group, Slick Hills, SW Oklahoma, USA: Geochimica et Cosmochimica Acta, v. 55, p. 2911-2920.

Garlick, G. D., and Epstein, S., 1967, Oxygen isotope ratios in coexisting minerals of regionally metamorphosed rocks: Geochimica et Cosmochimica Acta, v. 31, p. 181-214.

Gratz, A. J., and Bird, P., 1993, Quartz dissolution: Negative crystal experiments and a rate law: Geochimica et Cosmochimica Acta, v. 57, p. 965-976.

Green, T. H., 1977, Garnet in silicic liquids and its possible use as a P-T indicator: Contributions to Mineralogy and Petrology, v. 65, p. 59-67.

Hammarstrom, J. M., and Zen, E-an, 1986, Aluminum in hornblende: An empirical igneous geobarometer: American Mineralogist, v. 71, p. 1297-1313.

Hammarstrom, J. M., and Zen, E-an, 1992, Discussion of Blundy and Holland's (1990) "Calcic amphibole equilibria and a new amphibole-plagioclase geothermometer": Contributions to Mineralogy and Petrology, v. 111, p. 264-266.

Hanson, R. B., 1992, Effects of fluid production on fluid flow during regional and contact metamorphism: Journal of Metamorphic Geology, v. 10, p. 87-97.

Hochella, M. F., Liou, J. G., Keskinen, M. J., and Kim, H. S., 1982, Synthesis and stability relations of magnesium idocrase: Economic Geology, v. 77, p. 798-808.

Holdaway, M. J., 1972, Thermal stability of Al-Fe epidote as a function of fO_2 and Fe content: Contributions to Mineralogy and Petrology, v. 37, p. 307-340.

Holdaway, M. J., and Mukhopadhyay, B., 1993, A reevaluation of the stability relations of andalusite: thermochemical data and phase diagram for the aluminum silicates: American Mineralogist, v. 78, p. 298-315.

Holland, T. J. B., and Powell, R., 1991, An enlarged and updated internally consistent thermodynamic dataset with uncertainties and correlations: the system K_2O-Na_2O-CaO-MgO-MnO-FeO-Fe_2O_3-Al_2O_3-TiO_2-SiO_2-C-H_2-O_2: Journal of Metamorphic Geology, v. 8, p. 89-124.

Hollister, L. S., Grissom, G. C., Peters, E. K., Stowell, H. H., and Sisson, V. B., 1987, Confirmation of the empirical correlation of Al in hornblende with pressure of solidification of calc-alkaline plutons: American Mineralogist, v. 72, p. 231-239.

Jamtveit, B., Grorud, H. F., and Bucher-Nurminen, K., 1992, Contact metamorphism of layered carbonate-shale sequences in the Oslo Rift. II: Migration of isotopic and reaction fronts around cooling plutons: Earth and Planetary Science Letters, v. 114, p. 131-148.

Jezek, P. A., Sinton, J. M., Jarosewich, E., and Obeymeyer, C. R., 1978, Fusion of rock and mineral powders for electron microprobe analysis: Smithsonian Contributions to the Earth Sciences, v. 22, p. 46-52.

John, D. A., and Robinson, A. C., 1989, Rb-Sr whole-rock isotopic ages of granitic plutons in the western part of the Tonopah 1° by 2° quadrangle, Nevada: Isochron/West, v. 53, p. 20-27.

Johnson, M. C., and Rutherford, M. J., 1989, Experimental calibration of the aluminum-in-hornblende geobarometer with application to Long Valley caldera (California) volcanic rocks: Geology, v. 17, p. 837-841.

Katz, A., and Matthews, A., 1977, The dolomitization of $CaCO_3$: An experimental study at 25-295°C: Geochimica et Cosmochimica Acta, v. 41, p. 297-308.

Katz, A., Sass, E., Starinsky, A., and Holland, H. D., 1972, Strontium behavior in the aragonite-calcite transformation: An experimental study at 40-98°C: Geochimica et Cosmochimica Acta, v. 36, p. 481-496.

Kinsman, D. J. J., 1969, Interpretation of Sr^{+2} concentrations in carbonate minerals and rocks: Journal of Sedimentary Petrology, v. 39, p. 486-508.

Kistler, R. W., 1990, Two different lithospheric type in the Sierra Nevada, California, *in* Anderson, J. L., ed., The nature and origin of Cordilleran magmatism: Geological Society of America Memoir 174, p.271-281.

Knoll, A. H., Hayes, J. M., Kaufman, A. J., Swett, K., and Lambert, I. B., 1986, Secular variation in carbon isotope ratios from Upper Proterozoic successions of Svalbard and East Greenland: Nature, v. 321, p. 832-838.

Kretz, R., 1983, Symbols for rock-forming minerals: American Mineralogist, v. 68, p. 277-279.

Krinsley, D. H., and Doornkamp, J. C., 1973, Atlas of quartz sand surface textures: Cambridge University Press, 91 p.

Labotka, T. C., White, C. E., and Papike, J. J., 1984, The evolution of water in the contact metamorphic aureole of the Duluth Complex, northeastern Minnesota: Geological Society of America Bulletin, v. 95, p. 788-804.

Labotka, T. C., Nabelek, P. I., Papike, J. J., Hover-Granath, V. C., and Laul, J. C., 1988 a, Effects of contact metamorphism on the chemistry of calcareous rocks in the Big Horse Limestone Member, Notch Peak, Utah: American Mineralogist, v. 73, p. 1095-1110.

Labotka, T. C., Nabelek, P. I., and Papike, J. J., 1988 b, Fluid infiltration through the Big Horse Limestone Member in the Notch Peak contact-metamorphic aureole, Utah: American Mineralogist, v. 73, p. 1302-1324.

Lambert, I. B., Walter, M. R., Zang, W., Lu, S., and Ma, G., 1987, Paleoenvironment and carbon isotope stratigraphy of Upper Proterozoic carbonates of the Yangtze Platform: Nature, v. 325, p. 140-142.

Land, L. S., 1980, The isotopic and trace element geochemistry of dolomite: The state of the art, *in* Zenger, D. H., Dunham, J. B., and Ethington, R. L., eds., Concepts and Models of Dolomitization: Society of Economic Paleontologists and Mineralogists Special Publication 28, p.87-110.

Land, L. S., and Hoops, G. K., 1973, Sodium in carbonate sediments and rocks: A possible index to the salinity of diagenetic solutions: Journal of Sedimentary Petrology, v. 43, p. 614-617.

Leake, B. E., 1978, Nomenclature of amphiboles: American Mineralogist, v. 63, p. 1023-1052.

Liou, J. G., 1973, Synthesis and stability relations of epidote, $Ca_2Al_2FeSi_3O_{12}(OH)$: Journal of Petrology, v. 14, p. 381-413.

Machel, H. G., Mason, R. A., Mariano, A. N., and Mucci, A., 1991, Causes and emission of luminescence in calcite and dolomite, *in* Barker, C. E., and Kopp, O. C., eds., Luminescence Microscopy and Spectroscopy: Qualitative and Quantitative Applications: Society of Economic Paleontologists and Mineralogists Short Course 25, p.9-25.

Magaritz, M., Kirschvink, J. L., Latham, A. J., Zhuravlev, A. Y., Rozanov, A. Y., 1991, Precambrian/Cambrian boundary problem: Carbon isotope correlations for Vendian and Tommotian time between Siberia and Morocco: Geology, v. 19, p. 847-850.

Maldonado, F., 1984, Bedrock geologic map of the Lone Mountain pluton area, Esmeralda County, Nevada: United States Geological Survey Miscellaneous Investigation Series Map I-1533, scale 1: 24,000.

McCrea, J. M., 1950, On the oxygen isotope geochemistry of carbonates and a paleotemperature scale: Journal of Chemical Physics, v. 18, p. 849-857.

McKee, E. H., and Moiola, R. J., 1962, Precambrian and Cambrian rocks of south-central Esmeralda County, Nevada: American Journal of Science, v. 260, p. 530-538.

Miller, C. F., and Barton, M. D., 1990, Phanerozoic plutonism in the Cordilleran Interior, U.S.A., *in* Kay, S. M., and Rapela, C. W., eds., Plutonism from Antarctica to Alaska: Geological Society of America Special Paper 241, p.213-231.

Miller, C. F., and Stoddard, E. F., 1981, The role of manganese in the paragenesis of magmatic garnet; An example from the Old Woman-Piute Range, California: Journal of Geology, v. 89, p. 233-246.

Miller, C. F., Stoddard, E. F., Bradfish, L. J., and Dollasse, W. A., 1981, Composition of plutonic muscovite; Genetic implications: Canadian Mineralogist, v. 19, p. 25-34.

Miller, C. F., Watson, E. B., and Harrison, T. M., 1988, Perspectives on the source, segregation, and transport of granitoid magmas: Transactions of the Royal Society of Edinburgh, v. 79, p. 135-156.

Miyashiro, A., 1974, Volcanic rock series in island arcs and active continental margins: American Journal of Science, v. 274, p. 321-355.

Nabelek, P. I., Labotka, T. C., O'Neil, J. R., and Papike, J. J., 1984, Contrasting fluid/rock interaction between the Notch Peak granitic intrusion and argillites and limestones in western Utah: evidence from stable isotopes and phase assemblages: Contributions to Mineralogy and Petrology, v. 86, p. 25-34.

Nabelek, P. I., Labotka, T. C., and Russ-Nabelek, C., 1992, Stable isotope evidence for the role of diffusion, infiltration, and local structure on contact metamorphism of calc-silicate rocks at Notch Peak, Utah: Journal of Petrology, v. 33, p. 557-583.

Naney, M. T., 1983, Phase equilibria of rock-forming ferromagnesian silicates in granitic systems: American Journal of Science, v. 283, p. 993-1033.

Nelson, C. A., 1962, Lower Cambrian-Precambrian succession, White-Inyo Mountains, California: Geological Society of America Bulletin, v. 73, p. 139-144.

O'Neil, J. R., 1987, Preservation of H, C, and O isotopic ratios in the low temperature environment, *in* Kyser, T. K., ed., Stable Isotope Geochemistry of Low Temperature Processes: Mineralogical Association of Canada Short Course 13, p.85-128.

O'Neil, J. R., Clayton, R. N., and Mayeda, T. K., 1969, Oxygen isotope fractionation in divalent metal carbonates: Journal of Chemical Physics, v. 51, p. 1414-1437.

O'Neil, J. R., and Silberman, M. L., 1974, Stable isotope relations in epithermal Au-Ag deposits: Economic Geology, v. 69, p. 902-909.

Patino Douce, A. E., and Johnston, A. D., 1991, Phase equilibria and melt productivity in the pelitic system: implications for the origin of peraluminous granitoids and aluminous granulites: Contributions to Mineralogy and Petrology, v. 107, p.202-218.

Phariss, E. I., 1974. Geology and ore deposits of the Alpine mining district, Esmeralda County, Nevada. M. S. thesis, Nevada. University of Nevada, Reno.

Poli, S., and Schmidt, M. W., 1992, A comment on "Calcic amphibole equilibria and a new amphibole-plagioclase geothermometer" by J. D. Blundy and T. J. B. Holland (Contrib Mineral Petrol (1990) 104: 208-224): Contributions to Mineralogy and Petrology, v. 111, p. 273-278.

Ramseyer, K., Baumann, J., Matter, A., and Mullis, J., 1988, Cathodoluminescence colors of α-quartz: Mineralogical Magazine, v. 52, p. 669-677.

Rice, J. M., 1977, Progressive metamorphism of impure dolomitic limestone in the Marysville aureole, Montana: American Journal of Science, v. 277, p. 1-24.

Rice, J. M., and Ferry, J. M., 1982, Buffering, infiltration, and the control of intensive variables during metamorphism, *in* Ferry, J. M., ed., Characterization of metamorphism through mineral equilibria: Reviews in Mineralogy, v. 10, p.263-326.

Rosenbaum, J., and Sheppard, S. M. F., 1986, An isotopic study of siderites, dolomites and ankerites at high temperatures: Geochimica et Cosmochimica Acta, v. 50, p. 1147-1150.

Rumble, D., III., and Spear, F. S., 1983, Oxygen-isotope equilibration and permeability enhancement during regional metamorphism: Journal of the Geological Society of London, v. 140, p. 619-628.

Rumble, D., III, Ferry, J. M., Hoering, T. C., and Boucot, A. J., 1982, Fluid flow during metamorphism at the Beaver Brook Fossil Locality, New Hampshire: American Journal of Science, 282, 886-919.

Rumble, D., III, Oliver, N. H. S., Ferry, J. M., and Hoering, T. C., 1991, Carbon and oxygen isotope geochemistry of chlorite-zone rocks of the Waterville Formation, Maine, U.S.A.: American Mineralogist, v. 76, p. 857-866.

Rutherford, M. J., and Johnson, M. C., 1992, Comment on Blundy and Holland's (1990) "Calcic amphibole equilibria and a new amphibole-plagioclase geothermometer": Contributions to Mineralogy and Petrology, v. 111, p. 266-268.

Sandy, J., Jr., 1965. Geology of the Lone Mountain intrusive, Esmeralda County, Nevada. M. S. thesis, Tulane University.

Savin, S., and Epstein, S., 1970, The oxygen and hydrogen isotope geochemistry of clay minerals: Geochimica et Cosmochimica Acta, v. 34, p. 25-42.

Schmidt, M. W., 1992, Amphibole composition in tonalite as a function of pressure: an experimental calibration of the Al-in-hornblende barometer: Contributions to Mineralogy and Petrology, v. 110, p. 304-310.

Shand, S. J., 1951, The Study of Rocks: London, Thomas Murby and Company, 236 p.

Sharp, Z. D., and Kirschner, D. L., 1993, Quartz-calcite oxygen isotope thermometry: An empirical calibration: Geological Society of America Abstracts with Programs, v. 25, p. 204.

Sheppard, S. M. F., and Schwarcz, H. P., 1970, Fractionation of carbon and oxygen isotopes and magnesium between coexisting metamorphic calcite and dolomite: Contributions to Mineralogy and Petrology, v. 26, p. 161-198.

Shmonov, V. M., and Shmulovich, K. I., 1974, Molal volumes and equation of state of CO_2 at temperatures from 100 to 1,000°C and pressures from 2,000 to 10,000 bars: Akademiya Nauk SSSR Doklady, v. 217, p. 206-209.

Silberman, M. L., Bonham, H. F., Jr., Garside, L. J., and Osborne, D. H., 1975, New K-Ar ages of volcanic and plutonic rocks and ore deposits in western Nevada: Isochron/West, v. 13, p. 13-21.

Solomon, G. C., and Taylor, H. P., Jr., 1989, Isotopic evidence for the origin of Mesozoic and Cenozoic granitic plutons in the northern Great Basin: Geology, v. 17, p. 591-594.

Sonderman, F. J., 1971, Geology of the Weepah mining district, Esmeralda County, Nevada. M. S. thesis, Nevada. University of Nevada, Reno.

Sprunt, E. S., Dengler, L. A., and Sloan, D., 1978, Effects of metamorphism on quartz cathodoluminescence: Geology, v. 6, p. 305-308.

Stewart, J. H., 1970, Upper Precambrian and lower Cambrian strata in the southern Great Basin, California and Nevada: United States Geological Survey Professional Paper 620, p. 206.

Stewart, J. H., 1985, East-trending dextral faults in the western Great Basin; An explanation for anomalous trends of pre-Cenozoic strata and Cenozoic faults: Tectonics, v. 4, p. 547-564.

Stewart, J. H., 1988, Tectonics of the Walker Lane belt, western Great Basin: Mesozoic and Cenozoic deformation in a zone of shear, *in* Ernst, W. G., ed., Metamorphism and crustal structure of the western United States: Rubey Volume 7: Englewood-Cliffs, New Jersey, Prentice-Hall, p.683-713.

Stewart, J. H., and Diamond, D. S., 1990, Changing patterns of extensional tectonics; Overprinting of the basin of the middle and upper Miocene Esmeralda Formation in western Nevada by younger structural basins, *in* Wernicke, B. P., ed., Basin and Range extensional tectonics near the latitude of Las Vegas, Nevada: Geological Society of America Memoir 176, p.447-475.

Stormer, J. C., Jr., and Nicholls, J., 1978, XLFRAC: a program for the interactive testing of magmatic differentiation models: Computers and Geosciences, v. 4, p. 143-159.

Taylor, H. P., Jr., 1973, O^{18}/O^{16} evidence for meteoric hydrothermal alteration and ore deposition in the Tonopah, Comstock Lode, and Goldfield mining districts, Nevada: Economic Geology, v. 68, p. 747-764.

Taylor, H. P., Jr., 1974, The application of oxygen and hydrogen isotope studies to problems of hydrothermal alteration and ore deposition: Economic Geology, v. 69, p. 843-883.

Taylor, H. P., Jr., 1978, Oxygen and hydrogen isotope studies of plutonic granitic rocks: Earth and Planetary Science Letters, v. 38, p. 177-210.

Tulloch, A. J., 1979, Secondary Ca-Al silicates as low-grade alteration products of granitoid biotite: Contributions to Mineralogy and Petrology, v. 69, p. 105-117.

Tulloch, A. J., 1986, Comment on "Implications of magmatic epidote-bearing plutons on crustal evolution in the accreted terranes of northwestern North America" and "Magmatic epidote and its petrologic significance": Geology, v. 14, p. 186-187.

Valley, J. W., 1986, Stable isotope geochemistry of metamorphic rocks, *in* Valley, J. W., Taylor, H. P., Jr., and O'Neil, J. R., eds., Stable isotopes in high temperature geological processes: Reviews in Mineralogy, v. 16, p.445-489.

Valley, J. W., Peacor, D. R., Bowman, J. R., Essene, E. J. and Allard, M. J., 1985. Crystal chemistry of a Mg-vesuvianite and implications of phase equilibria in the system CaO-MgO-Al_2O_3-SiO_2-H_2O-CO_2. Journal of Metamorphic Geology, 3, 137-153.

Veizer, J., 1983, Chemical diagenesis of carbonates: Theory and application of trace element technique, *in* Arthur, M. M., ed., Stable Isotopes in Sedimentary Geology: Society of Economic Paleontologists and Mineralogists Short Course 10, p. 3-1 to 3-100.

Veizer, J., and Hoefs, J., 1976, The nature of O^{18}/O^{16} and C^{13}/C^{12} secular trends in sedimentary carbonate rocks: Geochimica et Cosmochimica Acta, v. 40, p. 1387-1395.

Weber, J. N., 1964, Trace element composition of dolostones and dolomite and its bearing on the dolomite problem: Geochimica et Cosmochimica Acta, v. 28, p. 1817-1868.

Wenk, H.-R., 1985, Carbonates, *in* Wenk, H.-R., ed., Preferred orientation in deformed metals and rocks: an introduction to modern texture analysis: Orlando, Academic Press, p.361-384.

Wickham, S. M., and Peters, M. T., 1993, High $\delta^{13}C$ Neoproterozoic carbonate rocks in western North America: Geology, v. 21, p. 165-168.

Wyllie, P. J., 1977, Crustal anatexis - An experimental review: Tectonophysics, v. 43, p. 41-71.

Yount, J. C., Bell, J. W., dePolo, C. M., and Ramelli, A. R., 1993, Neotectonics of the Walker lane, Pyramid Lake to Tonopah, Nevada, *in* Lahren, M. M., Trexler, J. H., Jr., and Spinosa, C., eds., Crustal Evolution of the Great Basin and the Sierra Nevada: p.383-408.

Zartman, R. E., 1974, Lead isotopic provinces of the western United States and their geologic significance: Economic Geology, v. 69, p. 792-805.

Zen, E-an., and Hammarstrom, J. M., 1984, Magmatic epidote and its petrologic significance: Geology, v. 12, p. 515-518.

Zenger, D. H., 1976, Dolomitization and dolomite "dikes" in the Wyman Formation (Precambrian), northeastern Inyo Mountains, California: Journal of Sedimentary Petrology, v. 64, p. 457-462.

Zhu, H., Newton, R. C., and Kleppa, O. J., 1994, Enthalpy of formation of wollastonite ($CaSiO_3$) and anorthite ($CaAl_2Si_2O_8$) by experimental phase equilibrium measurements and high-temperature solution calorimetry: American Mineralogist, v. 79, p. 134-144.

Zinkernagel, U., 1978, Cathodoluminescence of quartz and its application to sandstone petrology: Contributions to Sedimentology, v. 8, 69 p.

APPENDIX

ANALYTICAL METHODS

One hundred and thirty six samples were collected from one hundred and four locations. Metamorphic rocks were collected along four traverses approximately perpendicular to granite contacts. Sample locations are shown on Figure A1. Two rock chips were cut from the same area of each sample. A thin section was made from one chip, and the other chip was crushed to –500+250 μm for stable isotope and whole-rock chemical analyses. For marbles, between approximately 100 and 200 g, and for calc-silicate rocks approximately 20 g, of additional sample was crushed and dissolved in dilute hydrochloric at 25°C for calcite marbles and calc-silicate rocks and at 50°C for dolomite marbles. The resulting non-carbonate residue was filtered, dried, then resized. Silicate mineral grains were then hand picked under a binocular microscope and are estimated to be greater than 95% pure. After initial observation of quartz grains from marbles under the binocular microscope, replicates of calcite marble powders were dissolved in dilute glacial acetic acid at 25°C, and replicates of dolomite marble powders were dissolved in dilute formic acid at 25°C. Marbles were treated in this manner to ensure that the surface features of the quartz grains observed using the scanning electron microscope were not caused by reaction with hydrochloric acid. Quartz grains with conchoidal fracture were not considered for scanning electron microscope observation, because this feature may have been caused by crushing during sample preparation. The same features and the same isotopic compositions were observed and determined from the marbles irrespective of the type of acid used in the digestion of the sample.

Mineral and whole-rock chemical compositions were determined with a Cameca SX50 electron microprobe in the Department of Geological Sciences, University of Tennessee. Operating conditions in wavelength dispersive mode were an accelerating potential of 15 kV with a beam current of 30 nA and size of 5 μm for garnet and pyroxene, 20 nA, 5 μm for feldspar, mica, chlorite, epidote, amphibole, 10 nA, 20 μm

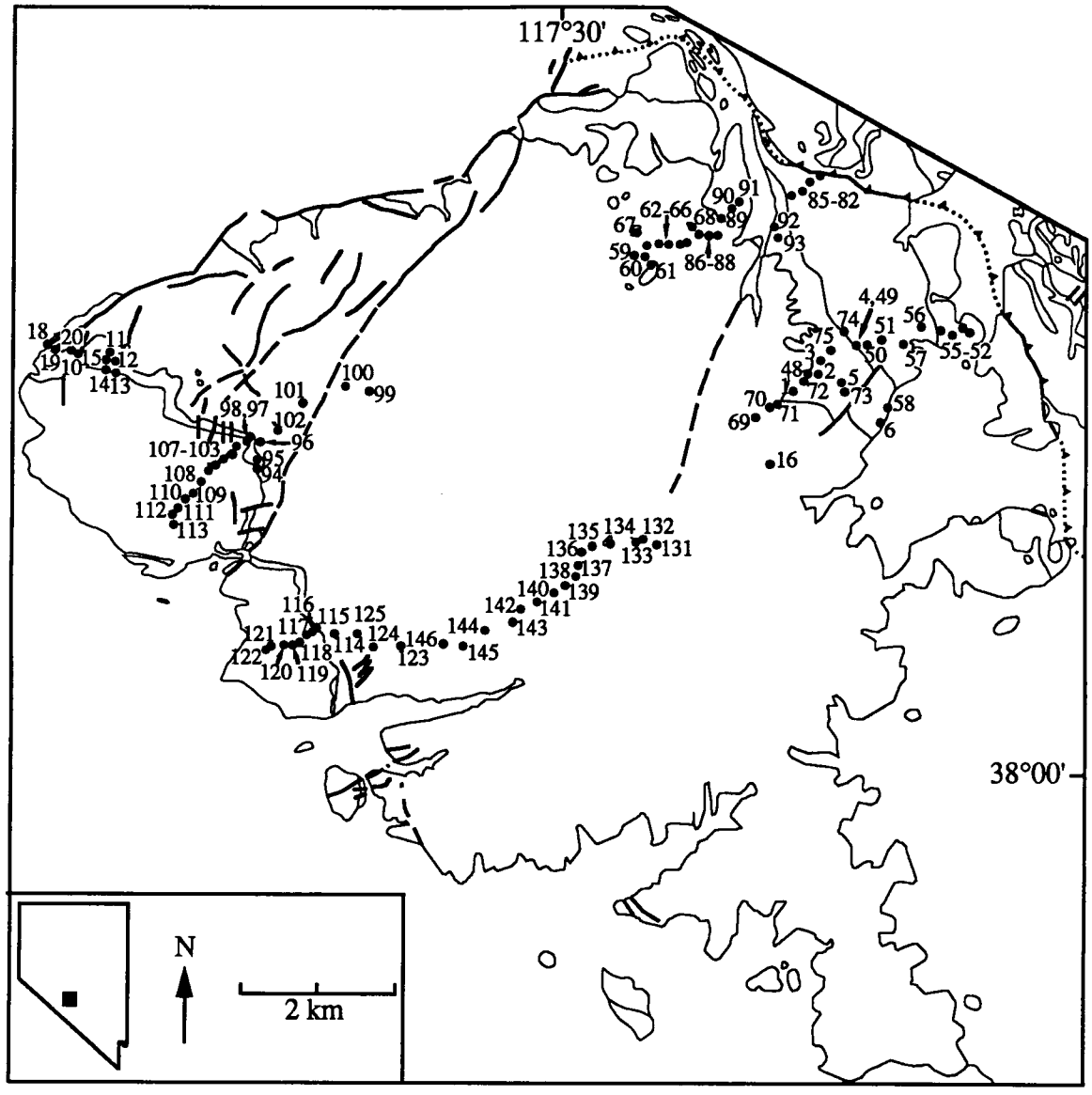

Figure A1: Sample location map.

for carbonate minerals, and 20 nA, 20 μm for whole rock glasses. With the exception of carbonate minerals, counting times for all elements was 20 s. For carbonate minerals counting times were 10 s for Ca and 40 s for Fe, Mg, and Mn. Natural and synthetic mineral standards were used to calibrate each element and standards were analyzed both before and after unknowns. Raw data were reduced on-line using ZAF corrections. The accuracy of analyses is approximately ± 2% for major elements and ± 10% for minor elements. Electron microprobe analyses of minerals are given in Tables A1 to A12, and analyses of standards in Table A13. Whole rock glass beads were prepared following the method of Jezek and others (1978). Approximately 10 mg of sample was fused on a Mo strip-heater in a nitrogen atmosphere. Each glass bead was analyzed at least 10 times and the average result used after being renormalized to the measured weight percentage totals, after correcting for the presence of Mo, which was assumed not to be originally present in any sample.

Whole-rock chemical compositions were also determined by X-ray fluorescence with a HNu energy-dispersive X-ray fluorescence spectrometer in the Department of Geological Sciences, University of Tennessee, using natural and synthetic standards. Samples were pulverized in a tungsten carbide mill and pressed into pellets using a boric acid mounting medium. The accuracy of analyses is approximately ± 5% for major elements and ± 20% for minor elements. Analyses of standards are given in Table A14. The LSDOL protocol was used for marbles, the TECLAY protocol for pelitic schists, and the IGROCK and SIAL protocols for igneous rocks. Comparisons between the IGROCK and SIAL protocols, and between electron microprobe and X-ray fluorescence analyses for granite samples are given in Tables A15 and A16, respectively. Loss on ignition for pelitic schists was determined by heating approximately 10 g of sample at 1000°C for approximately 1 hour.

The isotopic composition of carbonate minerals was determined by liberating CO_2 by reaction of approximately 15 mg of sample with orthophosphoric acid. Calcite (–500+250 μm) was reacted at 25°C for approximately 12 hours (McCrea, 1950). Dolomite (–75 μm) was reacted for approximately 24 hours at 50°C and the $\delta^{18}O$ values corrected using the dolomite-orthophosphoric acid fractionation factor of Rosenbaum and Sheppard (1986). Mixed calcite-dolomite samples (–75 μm) were reacted at 25°C for 2 hours, the CO_2 collected for calcite and then reacted again at 50°C for approximately 24 hours and the CO_2 collected for dolomite (Al-Assam and others, 1990). The weight percent CO_2 of each sample was determined by measuring the yield of CO_2 liberated from the orthophosphoric acid reaction. The isotopic composition of silicate minerals was determined using the method of Borthwick and Harmon (1983). Approximately 10 mg of sample was placed in a nickel reaction vessel with 150 torr of ClF_3 and reacted at 550°C for approximately 12 hours. The liberated O_2 was then converted to CO_2 by heating with a graphite rod. The δ-values are reported with respect to SMOW for oxygen and PDB for carbon. Replicate analyses of the carbonate standards NBS18 and NBS19 give average values of $\delta^{13}C = -5.07$, and $\delta^{18}O = 23.08$, and $\delta^{13}C = 1.88$, and $\delta^{18}O = 28.39$, respectively. Reproducibility of analyses is $\pm$ 0.1‰ for both $\delta^{13}C$ and $\delta^{18}O$. Replicate analyses of the quartz standard NBS28 give average values for $\delta^{18}O$ of 9.6‰. Reproducibility of analyses is $\pm$ 0.2‰ for $\delta^{18}O$. Carbonate stable isotope analyses were conducted in the Department of Geological Sciences at the University of Tennessee, and silicate stable isotope analyses and checks on carbonate stable isotope analyses were conducted in the Department of Geological Sciences at Southern Methodist University. Whole rock $\delta^{18}O$ values for marbles and calc-silicate rocks were calculated using the mass balance relationship $\delta^{18}O_{\text{whole rock}} = \Sigma\, \delta^{18}O_i X_i$, where $\delta^{18}O_i$ = oxygen isotopic composition of mineral , and X_i = fraction of mineral in rock.

Polished thin sections of marbles were examined using a Citl cold cathode luminoscope operating at an energy of between 15 and 17 kV, and a beam current of approximately 300 μA. The colors used to describe calcite, dolomite, and quartz are based on their appearance when viewed under cathodoluminescence.

Table A1: Electron microprobe analyses of calcite

Sample	LM10										LM48	
Analysis	1	2	3	4	5	6	7	8	9	10	1	2
FeO	0.09	0.09	0.09	<0.06	<0.06	<0.06	<0.06	<0.06	<0.06	<0.06	0.10	0.14
MnO	0.08	<0.05	<0.05	<0.05	<0.05	<0.05	<0.05	<0.05	<0.05	<0.05	<0.05	<0.05
MgO	0.02	<0.02	<0.02	<0.02	<0.02	<0.02	<0.02	<0.02	<0.02	<0.02	<0.02	<0.02
CaO	54.7	55.2	55.2	53.6	54.4	54.7	54.6	54.4	54.7	54.6	54.5	54.6
Total	54.93	55.30	55.24	53.63	54.52	54.82	54.67	54.52	54.82	54.67	54.59	54.71
						1 oxygen						
Fe	0.001	0.001	0.001	0.000	0.000	0.001	0.000	0.000	0.001	0.000	0.001	0.002
Mn	0.001	0.000	0.000	0.000	0.001	0.000	0.000	0.001	0.000	0.000	0.000	0.000
Mg	0.000	0.000	0.000	0.000	0.000	0.000	0.000	0.000	0.000	0.000	0.000	0.000
Ca	0.997	0.999	0.999	0.999	0.999	0.999	0.999	0.999	0.999	0.999	0.998	0.998
Total	0.999	1.000	1.000	0.999	1.000	1.000	0.999	1.000	1.000	0.999	0.999	1.000

Sample	LM55-2	LM58-2	LM68-2		LM72							
Analysis	1	1	1	2	1	2	3	4	5	6	7	8
FeO	0.09	0.14	0.49	0.37	<0.06	<0.06	0.06	0.09	<0.06	<0.06	<0.06	<0.06
MnO	<0.05	<0.05	<0.05	<0.05	<0.05	<0.05	<0.05	<0.05	<0.05	<0.05	<0.05	<0.05
MgO	0.09	0.43	0.17	0.15	0.09	0.08	0.08	0.09	0.02	0.07	0.05	0.05
CaO	54.9	55.6	53.5	54.8	54.7	54.5	55.2	54.9	55.4	55.3	54.9	55.3
Total	55.05	56.22	54.12	55.39	54.81	54.58	55.35	55.04	55.44	55.37	54.94	55.38
						1 oxygen						
Fe	0.001	0.002	0.007	0.005	0.001	0.000	0.001	0.001	0.000	0.000	0.000	0.000
Mn	0.000	0.000	0.000	0.001	0.000	0.000	0.000	0.000	0.000	0.000	0.000	0.000
Mg	0.002	0.011	0.004	0.004	0.002	0.002	0.002	0.002	0.001	0.002	0.001	0.001
Ca	0.996	0.987	0.988	0.990	0.997	0.998	0.997	0.996	0.999	0.998	0.999	0.998
Total	0.999	1.000	0.999	1.000	1.000	1.000	1.000	0.999	1.000	1.000	1.000	0.999

Sample	LM74-1	LM75-1				LM75-2		LM90	LM92-1		LM94	
Analysis	1	1	2	3	4	1	2	1	1	2	1	2
FeO	0.76	0.38	0.67	0.52	0.28	<0.06	<0.06	0.30	0.50	0.47	0.37	0.22
MnO	0.22	<0.05	<0.05	0.05	0.08	<0.05	<0.05	0.06	0.16	0.08	0.19	0.32
MgO	0.16	0.10	0.11	0.06	0.09	0.15	0.10	0.11	0.17	0.18	0.12	0.09
CaO	53.8	54.0	54.2	54.4	54.4	54.5	54.7	54.1	54.5	54.0	53.8	54.4
Total	54.94	54.48	55.00	54.98	54.80	54.61	54.80	54.59	55.34	54.72	54.48	55.07
						1 oxygen						
Fe	0.011	0.005	0.009	0.007	0.004	0.000	0.000	0.004	0.007	0.007	0.005	0.003
Mn	0.003	0.001	0.000	0.001	0.001	0.000	0.000	0.001	0.002	0.001	0.003	0.005
Mg	0.004	0.003	0.003	0.001	0.002	0.004	0.003	0.003	0.004	0.004	0.003	0.002
Ca	0.982	0.991	0.987	0.990	0.993	0.996	0.997	0.992	0.986	0.988	0.989	0.990
Total	1.000	1.000	0.999	0.999	1.000	1.000	1.000	1.000	1.000	1.000	1.000	1.000

Table A1: (continued)

Sample	LM97-2	LM105-4		LM111-2								
Analysis	1	1	2	1	2	3	4	5	6	7	8	9
FeO	0.11	0.20	0.34	<0.06	<0.06	<0.06	<0.06	0.06	<0.06	<0.06	<0.06	<0.06
MnO	<0.05	<0.05	<0.05	0.05	<0.05	<0.05	<0.05	<0.05	<0.05	<0.05	<0.05	<0.05
MgO	1.15	0.67	0.59	1.43	1.45	0.35	0.59	1.44	0.68	1.69	0.54	1.05
CaO	54.4	54.0	54.1	54.0	54.1	55.4	55.3	53.2	54.4	53.2	55.3	54.3
Total	55.60	54.90	55.09	55.51	55.58	55.72	55.88	54.75	55.12	54.98	55.82	55.38
						1 oxygen						
Fe	0.002	0.003	0.005	0.000	0.001	0.000	0.000	0.001	0.000	0.001	0.000	0.000
Mn	0.000	0.000	0.000	0.001	0.000	0.000	0.000	0.000	0.000	0.000	0.000	0.001
Mg	0.028	0.017	0.015	0.035	0.036	0.009	0.015	0.036	0.017	0.042	0.013	0.026
Ca	0.970	0.980	0.980	0.964	0.963	0.991	0.985	0.963	0.982	0.957	0.986	0.973
Total	1.000	1.000	1.000	1.000	1.000	1.000	1.000	1.000	0.999	1.000	0.999	1.000

Sample	LM111-2							LM112				
Analysis	10	11	12	13	14	15	16	1	2	3	4	5
FeO	0.06	0.06	0.07	0.06	<0.06	<0.06	<0.06	<0.06	<0.06	0.06	<0.06	0.06
MnO	<0.05	<0.05	<0.05	<0.05	<0.05	<0.05	<0.05	<0.05	<0.05	<0.05	<0.05	<0.05
MgO	2.23	1.22	0.27	0.39	4.97	0.73	1.29	1.16	2.27	1.05	0.77	0.22
CaO	52.7	54.4	55.0	54.7	49.7	54.7	54.4	54.7	52.6	54.6	54.7	55.4
Total	54.99	55.68	55.38	55.15	54.75	55.45	55.76	55.93	54.98	55.69	55.54	55.70
						1 oxygen						
Fe	0.001	0.001	0.001	0.001	0.001	0.000	0.000	0.000	0.001	0.001	0.000	0.001
Mn	0.000	0.000	0.000	0.000	0.000	0.000	0.000	0.000	0.001	0.000	0.000	0.000
Mg	0.056	0.030	0.007	0.010	0.122	0.018	0.032	0.029	0.056	0.026	0.019	0.006
Ca	0.943	0.969	0.992	0.989	0.877	0.981	0.968	0.971	0.942	0.973	0.980	0.994
Total	1.000	1.000	1.000	1.000	1.000	0.999	1.000	1.000	1.000	1.000	0.999	1.001

Sample	LM112											
Analysis	6	7	8	9	10	11	12	13	14	15	16	17
FeO	<0.06	<0.06	<0.06	<0.06	<0.06	<0.06	<0.06	0.07	<0.06	<0.06	0.07	<0.06
MnO	<0.05	<0.05	0.07	0.06	<0.05	<0.05	<0.05	<0.05	<0.05	<0.05	0.06	<0.05
MgO	0.32	0.38	0.42	0.93	0.21	0.30	0.59	0.47	0.28	5.32	1.70	0.22
CaO	55.6	55.8	55.5	54.6	55.4	55.1	54.4	55.1	54.7	49.8	53.7	54.8
Total	56.00	56.15	56.02	55.58	55.64	55.39	54.99	55.61	55.03	55.16	55.49	55.12
						1 oxygen						
Fe	0.001	0.000	0.000	0.000	0.000	0.000	0.000	0.001	0.001	0.001	0.001	0.001
Mn	0.000	0.000	0.001	0.001	0.000	0.000	0.000	0.000	0.000	0.000	0.001	0.001
Mg	0.008	0.009	0.010	0.023	0.005	0.008	0.015	0.012	0.007	0.129	0.042	0.006
Ca	0.991	0.991	0.988	0.976	0.994	0.992	0.985	0.987	0.992	0.870	0.956	0.993
Total	1.000	1.000	0.999	1.000	0.999	1.000	1.000	1.000	1.000	1.000	1.000	1.001

Table A1: (continued)

Sample	LM112										
Analysis	18	19	20	21	22	23	24	25	26	27	28
FeO	<0.06	<0.06	<0.06	<0.06	<0.06	0.06	0.07	<0.06	<0.06	<0.06	<0.06
MnO	<0.05	<0.05	0.06	<0.05	<0.05	<0.05	<0.05	<0.05	<0.05	0.06	<0.05
MgO	0.70	0.29	1.07	0.45	0.58	1.70	1.46	0.25	1.39	1.47	1.40
CaO	54.7	55.3	54.2	55.5	54.5	53.3	53.2	55.5	53.8	54.1	54.1
Total	55.49	55.61	55.38	56.01	55.07	55.06	54.75	55.72	55.27	55.64	55.51
						1 oxygen					
Fe	0.000	0.000	0.000	0.000	0.000	0.001	0.001	0.000	0.000	0.000	0.000
Mn	0.000	0.000	0.001	0.000	0.000	0.000	0.000	0.000	0.000	0.001	0.000
Mg	0.017	0.007	0.027	0.011	0.015	0.042	0.037	0.006	0.035	0.036	0.035
Ca	0.982	0.992	0.972	0.988	0.985	0.957	0.962	0.993	0.964	0.962	0.965
Total	0.999	0.999	1.000	0.999	1.000	1.000	1.000	0.999	0.999	0.999	1.000

Table A2: Electron microprobe analyses of dolomite

Sample	LM85		LM105-5	LM107	LM111-2							
Analysis	1	2	1	1	1	2	3	4	5	6	7	8
FeO	0.21	0.24	0.34	0.28	0.21	0.23	0.17	0.23	0.21	0.18	0.23	0.18
MnO	<0.05	<0.05	<0.05	<0.05	<0.05	<0.05	<0.05	<0.05	<0.05	<0.05	<0.05	<0.05
MgO	21.6	21.6	21.6	21.8	21.6	21.6	21.4	21.4	21.4	21.6	21.6	21.5
CaO	30.7	30.8	29.9	31.1	30.6	30.3	30.2	30.5	30.2	30.6	30.2	30.6
Total	52.48	52.67	51.92	53.17	52.41	52.07	51.82	52.08	51.78	52.31	52.05	52.24
						2 oxygens						
Fe	0.005	0.007	0.009	0.007	0.005	0.006	0.004	0.006	0.005	0.005	0.006	0.005
Mn	0.001	0.000	0.001	0.001	0.001	0.000	0.001	0.000	0.000	0.000	0.001	0.001
Mg	0.986	0.985	0.998	0.983	0.988	0.994	0.990	0.986	0.990	0.989	0.993	0.986
Ca	1.008	1.008	0.992	1.009	1.006	1.000	1.005	1.008	1.004	1.006	1.000	1.009
Total	2.000	2.000	2.000	2.000	2.000	2.000	2.000	2.000	1.999	2.000	2.000	2.001
Sample	LM111-2										LM112	
Analysis	9	10	11	12	13	14	15	16	17	18	1	2
FeO	0.23	0.20	0.26	0.17	0.22	0.23	0.19	0.24	0.26	0.25	0.21	0.26
MnO	0.06	<0.05	<0.05	<0.05	0.05	0.06	<0.05	<0.05	<0.05	<0.05	0.05	<0.05
MgO	21.5	21.5	21.5	21.4	21.4	21.4	21.5	21.3	21.5	21.5	21.3	21.5
CaO	29.8	31.0	30.1	30.8	30.8	29.9	29.7	30.2	31.0	30.2	30.8	31.0
Total	51.63	52.63	51.94	52.47	52.44	51.59	51.43	51.68	52.70	51.93	52.37	52.72
						2 oxygens						
Fe	0.006	0.005	0.007	0.004	0.006	0.006	0.005	0.006	0.007	0.006	0.006	0.007
Mn	0.002	0.000	0.000	0.001	0.001	0.002	0.001	0.000	0.000	0.000	0.001	0.000
Mg	0.998	0.980	0.994	0.981	0.981	0.995	1.002	0.987	0.978	0.991	0.978	0.977
Ca	0.994	1.015	0.999	1.013	1.012	0.997	0.993	1.006	1.015	1.003	1.015	1.016
Total	2.000	2.000	2.000	1.999	2.000	2.000	2.001	1.999	2.000	2.000	2.000	2.000
Sample	LM112											
Analysis	3	4	5	6	7	8	9	10	11	12	13	14
FeO	0.19	0.25	0.27	0.26	0.15	0.18	0.18	0.23	0.15	0.20	0.21	0.23
MnO	<0.05	<0.05	<0.05	<0.05	<0.05	<0.05	<0.05	0.06	<0.05	<0.05	<0.05	<0.05
MgO	21.5	21.5	21.5	21.4	21.4	21.3	21.4	21.5	21.6	21.3	21.4	21.4
CaO	31.0	31.1	30.7	30.2	30.8	29.9	30.7	29.8	29.7	30.2	30.2	30.4
Total	52.73	52.88	52.41	51.94	52.42	51.40	52.24	51.63	51.39	51.62	51.76	52.07
						2 oxygens						
Fe	0.005	0.006	0.007	0.007	0.004	0.005	0.005	0.006	0.004	0.005	0.005	0.006
Mn	0.001	0.000	0.000	0.000	0.000	0.001	0.001	0.002	0.001	0.000	0.000	0.000
Mg	0.980	0.977	0.984	0.990	0.982	0.992	0.982	0.998	1.004	0.987	0.990	0.987
Ca	1.014	1.016	1.009	1.003	1.014	1.002	1.013	0.995	0.992	1.007	1.004	1.007
Total	2.000	1.999	2.000	2.000	2.000	2.000	2.001	2.001	2.001	1.999	1.999	2.000

Table A2: (continued)

Sample	LM112						LM117		LM121
Analysis	15	16	17	18	19	20	1	2	1
FeO	0.25	0.20	0.17	0,20	0.21	0.27	0.23	0.27	0.21
MnO	<0.05	<0.05	<0.05	<0.05	<0.05	<0.05	<0.05	<0.05	<0.05
MgO	21.3	21.6	21.4	21.6	21.6	21.5	21.8	21.9	21.9
CaO	30.6	30.4	30.1	30.3	30.5	31.3	31.2	31.2	31.1
Total	52.11	52.23	51.72	52.04	52.37	53.04	53.21	53.41	53.25
					2 oxygens				
Fe	0.006	0.005	0.004	0.005	0.005	0.005	0.006	0.007	0.005
Mn	0.001	0.001	0.001	0.000	0.001	0.001	0.001	0.001	0.001
Mg	0.980	0.989	0.991	0.994	0.988	0.988	0.983	0.984	0.987
Ca	1.013	1.004	1.003	1.001	1.006	1.005	1.011	1.009	1.007
Total	2.000	1.999	1.999	2.000	2.000	1.999	2.001	2.001	2.000

Table A3: Electron microprobe analyses of pyroxene

Sample	LM10											
Analysis	1	2	3	4	5	6	7	8	9	10	11	12
SiO_2	53.5	53.1	53.0	52.8	53.2	53.1	53.2	53.8	53.7	54.4	54.3	54.2
TiO_2	<0.02	<0.02	<0.02	<0.02	0.02	<0.02	<0.02	<0.02	<0.02	<0.02	<0.02	<0.02
Al_2O_3	0.16	0.33	0.34	0.36	0.34	0.35	0.36	0.59	0.51	0.28	0.51	0.15
Cr_2O_3	<0.05	0.05	<0.05	<0.05	0.05	0.10	<0.05	0.13	0.07	<0.05	0.06	<0.05
FeO	5.56	7.25	7.24	7.17	7.09	7.54	7.26	5.56	5.80	6.18	5.49	2.64
MnO	0.10	0.07	0.11	0.08	0.09	0.09	0.04	0.10	0.06	0.12	0.08	0.10
MgO	14.8	13.8	13.6	13.7	13.6	13.4	13.8	14.8	14.6	14.1	14.8	16.7
CaO	25.0	24.6	24.8	25.0	25.0	24.9	24.7	25.1	25.0	25.2	25.3	25.5
Na_2O	0.13	0.22	0.24	0.20	0.23	0.22	0.23	0.30	0.26	0.17	0.25	0.13
Total	99.24	99.45	99.35	99.34	99.56	99.70	99.63	100.28	100.02	100.38	100.69	99.32
						6 oxygens						
Si	1.995	1.991	1.989	1.983	1.990	1.990	1.990	1.983	1.989	2.005	1.992	1.992
Ti	0.000	0.000	0.000	0.000	0.001	0.000	0.000	0.000	0.000	0.000	0.000	0.000
Al	0.007	0.015	0.015	0.016	0.015	0.015	0.016	0.025	0.022	0.012	0.022	0.006
Cr	0.001	0.002	0.001	0.001	0.001	0.003	0.001	0.004	0.002	0.000	0.002	0.000
Fe	0.173	0.227	0.227	0.225	0.222	0.236	0.227	0.171	0.179	0.191	0.168	0.081
Mn	0.003	0.002	0.003	0.003	0.003	0.003	0.001	0.003	0.002	0.004	0.003	0.003
Mg	0.821	0.768	0.761	0.767	0.761	0.746	0.767	0.814	0.804	0.774	0.807	0.913
Ca	0.997	0.989	0.997	1.006	1.001	1.001	0.991	0.990	0.991	0.996	0.994	1.004
Na	0.009	0.016	0.018	0.015	0.016	0.016	0.016	0.021	0.019	0.012	0.018	0.009
Total	4.006	4.010	4.011	4.016	4.010	4.010	4.009	4.011	4.008	3.994	4.006	4.008

Sample	LM10											
Analysis	13	14	15	16	17	18	19	20	21	22	23	24
SiO_2	53.2	54.2	53.4	53.6	53.9	54.0	52.9	52.7	52.9	53.1	52.8	53.5
TiO_2	<0.02	<0.02	<0.02	<0.02	0.02	<0.02	<0.02	0.02	0.02	0.02	<0.02	<0.02
Al_2O_3	0.25	0.12	0.83	0.29	0.35	0.58	0.54	0.65	0.57	0.65	0.66	0.38
Cr_2O_3	<0.05	<0.05	<0.05	<0.05	<0.05	0.10	<0.05	<0.05	<0.05	<0.05	0.08	<0.05
FeO	6.57	3.99	6.05	6.53	6.93	5.89	6.26	5.38	6.86	7.21	7.05	4.93
MnO	<0.04	0.09	0.05	0.04	0.07	0.11	0.07	0.05	0.09	0.08	0.11	0.08
MgO	14.2	16.2	14.5	14.0	13.7	14.5	14.0	14.1	13.8	13.5	13.5	15.1
CaO	24.9	25.6	24.9	25.0	25.1	24.9	24.9	24.9	24.9	24.8	24.7	25.2
Na_2O	0.16	0.14	0.30	0.21	0.24	0.28	0.28	0.31	0.29	0.29	0.35	0.22
Total	99.40	100.23	100.04	99.65	100.31	100.32	98.95	98.08	99.53	99.61	99.24	99.43
						6 oxygens						
Si	1.990	1.987	1.979	1.998	1.998	1.992	1.985	1.989	1.981	1.985	1.984	1.986
Ti	0.000	0.000	0.001	0.000	0.001	0.000	0.000	0.000	0.000	0.001	0.000	0.000
Al	0.011	0.005	0.036	0.013	0.015	0.025	0.024	0.029	0.025	0.028	0.029	0.017
Cr	0.001	0.000	0.000	0.001	0.000	0.003	0.001	0.000	0.001	0.001	0.002	0.001
Fe	0.205	0.122	0.188	0.203	0.215	0.182	0.197	0.170	0.215	0.226	0.222	0.153
Mn	0.001	0.003	0.002	0.001	0.002	0.003	0.002	0.002	0.003	0.002	0.004	0.002
Mg	0.794	0.884	0.798	0.776	0.759	0.797	0.782	0.790	0.770	0.752	0.756	0.837
Ca	0.996	1.005	0.989	0.996	0.996	0.982	1.001	1.006	1.000	0.994	0.992	1.000
Na	0.012	0.010	0.022	0.015	0.017	0.020	0.020	0.023	0.021	0.021	0.025	0.016
Total	4.010	4.016	4.015	4.003	4.003	4.004	4.012	4.009	4.016	4.010	4.014	4.012

Table A3: (continued)

Sample	LM68-1											
Analysis	1	2	3	4	5	6	7	8	9	10	11	12
SiO_2	52.2	52.7	52.5	52.4	51.7	52.3	51.9	52.9	52.1	52.0	51.6	51.8
TiO_2	<0.02	<0.02	<0.02	<0.02	<0.02	<0.02	<0.02	<0.02	<0.02	<0.02	<0.02	<0.02
Al_2O_3	0.06	0.07	0.04	0.19	0.16	0.17	0.15	0.12	0.18	0.16	0.21	0.19
Cr_2O_3	<0.05	<0.05	<0.05	<0.05	0.07	0.06	<0.05	<0.05	0.07	<0.05	<0.05	<0.05
FeO	12.1	10.8	11.3	12.9	12.9	12.2	12.3	9.86	12.0	12.1	12.6	12.4
MnO	0.19	0.12	0.14	0.12	0.14	0.15	0.15	0.14	0.14	0.19	0.18	0.16
MgO	10.7	11.4	11.5	10.3	10.4	10.7	10.6	12.1	10.5	10.7	10.4	10.7
CaO	24.5	24.8	24.7	24.2	24.0	24.2	24.6	24.6	24.3	24.4	24.2	24.3
Na_2O	0.06	0.07	0.05	0.16	0.15	0.14	0.16	0.11	0.16	0.14	0.16	0.14
Total	99.86	99.99	100.17	100.29	99.81	99.95	99.83	99.82	99.40	99.67	99.38	99.70
						6 oxygens						
Si	1.994	1.996	1.992	1.995	1.985	1.995	1.986	1.997	1.996	1.991	1.985	1.986
Ti	0.000	0.000	0.000	0.000	0.000	0.000	0.000	0.000	0.000	0.000	0.000	0.000
Al	0.003	0.003	0.002	0.008	0.007	0.007	0.007	0.005	0.008	0.007	0.010	0.009
Cr	0.001	0.001	0.000	0.000	0.002	0.002	0.001	0.001	0.002	0.001	0.000	0.001
Fe	0.387	0.341	0.358	0.412	0.414	0.390	0.393	0.311	0.385	0.388	0.406	0.396
Mn	0.006	0.004	0.004	0.004	0.004	0.005	0.005	0.004	0.004	0.006	0.006	0.005
Mg	0.611	0.645	0.647	0.587	0.594	0.607	0.603	0.681	0.600	0.609	0.598	0.610
Ca	1.000	1.008	1.002	0.987	0.999	0.989	1.008	0.997	0.996	0.999	1.000	0.998
Na	0.005	0.005	0.004	0.011	0.011	0.010	0.012	0.008	0.011	0.010	0.012	0.010
Total	4.007	4.003	4.009	4.004	4.016	4.005	4.015	4.004	4.002	4.011	4.017	4.015

Sample	LM68-1	LM72									
Analysis	13	1	2	3	4	5	6	7	8	9	10	11
SiO_2	51.6	53.7	53.9	53.5	52.5	53.7	54.2	53.8	53.7	53.6	54.0	54.3
TiO_2	<0.02	<0.02	<0.02	<0.02	<0.02	<0.02	0.02	<0.02	0.03	0.02	<0.02	0.02
Al_2O_3	0.08	0.26	0.25	0.32	0.22	0.43	0.20	0.24	0.20	0.20	0.44	0.30
Cr_2O_3	<0.05	<0.05	<0.05	<0.05	<0.05	<0.05	<0.05	<0.05	<0.05	<0.05	<0.05	<0.05
FeO	13.6	4.08	4.33	4.25	4.06	5.61	3.88	4.97	3.59	3.46	3.84	3.13
MnO	0.12	<0.04	<0.04	0.05	<0.04	0.06	0.04	0.05	0.05	<0.04	<0.04	0.04
MgO	9.97	16.0	16.0	15.8	15.5	14.9	16.2	15.3	16.2	16.4	16.1	16.8
CaO	24.2	25.1	25.1	25.0	24.7	25.0	25.3	25.2	25.0	24.9	25.1	25.3
Na_2O	0.09	0.12	0.12	0.10	0.10	0.15	0.08	0.12	0.14	0.13	0.21	0.09
Total	99.68	99.34	99.67	99.03	97.00	99.82	99.91	99.66	98.86	98.65	99.69	100.01
						6 oxygens						
Si	1.987	1.986	1.988	1.986	1.988	1.988	1.991	1.992	1.990	1.988	1.987	1.986
Ti	0.000	0.000	0.000	0.000	0.000	0.000	0.000	0.000	0.001	0.001	0.000	0.001
Al	0.004	0.011	0.011	0.014	0.010	0.019	0.009	0.010	0.009	0.009	0.019	0.013
Cr	0.001	0.000	0.000	0.000	0.000	0.001	0.000	0.000	0.000	0.000	0.000	0.000
Fe	0.439	0.126	0.133	0.132	0.129	0.174	0.119	0.154	0.111	0.107	0.118	0.096
Mn	0.004	0.001	0.000	0.002	0.000	0.002	0.001	0.002	0.002	0.000	0.000	0.001
Mg	0.573	0.884	0.877	0.875	0.874	0.822	0.885	0.841	0.895	0.908	0.882	0.915
Ca	1.000	0.995	0.993	0.994	1.002	0.993	0.995	0.998	0.992	0.989	0.989	0.992
Na	0.006	0.009	0.009	0.007	0.007	0.011	0.005	0.008	0.010	0.009	0.015	0.006
Total	4.014	4.012	4.011	4.010	4.010	4.010	4.005	4.005	4.010	4.011	4.010	4.010

Table A3: (continued)

Sample	LM72				LM95-1							
Analysis	12	13	14	15	1	2	3	4	5	6	7	8
SiO_2	54.0	54.3	54.2	54.2	50.8	51.4	51.4	51.2	51.2	51.2	51.1	51.1
TiO_2	<0.02	0.02	<0.02	0.04	0.03	<0.02	<0.02	<0.02	0.02	<0.02	0.02	<0.02
Al_2O_3	0.35	0.19	0.28	0.65	0.46	0.35	0.35	0.34	0.37	0.45	0.45	0.44
Cr_2O_3	<0.05	<0.05	<0.05	<0.05	<0.05	<0.05	<0.05	<0.05	<0.05	<0.05	<0.05	<0.05
FeO	3.10	1.87	4.23	2.69	14.4	12.4	11.7	12.5	13.9	13.4	12.2	13.9
MnO	0.04	<0.04	<0.04	0.05	0.23	0.20	0.18	0.20	0.16	0.21	0.23	0.22
MgO	16.6	17.6	15.7	16.7	9.32	10.6	10.9	10.6	9.86	10.0	10.5	9.69
CaO	25.5	25.6	25.5	25.3	23.6	24.1	24.2	23.8	24.1	23.9	23.9	23.9
Na_2O	0.10	0.11	0.13	0.18	0.12	0.11	0.12	0.10	0.11	0.11	0.13	0.12
Total	99.69	99.66	100.03	99.74	98.97	99.02	98.90	98.77	99.73	99.27	98.47	99.44
						6 oxygens						
Si	1.982	1.984	1.991	1.983	1.980	1.981	1.982	1.982	1.982	1.978	1.980	1.979
Ti	0.000	0.001	0.000	0.001	0.001	0.000	0.000	0.000	0.000	0.000	0.001	0.000
Al	0.015	0.008	0.012	0.028	0.021	0.016	0.016	0.015	0.015	0.021	0.020	0.020
Cr	0.000	0.001	0.000	0.000	0.000	0.000	0.001	0.001	0.001	0.000	0.000	0.000
Fe	0.095	0.057	0.130	0.082	0.469	0.399	0.376	0.405	0.405	0.434	0.395	0.451
Mn	0.001	0.000	0.000	0.002	0.008	0.007	0.006	0.007	0.007	0.007	0.007	0.007
Mg	0.910	0.956	0.861	0.909	0.541	0.608	0.625	0.610	0.610	0.578	0.608	0.559
Ca	1.003	1.000	1.004	0.991	0.984	0.995	1.000	0.986	0.986	0.989	0.993	0.991
Na	0.007	0.007	0.009	0.013	0.009	0.008	0.009	0.008	0.008	0.008	0.010	0.009
Total	4.013	4.014	4.007	4.009	4.013	4.014	4.015	4.014	4.013	4.015	4.014	4.016

Table A4: Electron microprobe analyses of amphibole

Sample	LM11																	
Analysis	1	2	3	4	5	6	7	8	9	10	11	12	13	14	15	16	17	18
SiO_2	43.5	43.1	43.8	43.1	47.7	43.2	42.0	42.7	43.6	43.3	43.7	43.6	42.5	42.7	42.9	42.9	42.7	42.9
TiO_2	0.51	0.43	0.29	0.45	0.21	0.33	0.39	0.26	0.33	0.26	0.34	0.28	0.38	0.40	0.40	0.35	0.46	0.43
Al_2O_3	11.4	11.3	11.5	11.3	7.51	11.3	11.3	11.6	11.6	11.0	11.2	10.8	12.4	11.8	12.0	11.5	11.4	11.7
FeO	18.9	18.6	17.9	18.8	17.8	18.1	17.9	17.8	18.3	18.2	18.4	18.7	18.6	19.2	18.7	19.6	19.6	18.8
MnO	0.14	0.24	0.26	0.25	0.22	0.22	0.21	0.25	0.20	0.22	0.27	0.25	0.30	0.19	0.19	0.19	0.22	0.16
MgO	9.01	9.13	9.34	8.85	10.64	9.19	9.41	9.11	9.19	9.42	8.97	9.51	8.45	8.60	8.49	8.81	8.26	8.67
CaO	12.0	12.0	12.0	12.0	12.3	12.2	12.0	12.2	12.2	12.1	12.1	12.2	12.0	12.1	12.2	12.1	11.9	11.9
Na_2O	0.95	0.85	0.84	0.84	0.55	0.86	0.90	0.83	0.78	0.82	0.88	0.83	0.87	0.88	0.95	0.83	0.82	0.97
K_2O	1.59	1.65	1.63	1.78	1.00	1.71	1.71	1.61	1.78	1.55	1.76	1.48	1.82	1.75	1.80	1.70	1.78	1.81
Total	97.97	97.37	97.57	97.29	97.90	97.10	95.79	96.40	97.83	96.89	97.55	97.62	97.33	97.76	97.56	97.99	97.15	97.37
									23 oxygens									
Si	6.534	6.521	6.576	6.535	7.084	6.543	6.447	6.505	6.555	6.563	6.603	6.560	6.445	6.464	6.504	6.467	6.518	6.511
Al^{IV}	1.466	1.479	1.424	1.465	0.916	1.457	1.553	1.495	1.445	1.437	1.397	1.440	1.555	1.536	1.496	1.533	1.482	1.489
Al^{VI}	0.558	0.539	0.620	0.557	0.399	0.571	0.485	0.595	0.602	0.529	0.598	0.467	0.664	0.575	0.648	0.515	0.569	0.607
Ti	0.058	0.048	0.032	0.051	0.023	0.038	0.045	0.030	0.038	0.030	0.039	0.032	0.043	0.046	0.046	0.040	0.053	0.049
Fe^{3+}	0.284	0.331	0.244	0.266	0.173	0.242	0.399	0.285	0.245	0.349	0.170	0.414	0.247	0.311	0.149	0.423	0.284	0.218
Mg	2.019	2.057	2.093	2.003	2.356	2.077	2.153	2.070	2.059	2.127	2.022	2.131	1.910	1.938	1.920	1.977	1.878	1.961
Fe^{2+}	2.096	2.018	2.005	2.115	2.044	2.051	1.902	1.989	2.050	1.955	2.157	1.937	2.119	2.123	2.222	2.044	2.216	2.174
Mn	0.017	0.031	0.033	0.031	0.027	0.028	0.027	0.032	0.025	0.028	0.034	0.032	0.038	0.024	0.024	0.025	0.029	0.021
Ca	1.932	1.949	1.940	1.949	1.953	1.987	1.977	1.996	1.958	1.961	1.957	1.972	1.954	1.963	1.981	1.948	1.937	1.935
Na^{M4}	0.036	0.027	0.032	0.027	0.025	0.007	0.012	0.002	0.023	0.021	0.023	0.015	0.025	0.020	0.010	0.028	0.034	0.035
Na^{A}	0.240	0.221	0.213	0.221	0.134	0.245	0.256	0.242	0.204	0.221	0.236	0.226	0.231	0.239	0.270	0.216	0.209	0.250
K	0.306	0.319	0.313	0.345	0.190	0.330	0.335	0.313	0.341	0.299	0.340	0.283	0.352	0.338	0.348	0.326	0.347	0.351
Total	15.546	15.540	15.525	15.565	15.324	15.576	15.591	15.554	15.545	15.520	15.576	15.509	15.583	15.577	15.618	15.542	15.556	15.601

Table A4: (continued)

Sample	LM11				LM68-2					LM74-1								
Analysis	19	20	21	22	1	2	3	4	5	1	2	3	4	5	6	7	8	9
SiO_2	42.7	42.5	42.2	42.6	45.8	45.1	44.5	45.8	46.0	43.8	41.2	42.6	40.6	42.1	41.5	41.8	45.2	41.4
TiO_2	0.52	0.42	0.47	0.53	0.25	0.27	0.31	0.21	0.26	0.30	0.48	0.41	0.62	0.41	0.53	0.55	0.29	0.54
Al_2O_3	11.6	11.9	11.5	11.5	9.53	10.1	9.97	9.28	9.25	10.3	12.6	11.6	12.7	11.9	12.7	12.3	9.91	13.4
FeO	19.5	19.3	20.3	19.2	17.2	17.2	17.1	17.0	17.3	18.9	19.7	19.2	20.2	20.1	20.0	19.9	18.7	19.7
MnO	0.17	0.16	0.16	0.17	<0.04	<0.04	<0.04	<0.04	<0.04	0.30	0.37	0.38	0.35	0.34	0.34	0.32	0.32	0.38
MgO	8.64	8.53	8.51	8.57	10.7	10.3	10.1	10.7	10.7	8.74	7.06	7.78	6.60	7.66	7.22	7.36	9.31	7.37
CaO	12.2	12.2	11.5	12.2	12.6	12.4	12.3	12.2	12.4	11.9	11.9	11.9	11.7	12.1	12.0	11.8	12.2	12.0
Na_2O	0.91	0.81	1.05	0.85	0.80	0.74	0.76	0.81	0.87	0.76	0.83	0.81	0.94	1.00	0.95	1.01	0.74	0.94
K_2O	1.81	1.80	1.81	1.88	0.98	1.19	1.43	0.95	1.04	1.15	1.62	1.35	1.74	1.48	1.59	1.56	1.13	1.82
Total	98.05	97.58	97.49	97.54	97.80	97.32	96.47	97.00	97.79	96.15	95.79	96.06	95.41	97.17	96.84	96.70	97.70	97.50
									23 oxygens									
Si	6.456	6.446	6.419	6.475	6.805	6.743	6.736	6.853	6.842	6.700	6.396	6.556	6.361	6.445	6.372	6.436	6.774	6.310
Al^{IV}	1.544	1.554	1.581	1.525	1.195	1.257	1.264	1.147	1.158	1.300	1.604	1.444	1.639	1.555	1.628	1.564	1.226	1.690
Al^{VI}	0.514	0.567	0.486	0.541	0.473	0.518	0.515	0.488	0.463	0.546	0.704	0.667	0.706	0.598	0.674	0.667	0.525	0.716
Ti	0.060	0.048	0.054	0.061	0.028	0.031	0.035	0.024	0.029	0.035	0.056	0.047	0.073	0.047	0.061	0.063	0.033	0.062
Fe^{3+}	0.321	0.321	0.471	0.266	0.253	0.255	0.192	0.247	0.220	0.282	0.229	0.215	0.187	0.304	0.259	0.213	0.251	0.261
Mg	1.946	1.927	1.926	1.941	2.362	2.304	2.285	2.379	2.361	1.990	1.634	1.784	1.543	1.746	1.654	1.688	2.080	1.675
Fe^{2+}	2.149	2.123	2.105	2.177	1.885	1.896	1.975	1.880	1.937	2.130	2.333	2.255	2.458	2.272	2.318	2.349	2.091	2.255
Mn	0.022	0.021	0.020	0.022	0.000	0.004	0.003	0.004	0.003	0.038	0.049	0.049	0.047	0.045	0.044	0.041	0.040	0.049
Ca	1.976	1.985	1.866	1.984	1.997	1.982	1.989	1.954	1.969	1.955	1.988	1.965	1.972	1.976	1.980	1.953	1.956	1.961
Na^{M4}	0.013	0.008	0.072	0.009	0.001	0.010	0.006	0.025	0.016	0.024	0.007	0.019	0.015	0.013	0.011	0.025	0.023	0.021
Na^{A}	0.253	0.230	0.237	0.242	0.229	0.205	0.216	0.209	0.234	0.202	0.245	0.223	0.269	0.284	0.271	0.276	0.191	0.257
K	0.350	0.348	0.350	0.364	0.186	0.227	0.277	0.181	0.198	0.225	0.320	0.265	0.347	0.289	0.313	0.306	0.217	0.353
Total	15.604	15.578	15.587	15.607	15.414	15.432	15.493	15.391	15.430	15.427	15.565	15.489	15.617	15.574	15.585	15.581	15.407	15.610

Table A4: (continued)

Sample	LM75-1						LM94			LM95-1								LM134-2
Analysis	1	2	3	4	5	6	1	2	3	1	2	3	4	5	6	7	8	1
SiO_2	42.9	39.7	41.8	44.0	44.3	42.6	46.9	46.4	43.6	43.7	43.9	44.3	43.7	44.8	43.0	44.4	43.5	42.9
TiO_2	0.25	0.16	0.20	0.23	0.29	0.24	0.30	0.13	0.54	0.32	0.36	0.17	0.30	0.27	0.35	0.29	0.32	0.89
Al_2O_3	11.3	11.4	12.3	9.58	9.12	11.4	8.51	9.63	11.4	10.9	10.6	11.1	11.0	10.4	11.5	10.5	11.0	8.34
FeO	19.3	22.5	19.0	20.0	19.6	20.1	18.0	16.4	18.6	17.5	18.0	17.6	17.7	17.0	17.9	17.5	18.2	21.2
MnO	0.09	0.10	0.08	0.09	0.07	<0.04	0.31	0.32	0.26	0.12	0.18	0.09	0.14	0.15	0.10	0.15	0.11	1.08
MgO	8.40	7.37	8.09	9.27	9.50	8.27	10.1	10.3	8.47	9.66	9.70	9.62	9.65	10.5	9.28	9.97	9.50	8.30
CaO	12.1	11.3	12.0	12.1	12.1	12.1	12.2	12.5	12.2	12.2	12.2	12.2	12.3	12.4	12.3	12.2	12.2	11.1
Na_2O	1.14	1.02	1.24	1.07	0.89	1.10	0.50	0.59	0.81	1.02	0.99	0.94	1.01	0.69	1.09	0.75	0.94	1.72
K_2O	1.56	1.55	1.82	1.49	1.58	1.69	0.86	0.78	1.28	1.58	1.42	1.31	1.47	1.34	1.63	1.27	1.46	1.12
Total	97.00	95.12	96.45	97.79	97.43	97.39	97.72	97.10	97.19	97.01	97.41	97.31	97.22	97.42	97.12	97.09	97.24	96.62
									23 oxygens									
Si	6.561	6.222	6.437	6.660	6.711	6.494	6.978	6.921	6.602	6.616	6.618	6.654	6.594	6.690	6.523	6.674	6.568	6.645
Al^{IV}	1.439	1.778	1.563	1.340	1.289	1.506	1.022	1.079	1.398	1.384	1.382	1.346	1.406	1.310	1.477	1.326	1.432	1.355
Al^{VI}	0.590	0.333	0.663	0.368	0.341	0.540	0.470	0.613	0.644	0.563	0.504	0.619	0.546	0.515	0.578	0.529	0.522	0.167
Ti	0.029	0.019	0.024	0.026	0.033	0.027	0.033	0.014	0.062	0.037	0.041	0.019	0.034	0.031	0.040	0.033	0.036	0.104
Fe^{3+}	0.179	0.891	0.143	0.369	0.343	0.281	0.233	0.125	0.163	0.174	0.272	0.197	0.218	0.303	0.190	0.307	0.308	0.404
Mg	1.913	1.722	1.859	2.089	2.147	1.881	2.243	2.290	1.912	2.180	2.177	2.155	2.171	2.327	2.099	2.232	2.138	1.917
Fe^{2+}	2.290	2.066	2.308	2.157	2.140	2.282	2.005	1.921	2.194	2.044	1.999	2.013	2.015	1.815	2.084	1.897	1.994	2.337
Mn	0.012	0.013	0.011	0.012	0.009	0.000	0.040	0.040	0.034	0.016	0.023	0.011	0.018	0.019	0.013	0.019	0.014	0.141
Ca	1.973	1.902	1.984	1.953	1.972	1.977	1.948	1.993	1.983	1.971	1.967	1.969	1.995	1.977	1.993	1.967	1.974	1.847
Na^{M4}	0.014	0.053	0.009	0.025	0.015	0.012	0.028	0.004	0.009	0.015	0.018	0.016	0.003	0.012	0.004	0.018	0.014	0.082
Na^{A}	0.322	0.257	0.361	0.288	0.248	0.314	0.116	0.168	0.228	0.284	0.270	0.257	0.292	0.187	0.317	0.200	0.262	0.435
K	0.305	0.310	0.358	0.288	0.305	0.330	0.164	0.148	0.247	0.305	0.272	0.252	0.283	0.255	0.316	0.243	0.281	0.222
Total	15.627	15.566	15.720	15.575	15.553	15.644	15.280	15.316	15.476	15.589	15.543	15.508	15.575	15.441	15.634	15.445	15.543	15.656

Table A4: (continued)

Sample	LM134-2																	
Analysis	2	3	4	5	6	7	8	9	10	11	12	13	14	15	16	17	18	19
SiO_2	41.5	43.0	42.9	43.2	42.9	42.8	43.3	43.0	42.8	42.0	41.6	40.9	43.0	44.2	42.3	43.0	42.8	40.7
TiO_2	0.39	0.86	0.98	0.80	0.89	0.90	0.73	0.82	0.87	0.87	0.48	0.38	0.78	0.71	0.97	0.81	0.92	0.55
Al_2O_3	9.78	8.44	8.47	8.32	8.42	8.54	8.29	8.24	8.38	8.63	9.24	9.76	8.66	7.65	8.56	8.48	8.72	9.77
FeO	21.9	21.4	21.4	20.9	20.9	22.1	20.7	21.1	22.3	23.6	23.2	24.1	20.1	20.4	22.0	20.5	21.3	23.2
MnO	1.08	1.19	1.07	1.07	1.03	1.11	1.11	1.09	1.15	1.12	1.11	1.00	0.98	1.10	1.13	1.10	0.95	1.12
MgO	7.72	8.32	8.16	8.70	8.43	7.82	8.94	8.25	7.67	6.93	7.06	6.15	9.08	9.14	7.65	8.76	8.44	6.88
CaO	11.3	11.1	10.9	10.9	11.1	11.0	11.1	11.2	11.0	11.1	11.4	11.2	11.1	11.2	11.3	11.0	10.8	11.2
Na_2O	1.43	1.77	1.81	1.80	1.80	1.65	1.80	1.74	1.76	1.57	1.34	1.35	1.83	1.67	1.65	1.85	1.86	1.51
K_2O	1.59	1.11	1.15	1.12	1.14	1.10	1.09	0.98	1.12	1.21	1.32	1.54	1.22	1.05	1.18	1.09	1.25	1.54
Total	96.62	97.22	96.78	96.83	96.60	97.01	97.04	96.39	97.04	97.01	96.62	96.35	96.73	97.10	96.70	96.60	97.02	96.55
									23 oxygens									
Si	6.450	6.623	6.637	6.656	6.644	6.621	6.654	6.668	6.638	6.548	6.482	6.441	6.625	6.770	6.588	6.642	6.599	6.379
Al^{IV}	1.550	1.377	1.363	1.344	1.356	1.379	1.346	1.332	1.362	1.452	1.518	1.559	1.375	1.230	1.412	1.358	1.401	1.621
Al^{VI}	0.241	0.155	0.183	0.168	0.183	0.178	0.154	0.176	0.169	0.134	0.181	0.253	0.196	0.151	0.158	0.185	0.184	0.185
Ti	0.046	0.100	0.114	0.092	0.104	0.104	0.085	0.095	0.102	0.102	0.056	0.045	0.090	0.081	0.114	0.094	0.107	0.065
Fe^{3+}	0.603	0.447	0.393	0.444	0.365	0.467	0.463	0.405	0.422	0.550	0.660	0.619	0.397	0.396	0.427	0.402	0.426	0.659
Mg	1.788	1.909	1.884	1.999	1.946	1.802	2.046	1.908	1.773	1.611	1.641	1.445	2.083	2.087	1.774	2.015	1.941	1.608
Fe^{2+}	2.238	2.308	2.377	2.250	2.338	2.383	2.190	2.339	2.463	2.520	2.361	2.558	2.187	2.221	2.434	2.240	2.315	2.386
Mn	0.141	0.155	0.140	0.139	0.136	0.145	0.144	0.144	0.151	0.147	0.147	0.133	0.127	0.143	0.150	0.144	0.124	0.149
Ca	1.876	1.839	1.803	1.803	1.846	1.827	1.824	1.856	1.829	1.861	1.904	1.887	1.828	1.830	1.876	1.827	1.791	1.889
Na^{M4}	0.066	0.086	0.105	0.106	0.083	0.093	0.094	0.077	0.091	0.075	0.051	0.061	0.092	0.091	0.067	0.093	0.112	0.060
Na^{A}	0.365	0.443	0.438	0.433	0.457	0.401	0.442	0.445	0.438	0.398	0.353	0.350	0.455	0.406	0.431	0.461	0.444	0.399
K	0.316	0.219	0.227	0.220	0.226	0.218	0.213	0.193	0.221	0.240	0.263	0.309	0.239	0.205	0.234	0.214	0.245	0.309
Total	15.680	15.661	15.664	15.654	15.684	15.618	15.655	15.638	15.659	15.638	15.617	15.660	15.694	15.611	15.665	15.675	15.689	15.709

Table A5: Electron microprobe analyses of biotite

Sample	LM11		LM12									LM65
Analysis	1	2	1	2	3	4	5	6	7	8	9	1
SiO_2	37.3	37.4	29.5	30.9	38.8	30.3	28.2	26.9	34.8	33.1	26.4	35.0
TiO_2	1.05	1.15	0.20	0.19	0.48	0.18	0.24	0.12	0.44	0.68	0.17	2.03
Al_2O_3	13.7	14.0	18.0	18.5	31.2	22.5	23.7	24.1	26.1	24.4	23.0	19.1
FeO	17.7	17.7	27.9	26.5	11.0	22.4	24.9	24.6	15.9	19.6	25.8	23.7
MnO	0.12	0.17	0.11	<0.04	0.04	0.17	0.18	0.22	0.18	0.04	0.22	0.88
MgO	14.2	14.2	9.28	9.80	3.07	11.2	9.80	11.2	6.81	7.48	10.5	5.37
CaO	0.06	0.08	0.21	0.10	0.04	0.04	0.08	<0.02	0.17	0.16	0.09	<0.02
Na_2O	0.08	0.07	0.06	0.06	0.62	0.08	0.15	0.11	0.36	0.27	0.14	0.13
K_2O	9.91	10.1	9.39	8.70	9.16	8.59	8.97	8.38	10.6	10.2	9.14	9.45
Total	94.14	94.85	94.58	94.70	94.46	95.43	96.16	95.46	95.36	95.78	95.39	95.65
						11 oxygens						
Si	2.869	2.857	2.408	2.475	2.776	2.353	2.211	2.121	2.596	2.512	2.115	2.718
Ti	0.061	0.066	0.012	0.012	0.026	0.010	0.014	0.007	0.025	0.039	0.010	0.119
Al	1.242	1.263	1.736	1.745	2.630	2.058	2.190	2.243	2.297	2.186	2.172	1.751
Fe	1.139	1.133	1.904	1.777	0.658	1.451	1.637	1.621	0.996	1.243	1.730	1.542
Mn	0.008	0.011	0.008	0.002	0.002	0.011	0.012	0.015	0.011	0.003	0.015	0.058
Mg	1.633	1.612	1.130	1.172	0.327	1.292	1.147	1.313	0.759	0.847	1.259	0.622
Ca	0.005	0.007	0.019	0.009	0.003	0.003	0.007	0.000	0.013	0.013	0.008	0.000
Na	0.012	0.011	0.009	0.009	0.086	0.012	0.022	0.016	0.052	0.040	0.022	0.020
K	0.973	0.983	0.979	0.890	0.835	0.850	0.899	0.845	1.014	0.984	0.935	0.937
Total	7.942	7.943	8.205	8.091	7.343	8.040	8.139	8.181	7.763	7.867	8.266	7.766

Sample	LM65		LM68-2								LM75-1	
Analysis	2	3	1	2	3	4	5	6	7	8	1	2
SiO_2	34.6	33.6	37.0	37.3	36.9	37.2	37.2	37.1	37.8	37.8	37.3	37.6
TiO_2	2.09	1.97	0.94	1.00	0.99	0.98	0.86	0.87	0.99	1.03	0.58	0.55
Al_2O_3	19.7	19.3	16.4	15.9	16.0	16.1	16.7	16.2	16.0	15.8	15.0	15.1
FeO	23.6	26.4	18.8	18.0	18.1	17.8	16.8	16.3	16.4	16.3	18.2	18.1
MnO	0.79	0.73	<0.04	0.05	<0.04	0.04	0.07	0.08	<0.04	0.07	<0.04	<0.04
MgO	5.46	4.17	12.1	12.5	13.1	13.4	13.1	13.4	13.7	13.6	12.4	12.4
CaO	0.00	0.00	0.21	0.10	0.02	0.02	0.04	0.35	0.05	0.09	0.20	0.20
Na_2O	0.11	0.08	0.07	0.05	0.05	0.07	0.04	0.06	0.11	0.07	0.05	0.05
K_2O	8.98	9.15	8.86	9.84	9.67	9.81	9.50	9.94	9.78	9.75	8.97	8.84
Total	95.33	95.40	94.26	94.71	94.81	95.46	94.29	94.29	94.85	94.42	92.58	92.77
						11 oxygens						
Si	2.691	2.659	2.825	2.842	2.812	2.810	2.822	2.821	2.848	2.858	2.897	2.908
Ti	0.122	0.117	0.054	0.057	0.057	0.056	0.049	0.050	0.056	0.059	0.034	0.032
Al	1.803	1.799	1.473	1.428	1.433	1.432	1.492	1.449	1.424	1.411	1.371	1.377
Fe	1.531	1.742	1.204	1.150	1.150	1.127	1.065	1.040	1.035	1.031	1.183	1.172
Mn	0.052	0.049	0.000	0.003	0.000	0.003	0.005	0.005	0.002	0.005	0.000	0.000
Mg	0.632	0.491	1.373	1.417	1.488	1.511	1.485	1.525	1.536	1.531	1.434	1.427
Ca	0.000	0.000	0.017	0.008	0.002	0.002	0.003	0.029	0.004	0.007	0.017	0.016
Na	0.017	0.012	0.011	0.007	0.007	0.010	0.006	0.009	0.016	0.010	0.007	0.007
K	0.890	0.923	0.864	0.957	0.939	0.946	0.920	0.965	0.940	0.942	0.890	0.873
Total	7.738	7.792	7.821	7.869	7.888	7.897	7.847	7.893	7.861	7.854	7.833	7.812

Table A5: (continued)

Sample	LM75-1					LM92-1			LM95-1			LM97-2
Analysis	3	4	5	6	7	1	2	3	1	2	3	1
SiO_2	37.5	36.7	37.0	36.7	36.9	35.1	34.8	34.9	37.5	37.6	37.9	41.6
TiO_2	0.49	0.59	0.58	0.59	0.62	2.09	1.17	1.39	1.00	0.92	0.72	0.24
Al_2O_3	14.5	14.6	14.5	14.7	14.6	16.8	16.6	16.9	15.5	15.8	15.4	14.5
FeO	17.8	19.0	19.0	19.2	18.7	19.0	20.0	20.4	16.1	16.4	16.4	0.99
MnO	<0.04	0.05	0.05	<0.04	<0.04	0.08	0.07	<0.04	0.13	0.08	0.13	<0.04
MgO	12.9	12.1	12.4	12.1	12.5	9.91	9.97	9.33	14.3	13.6	13.9	26.9
CaO	0.22	0.54	0.36	0.40	0.45	0.41	0.64	0.69	0.07	0.13	0.13	0.07
Na_2O	0.09	0.10	0.12	0.08	0.08	0.08	0.05	0.10	0.08	0.08	0.09	0.23
K_2O	8.87	8.51	8.22	8.40	8.50	9.29	8.86	8.80	9.76	9.17	9.14	10.2
Total	92.48	92.27	92.21	92.17	92.42	92.71	92.14	92.49	94.45	93.73	93.76	94.72
						11 oxygens						
Si	2.914	2.918	2.895	2.877	2.885	2.755	2.757	2.761	2.839	2.860	2.881	2.914
Ti	0.029	0.034	0.034	0.035	0.036	0.123	0.070	0.083	0.057	0.053	0.041	0.013
Al	1.329	1.330	1.336	1.361	1.345	1.550	1.555	1.573	1.388	1.417	1.380	1.201
Fe	1.159	1.230	1.245	1.257	1.223	1.247	1.325	1.346	1.022	1.044	1.042	0.058
Mn	0.000	0.003	0.003	0.001	0.001	0.005	0.005	0.002	0.008	0.005	0.008	0.000
Mg	1.498	1.395	1.441	1.417	1.449	1.160	1.179	1.100	1.613	1.538	1.575	2.808
Ca	0.018	0.045	0.030	0.034	0.038	0.034	0.054	0.058	0.006	0.010	0.010	0.005
Na	0.014	0.015	0.018	0.012	0.012	0.012	0.008	0.008	0.012	0.012	0.013	0.031
K	0.879	0.839	0.820	0.840	0.847	0.930	0.896	0.887	0.943	0.890	0.887	0.914
Total	7.840	7.809	7.822	7.834	7.836	7.816	7.849	7.818	7.888	7.829	7.837	7.944

Sample	LM97-2			LM105-5			LM121	
Analysis	2	3	4	1	2	3	1	2
SiO_2	42.2	42.3	42.6	41.8	42.0	40.6	38.0	38.2
TiO_2	0.19	0.18	0.21	0.86	0.83	0.80	0.34	0.35
Al_2O_3	13.4	13.8	13.0	16.0	15.4	16.9	19.6	19.5
FeO	0.78	1.06	0.99	0.61	0.59	0.67	0.68	0.62
MnO	<0.04	<0.04	<0.04	<0.04	<0.04	<0.04	<0.04	<0.04
MgO	27.5	26.7	26.8	25.8	25.9	25.1	25.7	25.6
CaO	0.10	0.08	0.05	0.04	0.27	0.15	0.15	0.14
Na_2O	0.24	0.14	0.16	0.13	0.08	0.13	0.19	0.23
K_2O	10.2	10.1	10.1	9.53	9.08	9.58	9.42	9.67
Total	94.58	94.32	93.90	94.73	94.17	93.80	94.12	94.35
				11 oxygens				
Si	2.960	2.971	3.003	2.902	2.930	2.852	2.671	2.682
Ti	0.010	0.010	0.011	0.045	0.044	0.042	0.018	0.018
Al	1.106	1.140	1.083	1.307	1.266	1.397	1.626	1.615
Fe	0.046	0.062	0.059	0.035	0.034	0.039	0.040	0.036
Mn	0.001	0.002	0.001	0.001	0.002	0.000	0.001	0.000
Mg	2.875	2.798	2.820	2.675	2.689	2.626	2.694	2.681
Ca	0.008	0.006	0.004	0.003	0.020	0.011	0.011	0.011
Na	0.033	0.019	0.022	0.018	0.011	0.018	0.026	0.031
K	0.913	0.903	0.907	0.844	0.808	0.859	0.845	0.866
Total	7.952	7.911	7.910	7.830	7.804	7.844	7.932	7.941

Table A6: Electron microprobe analyses of muscovite

Sample	LM12											
Analysis	1	2	3	4	5	6	7	8	9	10	11	12
SiO_2	45.6	45.4	45.4	45.4	45.7	44.5	45.5	45.7	46.7	44.7	45.3	45.4
TiO_2	0.73	0.69	0.63	0.65	0.66	0.65	0.66	0.68	0.23	0.60	0.70	0.70
Al_2O_3	36.1	36.1	35.9	36.0	35.9	34.8	35.7	36.1	34.9	35.6	35.8	35.7
FeO	1.32	1.32	1.27	1.28	1.10	3.28	1.21	1.11	1.94	1.09	1.09	1.20
MnO	<0.04	<0.04	<0.04	<0.04	<0.04	<0.04	<0.04	<0.04	<0.04	0.04	<0.04	0.04
MgO	0.60	0.54	0.53	0.61	0.62	0.72	0.54	0.62	1.24	0.58	0.66	0.55
CaO	<0.02	0.02	<0.02	0.04	<0.02	0.04	<0.02	0.02	<0.02	0.03	<0.02	0.02
Na_2O	0.79	0.81	0.82	0.93	0.86	0.77	0.76	0.81	0.52	0.92	0.89	0.74
K_2O	10.2	10.3	10.2	9.87	10.1	9.70	10.1	10.4	9.98	10.1	10.1	10.4
Total	95.31	95.16	94.68	94.81	94.88	94.48	94.48	95.33	95.50	93.65	94.58	94.77
						11 oxygens						
Si	3.036	3.028	3.037	3.033	3.050	3.015	3.050	3.037	3.099	3.027	3.034	3.041
Ti	0.036	0.035	0.032	0.033	0.033	0.033	0.033	0.034	0.011	0.031	0.035	0.035
Al	2.827	2.838	2.833	2.834	2.818	2.782	2.820	2.827	2.729	2.842	2.829	2.821
Fe	0.074	0.074	0.071	0.071	0.061	0.186	0.068	0.062	0.108	0.062	0.061	0.067
Mn	0.000	0.000	0.000	0.001	0.000	0.000	0.000	0.001	0.001	0.002	0.000	0.002
Mg	0.059	0.053	0.053	0.061	0.062	0.073	0.054	0.062	0.122	0.059	0.066	0.055
Ca	0.000	0.001	0.001	0.003	0.001	0.003	0.001	0.001	0.000	0.002	0.000	0.001
Na	0.102	0.105	0.106	0.120	0.111	0.101	0.098	0.104	0.067	0.121	0.115	0.096
K	0.864	0.874	0.869	0.841	0.857	0.838	0.862	0.879	0.845	0.871	0.864	0.888
Total	6.998	7.007	7.002	6.997	6.992	7.031	6.986	7.008	6.981	7.017	7.006	7.006

Sample	LM12							LM58-2				
Analysis	13	14	15	16	17	18	19	1	2	3	4	5
SiO_2	43.4	45.4	45.4	45.2	43.3	46.0	45.2	47.1	47.4	46.8	47.0	47.0
TiO_2	0.61	0.69	0.66	0.74	0.67	0.44	0.71	0.30	0.19	0.13	0.04	0.25
Al_2O_3	34.1	36.1	36.0	35.6	34.6	33.9	36.0	32.5	33.0	34.5	34.3	33.4
FeO	1.42	1.13	1.02	1.36	3.86	1.59	1.30	0.71	0.48	0.32	0.34	0.43
MnO	<0.04	<0.04	<0.04	<0.04	0.05	<0.04	<0.04	<0.04	<0.04	<0.04	<0.04	<0.04
MgO	0.77	0.61	0.65	0.68	1.93	1.14	0.69	3.23	2.80	1.89	1.94	2.41
CaO	<0.02	<0.02	<0.02	<0.02	<0.02	<0.02	<0.02	0.03	0.06	0.02	0.15	0.08
Na_2O	0.78	1.21	0.88	0.72	0.72	0.67	0.82	0.18	0.16	0.22	0.17	0.21
K_2O	10.0	10.3	10.2	10.1	9.11	10.3	10.2	11.1	11.2	11.3	11.1	11.2
Total	91.15	95.51	94.83	94.37	94.21	93.97	94.98	95.13	95.23	95.21	95.01	94.91
						11 oxygens						
Si	3.027	3.023	3.032	3.036	2.953	3.110	3.023	3.145	3.154	3.114	3.128	3.136
Ti	0.032	0.035	0.033	0.037	0.035	0.022	0.036	0.015	0.010	0.007	0.002	0.013
Al	2.801	2.831	2.837	2.818	2.775	2.696	2.834	2.555	2.585	2.706	2.690	2.630
Fe	0.102	0.063	0.057	0.076	0.220	0.090	0.072	0.040	0.027	0.018	0.019	0.024
Mn	0.000	0.001	0.002	0.001	0.003	0.000	0.000	0.001	0.001	0.000	0.000	0.000
Mg	0.008	0.060	0.064	0.068	0.196	0.114	0.068	0.321	0.278	0.187	0.193	0.240
Ca	0.000	0.000	0.000	0.000	0.000	0.001	0.000	0.002	0.004	0.001	0.011	0.006
Na	0.196	0.156	0.114	0.093	0.095	0.087	0.106	0.023	0.021	0.028	0.022	0.027
K	0.890	0.873	0.866	0.865	0.792	0.883	0.873	0.943	0.950	0.959	0.944	0.952
Total	7.056	7.042	7.006	6.996	7.068	7.005	7.014	7.045	7.030	7.020	7.009	7.028

Table A6: (continued)

Sample	LM65				LM104-1							
Analysis	1	2	3	4	1	2	3	4	5	6	7	8
SiO_2	46.6	46.1	46.1	46.0	45.6	45.5	45.2	45.8	45.1	44.9	45.9	45.3
TiO_2	0.04	0.04	0.08	0.37	0.28	0.25	0.98	0.51	0.93	0.81	0.51	0.55
Al_2O_3	32.2	33.2	33.4	33.6	33.9	34.0	33.6	32.9	33.8	33.2	32.9	32.9
FeO	3.50	3.14	2.89	1.75	1.81	1.85	1.79	2.20	1.84	2.42	1.82	2.04
MnO	0.09	0.10	0.10	<0.04	<0.04	<0.04	0.05	<0.04	<0.04	0.05	<0.04	<0.04
MgO	1.19	0.91	1.05	1.50	1.43	1.38	1.30	1.68	1.35	1.71	1.46	1.61
CaO	<0.02	0.02	<0.02	<0.02	0.02	0.02	<0.02	0.11	<0.02	0.07	0.05	0.05
Na_2O	0.15	0.16	0.16	0.27	0.23	0.28	0.27	0.45	0.30	0.31	0.30	0.32
K_2O	11.2	11.3	11.4	11.1	11.2	11.0	11.0	10.8	10.8	10.9	10.9	10.8
Total	94.92	94.89	95.15	94.51	94.42	94.19	94.17	94.35	94.09	94.33	93.84	93.52
						11 oxygens						
Si	3.158	3.122	3.113	3.104	3.085	3.083	3.071	3.105	3.063	3.054	3.121	3.098
Ti	0.002	0.002	0.004	0.019	0.014	0.013	0.050	0.026	0.048	0.042	0.026	0.028
Al	2.576	2.651	2.660	2.673	2.703	2.713	2.685	2.628	2.701	2.665	2.638	2.648
Fe	0.199	0.178	0.163	0.099	0.102	0.105	0.102	0.125	0.104	0.138	0.104	0.117
Mn	0.005	0.006	0.005	0.000	0.001	0.001	0.003	0.000	0.000	0.003	0.001	0.000
Mg	0.120	0.092	0.106	0.151	0.144	0.139	0.132	0.170	0.137	0.173	0.148	0.164
Ca	0.000	0.002	0.001	0.001	0.001	0.001	0.001	0.008	0.000	0.005	0.004	0.004
Na	0.020	0.020	0.021	0.035	0.030	0.037	0.035	0.059	0.040	0.041	0.040	0.042
K	0.965	0.976	0.980	0.954	0.965	0.948	0.953	0.931	0.933	0.947	0.945	0.938
Total	7.045	7.049	7.054	7.036	7.047	7.040	7.031	7.052	7.026	7.068	7.027	7.039

Table A7: Electron microprobe analyses of chlorite

Sample	LM11				LM12							
Analysis	1	2	3	4	1	2	3	4	5	6	7	8
SiO_2	25.7	26.4	26.9	25.8	24.9	24.9	25.5	24.9	25.4	23.3	23.8	25.5
TiO_2	0.03	0.09	0.03	0.11	0.10	0.03	0.10	0.06	0.23	0.09	0.09	0.09
Al_2O_3	18.5	18.6	18.5	17.9	19.6	19.3	20.0	19.4	20.3	18.0	21.1	21.1
FeO	27.4	28.3	25.0	28.7	29.4	30.1	29.8	29.6	28.9	35.1	29.3	28.3
MnO	0.19	0.19	0.19	0.19	0.26	0.15	0.20	0.16	0.25	0.18	0.24	0.24
MgO	13.7	13.1	15.4	13.4	11.8	11.5	10.9	12.0	12.0	8.82	11.2	10.6
Total	85.64	86.56	86.05	86.09	85.99	85.99	86.48	86.21	87.17	85.50	85.75	85.85
						14 oxygens						
Si	2.819	2.859	2.878	2.832	2.749	2.759	2.794	2.743	2.750	2.691	2.635	2.782
Ti	0.002	0.007	0.002	0.009	0.008	0.003	0.008	0.005	0.019	0.008	0.007	0.007
Al	2.391	2.384	2.341	2.314	2.542	2.515	2.575	2.524	2.592	2.449	2.755	2.716
Fe	2.513	2.563	2.244	2.638	2.712	2.788	2.729	2.731	2.616	3.392	2.708	2.591
Mn	0.018	0.018	0.017	0.018	0.024	0.014	0.018	0.015	0.023	0.018	0.023	0.022
Mg	2.240	2.111	2.466	2.193	1.937	1.902	1.784	1.972	1.938	1.518	1.853	1.734
Total	9.983	9.942	9.949	10.002	9.972	9.981	9.910	9.990	9.936	10.076	9.981	9.852

Sample	LM92-1								LM94			
Analysis	1	2	3	4	5	6	7	8	1	2	3	4
SiO_2	24.8	25.5	25.0	25.3	24.9	25.2	25.5	25.6	26.2	27.4	26.4	26.0
TiO_2	0.03	<0.02	0.02	0.05	0.02	0.04	<0.02	0.04	<0.02	0.04	0.02	0.02
Al_2O_3	20.1	19.2	19.4	19.1	19.7	20.0	20.0	20.1	18.7	17.9	18.0	18.5
FeO	12.8	13.1	12.7	13.1	12.7	13.0	13.2	13.1	27.9	23.2	29.2	27.7
MnO	0.24	0.14	0.14	0.21	0.18	0.18	0.19	0.14	0.19	0.33	0.12	0.21
MgO	27.4	26.6	27.9	27.7	27.9	27.3	28.0	27.5	13.8	17.1	12.9	14.4
Total	85.32	84.47	85.14	85.50	85.40	85.82	86.95	86.37	86.72	86.02	86.62	86.80
						14 oxygens						
Si	2.724	2.820	2.760	2.785	2.747	2.750	2.753	2.769	2.830	2.916	2.882	2.809
Ti	0.002	0.000	0.002	0.004	0.002	0.003	0.001	0.003	0.001	0.003	0.002	0.002
Al	2.599	2.496	2.528	2.469	2.556	2.577	2.548	2.562	2.383	2.237	2.308	2.357
Fe	2.104	2.149	2.092	2.151	2.084	2.121	2.126	2.114	2.519	2.062	2.660	2.501
Mn	0.022	0.013	0.013	0.020	0.017	0.016	0.018	0.013	0.018	0.030	0.011	0.019
Mg	2.524	2.453	2.578	2.547	2.566	2.493	2.527	2.486	2.228	2.715	2.099	2.324
Total	9.975	9.931	9.973	9.976	9.972	9.960	9.973	9.947	9.979	9.963	9.962	10.012

Table A7: (continued)

Sample	LM95-1									LM121		
Analysis	1	2	3	4	5	6	7	8	9	1	2	3
SiO_2	27.4	26.7	26.9	29.3	27.8	27.3	26.4	28.0	27.3	28.3	28.5	28.0
TiO_2	0.01	0.00	0.01	0.19	0.04	0.03	0.05	0.10	0.05	0.02	0.02	0.01
Al_2O_3	19.3	18.4	17.9	17.3	18.7	18.7	19.0	17.9	18.7	24.3	23.9	24.2
FeO	25.9	25.6	25.4	20.8	21.8	21.8	24.6	21.2	22.0	0.94	1.19	1.16
MnO	0.16	0.15	0.21	0.20	0.10	0.14	0.16	0.08	0.11	<0.04	<0.04	<0.04
MgO	14.5	14.4	15.2	16.6	18.2	18.4	16.1	18.6	17.9	33.0	33.1	33.0
Total	87.15	85.37	85.59	84.26	86.53	86.29	86.28	85.91	86.01	86.50	86.71	86.38
						14 oxygens						
Si	2.899	2.899	2.909	3.113	2.901	2.868	2.820	2.938	2.876	2.650	2.662	2.633
Ti	0.001	0.000	0.001	0.015	0.003	0.002	0.004	0.008	0.004	0.002	0.002	0.001
Al	2.404	2.356	2.282	2.166	2.297	2.311	2.388	2.220	2.320	2.679	2.632	2.680
Fe	2.296	2.323	2.296	1.848	1.902	1.910	2.195	1.860	1.940	0.074	0.093	0.091
Mn	0.015	0.013	0.019	0.018	0.009	0.013	0.015	0.007	0.009	0.003	0.000	0.000
Mg	2.283	2.331	2.442	2.629	2.836	2.870	2.561	2.911	2.810	4.602	4.611	4.621
Total	9.898	9.922	9.949	9.789	9.948	9.974	9.983	9.944	9.959	10.010	10.000	10.026

Table A8: Electron microprobe analyses of garnet

Sample	LM10											
Analysis	1	2	3	4	5	6	7	8	9	10	11	12
SiO_2	37.8	38.3	38.0	37.9	37.4	37.6	38.1	38.3	37.8	38.6	39.0	38.3
TiO_2	0.59	0.54	0.59	0.89	0.90	0.74	0.88	0.54	0.85	0.55	0.10	0.36
Al_2O_3	16.3	16.7	16.8	16.5	16.0	15.8	16.7	16.5	16.0	17.0	20.5	17.6
Cr_2O_3	<0.05	<0.05	<0.05	<0.05	<0.05	0.06	<0.05	<0.05	<0.05	<0.05	<0.05	0.25
FeO	7.83	7.69	7.11	7.92	7.94	8.44	7.15	7.60	7.84	7.48	2.79	6.02
MnO	0.10	0.07	0.04	<0.04	0.08	<0.04	0.04	0.06	0.08	0.10	0.05	0.10
MgO	0.06	0.04	0.06	0.08	0.08	0.09	0.08	0.07	0.10	0.07	0.03	0.06
CaO	36.1	36.2	36.2	35.9	36.1	35.8	36.1	35.9	36.1	36.4	37.0	36.1
Total	98.75	99.45	98.79	99.35	98.53	98.59	99.17	99.06	98.73	100.21	99.38	98.69
						12 oxygens						
Si	2.944	2.956	2.951	2.938	2.927	2.941	2.952	2.971	2.947	2.959	2.968	2.966
Ti	0.035	0.031	0.035	0.052	0.053	0.044	0.051	0.031	0.050	0.032	0.006	0.021
Al	1.501	1.518	1.537	1.509	1.480	1.460	1.527	1.509	1.468	1.531	1.838	1.604
Cr	0.000	0.000	0.002	0.001	0.000	0.003	0.000	0.002	0.000	0.002	0.000	0.015
Fe^{3+}	0.510	0.495	0.462	0.500	0.519	0.552	0.463	0.487	0.512	0.475	0.178	0.390
Fe^{2+}	0.000	0.002	0.000	0.012	0.000	0.000	0.000	0.005	0.000	0.004	0.000	0.000
Mn	0.007	0.005	0.002	0.002	0.005	0.001	0.003	0.004	0.005	0.006	0.003	0.006
Mg	0.008	0.005	0.007	0.009	0.010	0.011	0.009	0.008	0.012	0.008	0.004	0.007
Ca	3.010	2.995	3.018	2.982	3.026	2.997	2.997	2.981	3.019	2.986	3.021	2.998
Total	8.015	8.007	8.014	8.005	8.020	8.009	8.002	7.998	8.013	8.003	8.018	8.007

Sample	LM10											
Analysis	13	14	15	16	17	18	19	20	21	22	23	24
SiO_2	39.0	37.8	38.1	37.9	37.7	38.0	37.9	37.8	38.3	39.1	38.8	37.8
TiO_2	0.58	0.59	0.52	0.44	0.55	0.57	0.51	1.40	0.64	0.05	0.28	1.09
Al_2O_3	19.3	16.3	17.7	17.1	15.7	16.8	17.4	16.5	14.5	19.1	18.5	18.1
Cr_2O_3	0.10	<0.05	<0.05	0.06	<0.05	<0.05	<0.05	<0.05	0.06	<0.05	<0.05	<0.05
FeO	3.67	7.66	6.34	6.81	8.49	7.29	6.83	6.66	8.70	4.58	5.42	5.09
MnO	0.04	0.09	0.08	0.11	0.07	0.05	0.07	0.04	0.05	0.07	<0.04	0.05
MgO	0.14	0.07	0.06	0.07	0.13	0.07	0.06	0.15	0.07	0.02	0.04	0.15
CaO	36.8	36.0	36.3	36.1	35.8	36.0	36.1	36.2	36.2	36.9	36.9	36.5
Total	99.66	98.58	99.10	98.60	98.40	98.86	98.87	98.77	98.58	99.76	100.01	98.78
						12 oxygens						
Si	2.974	2.952	2.944	2.951	2.952	2.953	2.939	2.938	3.002	2.980	2.964	2.927
Ti	0.033	0.035	0.030	0.026	0.033	0.033	0.030	0.082	0.038	0.003	0.016	0.063
Al	1.736	1.502	1.613	1.569	1.448	1.541	1.591	1.516	1.340	1.717	1.666	1.650
Cr	0.006	0.002	0.001	0.004	0.001	0.000	0.002	0.000	0.004	0.000	0.000	0.000
Fe^{3+}	0.234	0.500	0.409	0.443	0.556	0.472	0.438	0.433	0.570	0.292	0.346	0.330
Fe^{2+}	0.000	0.000	0.000	0.000	0.000	0.001	0.005	0.000	0.000	0.000	0.000	0.000
Mn	0.003	0.006	0.005	0.007	0.005	0.003	0.005	0.002	0.003	0.005	0.001	0.003
Mg	0.016	0.008	0.007	0.008	0.015	0.008	0.007	0.017	0.008	0.002	0.005	0.017
Ca	3.002	3.007	3.004	3.008	3.002	2.995	2.999	3.017	3.038	3.012	3.015	3.029
Total	8.004	8.012	8.013	8.016	8.012	8.006	8.016	8.005	8.003	8.011	8.013	8.019

Table A8: (continued)

Sample	LM10		LM65									LM68-1
Analysis	25	26	1	2	3	4	5	6	7	8	9	1
SiO_2	38.0	37.8	35.3	35.2	36.0	36.1	36.1	35.1	35.3	35.3	35.1	37.2
TiO_2	1.38	1.37	0.55	0.56	0.14	0.16	0.11	0.48	0.50	0.57	0.52	0.37
Al_2O_3	17.0	16.4	18.9	18.9	20.0	19.9	20.4	19.0	19.0	19.1	19.2	16.8
Cr_2O_3	<0.05	<0.05	<0.05	<0.05	<0.05	<0.05	<0.05	<0.05	<0.05	<0.05	<0.05	<0.05
FeO	6.08	7.04	10.6	10.8	13.6	13.5	11.9	11.7	11.7	11.2	11.0	8.48
MnO	0.07	0.06	28.2	28.1	22.7	22.5	24.2	26.5	26.8	27.0	27.6	0.10
MgO	0.14	0.11	0.58	0.54	0.47	0.48	0.40	0.46	0.45	0.51	0.55	0.02
CaO	36.1	36.2	3.35	3.31	5.55	5.78	5.49	3.52	3.52	3.43	3.21	35.3
Total	98.74	98.97	97.43	97.33	98.51	98.40	98.56	96.84	97.31	97.06	97.25	98.23
						12 oxygens						
Si	2.945	2.934	2.982	2.981	2.982	2.990	2.982	2.983	2.985	2.984	2.970	2.922
Ti	0.081	0.080	0.035	0.035	0.009	0.010	0.006	0.030	0.032	0.036	0.033	0.022
Al	1.553	1.501	1.884	1.882	1.954	1.944	1.983	1.901	1.893	1.903	1.914	1.551
Cr	0.000	0.000	0.000	0.001	0.000	0.000	0.001	0.002	0.002	0.000	0.000	0.001
Fe^{3+}	0.395	0.458	0.748	0.762	0.943	0.932	0.820	0.834	0.825	0.792	0.781	0.504
Fe^{2+}	0.000	0.000										0.053
Mn	0.005	0.004	2.016	2.013	1.594	1.581	1.691	1.907	1.922	1.936	1.981	0.007
Mg	0.017	0.013	0.073	0.068	0.058	0.059	0.049	0.058	0.057	0.064	0.069	0.003
Ca	3.004	3.016	0.303	0.301	0.493	0.513	0.486	0.320	0.319	0.311	0.291	2.966
Total	8.000	8.006	8.041	8.043	8.033	8.029	8.018	8.035	8.035	8.026	8.039	8.029

Sample	LM68-1			
Analysis	2	3	4	5
SiO_2	39.0	37.8	38.1	37.9
TiO_2	0.58	0.59	0.52	0.44
Al_2O_3	19.3	16.3	17.7	17.1
Cr_2O_3	0.10	<0.05	<0.05	0.06
FeO	3.67	7.66	6.34	6.81
MnO	0.04	0.09	0.08	0.11
MgO	0.14	0.07	0.06	0.07
CaO	36.8	36.0	36.3	36.1
Total	99.66	98.58	99.10	98.60
		12 oxygens		
Si	2.974	2.952	2.944	2.951
Ti	0.033	0.035	0.030	0.026
Al	1.736	1.502	1.613	1.569
Cr	0.006	0.002	0.001	0.004
Fe^{3+}	0.234	0.500	0.409	0.443
Fe^{2+}	0.000	0.000	0.000	0.000
Mn	0.003	0.006	0.005	0.007
Mg	0.016	0.008	0.007	0.008
Ca	3.002	3.007	3.004	3.008
Total	8.004	8.012	8.013	8.016

Table A9: Electron microprobe analyses of epidote

Sample	LM11					LM68-1			LM68-2			
Analysis	1	2	3	4	5	1	2	3	1	2	3	4
SiO_2	37.6	37.6	38.7	38.1	38.2	37.9	37.9	37.4	38.2	38.1	38.1	38.0
TiO_2	0.07	0.07	0.14	0.08	0.11	0.07	0.07	0.08	0.06	0.03	0.12	0.17
Al_2O_3	23.3	24.7	27.7	28.0	28.2	26.2	26.0	25.1	28.5	28.9	28.7	28.8
FeO	12.2	10.6	6.78	6.46	6.41	8.44	8.68	10.4	6.39	6.12	6.62	6.37
MnO	0.11	0.13	0.02	0.06	0.07	<0.04	<0.04	0.05	<0.04	<0.04	0.04	<0.04
MgO	0.02	<0.02	<0.02	0.04	0.03	0.03	0.03	0.04	<0.02	<0.02	0.03	0.02
CaO	23.2	23.1	23.9	24.2	24.0	21.9	22.7	21.1	23.1	23.3	23.5	23.7
Total	96.49	96.33	97.21	96.97	96.99	94.47	95.48	94.17	96.21	96.50	97.07	97.04
						8 cations						
Si	2.999	2.990	3.012	2.971	2.979	3.050	3.025	3.041	2.997	2.977	2.963	2.958
Ti	0.004	0.004	0.008	0.005	0.006	0.004	0.004	0.005	0.004	0.002	0.007	0.010
Al	2.191	2.319	2.540	2.572	2.588	2.485	2.446	2.402	2.638	2.663	2.632	2.638
Fe	0.810	0.706	0.442	0.421	0.418	0.568	0.579	0.706	0.420	0.400	0.431	0.415
Mn	0.007	0.009	0.001	0.004	0.005	0.001	0.002	0.003	0.000	0.002	0.003	0.000
Mg	0.002	0.001	0.001	0.005	0.003	0.004	0.004	0.005	0.001	0.000	0.003	0.002
Ca	1.986	1.971	1.995	2.023	2.001	1.888	1.940	1.838	1.941	1.955	1.960	1.977
Total	8.000	8.000	8.000	8.000	8.000	8.000	8.000	8.000	8.000	8.000	8.000	8.000

Sample	LM68-2	LM74-1									LM75-1	
Analysis	5	1	2	3	4	5	6	7	8	9	1	2
SiO_2	38.2	37.6	37.5	38.0	38.3	38.3	38.2	38.4	38.3	38.4	38.0	37.7
TiO_2	0.17	0.09	0.05	0.14	0.04	0.15	0.10	0.20	0.09	0.10	0.02	0.07
Al_2O_3	28.7	28.0	27.8	28.2	28.7	28.2	28.3	28.7	28.6	28.8	28.0	27.8
FeO	6.26	7.14	6.93	6.83	6.43	7.14	7.12	6.51	6.68	6.57	7.47	7.51
MnO	<0.04	0.13	0.07	0.15	0.10	0.11	0.14	0.13	0.11	0.09	<0.04	0.05
MgO	0.03	<0.02	0.02	0.02	0.02	0.02	0.02	0.02	0.03	0.04	<0.02	0.02
CaO	23.6	23.8	23.5	23.5	23.7	23.6	23.8	23.9	23.9	23.7	23.4	23.0
Total	97.07	96.74	95.79	96.87	97.31	97.49	97.66	97.88	97.81	97.70	96.97	96.14
						8 cations						
Si	2.974	2.940	2.959	2.969	2.970	2.973	2.960	2.969	2.962	2.967	2.969	2.967
Ti	0.010	0.005	0.003	0.008	0.002	0.009	0.006	0.012	0.005	0.006	0.001	0.004
Al	2.635	2.584	2.588	2.595	2.628	2.579	2.585	2.610	2.609	2.625	2.580	2.583
Fe	0.407	0.467	0.458	0.446	0.417	0.464	0.461	0.420	0.432	0.425	0.488	0.495
Mn	0.000	0.009	0.005	0.010	0.007	0.007	0.009	0.009	0.007	0.006	0.001	0.003
Mg	0.003	0.000	0.002	0.002	0.002	0.002	0.002	0.002	0.003	0.005	0.000	0.002
Ca	1.969	1.995	1.985	1.969	1.973	1.966	1.976	1.979	1.981	1.966	1.962	1.945
Total	8.000	8.000	8.000	8.000	8.000	8.000	8.000	8.000	8.000	8.000	8.000	8.000

Table A9: (continued)

Sample	LM75-1					LM94						LM95-1
Analysis	3	4	5	6	7	1	2	3	4	5	6	1
SiO_2	37.3	37.9	37.4	38.0	37.6	37.1	38.3	37.7	38.5	38.5	38.2	40.9
TiO_2	0.12	0.08	0.10	0.05	0.13	0.50	0.17	0.04	0.04	0.03	0.03	<0.02
Al_2O_3	28.1	27.9	27.7	27.8	28.0	22.3	29.1	30.4	30.8	29.5	29.2	32.3
FeO	7.16	7.19	6.81	7.65	6.97	13.0	5.66	4.54	4.01	5.60	6.39	1.17
MnO	<0.04	<0.04	0.05	<0.04	<0.04	0.05	0.07	0.19	0.09	0.15	0.08	0.04
MgO	0.02	0.03	0.06	0.05	0.05	0.04	0.09	0.03	0.04	0.02	0.02	0.03
CaO	23.2	23.1	23.1	23.1	23.3	23.2	24.0	23.6	23.9	24.0	24.1	22.7
Total	95.93	96.18	95.17	96.63	96.17	96.16	97.40	96.49	97.32	97.67	97.99	97.05
						8 cations						
Si	2.945	2.980	2.969	2.977	2.961	2.981	2.961	2.935	2.962	2.968	2.945	3.136
Ti	0.007	0.005	0.006	0.003	0.008	0.030	0.010	0.002	0.002	0.002	0.002	0.000
Al	2.614	2.588	2.592	2.567	2.600	2.115	2.657	2.783	2.799	2.678	2.648	2.919
Fe	0.472	0.473	0.453	0.502	0.459	0.871	0.366	0.295	0.258	0.361	0.412	0.075
Mn	0.001	0.000	0.003	0.001	0.000	0.003	0.005	0.013	0.006	0.010	0.005	0.003
Mg	0.002	0.004	0.007	0.006	0.006	0.005	0.010	0.003	0.005	0.002	0.002	0.003
Ca	1.958	1.951	1.970	1.944	1.967	1.994	1.991	1.969	1.969	1.979	1.986	1.864
Total	8.000	8.000	8.000	8.000	8.000	8.000	8.000	8.000	8.000	8.000	8.000	8.000

Sample	LM95-1	LM134-2				
Analysis	2	1	2	3	4	5
SiO_2	40.1	37.5	37.4	37.2	37.5	36.9
TiO_2	<0.02	0.14	0.08	0.05	0.03	0.05
Al_2O_3	29.8	27.5	26.2	22.4	26.7	23.3
FeO	4.39	7.78	9.26	13.7	8.49	12.2
MnO	0.04	0.30	0.64	0.24	0.39	0.31
MgO	0.02	0.03	<0.02	0.03	0.20	0.36
CaO	23.7	23.3	22.8	22.6	22.6	21.6
Total	97.92	96.60	96.31	96.28	95.91	94.76
			8 cations			
Si	3.075	2.949	2.960	2.984	2.975	2.993
Ti	0.000	0.008	0.004	0.003	0.002	0.003
Al	2.692	2.550	2.445	2.122	2.496	2.231
Fe	0.282	0.511	0.614	0.922	0.563	0.829
Mn	0.003	0.020	0.043	0.017	0.026	0.022
Mg	0.002	0.003	0.001	0.004	0.023	0.044
Ca	1.946	1.958	1.933	1.948	1.915	1.878
Total	8.000	8.000	8.000	8.000	8.000	8.000

Table A10: Electron microprobe analyses of vesuvianite

Sample	LM10								
Analysis	1	2	3	4	5	6	7	8	9
SiO_2	36.5	36.2	36.4	36.3	35.9	36.2	36.3	36.6	36.2
TiO_2	2.54	2.56	2.44	2.60	1.51	1.84	2.77	2.18	2.27
Al_2O_3	15.9	15.7	16.1	15.8	16.6	16.3	15.5	16.6	16.0
FeO	3.52	3.51	3.75	3.64	3.78	3.90	3.64	3.43	3.56
MnO	<0.04	0.07	0.05	<0.04	<0.04	0.05	<0.04	0.05	0.04
MgO	1.83	1.89	1.83	1.89	1.76	1.63	1.97	1.60	1.84
CaO	35.5	35.3	35.4	35.7	35.7	35.6	35.2	35.8	35.5
Na_2O	0.15	0.15	0.13	0.13	0.13	0.10	0.13	0.15	0.13
K_2O	<0.02	<0.02	<0.02	<0.02	0.02	<0.02	<0.02	<0.02	<0.02
F	1.70	1.56	1.31	1.44	1.47	1.67	1.35	1.59	1.55
Total	97.57	96.91	97.35	97.49	96.89	97.25	96.89	97.97	97.05
–O≡F	0.71	0.66	0.55	0.61	0.62	0.70	0.57	0.67	0.65
Total	96.86	96.25	96.80	96.88	96.27	96.54	96.32	97.30	96.39
					50 cations				
Si	18.045	17.991	17.951	17.939	17.806	17.948	18.042	17.984	17.958
Ti	0.943	0.958	0.907	0.967	0.562	0.686	1.035	0.807	0.847
Al	9.275	9.220	9.351	9.200	9.696	9.530	9.072	9.601	9.342
Fe	1.454	1.460	1.547	1.502	1.565	1.616	1.512	1.410	1.477
Mn	0.000	0.029	0.022	0.011	0.009	0.021	0.002	0.021	0.017
Mg	1.352	1.404	1.347	1.389	1.299	1.203	1.457	1.175	1.359
Ca	18.788	18.798	18.750	18.872	18.925	18.904	18.756	18.855	18.868
Na	0.143	0.140	0.121	0.120	0.128	0.092	0.120	0.147	0.121
K	0.000	0.000	0.005	0.000	0.010	0.000	0.004	0.000	0.009
Total	50.000	50.000	50.000	50.000	50.000	50.000	50.000	50.000	50.000

Table A11: Electron microprobe analyses of alkali feldspar

Sample	LM11											
Analysis	1	2	3	4	5	6	7	8	9	10	11	12
SiO_2	64.4	64.2	64.7	64.6	64.5	64.9	64.2	64.6	64.9	64.4	64.4	64.6
Al_2O_3	18.4	18.5	18.7	18.7	18.5	18.7	18.6	18.8	18.7	18.7	18.7	18.8
FeO	0.17	0.13	<0.06	0.13	0.14	0.11	0.06	0.13	0.14	0.14	0.36	0.21
CaO	0.04	0.04	0.02	0.03	<0.02	0.02	0.04	0.04	0.05	0.02	0.05	0.05
Na_2O	0.94	0.92	0.93	0.75	0.77	0.91	0.82	1.02	1.14	0.85	0.72	0.85
K_2O	15.6	15.5	15.6	15.7	15.6	15.6	15.5	15.9	15.7	16.2	16.2	16.2
Total	99.59	99.29	99.88	99.83	99.51	100.27	99.26	100.46	100.59	100.32	100.47	100.69
						8 oxygens						
Si	2.989	2.986	2.987	2.987	2.990	2.987	2.985	2.974	2.982	2.976	2.973	2.973
Al	1.007	1.013	1.015	1.016	1.013	1.015	1.019	1.022	1.012	1.017	1.019	1.018
Fe	0.007	0.005	0.002	0.005	0.005	0.004	0.002	0.005	0.005	0.005	0.014	0.008
Ca	0.002	0.002	0.001	0.002	0.001	0.001	0.002	0.002	0.002	0.001	0.002	0.002
Na	0.084	0.083	0.083	0.067	0.069	0.081	0.074	0.091	0.102	0.076	0.065	0.076
K	0.922	0.919	0.916	0.923	0.921	0.914	0.919	0.933	0.919	0.955	0.952	0.954
Total	5.011	5.008	5.004	5.000	4.999	5.002	5.001	5.027	5.022	5.030	5.026	5.032

Sample	LM11		LM65							LM68-1		
Analysis	13	14	1	2	3	4	5	6	7	1	2	3
SiO_2	64.9	64.5	63.8	64.1	64.3	64.3	64.1	63.9	64.4	63.5	64.0	62.8
Al_2O_3	18.7	18.7	18.8	18.7	18.9	18.9	18.9	18.9	18.9	18.6	18.8	18.6
FeO	0.17	0.14	<0.06	0.06	0.12	<0.06	<0.06	<0.06	0.07	<0.06	0.08	<0.06
CaO	0.02	0.04	0.02	0.03	0.02	0.03	0.04	0.03	0.02	<0.02	<0.02	0.07
Na_2O	0.95	0.93	0.53	0.56	0.67	0.61	0.63	0.49	0.60	0.50	0.62	0.63
K_2O	15.9	16.0	16.3	16.3	16.2	16.2	16.2	16.3	16.2	16.4	16.2	16.0
Total	100.53	100.36	99.42	99.71	100.24	99.98	99.85	99.61	100.23	99.07	99.62	98.13
						8 oxygens						
Si	2.983	2.978	2.973	2.976	2.972	2.974	2.971	2.971	2.975	2.973	2.973	2.966
Al	1.012	1.015	1.029	1.025	1.028	1.030	1.033	1.033	1.028	1.026	1.029	1.036
Fe	0.006	0.005	0.002	0.002	0.005	0.000	0.001	0.001	0.003	0.002	0.003	0.001
Ca	0.001	0.002	0.001	0.002	0.001	0.002	0.002	0.002	0.001	0.001	0.000	0.004
Na	0.084	0.083	0.048	0.051	0.060	0.055	0.057	0.044	0.054	0.046	0.056	0.057
K	0.931	0.944	0.966	0.965	0.957	0.957	0.955	0.967	0.956	0.977	0.959	0.963
Total	5.017	5.027	5.019	5.021	5.023	5.018	5.019	5.018	5.017	5.026	5.020	5.027

Table A11: (continued)

Sample	LM68-1		LM68-2					LM72				
Analysis	4	5	1	2	3	4	5	6	1	2	3	4
SiO_2	63.8	63.4	63.4	63.2	63.2	63.2	63.5	63.6	63.6	63.9	64.0	63.8
Al_2O_3	18.4	18.6	19.5	19.5	19.4	19.5	19.2	19.4	19.1	18.9	18.8	18.9
FeO	<0.06	0.10	<0.06	<0.06	<0.06	0.10	0.09	0.06	<0.06	<0.06	<0.06	<0.06
CaO	0.05	0.02	0.09	0.10	0.08	0.06	0.08	0.04	0.21	0.02	0.07	0.10
Na_2O	0.41	0.33	0.59	0.71	0.59	0.55	0.72	0.66	0.51	0.52	0.35	0.43
K_2O	16.4	16.6	15.6	15.5	15.6	15.7	15.4	15.3	15.8	16.0	16.3	16.2
Total	99.16	99.01	99.15	98.96	98.91	99.09	99.10	99.10	99.14	99.30	99.51	99.44
						8 oxygens						
Si	2.982	2.973	2.952	2.946	2.950	2.946	2.959	2.957	2.962	2.975	2.975	2.968
Al	1.016	1.025	1.067	1.073	1.068	1.074	1.056	1.065	1.048	1.034	1.032	1.039
Fe	0.001	0.004	0.001	0.001	0.001	0.004	0.004	0.002	0.000	0.000	0.001	0.002
Ca	0.003	0.001	0.005	0.005	0.004	0.003	0.004	0.002	0.010	0.001	0.004	0.005
Na	0.037	0.030	0.054	0.064	0.053	0.050	0.065	0.059	0.046	0.047	0.031	0.039
K	0.979	0.990	0.926	0.920	0.932	0.932	0.916	0.910	0.938	0.948	0.964	0.960
Total	5.018	5.023	5.005	5.009	5.009	5.008	5.004	4.995	5.004	5.005	5.007	5.013

Sample	LM74-1											
Analysis	1	2	3	4	5	6	7	8	9	10	11	12
SiO_2	63.6	63.7	63.4	63.8	64.0	64.1	63.1	64.1	64.4	64.2	64.3	64.4
Al_2O_3	18.9	19.0	18.7	18.8	18.9	18.9	19.0	19.0	19.1	19.0	18.9	19.1
FeO	<0.06	<0.06	0.10	0.19	0.14	0.39	0.15	0.10	0.15	0.08	0.08	0.14
CaO	0.10	0.06	0.03	0.03	0.07	0.04	0.60	0.06	0.03	0.04	<0.02	0.03
Na_2O	0.44	0.59	0.39	0.60	0.56	0.58	0.50	0.50	0.47	0.42	0.60	0.55
K_2O	16.0	15.9	15.8	16.0	15.8	16.1	15.6	16.3	16.0	16.1	15.9	16.1
Total	99.05	99.25	98.37	99.47	99.37	100.18	98.96	100.01	100.11	99.90	99.83	100.31
						8 oxygens						
Si	2.969	2.968	2.977	2.970	2.975	2.967	2.952	2.967	2.971	2.973	2.976	2.970
Al	1.038	1.042	1.033	1.032	1.033	1.032	1.048	1.037	1.040	1.037	1.031	1.037
Fe	0.001	0.000	0.004	0.007	0.005	0.015	0.006	0.004	0.006	0.003	0.003	0.005
Ca	0.005	0.003	0.002	0.001	0.003	0.002	0.030	0.003	0.002	0.002	0.001	0.001
Na	0.040	0.053	0.036	0.054	0.050	0.052	0.045	0.044	0.042	0.038	0.054	0.049
K	0.956	0.944	0.949	0.952	0.934	0.952	0.929	0.963	0.939	0.950	0.941	0.948
Total	5.009	5.010	5.001	5.016	5.000	5.020	5.010	5.018	5.000	5.003	5.006	5.010

Table A11: (continued)

Sample	LM75-1		LM92-1	LM94				LM95-1				
Analysis	1	2	1	1	2	3	4	5	1	2	3	4
SiO_2	63.4	63.8	64.1	64.2	63.8	63.9	63.7	64.1	64.0	63.5	63.9	64.6
Al_2O_3	19.5	19.4	18.8	18.7	18.9	18.8	19.0	19.0	19.1	19.2	19.1	18.7
FeO	0.10	<0.06	0.07	0.16	0.14	0.16	0.11	<0.06	<0.06	0.07	0.14	0.13
CaO	0.09	0.09	0.08	<0.02	0.10	<0.02	0.05	<0.02	0.02	0.02	0.02	0.09
Na_2O	0.76	0.68	0.56	0.40	0.32	0.34	0.37	0.53	0.63	0.62	0.66	0.84
K_2O	15.3	15.4	16.1	16.1	16.0	16.3	16.3	16.1	15.9	16.1	15.9	15.3
Total	99.13	99.28	99.73	99.49	99.29	99.57	99.49	99.71	99.76	99.48	99.79	99.67
						8 oxygens						
Si	2.949	2.960	2.974	2.981	2.973	2.971	2.965	2.971	2.967	2.955	2.964	2.987
Al	1.071	1.060	1.030	1.024	1.037	1.035	1.041	1.039	1.044	1.055	1.044	1.020
Fe	0.004	0.001	0.003	0.006	0.005	0.006	0.004	0.001	0.001	0.003	0.005	0.005
Ca	0.004	0.005	0.004	0.000	0.005	0.000	0.003	0.000	0.001	0.001	0.001	0.005
Na	0.069	0.061	0.050	0.036	0.029	0.031	0.033	0.047	0.056	0.056	0.059	0.075
K	0.907	0.909	0.951	0.953	0.950	0.970	0.969	0.949	0.941	0.953	0.941	0.900
Total	5.004	4.996	5.012	5.000	4.999	5.013	5.015	5.007	5.010	5.023	5.014	4.992

Sample	LM95-1				LM134-2		
Analysis	5	6	7	8	1	2	3
SiO_2	63.7	63.8	63.7	62.5	64.2	63.4	63.9
Al_2O_3	19.2	19.0	19.2	18.6	18.9	18.9	19.0
FeO	<0.06	0.10	0.08	<0.06	<0.06	0.09	<0.06
CaO	0.02	0.03	0.04	0.02	0.13	0.02	<0.02
Na_2O	0.58	0.44	0.53	0.58	0.77	0.48	0.54
K_2O	16.1	16.3	16.1	15.7	15.7	16.2	15.9
Total	99.65	99.68	99.62	97.43	99.63	99.06	99.32
				8 oxygens			
Si	2.958	2.965	2.960	2.968	2.977	2.966	2.971
Al	1.053	1.042	1.049	1.039	1.030	1.039	1.039
Fe	0.002	0.004	0.003	0.002	0.000	0.003	0.001
Ca	0.001	0.002	0.002	0.001	0.005	0.001	0.001
Na	0.052	0.039	0.048	0.054	0.069	0.044	0.049
K	0.952	0.964	0.956	0.951	0.926	0.966	0.946
Total	5.018	5.016	5.018	5.015	5.007	5.019	5.007

Table A12: Electron microprobe analyses of plagioclase

Sample	LM10						LM11					
Analysis	1	2	3	4	5	6	1	2	3	4	5	6
SiO_2	67.0	67.2	66.5	67.2	67.4	66.7	56.8	57.4	56.8	57.9	55.5	57.5
Al_2O_3	20.6	20.0	20.4	20.0	20.7	20.7	26.9	27.0	26.8	27.1	28.7	27.0
FeO	<0.06	0.06	0.09	<0.06	<0.06	<0.06	0.27	0.10	0.16	0.10	0.09	0.08
CaO	0.60	0.34	0.51	0.41	0.69	0.84	8.91	8.85	8.96	8.89	10.78	8.93
Na_2O	11.1	11.0	10.9	11.3	10.1	11.0	6.63	6.63	6.60	6.39	5.33	6.34
K_2O	0.10	0.10	0.13	0.06	0.09	0.11	0.18	0.16	0.13	0.19	0.18	0.20
Total	99.44	98.78	98.55	98.99	99.03	99.33	99.75	100.12	99.40	100.60	100.60	100.06
						8 oxygens						
Si	2.947	2.971	2.949	2.966	2.964	2.937	2.560	2.570	2.566	2.577	2.484	2.575
Al	1.069	1.043	1.068	1.042	1.071	1.076	1.431	1.426	1.424	1.423	1.516	1.426
Fe	0.000	0.002	0.003	0.001	0.000	0.001	0.010	0.004	0.006	0.004	0.003	0.003
Ca	0.028	0.016	0.024	0.019	0.033	0.040	0.430	0.425	0.434	0.424	0.517	0.428
Na	0.942	0.942	0.936	0.963	0.862	0.936	0.579	0.576	0.578	0.551	0.462	0.550
K	0.006	0.006	0.008	0.003	0.005	0.006	0.011	0.009	0.007	0.011	0.010	0.011
Total	4.992	4.980	4.988	4.994	4.935	4.997	5.021	5.010	5.015	4.991	4.992	4.993

Sample	LM11					LM65						
Analysis	7	8	9	10	11	1	2	3	4	5	6	7
SiO_2	58.1	57.6	56.9	57.1	57.1	64.1	64.5	64.4	64.2	64.3	63.5	64.1
Al_2O_3	27.0	27.3	27.2	26.9	27.5	22.7	22.5	22.6	22.8	22.8	23.0	22.8
FeO	0.16	0.08	0.09	0.10	0.19	<0.06	0.07	<0.06	<0.06	0.08	<0.06	<0.06
CaO	8.70	8.93	9.00	9.01	9.22	3.31	3.05	3.04	3.34	3.33	3.64	3.22
Na_2O	6.55	6.35	6.23	6.28	6.15	9.84	9.77	9.96	9.70	9.62	9.43	9.68
K_2O	0.20	0.18	0.20	0.19	0.21	0.12	0.11	0.11	0.10	0.16	0.13	0.19
Total	100.62	100.44	99.64	99.59	100.30	100.06	99.97	100.10	100.19	100.30	99.68	99.99
						8 oxygens						
Si	2.584	2.567	2.562	2.570	2.553	2.824	2.842	2.833	2.824	2.827	2.809	2.825
Al	1.414	1.437	1.441	1.428	1.448	1.180	1.167	1.175	1.184	1.182	1.200	1.185
Fe	0.006	0.003	0.003	0.004	0.007	0.001	0.002	0.000	0.001	0.003	0.001	0.002
Ca	0.415	0.427	0.434	0.435	0.442	0.156	0.144	0.143	0.157	0.157	0.172	0.152
Na	0.566	0.549	0.544	0.548	0.533	0.841	0.834	0.850	0.827	0.820	0.809	0.827
K	0.011	0.010	0.011	0.011	0.012	0.007	0.006	0.006	0.006	0.009	0.008	0.011
Total	4.996	4.993	4.995	4.996	4.996	5.009	4.995	5.007	4.999	4.998	4.999	5.002

Table A12: (continued)

Sample	LM65						LM68-1					
Analysis	8	9	10	11	12	13	1	2	3	4	5	6
SiO_2	63.7	67.7	66.4	64.3	64.3	63.8	68.4	68.4	69.4	68.2	65.4	67.9
Al_2O_3	22.9	20.5	21.0	22.7	22.7	23.0	19.7	20.4	19.7	19.5	19.1	19.6
FeO	<0.06	<0.06	<0.06	<0.06	0.08	<0.06	0.18	<0.06	0.06	0.07	<0.06	0.07
CaO	3.49	0.51	1.27	3.25	3.16	3.67	0.50	0.64	0.08	0.16	1.87	0.25
Na_2O	9.54	11.2	10.8	9.72	9.64	9.45	11.3	11.2	11.5	11.5	11.1	11.5
K_2O	0.22	0.12	0.10	0.11	0.20	0.13	0.10	0.14	0.08	0.07	0.09	0.11
Total	99.86	100.16	99.63	100.16	100.11	100.10	100.25	100.86	100.77	99.48	97.58	99.36
						8 oxygens						
Si	2.814	2.956	2.922	2.830	2.832	2.813	2.982	2.965	3.002	2.993	2.950	2.985
Al	1.193	1.056	1.088	1.178	1.178	1.196	1.015	1.042	1.003	1.010	1.015	1.015
Fe	0.002	0.001	0.000	0.002	0.003	0.000	0.007	0.002	0.002	0.003	0.001	0.003
Ca	0.165	0.024	0.060	0.153	0.149	0.173	0.023	0.030	0.004	0.008	0.090	0.012
Na	0.818	0.951	0.924	0.830	0.823	0.807	0.954	0.944	0.967	0.974	0.966	0.980
K	0.012	0.007	0.005	0.006	0.011	0.007	0.005	0.008	0.004	0.004	0.005	0.006
Total	5.004	4.995	4.999	4.999	4.996	4.996	4.991	4.991	4.982	4.992	5.027	5.001

Sample	LM68-1			LM68-2		LM72			LM75-1		LM92-1	
Analysis	7	8	9	1	2	1	2	3	1	2	1	2
SiO_2	67.2	68.4	67.9	53.8	55.2	68.4	68.0	68.0	54.4	57.5	57.5	53.1
Al_2O_3	19.4	19.7	19.7	29.8	28.6	19.9	19.8	20.2	29.3	27.0	26.9	28.5
FeO	0.07	0.06	<0.06	<0.06	0.07	<0.06	<0.06	<0.06	0.14	0.06	0.14	1.02
CaO	0.82	0.20	0.62	10.77	9.36	<0.02	0.08	0.09	10.24	7.39	8.04	10.01
Na_2O	11.5	11.5	11.6	5.14	5.68	11.7	11.4	11.4	5.41	6.92	6.83	5.09
K_2O	0.13	0.07	0.08	0.13	0.22	0.06	0.05	0.06	0.10	0.21	0.11	0.46
Total	99.11	99.84	99.92	99.68	99.15	100.12	99.36	99.75	99.52	99.08	99.52	98.15
						8 oxygens						
Si	2.972	2.990	2.974	2.434	2.498	2.983	2.986	2.976	2.458	2.591	2.584	2.451
Al	1.010	1.014	1.019	1.587	1.527	1.025	1.024	1.039	1.562	1.433	1.426	1.547
Fe	0.002	0.002	0.002	0.001	0.003	0.000	0.000	0.001	0.005	0.002	0.005	0.040
Ca	0.039	0.009	0.029	0.522	0.454	0.000	0.004	0.004	0.496	0.357	0.387	0.495
Na	0.990	0.971	0.982	0.451	0.498	0.991	0.974	0.965	0.474	0.605	0.595	0.456
K	0.007	0.004	0.005	0.007	0.013	0.003	0.003	0.004	0.006	0.012	0.006	0.027
Total	5.020	4.990	5.011	5.002	4.993	5.002	4.991	4.989	5.001	5.000	5.003	5.016

Table A12: (continued)

Sample	LM94				LM95-1							LM104-1
Analysis	1	2	3	4	1	2	3	4	5	6	7	1
SiO_2	67.8	68.4	68.3	67.9	52.7	50.6	53.7	53.5	50.4	51.9	52.7	61.5
Al_2O_3	20.5	20.5	20.4	20.6	30.6	26.4	30.0	30.1	32.0	30.7	30.6	24.1
FeO	0.17	0.14	0.13	0.08	<0.06	3.38	0.06	0.10	0.14	0.23	0.03	0.14
CaO	0.69	0.29	0.32	0.56	12.1	17.1	11.2	11.6	13.9	12.5	12.1	4.96
Na_2O	11.03	11.28	10.77	11.06	4.56	1.73	4.88	4.91	3.52	4.28	4.56	8.69
K_2O	0.17	0.13	0.14	0.12	0.12	0.06	0.10	0.12	0.07	0.12	0.12	0.08
Total	100.36	100.73	100.02	100.39	100.12	99.29	99.96	100.29	100.01	99.75	100.12	99.47
						8 oxygens						
Si	2.954	2.966	2.964	2.957	2.382	2.372	2.421	2.411	2.294	2.361	2.382	2.739
Al	1.055	1.047	1.044	1.058	1.630	1.456	1.598	1.597	1.715	1.644	1.630	1.268
Fe	0.006	0.005	0.005	0.003	0.001	0.132	0.002	0.004	0.005	0.009	0.001	0.005
Ca	0.032	0.013	0.015	0.026	0.587	0.859	0.543	0.561	0.677	0.611	0.587	0.237
Na	0.932	0.948	0.907	0.934	0.400	0.157	0.427	0.429	0.311	0.377	0.400	0.751
K	0.009	0.007	0.063	0.006	0.007	0.004	0.006	0.007	0.004	0.007	0.007	0.005
Total	4.988	4.986	4.998	4.984	5.007	4.980	4.997	5.009	5.006	5.009	5.007	5.005

Sample	LM104-1				LM134-2							
Analysis	2	3	4	5	1	2	3	4	5	6	7	8
SiO_2	61.0	57.4	56.9	58.1	64.0	65.0	63.9	65.1	65.1	64.0	65.2	64.1
Al_2O_3	24.2	27.1	27.7	26.7	22.9	22.4	22.8	22.5	21.9	22.6	21.9	22.8
FeO	0.14	0.07	0.09	0.08	0.25	<0.06	<0.06	<0.06	0.11	<0.06	2.29	3.19
CaO	4.83	8.01	8.87	7.78	3.36	2.75	3.38	2.59	2.40	2.95	0.06	0.05
Na_2O	8.34	6.85	6.51	7.07	9.65	9.99	9.67	9.94	10.4	9.87	10.3	9.54
K_2O	0.15	0.09	0.10	0.12	0.11	0.14	0.14	0.19	0.15	0.11	0.18	0.10
Total	98.64	99.49	100.17	99.93	100.26	100.22	99.93	100.30	99.98	99.56	99.82	99.81
						8 oxygens						
Si	2.736	2.579	2.547	2.600	2.817	2.852	2.821	2.852	2.866	2.833	2.872	2.829
Al	1.282	1.435	1.461	1.409	1.188	1.159	1.186	1.163	1.136	1.178	1.135	1.186
Fe	0.005	0.003	0.003	0.003	0.009	0.000	0.001	0.001	0.004	0.001	0.108	0.151
Ca	0.232	0.386	0.425	0.373	0.158	0.129	0.160	0.122	0.113	0.140	0.002	0.002
Na	0.726	0.597	0.565	0.613	0.824	0.850	0.827	0.845	0.885	0.847	0.875	0.816
K	0.008	0.005	0.006	0.007	0.006	0.008	0.008	0.946	0.008	0.006	0.010	0.006
Total	4.989	5.005	5.007	5.005	5.002	4.998	5.003	5.929	5.012	5.005	5.002	4.990

Table A13: Electron microprobe standard analyses

Standard	ALB4		ORTH4		BIO7	
	Measured	Expected	Measured	Expected	Measured	Expected
SiO_2	68.4 (4)	68.14	64.6 (3)	64.80	36.0 (2)	36.5
TiO_2					2.26 (25)	2.30
Al_2O_3	20.1 (3)	19.77	16.6 (3)	16.74	18.2 (2)	18.30
FeO	0.03 (3)	0.01	1.75 (8)	2.01	13.7 (3)	13.61
MnO					0.03 (3)	0.06
MgO					15.0 (3)	15.1
CaO	0.09 (5)	0.38	0.00		0.02 (1)	0.33
Na_2O	11.4 (1)	11.46	0.96 (3)	0.91	0.66 (4)	0.55
K_2O	0.15 (3)	0.23	15.6 (2)	15.49	8.67 (17)	9.00
Total	100.17	99.99	99.51	99.95	94.54	95.75
n	33		27		12	

Standard	MUSC7		BIO4		HORN7	
	Measured	Expected	Measured	Expected	Measured	Expected
SiO_2	44.9 (3)	47.24	37.1 (1)	38.33	41.3 (2)	41.92
TiO_2	0.59 (2)	0.48	1.31 (21)	1.67	2.64 (13)	2.81
Al_2O_3	32.9 (4)	30.9	15.7 (1)	15.30	12.3 (2)	12.48
FeO	4.25 (13)	4.91	10.9 (8)	10.36	16.5 (2)	17.18
MnO	0.07 (2)	0.12	0.11 (2)	0.11	0.15 (2)	0.19
MgO	0.86 (4)	0.93	18.3 (6)	19.35	9.67 (13)	9.72
CaO	0.00 (1)		0.02 (2)	0.21	11.5 (1)	11.63
Na_2O	0.58 (3)	0.67	0.08 (2)	0.09	1.54 (10)	1.61
K_2O	10.7 (2)	10.22	10.2 (1)	10.03	1.56 (6)	1.51
Total	94.85	95.47	93.72	95.45	97.16	99.05
n	8		6		14	

Table A13: (continued)

Standard	SPESS4		PYR4		DIOP4	
	Measured	Expected	Measured	Expected	Measured	Expected
SiO_2	34.9 (2)	36.39	41.6 (6)	42.50	55.1 (3)	55.19
TiO_2	0.03(1)	0.03	0.70(4)	0.65	0.03(1)	0.02
Al_2O_3	20.6 (3)	20.62	21.4 (2)	21.39	0.65(3)	0.43
Cr_2O_3	0.01(2)		1.58(5)	1.55	0.01(1)	
FeO	1.26(7)	1.78	9.38(8)	9.39	0.80(3)	0.89
MnO	40.7 (4)	40.71	0.33(2)	0.35	0.06(3)	0.05
MgO	0.00		21.2 (1)	20.76	17.8 (4)	17.94
CaO	0.35(2)	0.36	4.21(5)	4.19	25.2 (1)	25.18
Na_2O					0.42(2)	0.38
K_2O						
Total	97.85	99.89	100.40	100.78	100.07	100.08
n	9		8		28	

Note: Number in () is the standard deviation in terms of the least units cited, determined by n replicate analyses.

Table A14: X-ray fluorescence standard analyses

Protocol	LSDOL					
Standard	L88A		L7011		AP35L	
	Measured	Expected	Measured	Expected	Measured	Expected
SiO_2	0.96 (2)	0.98	2.18 (3)	2.21	2.29 (3)	2.32
TiO_2	0.01 (0)	0.01	0.04 (0)	0.04	0.02 (0)	0.02
Al_2O_3	0.38 (1)	0.44	0.56 (6)	0.61	0.29 (2)	0.29
Fe_2O_3	0.32 (0)	0.32	1.08 (1)	1.08	0.13 (0)	0.13
MgO	21.6 (4)	21.6	0.70 (1)	0.69	0.83 (3)	0.80
CaO	30.3 (2)	30.2	52.7 (1)	52.6	53.8 (2)	53.4
Na_2O	0.03 (6)	0.00	0.02 (0)	0.03	0.04 (4)	0.02
K_2O	0.10 (7)	0.14	0.12 (1)	0.13	0.08 (4)	0.11
P_2O_5	0.03 (1)	0.03	0.05 (0)	0.05	0.01 (1)	0.01
Total	53.70	53.71	57.40	57.43	57.48	57.11
S			779 (17)	806	995 (51)	927
Mn	236 (5)	238	173 (3)	174	63 (3)	69
Zn	77 (5)	75	18 (3)	18	27 (6)	23
Rb	182 (137)	43	27 (1)		31 (6)	13
Sr	72 (10)	76	280 (9)	298	294 (7)	298
n	4		3		4	

Table A14: (continued)

Protocol	LSDOL					
Standard	KH2L		KH1L		AP48L	
	Measured	Expected	Measured	Expected	Measured	Expected
SiO_2	8.61 (7)	8.63	8.47 (5)	8.42	0.80 (1)	0.82
TiO_2	0.11 (0)	0.11	0.11 (0)	0.11	0.01 (0)	0.01
Al_2O_3	2.37 (9)	2.51	2.39 (13)	2.26	0.13 (6)	0.10
Fe_2O_3	0.87 (1)	0.87	0.84 (0)	0.83	0.21 (0)	0.21
MgO	0.84 (8)	0.81	0.85 (8)	0.82	21.2 (5)	21.1
CaO	48.0 (2)	47.9	47.8 (2)	47.3	30.7 (0)	30.6
Na_2O	0.22 (16)	0.13	0.12 (1)	0.11	0.00	0.00
K_2O	0.32 (18)	0.04	0.42 (1)	0.41	0.00	0.00
P_2O_5	0.10 (0)	0.11	0.11 (0)	0.11	0.03 (0)	0.03
Total	61.39	61.15	61.08	60.36	53.13	52.87
S	831 (72)	828	802 (4)	791		
Mn	577 (11)	581	593 (8)	557	114 (5)	112
Zn	29 (7)	19	21 (1)	27	79 (10)	76
Rb	22 (0)	19	46 (26)	25	355 (24)	325
Sr	594 (33)	554	535 (11)	550	81 (1)	81
n	3		2		2	

Table A14: (continued)

Protocol	SIAL					
Standard	G2		GSP1		SARM1	
	Measured	Expected	Measured	Expected	Measured	Expected
SiO_2	68.9 (7)	69.3	68.6 (5)	67.2	75.9 (8)	78.1
TiO_2	0.49 (0)	0.48	0.64(2)	0.62	0.06(1)	0.05
Al_2O_3	15.0 (5)	14.9	14.8 (2)	15.3	12.3 (4)	12.5
Fe_2O_3	2.57 (11)	2.66	3.88(7)	4.11	1.98(18)	2.01
MnO	0.04 (0)	0.03	0.06(0)	0.04	0.03(0)	0.03
MgO	0.78 (12)	0.77	1.02(4)	0.95	0.05(5)	0.07
CaO	1.81 (3)	1.84	1.75(0)	1.85	0.77(3)	0.79
Na_2O	4.06 (16)	4.07	2.68(18)	3.00	3.37(21)	3.54
K_2O	4.42 (10)	4.27	5.42(18)	5.54	5.19(7)	5.02
P_2O_5	0.15 (5)	0.14	0.28(5)	0.27	0.04(4)	0.03
Total	98.20	98.43	99.09	98.86	99.61	102.12
Cu	15 (2)	9	27 (3)	21	20 (4)	17
V	32 (13)	27	63 (17)	62	10 (8)	1
Cr	36 (4)	34	86 (26)	66	22 (22)	20
Co	6 (4)	7	12 (1)	6	3 (1)	5
Ni	8 (11)	15	20 (0)	13	6 (2)	5
Zn	52 (30)	79	103 (6)	77	49 (14)	71
Pb	23 (2)	25	41 (1)	44	40 (9)	49
Rb	181 (11)	162	259 (14)	267	359 (12)	344
Sr	469 (19)	441	226 (10)	227	9 (1)	
Y	17 (3)	14	37 (1)	38	151 (1)	144
Zr	360 (32)	330	564 (12)	555	304 (18)	287
Nb	13 (4)	17	27 (1)	22	37 (27)	51
Mo	3 (4)	3	1 (1)		13 (2)	9
Ba	1645 (359)	1410	1126 (31)	1259	306 (28)	319
n	2		3		3	

Table A14: (continued)

Protocol	TECLAY			
Standard	TSO2S1		TNB97B	
	Measured	Expected	Measured	Expected
SiO2	52.8 (4)	53.6	41.8 (10)	42.3
TiO2	1.40 (3)	1.40	2.42 (4)	2.41
Al2O3	15.3 (1)	15.0	39.9 (2)	39.2
Fe2O3	7.62 (24)	7.80	1.12 (2)	1.13
MnO	0.09 (0)	0.09	0.01 (0)	0.01
MgO	1.21 (6)	1.26	0.10 (5)	0.26
CaO	2.43 (3)	2.57	0.00 (0)	0.00
Na2O	2.70 (23)	2.51	0.01 (2)	0.01
K2O	2.71 (3)	2.91	0.60 (1)	0.65
P2O5	0.26 (0)	0.28	0.06 (0)	0.06
S	0.03 (0)	0.03	0.18 (3)	0.16
Cl	0.08 (2)	0.22		
Total	86.57	87.43	86.57	86.03
V	111 (23)	109	224 (11)	227
Cr	31 (2)	32	241 (6)	239
Co	24 (2)	26	10 (0)	10
Ni	36 (19)	32		
Zn	1345 (166)	1099	297 (33)	214
Pb	14 (7)	10	38 (4)	36
As	34 (2)	33	0 (0)	
Rb	70 (5)	72	46 (1)	45
Sr	302 (13)	305	96 (53)	120
Zr	673 (26)	686	500 (6)	506
Ba	815 (47)	797	355 (38)	334
Cu	29 (29)	25	29 (5)	24
n	5		5	

Note: Number in () is the standard deviation in terms of the least units cited, determined by n replicate analyses.

Table A 15: Comparison of X-ray fluorescence whole-rock chemical analyses using IGROCK and SIAL protocols

Sample	LM138		LM140		LM142		LM144		LM146	
Protocol	IGROCK	SIAL	IGROCK	SIAL	IGROCK	SIAL	IGROCK	SIAL	IGROCK	SIAL
SiO_2	68.7	71.5	68.5	71.0	68.4	71.5	71.1	73.2	64.6	68.9
TiO_2	0.23	0.30	0.20	0.26	0.16	0.24	0.25	0.31	0.27	0.32
Al_2O_3	15.9	16.1	15.8	15.9	15.6	16.0	14.5	15.0	17.4	17.6
Fe_2O_3	1.44	1.50	1.41	1.43	1.34	1.38	1.78	1.75	1.54	1.58
MnO	0.01	0.03	0.01	0.03	0.00	0.03	0.02	0.04	0.00	0.03
MgO	0.63	0.33	0.72	0.40	0.69	0.30	0.98	0.42	0.62	0.44
CaO	1.90	1.84	2.03	2.01	1.83	1.77	2.04	2.03	2.26	2.25
Na_2O	4.23	4.53	4.47	4.58	4.62	4.74	4.23	4.70	4.92	4.77
K_2O	4.52	4.67	4.20	4.29	4.31	4.40	3.60	3.69	4.49	4.71
P_2O_5	0.05	0.06	0.03	0.06	0.02	0.05	0.08	0.09	0.06	0.07
Total	97.60	100.89	97.32	99.96	96.95	100.46	98.56	101.32	96.19	100.68
V	24	17	9	16	5	17	14	17	29	18
Rb	169	181	134	147	165	184	128	157	162	190
Sr	748	764	789	787	709	731	751	740	856	859
Y	6	21	7	20	6	22	8	19	6	24
Zr	242	378	237	374	228	349	254	401	263	450
Nb	8	6	9	7	8	6	9	8	9	8

Table A 16: Comparison of electron microprobe and X-ray fluorescence whole-rock chemical analyses

Sample	LM115-1		LM123		LM131-2		LM134-2		LM138	
Instrument	EMP	XRF	EMP	XRF	EMP	XRF	EMP	XRF	EMP	XRF
SiO_2	67.2	68.8	70.8	71.4	72.8	74.6	69.2	71.3	69.2	71.5
TiO_2	0.41	0.34	0.29	0.28	0.19	0.23	0.26	0.23	0.28	0.30
Al_2O_3	16.7	17.1	15.6	15.3	14.6	14.8	16.40	16.6	16.2	16.1
FeO	1.78	2.03	1.43	1.59	1.18	1.23	1.12	1.39	1.49	1.50
MnO	0.03	0.04	0.04	0.03	0.02	0.03	0.04	0.04	0.03	0.03
MgO	0.52	0.52	0.42	0.43	0.28	0.26	0.30	0.31	0.41	0.33
CaO	2.11	2.01	1.49	1.41	1.46	1.44	2.16	2.24	1.96	1.84
Na_2O	4.49	5.09	3.94	4.27	3.87	4.54	4.58	5.16	4.11	4.53
K_2O	3.40	3.80	4.46	4.53	4.14	4.19	4.17	4.48	4.54	4.67
Total	97.69	99.73	98.60	99.28	98.64	101.21	98.39	101.75	98.24	100.83

Note: Instrument: EMP = electron microprobe, XRF = X-ray fluorescence.

VITA

Ian James Richards was born in Melbourne, Australia on December 11, 1958. Ian is the eldest son of Roy and Nancy Richards, and has a younger brother, Murray. Ian grew up in Melbourne. After attending Moorabin Technical School and then Mentone Grammar School, Ian finished high school in 1977. Needing a break from study, Ian took a job as a technical assistant with the Commonwealth Scientific and Industrial Research Organization Division of Mineral Engineering in 1978. In order to escape from the real world, Ian began studying part-time at LaTrobe University in 1980. Unsure of his specific interests within the broad realm of science, Ian began his studies with geology, a pursuit that he still continues to enjoy. In 1983 Ian decided to continue his education full-time and in 1985 received a Bachelor of Science (Honors) Degree from Monash University. Ian then worked for two years in the stable isotope laboratory of the Department of Earth Sciences at Monash University. Ian left Australia and began his studies at the University of Tennessee in 1987. Ian will next travel to Dallas, Texas where he will work in the stable isotope laboratory in the Department of Geological Sciences at Southern Methodist University. Ian will marry Maria Christine Leary on September 17 1994 in Michigan.